DOCTOR OF PHILOSOPHY

Evaluation of modern intraocular lenses

Phillip Buckhurst

2011

Aston University

EVALUATION OF MODERN INTRAOCULAR LENSES

PHILLIP JONATHAN BUCKHURST

Doctor of Philosophy

ASTON UNIVERSITY

January 2011

ASTON UNIVERSITY

EVALUATION OF MODERN INTRAOCULAR LENSES

PHILLIP JONATHAN BUCKHURST

DOCTOR OF PHILOSOPHY
JANUARY 2011

Summary

Accommodating Intraocular Lenses (IOLs), multifocal IOLs (MIOLs) and toric IOLs are designed to provide a greater level of spectacle independency post cataract surgery. All of these IOLs are reliant on the accurate calculation of intraocular lens power determined through reliable ocular biometry.

A standardised defocus area metric and reading performance index metric were devised for the evaluation of the range of focus and the reading ability of subjects implanted with presbyopic correcting IOLs. The range of clear vision after implantation of an MIOL is extended by a second focal point; however, this results in the prevalence of dysphotopsia. A bespoke halometer was designed and validated to assess this photopic phenomenon. There is a lack of standardisation in the methods used for determining IOL orientation and thus rotation. A repeatable, objective method was developed to allow the accurate assessment of IOL rotation, which was used to determine the rotational and positional stability of a closed loop haptic IOL. A new commercially available biometry device was validated for use with subjects prior to cataract surgery. The optical low coherence reflectometry instrument proved to be a valid method for assessing ocular biometry and covered a wider range of ocular parameters in comparison with previous instruments.

The advantages of MIOLs were shown to include an extended range of clear vision translating into greater reading ability. However, an increased prevalence of dysphotopsia was shown with a bespoke halometer, which was dependent on the MIOL optic design. Implantation of a single optic accommodating IOL did not improve reading ability but achieved high subjective ratings of near vision.

The closed-loop haptic IOL displayed excellent rotational stability in the late period but relatively poor rotational stability in the early period post implantation. The orientation error was compounded by the high frequency of positional misalignment leading to an extensive overall misalignment of the IOL.

This thesis demonstrates the functionality of new IOL lens designs and the importance of standardised testing methods, thus providing a greater understanding of the consequences of implanting these IOLs. Consequently, the findings of the thesis will influence future designs of IOLs and testing methods.

Key words: Intraocular lens, defocus curve, dysphotopsia, ocular biometry, toric rotation.

Dedicated to my auntie Margaret

Acknowledgements

Contents

LIST OF TABLES

13

LIST OF FIGURES

LIST OF ABBREVIATIONS

ACD	–	Anterior chamber depth
ADVS	–	Activities of daily vision scale
AL	–	Axial length
AMD	–	Age related macular degeneration
ANOVA	–	Analysis of variance
ANSI	–	American National Standards Institute
AOA	–	Amplitude of accommodation
ARE	–	Asymptotic relative efficiency
BAT	–	Brightness Acuity Tester
BSS	–	Balanced saline solution
BVD	–	Back vertex distance
CCT	–	Correlated colour temperature
CCI	–	Clear corneal incisions
CPS	–	Critical print size
CS	–	Contrast sensitivity
CSO	–	Costruzione Strumenti Oftalmici
CSS	–	Cataract symptom score
CTT	–	Classic test theory
C_W	–	Weber contrast units
ECCE	–	Extracapsular cataract extraction
ETDRS	–	Early treatment of diabetic retinopathy study
FGVS	–	Freedom from Glasses Value Scale
ICC	–	Intraclass correlation coefficent
ICCE	–	Intracapsular cataract extraction
IOL	–	Intraocular lens
IRM	–	Item response models
IVA	–	Intermediate visual acuity
LASIK	–	Laser-assisted in situ keratomileusis
LED	–	Light emitting diode
LOCS 111	–	Lens Opacities Classification Scale 111
LOGITS	–	Log-odd units
LRI	–	Limbal relaxing incision
LT	–	Lens thickness
MAR	–	Minimum angle of resolution
MIOL	–	Multifocal intraocular lenses
MK	–	Corneal reference markers
MNRead	–	Minnesota Near reading charts
MNSQ	–	Mean square
MRI	–	Magnetic resonance imaging
MRS	–	Maximum reading speed
NAVQ	–	Near Activity Visual Questionnaire
Nd:YAG	–	Neodymium-doped yttrium alumium garnet
NEI-RQL	–	National Eye Institute-Refractive Error Quality of Life
NHS	–	National Health Service
NVA	–	Near visual acuity
OLCR	–	Optical low coherence reflectometry
OP	–	Operative visit
OPD	–	Optical Path Difference

OVD	–	Ophthalmic viscoelastic device
P1	–	1ST Purkinje image
P2	–	2nd Purkinje image
P3	–	3rd Purkinje image
P4	–	4th Purkinje image
PCI	–	Partial coherence interferometry
PCO	–	Posterior capsular opacification
PMMA	–	Polymethylmethacrylate
PVD	–	Perceived visual disability
RA	–	Reading acuity
RAS	–	Reading ability score
RPI	–	Reading performance index
ROC	–	Receiver operating characteristic
QoV	–	Quality of vision
SA	–	Spherical aberration
SD	–	Standard deviation
V1	–	Visit 1
V2	–	Visit 2
V3	–	Visit 3
V4	–	Visit 4
VA	–	Visual acuity
VDA	–	Visual Disability Assessment
WHO	–	World health organisation
WPM	–	Words per minute

INTRAOCULAR LENSES EVALUATED IN THE THESIS

Monofocal intraocular lenses

IOL name	Manufacturer	Optic description	Haptic design
Softec 1	Lenstec	Hydophillic acrylic, 5.75 mm equal biconvex Spherical optic.	1-piece C-Loop haptic. 12 mm length
Akreos AO	Bausch and Lomb	Hydophillic acrylic, 6 mm aberration neutral aspherical optic	1-piece closed loop haptic. 11 mm length

Multifocal Intraocular Lenses

IOL name	Manufacturer	Optic description	Multifocal design	Near addition	Haptic design
Tecnis ZM900	Abbott medical optics	Silicone, 6 mm, biconvex, aberration control aspheric optic	Fully diffractive posterior surface	+4.00 D	3-piece C-Loop haptic. 12 mm length
ReZoom	Abbott medical optics	Hydrophillic acrylic, 6 mm, biconvex aberration control aspheric optic	Five zone concentric refractive. Distance dominant	+3.50 D	1-piece C-loop haptic. 13 mm length
Lentis Plus	Occulentis	Acrylic with hydrophobic surface, 6 mm, abberation neutral aspheric Optic	Sectorial refractive anterior surface.	+3.00 D (100° section of IOL)	1-piece C-Loop haptic. 12 mm length

Accommodative Intraocular Lens

IOL name	Manufacturer	Optic description	Accommodative design	Haptic design
Tetraflex	Lenstec	hydophillic acrylic, 5.75 mm equal biconvex Spherical optic.	Single Optic accommodative	1-piece closed Loop haptic. 11.5 mm length

Toric Intraocular Lens

IOL name	Manufacturer	Optic description	Toric design	Toricity	Haptic design
Akreos toric	Bausch and Lomb	Hydophillic acrylic, 6 mm aberration neutral aspherical optic	toric posterior surface	1.25, 2.00 & 2.75 D	1-piece closed loop haptic. 11 mm length

Chapter 1 Introduction

Cataracts are the main cause of blindness worldwide and are a particular issue in the developing world (Brian and Taylor, 2001). However, in the developed world, cataract extraction with intraocular lens (IOL) implantation is the most common surgical procedure. Approximately 2.5 million surgeries are preformed in the USA each year and approximately 250,000 are preformed in the UK (Dua *et al.,* 2009). The evolution of the IOL designs has been rapid and extensive development of new advanced IOLs has occurred in recent years; spherical monofocal IOL designs are no longer the only pseudophakic option. This chapter will provide a review outlining the evolution, outcomes and assessment of IOL implantation.

1.1   The Crystalline Lens

The transparent crystalline lens is a vital component of the human eye; it is responsible for one third of the eye's refractive power and facilitates accommodation in younger years (Pierscionek and Weale, 1995). The lens is composed of approximately 65% water and 35% protein – the largest concentration of protein for any tissue in the body (Schachar, 2006). The lens proteins are called crystallins; their high concentration and uniform structure gives the lens its transparency to the wavelengths of light detectable by the photoreceptors and allows its refractive index to be higher than the surrounding fluid (Andley, 2007). The crystalline lens separates the posterior and anterior segments of the eye. Its position, behind the pupil and in front of the vitreous, is maintained by the zonules of Zinn; which are elastic fibres connecting to the ciliary processes. The anterior and posterior zonular fibres attach to the anterior and posterior surface of the crystalline lens and equatorial fibres attach at the equatorial lens surface (Bron *et al.,* 1997). The interaction between the crystalline lens, zonules and ciliary body is an important consideration in the mechanism of accommodation. The crystalline lens diameter grows throughout life, examination of post-mortem eyes revealed an increase in lens diameter from 6 mm at birth to 9.3 mm at 16 years (Bluestein *et al.,* 1996). Using magnetic resonance imaging (MRI) scans, Fea and colleagues (2005) found an *in vivo* lens diameter of 9.43 mm for subjects in a non-accommodative state ranging from 20-79 years of age. In this study, lens thickness (in a non-accommodative state) was also found to increase with age; from 3.9 ± 0.41 mm in subjects aged 20-29 years to 4.75 ± 0.41 mm in subjects aged 70-79 years.

The human crystalline lens does not confirm to an equiconvex shape; the posterior lens surface has a steeper radius of curvature in comparison to the anterior surface (Koretz *et al.,* 2004). The lens can be divided into three distinct components:

- *the epithelium* – is made up of a characteristic layer of cuboidal cells located beneath the anterior capsule and extending from the central lens to the equatorial lens bow. Cell density is greatest in the central region where there is a relatively low occurrence of proliferation. In contrast epithelial cells close to the equator (within the germinative zone) display greater mitotic activity. Most of the newly formed cells are then forced into a transitional zone and differentiate into lens fibre cells. These cells elongate in a concentric pattern, whilst synthesizing crystallins, until meeting cells from the opposite side of the lens. The lens fibres then overlap to form the lens sutures. In the embryological stage these crystalline lens sutures form a simple three-branched structure, with age, this configuration increases in complexity until a twelve-suture arrangement has developed. The disparity of fibril arrangements in the transition zones – between lens suture regions – result in light scatter. These transition zones are known as the optical zones of discontinuity and are often used to differentiate regions within the lens fibre layers (Glasser *et al.,* 2007).

- *the lens fibres* – constitutes the main bulk of the lens. The lens fibres are densely packed and have little extracellular space assisting in their transparency. Throughout life new lens fibres are created but are not discarded, this results in an increased lens fibre density (Al-Ghoul and Costello, 1997). The lens regions can be described by there age of formation; the central portion – the lens nucleus – can be further subdivided into the embryonic nucleus, the fetal nucleus and the adult nucleus. Surrounding the nucleus is the cortex. The lens fibres in each region display distinct morphologies as a consequence of ageing (Al-Ghoul *et al.,* 2001). As lens fibre compaction increases towards the centre of the lens so does the refractive index of the lens. It is suggested that the central nucleus of the lens has a uniform refractive index (Brown, 1974). Matthiessen proposed a central refractive index of 1.41 and a peripheral refractive index of 1.383 (cited by Smith, 2003), however a higher peak refractive index of 1.42 has recently been proposed (Uhlhorn *et al.,* 2008). However, there is no general agreement on the uniformity or gradient of the refractive index change. Some models have proposed layered step

changes for the increase in refractive index (Mutti *et al.,* 1995) others use a continuous gradient (Pierscionek and Chan, 1989). The increasing refractive index towards the centre of the lens can partially correct for spherical aberration. The central portion of the lens also yellows with age and the increased lens fibre density can subsequently lead to reduced visual acuity (Snell and Lemp, 1998).

- *the elastic capsule* – is structurally difference in comparison to the lens fibres and epithelium. It is an elastic and transparent structure composed of collagen fibres, which are arranged to allow changes in lens shape. The shape of the capsule has been examined with interest. Fincham (1937) proposed that the thickest region of the anterior and posterior capsule was located at a point $2/5^{th}$ of the distance between the lens pole and equator. Studies have consistently demonstrated that the anterior capsule is thicker than the posterior capsule (Krag and Andreassen, 2003). Seland (1974) contradicted Fincham's proposal and suggested that the capsule was thickest that the equator however recent studies have supported Fincham's findings demonstrating an increase in thickness in the mid periphery of the lens (Barraquer *et al.,* 2006).

1.2 Cataracts

Cataracts are defined as any opacification of the crystalline lens. This reduced optical quality of the crystalline lens has a negative impact on the resultant retinal image, but is dependent on the extent and position of the cataract within the pupil margins. Cataracts can be classified by their location and aetiology. Cataracts can develop as a result of developmental abnormalities (Lloyd *et al.,* 1992), systemic and ocular diseases such as diabetes and uveitis, drug induced changes, and trauma, but the main cause remains to be ageing (Mitchell *et al.,* 1997; Livingston *et al.,* 1994).

Several classification systems, which use photographic illustrations to assist grading, exist for the assessment of cataract extent and location. The lens opacities classification scale 111 (LOCS 111)(Chylack *et al.,* 1993a), oxford clinical cataract classification and grading system (OCCCGS)(Sparrow *et al.,* 1986), world health organisation (WHO) simplified cataract grading system (Thylefors *et al.,* 2002) and the Wilmer nuclear grading system (West *et al.,* 1988) are all commonly used classification systems for the assessment of cataracts. An alternative to these subjective methods is the use of Scheimpflug photography with lens densitometry, which has shown good levels of

repeatability and validity for the measurement of nuclear cataracts (Datiles *et al.,* 1995; Grewal *et al.,* 2009).

Age related cataracts are generally categorised into cortical (the most common), nuclear or posterior subcapuslar cataracts although these do not have to occur in isolation (Beebe, 2003):

- *sub-capsular cataracts* – these form at the central posterior cortex at the position of the fourth purkinje image. Glare and reduced visual acuity are common visual symptoms associated with sub-capsular cataracts.
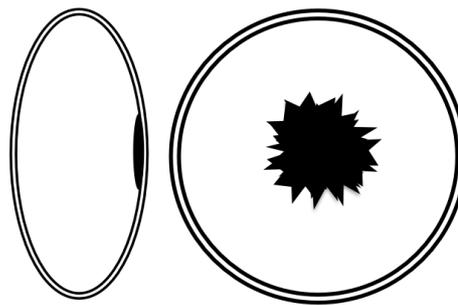
Figure 1.1 *Posterior sub-capsular cataract*

- *cortical Cataracts* – these opacities develop within the lens cortex and often appear as spokes within the crystalline lens. Visual symptoms are unlikely unless the cataract encroaches on the visual axis.
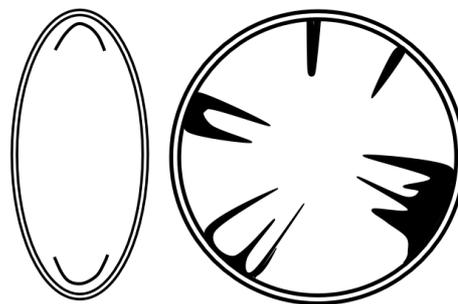
Figure 1.2 *Cortical cataract*

- *nuclear cataracts* – characteristically affect the lens nucleus often creating a myopic shift and cause a brown colouration known as brunescence (Millodot, 2002a).
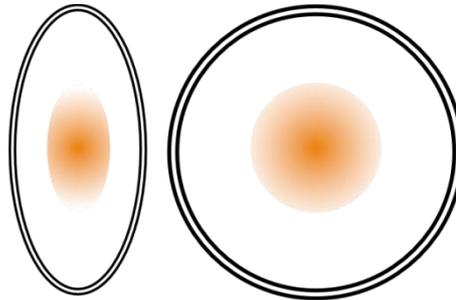
Figure 1.3 *Nuclear sclerotic cataract*

As well as reducing the overall light transmission through the lens cataracts can affect vision through refractive changes or by increasing ocular light scatter (Straylight). Light scatter does not always affect high contrast measurements of visual acuity and thus measurement of contrast sensitivity (Chylack *et al.,* 1993b) and Straylight (Michael *et al.,* 2009) can provide greater insight into the visual effects of the cataracts.

1.3 Cataract Surgery

The earliest forms of cataract surgery can be traced back to ancient civilisation where a procedure known as couching was used. This involved manually dislocating the lens into the vitreous allowing bright but blurred vision along the visual axis. Couching is still practiced in parts of the developing world where cataract surgery in its modern form is not accessible (Bamashmus, 2010). Couching can be traced back to 800BC and was the preferred method of treatment for over 2000 years. However, endophthalmitis, retinal detachment and uveitis were significant problems associated with this technique.

During the 1960s and 1970s most cataract operations were performed using the intracapsular cataract extraction (ICCE) technique. This surgery involves extracting the entire crystalline lens and capsule through a large incision using a cryoprobe (Kanski & Packard, 1985), leaving the patient either aphakic or with an anterior chamber IOL implanted. Using ICCE has a number of advantages: it avoids the possibility of capsular opacification, is relatively easy to perform without the use of an operating microscope and allows a clear view of the fundus (Absolon, 1991).

The extracapsular cataract extraction (ECCE) technique involves the extraction of the crystalline lens through an excision made in the anterior lens capsule. It leaves the posterior capsule intact allowing placement of a posterior IOL (Peckar, 1991). The capsule acts as a barrier between the anterior and posterior segments, reducing the risk of vitreous complications, retinal detachment and cystoid macular oedema. The rapid rise in popularity of the ECCE technique through the 1980s was a consequence of these reduced risks and new techniques and instruments were developed concurrently (Werner *et al.,* 2009):

- the surgical microscope was introduced
- stable posterior chamber IOLs were developed
- phacoemulsification, hydrodissection, and continuous curvilinear capsulorrhexis became established

Phacoemulsification was introduced by Charles Kelman. This technique uses an ultrasonic probe to emulsify the crystalline lens allowing it to be aspirated through an irrigation-aspiration system (Kelman, 1967). Phacoemulsification has evolved and now cataract surgery can be preformed through micro incisions sub-2 mm reducing disruption to the corneal shape, speeding wound recovery, and improving visual outcomes (Hoffman *et al.,* 2005). Furthermore small incision cataract surgery reduces the need for suturing and as a consequence the clear cornea has increased in popularity as an incision site.

1.4 Intraocular Lens Design

Sir Harold Ridley implanted the first IOL, *Transpex 1* (Rayner, Hove, UK), at St Thomas' Hospital on the 29th November 1949. This was a polymethylmethacrylate (PMMA) spherical IOL, 8.35mm in diameter, 2.40mm thick with a refractive power of 24.00D (Ridley, 1952). Ridley implanted around one thousand of his lenses, however, around 15% required extraction due to post-operative complications.

Ridley had concentrated on the posterior chamber as a viable site for IOL implantation, however, the IOL suffered from a high frequency of dislocation. Subsequently the anterior chamber was targeted as an alternative site. On May 13th 1952 the first anterior chamber IOL was implanted following crystalline lens extraction. The *Baron*

was designed to fixate within the anterior chamber angle (Baron, 1953), but the steep front-surface curvature resulted in a high rate of corneal decompensation, bullous keratopathy and endothelial atrophy (Jaffe, 1998).

To overcome these limitations several iris supported IOLs were subsequently developed to overcome the problem of IOL dislocation (found with posterior chamber IOLs) and corneal decomposition (found with anterior chamber IOLs). Blinkhorst and Epstein were the main pioneers of this technology. Epstein developed the Collar stud and the Maltese-Cross IOL in 1953 and incorporated haptics allowing lens fixation to the anterior and posterior section of the iris. Subsequently the *Blinkhorst Iris clip IOL* was developed in 1957 and implanted on August 11th 1958 (Jaffe, 1998). The design of the IOL and haptics were frequently adjusted to keep the IOL in place and the use of myotics, to aid fixation, became common. In February 1969, Worst began to suture the lens onto the iris, this led to the development of the Medallion lens: this IOL incorporated two holes to assist suturing (Blinkhorst, 1975). Even if fixated, this lens was not devoid of problems and a high frequency of iris deformation and atrophy occurred alongside the problem of corneal decomposition (Werner *et al.,* 2009).

The use of haptics to attain IOL stability was also incorporated in anterior chamber IOL designs and consequently a second generation of haptics were developed using PMMA and polypropylene. These allowed a more stable platform for the IOLs, and with the correct sizing and smoothing of the IOL haptics, a more precise fit to the anterior chamber could be achieved (Hoffer, 2009). Closed loop haptics had a high frequency of erosion, uveitis and secondary glaucoma, especially if the lens was too large. Open loop, one-piece haptics with smooth edges provided the best long-term results; the flexibility of the open loop meant that correct sizing of the IOL was not as critical (Werner *et al.,* 2009).

The vulnerability of the anterior angle structure advocated a return for the implantation of IOLs in the posterior chamber. The benefits of open loop haptics for IOL centration were established and the progression of the ECCE technique promised a more stable capsular bag for implantation. John Pierce implanted the first of the new generation of posterior chamber IOLs in 1975. Two of the haptics were in the posterior chamber and the third was secured to the iris. In 1977 the J-Loop haptic posterior chamber IOL was introduced, followed by the C-loop haptic (Werner *et al.,* 2009; Hoffer *et al.,* 2009).

The development of posterior chamber IOL technology coincided with the development of the ECCE technique – strongly advocated by Blinkhorst (Jaffe, 1998). This enabled surgeons to perform cataract surgery through a small incision and to successfully implant an IOL within a stable capsular bag. Ophthalmic viscoelastic devices were later introduced to assist placement of the IOL, aid maintenance of intraocular pressure, and protect the corneal endothelium.

Foldable silicone, hydrogel and acrylic posterior chamber IOLs have been developed some of which can be implanted through sub 2 mm incisions, reducing post-operative recovery time.

These IOLs were all of a spherical design. The power of the early lenses was fixed resulting in a high rate of post-operative residual error. Advancements in ocular biometry and IOL power formulae have allowed accurate determination of IOL power to reduce levels of post-operative residual error.

1.5   Intraocular Power Calculations with Ocular Biometry

IOL power calculation relies on the accurate measurement of ocular biometry (Norrby, 2008). Ultrasound and partial coherence interferometry (PCI) (using the *IOLMaster;* Carl Zeiss Meditec AG, Jena, Germany) are the most popular methods for measuring axial length. The *IOLMaster* was introduced in 2001 and since has become the technique of choice – by 2002 the *IOLMaster* was used in over a third of hospital eye units in the UK (Gale *et al.,* 2004). The popularity of the *IOLMaster* is attributable to its non-contact nature, superior resolution, and independence of examiner ability (Hill *et al.,* 2008). The *IOLMaster* thus improved the refractive outcome results of cataract surgery (Eleftheriadis, 2003; Rose and Moshegov, 2003).

The largest source of error with current IOL power predictions is error occurring whilst estimating the post-operative lens position (Norrby, 2008). The SRK/T (Retzlaff *et al.,* 1990), Hoffer Q (Hoffer, 1993) and Holladay 1 (Holladay *et al.,* 1988) use axial length (AL) and corneal power to determine the required IOL power; post-operative IOL position is assumed. The Haigis formulae (Haigis, 2004) predict post-operative IOL position using AL, anterior chamber depth (ACD) and corneal curvature. The Holladay 2 formulae incorporate multiple parameters in its estimation: AL, corneal power,

subject age, pre-operative refractive error, corneal diameter, ACD and lens thickness (LT) (Hoffer, 2000). However, the *IOLMaster* does not measure LT and ACD is not assessed using PCI. Ultrasound can measure both parameters but is limited by the resolution of the system (Butcher and O'Brien, 1991; Raj *et al.*, 1998).

New ocular biometry devices (such as the *LenStar LS900*; Haag-Streit, Koeniz, Switzerland) have been developed which measure a wide range of parameters with techniques similar to PCI. The validity of these systems needs to be assessed to evaluate their potential in reducing postoperative refractive error.

As the accuracy of IOL power calculations has improved, the use of IOLs for the correction of refractive error has increased. IOL optic technology has advanced to correct higher order aberrations, astigmatism and presbyopia. The increasing prevalence of elective clear lens extractions with IOL implantation highlights the advance of cataract surgery as a method of refractive surgery.

1.6   Aspherical Intraocular Lenses

Higher-order aberrations result in a reduction of visual acuity (VA) and contrast sensitivity (CS). The average human cornea induces positive spherical aberration (SA) into the eye's optical system. In the youthful eye, the crystalline lens compensates for this; however, with age the balance is lost as the crystalline lens starts to induce its own positive SA (Atchison, 1991; Glasser & Campbell, 1999).

Spherical IOLs induce their own positive SA, compounding rather than reducing the positive SA of the cornea (Kohnen *et al.*, 2009). To compensate for this, two forms of aspherical IOLs were introduced: aberration-control aspherical IOLs and aberration-neutral aspherical IOLs.

1.6.1   Aberration-Control Aspherical Intraocular Lenses

Aberration-control aspherical IOLs induce negative SA to compensate for the positive SA of the cornea. Reducing overall levels of SA can result in improved CS and VA (Kohnen *et al.*, 2009). These aberration-control lenses correct a specific amount of SA despite levels of corneal aberration being variable (Beiko, 2007). In a proportion of patients, with atypical levels of corneal SA, the negative SA of the IOL may not be

beneficial. Aberration-control aspherical IOLs are dependent on the centration of the IOL in relation to the visual axis. If an aspherical IOL is decentred by more than 0.5mm, its ability to reduce SA is lost; additionally, if decentration is coupled with tilt, the effects are compounded (Eppig *et al.,* 2009).

Modern IOLs are centrationally stable; this has increased the popularity of aspherical IOLs. However, in the presence of small pupils, the advantages of aspherical lenses may be lost providing no advantage over spherical IOLs.

1.6.2 Aberration-Neutral Aspherical Intraocular Lenses

Aberration-neutral aspherical IOLs do not introduce aberration into the eye, nor do they compensate for the positive SA of the cornea. These IOLs are minimally affected by centration when compared with aberration-control aspherical IOLs (Eppig *et al.,* 2009). Aberration-neutral aspherical IOLs show superior results compared with monofocal IOLs (Caporossi *et al.,* 2007).

To achieve optimum visual results, SA needs to be effectively and predictably controlled. Ideally, corneal SA would be measured pre-operatively and a lens selected in accordance with the measured aberration (Packer *et al.,* 2009).

1.7 Multifocal Intraocular Lenses

Multifocal IOLs (MIOLs) are popular for the surgical correction of presbyopia because their mechanism of action is independent of ciliary body function. MIOLs provide high levels of spectacle independence (Packer *et al.,* 2010) and currently are the most reliable lens for attaining both distance and near vision. MIOLs create at least two focal points within the eye, corresponding to different working distances. Several mechanisms can be employed to create the simultaneous focal points. It is important to consider an MIOL's method of action as each lens has its own unique optical properties. The design of the lens affects the light distribution, the number of focal points, the distance of their separation, and ultimately the quality of the images. MIOLs can be divided into diffractive and refractive designs. Refractive designs can be subdivided into concentric and sectorial, while diffractive designs can be categorised as fully diffractive or partially diffractive.

1.7.1 Concentric Refractive Multifocal Intraocular Lenses

1.7.1.1 Two-zone (button) Refractive Multifocal Intraocular Lenses

John Pearce implanted the first MIOL in June 1986. The *Kratz-Johnson/ Nuvue* MIOL (Precision Cosmet/IOLAB/Bausch & Lomb, Rochester, NY.) is a two-zone (button) PMMA refractive MIOL. It has a 7 mm optic and incorporates a 2 mm central optical element with an additional +4.00 D of refractive power.

The *Progress 3 Domilens* (Domilens/ Bausch & Lomb, Rochester, NY.) is a two-zone refractive multifocal IOL. The optic is 6.5 mm in diameter with a central 4.7 mm area that progresses from a mid point +5.00 D addition to a peripheral distance zone.

Both two-zone button MIOLs are pupil size dependent. Reduced pupil size increases the relative proportion of the near segment within the pupil zone; this increases the distribution of light in favour of the near zone. With the *Kratz-Johnson/Nuvue* a pupil less than 2 mm, if fully centred over the IOL, will result in a 100% distribution of light to the near focal point (Atebara and Millar, 1990). A 4 mm pupil − provided that the IOL is centred − results in 75% of light focused for distance and 25% for near (Percival, 1992). These designs of MIOLs are sensitive to decentration − malposition of the IOL can reduce the proportion of the near segment present within the pupil margin (Percival, 1992).

A good level of near visual acuity and spectacle independence has been found with both types of two-zone refractive MIOLs (Keates *et al.,* 1987; Fu and Yong, 1990; Bleckmann *et al.,* 1996). However, the IOLs can compromise distance vision in comparison to other MIOL types (Percival and Setty, 1991), and contrast sensitivity, in bright light conditions, is reduced (Bonnet *et al.,* 1991; Ravalico *et al.,* 1998)
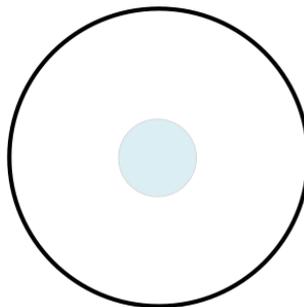
Figure 1.4 *Optic of a two zone (button) refractive multifocal intraocular lens*

1.7.1.2   Multiple Zone Concentric Refractive Multifocal Intraocular Lenses

Multi-zone concentric refractive MIOLs have several concentric zones that differ in curvature, creating two or more refractive powers.

The *Pharmacia Annular* (Pharmacia, Montreal, Canada), *Hoya SFX MV1* (Hoya, Tokyo, Japan)*, True Vista* (Storz/ Bausch and Lomb, Rochester, NY.) and *U370M* (Ioptex/ Bausch and Lomb, Rochester, NY.) MIOLs are three-zone concentric MIOLs with a central and peripheral distance zone and middle near zone. The middle-near zone is +4.00 D for the *Pharmacia Annular, True Vista* and *Norton U370* and +2.25 for the *Hoya SFX MV1* at the IOL plane. The *Nordan U370* has an aspheric transition between the zones facilitating intermediate vision.

Studies examining the effectiveness of these lenses are sparse. Optical bench tests have demonstrated an increase in depth of focus, but a potential decrease in contrast sensitivity with the *Pharmacia Annular* (Holladay *et al.,* 1990). Spectacle independence and near vision were superior with the *True Vista* and *U370M* when compared with a monofocal. However, compromises in contrast sensitivity were found and reports of dysphotopsia were common (Shoji and Shimizu, 1996; Shoji and Shimizu, 2002; Leyland *et al.,* 2002).

Only one clinical study has been published examining the *Hoya SFX MV1.* This study compared the MIOL with a monofocal lens, finding an extended range of focus and comparable contrast sensitivity levels. The study also reported 73% of the subjects experienced mild to severe dysphotopsia (Hayashi *et al.,* 2009).

The *Array* (Abbott Medical Optics, Inc., Santa Ana, CA, USA), *ReZoom* (Abbott Medical Optics, Inc., Santa Ana, CA, USA)*,* and *MFlex* (Rayner Intraocular Lenses Ltd, Hove, UK.) are all five-zone concentric refractive multifocal IOLs; the central distance zone is surrounded by alternating near and distance zones. The *Array* and *ReZoom* are similar in design: both have a near addition equivalent to +3.50 D at the IOL plane (approximately +2.60 D at the spectacle plane). The posterior surface of the *Array* optic is spherical, however, the *ReZoom* incorporates an aberration reducing aspheric posterior surface optic. The *MFlex* multifocal is available with either a +3.00 D or a +4.00 D addition and with four or five refractive zones depending on the base power of the IOL. The preliminary results of the *MFlex* are promising (Aslam *et al.,*

2009), but further evaluation is necessary before conclusions can be derived. The *MF-4* is a four-zone concentric refractive multifocal IOL with a centre near zone surrounded by alternating distance and near zones.

When compared with the two- and three-zone MIOLs, the five-zone MIOLs are less dependent on pupil size and are also minimally affected by decentration. However, the refractive zones in all refractive MIOLs are relatively large and so are still pupil-dependent. Centre-distance designs ensure the preservation of distance vision even with the smallest of pupils (Kawamorita *et al.,* 2009). The *MF-4* is a centre-near design; studies are needed to examine the effects of small pupils on the visual outcomes with this IOL.

There are few studies that have evaluated the *MF-4*. Pérez and colleagues (2003) reported that visual acuities with the *MF-4* were inferior when compared with a diffractive MIOL with an equivalent addition. Optical bench studies were unable to determine the disparity between the IOLs as they both produce equivalent image formations (Gobbi *et al.,* 2007). Rau and Bach (2003) noted a relatively high level of spectacle independence with the *MF-4*, but a prevalence of dysphotopsia of 45%.

The *Array* and *ReZoom* five-zone refractive MIOLs have been extensively evaluated in both *in vivo* and *in vitro* studies. Such studies have reported reduced contrast sensitivity in lower lighting conditions and lower spatial frequencies with the five-zone refractive MIOLs (Montés-Micó *et al.,* 2004; Cillino *et al.,* 2008) whilst the prevalence of dysphotopsia is higher than with a monofocal IOL (Pieh *et al.,* 2001; Häring *et al.,* 2001; Cillino *et al.,* 2008). In regards to near vision (Cillino *et al.,* 2008), spectacle dependence (Fujimoto *et al.,* 2010) and reading ability (Harman *et al.,* 2008) the five-zone refractive MIOLs are superior in comparison with a monofocal IOL.
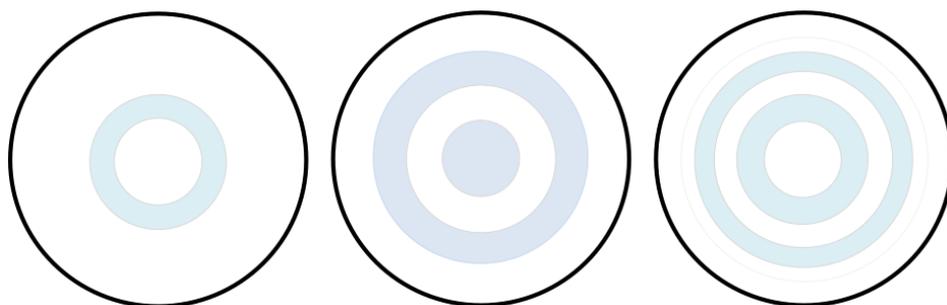
Figure 1.5 *Optics of a three, four, and five zone refractive multifocal intraocular lens*

1.7.2 Sectorial (Rotationally Asymmetrical) Refractive Multifocal Intraocular Lenses

Sectorial refractive MIOLs have the reading addition in a specific section of the lens. These lenses have the external appearance of a bifocal spectacle lens, but their mechanism of action, like all MIOLs, is simultaneous rather than translating vision.

The *Nordan* (Ioptex/ Bausch and Lomb, Rochester, NY.) MIOL has a straight edge top on the near segment (like a D-segment bifocal) and has an aspheric progression of power from the distance portion of the lens to a maximum +5.00 D addition in the inferior portion of the segment. An optical bench study on these lenses demonstrated an increased depth of focus at the expense of a lower contrast image. No *in vivo* studies have been published with this IOL.

The *Lentis MPlus* (Oculentis/ Topcon Europe, Capelle a/d IJssel, The Netherlands) has the appearance of a C-type bifocal spectacle lens; the near segment covers 100° of the inferior IOL and has a small in-cove for distance vision. The near portion of the IOL has an addition 3.00D over the distance portion of the IOL (Figure 1.4). The manufacturers of this lens recommend placing the IOL with the near segment inferiorly. No studies have yet been conducted to evaluate this IOL.
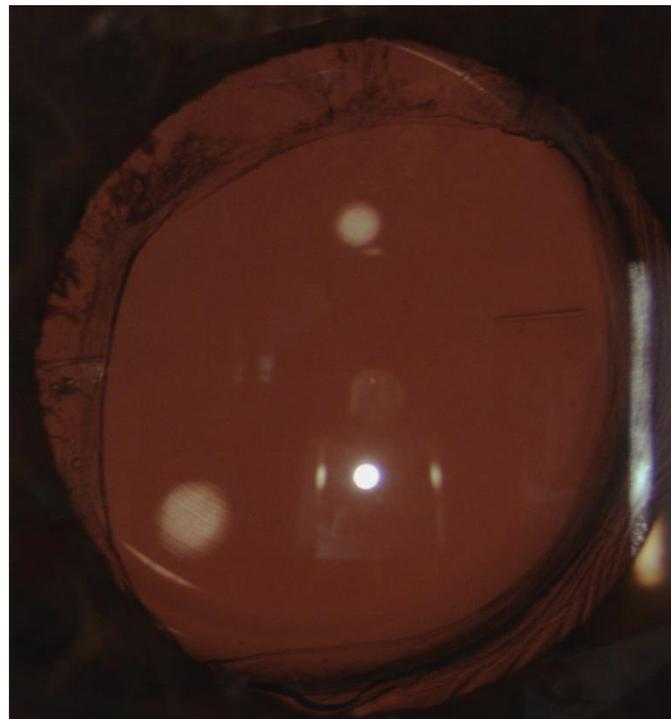
Figure 1.6 *Lentis MPlus*

Sectorial multifocal IOLs are dependent on IOL centration. The amount of light dedicated to distance or near is dependent on the proportion of the near segment occupying the pupil. The refractive power of the *Nordan* multifocal increases towards the periphery of the segment and is thus dependent on pupil size and centration. A sectorial MIOL requires the central radius points of the distance and near portions of the IOL to run along the same optical path, therefore negating image jump (Nordan, 1991).
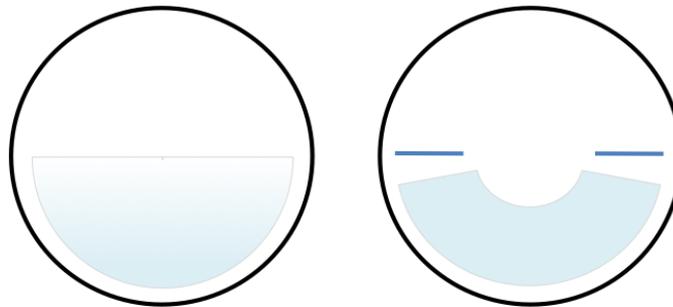
Figure 1.7 Optic of the Nordan and Lentis MPlus sectorial refractive multifocal intraocular lenses

1.7.3 Diffractive Multifocal Intraocular Lenses

Diffractive MIOLs use the principal of diffraction to create two or more focal points. A diffractive pattern is created by light diffracted by a boundary; this creates an interference pattern and results in multiple orders of light. The separation between these orders of light determines the IOL addition. The distance between the ring edges determines the order separation and thus the effective addition. However, not all of the light is distributed to the desired light orders and some is spread diffusely to the higher orders. In the case of a +4.00 D diffractive MIOL, designed to separate the light equally between two orders, 18% of the light is lost to higher orders (Hütz *et al.,* 2006).

Chromatic aberration occurs as a consequence of both refraction and diffraction, however, the spread of light into different colours occurs in the opposite direction to the spread through refraction (Miller, 1991).

1.7.3.1 Fully Diffractive Multifocal Intraocular lenses

With fully diffractive MIOLs, the concentric rings cover the entire optic of the IOL. These lenses are therefore pupil-independent and the split of light is maintained regardless of pupil size (Valle *et al.,* 2005).

The first fully diffractive MIOL was the *3M* (3M Vision Care, St Paul, USA) MIOL; this PMMA MIOL has an equal split between the two focal points, separated by +3.50 D at the IOL plane. The posterior surface hosts the diffractive pattern and the anterior surface is spherical. The *Morcher 53* (Morcher GmbH, Stuttgart, Germany) MIOL is similar in design to the *3M*.

The *CeeOn* (Pharmacia, Groningen, The Netherlands) MIOL is a PMMA, fully diffractive MIOL that has a diffractive pattern on the posterior lens surface and a spherical refractive surface on the anterior surface. The effective addition of the IOL is +4.00 D at the IOL plane; this IOL also has an equal split of light towards the distance and near focal points.

The *Tecnis ZM900* (Abbott Medical Optics, Inc., Santa Ana, CA, USA) has a silicone fully diffractive multifocal optic with the diffractive pattern on the posterior surface and an aspheric anterior surface. It has an equivalent addition of +4.00D at the IOL plane with the same light distribution as the *CeeOn*. There is also an acrylic version of the IOL, the *Tecnis ZA900*.
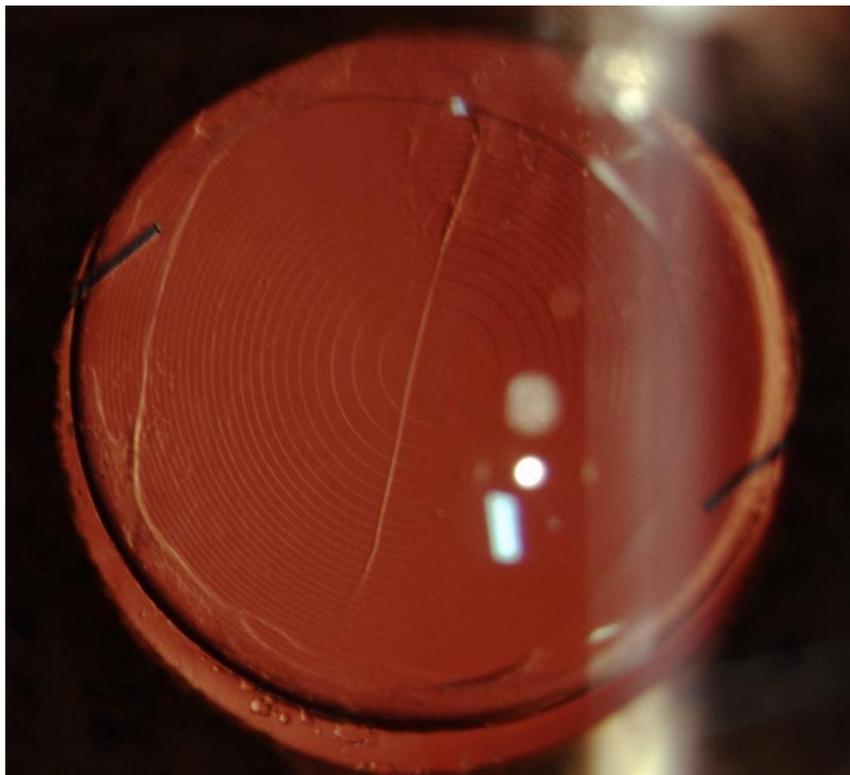
***Figure 1.8** Tecnis ZM900 fully diffractive multifocal intraocular lens*

Equal split fully concentric MIOLs offer a high level of near acuity and spectacle independence in comparison with a monofocal IOL and refractive concentric MIOL (Cilliano *et al.,* 2008; Packer *et al.,* 2010). The literature is equivocal in regards to the quality of intermediate vision with the equally split fully concentric MIOLs: defocus curve profiles (Schmidinger *et al.,* 2006), and optical bench tests (Terwee *et al.,* 2008) have demonstrated a reduction in intermediate vision whilst studies measuring VA at an intermediate distance have not corroborated these findings (Packer *et al.,* 2010).

Jacobi and Eisenmann (1993) proposed the principal of the asymmetrical distribution of diffractive power. This principal was incorporated into the *Acry.Twin* IOL system (Acri.Tec/ Carl Zeiss Meditec AG, Jena, Germany); two fully diffractive MIOLs with a +4.00D addition have asymmetrical light distributions. The Acry.Twin 737D is a distance dominant IOL with 70% light distribution to distance and 30% for near. The Acry.Twin 733D is the near dominant IOL with the opposite light distribution.

Distance VA is superior with the distance dominant lens, the reverse is true for near VA. Binocularly the vision is summated providing relatively good distance and near vision (Jacobi *et al.,* 1999). Optical bench studies (Gobbi *et al.,* 2007) and clinical studies (Alió *et al.,* 2004) have highlighted the presence of dysphotopsia. Moreover on assessment of distance contrast acuity via optical bench testing, contrast acuity has been found to be improved with the distance dominant MIOL when compared to the near dominant twin lens and an equal split fully diffractive MIOL (Gobbi *et al.,* 2007). Clinical studies have found comparable binocular contrast sensitivity values with the *Acri.Twin* MIOL and monofocal IOL system (Alfonso *et al.,* 2007)

The *Acri.Lisa* (Acri.Tec/ Carl Zeiss Meditec AG, Jena, Germany) MIOL is often described as a refractive/diffractive hybrid MIOL. The anterior surface of the IOL has a diffractive ring pattern, however, the ring edges are smooth rather than defined boundaries (these are described as phase zones). Each phase zone is curved and provides refractive power for distance vision matching the zero order light from diffraction. The *Acri.Lisa* has an effective +3.75 D addition at the IOL plane and has a 2:3 light distribution for the distance and near focal points.

Several clinical studies have evaluated the visual performance of the *Acri.Lisa* MIOL and found good distance and near acuities and high levels of contrast sensitivity.

However, no comparative studies between the *Acri.Lisa* and a monofocal IOL have been conducted. In a comparison study between a partially diffractive +3.00 D MIOL similar results were found for measures of VA at different distances and for various levels of defocus (Alfonso *et al.,* 2009).
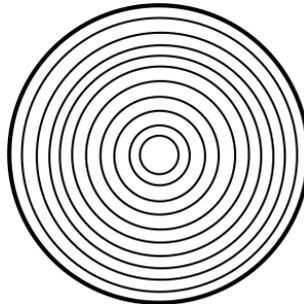
Figure 1.9 *Optic of a fully diffractive multifocal intraocular lens*

1.7.3.2 Partially Diffractive Multifocal Intraocular Lenses

Unlike fully diffractive MIOLs, partially diffractive MIOLs only have the diffractive pattern over a specific area of the optic. The *ReSTOR* (Alcon, Fort Worth, Texas) Apodized diffractive multifocal, has a diffractive pattern over the central 3.6mm of the anterior optic surface. The central area of this zone distributes light equally between distance and near vision; this distribution progressively becomes more distance dominant towards the peripheral section of the near zone. Surrounding the diffractive area is a single refractive surface dedicated to distance vision. Therefore the lens is pupil-dependent: the larger the pupil the greater the distribution of light to the distance. The IOL is available with two near additions: +3.00 and +4.00 D at the IOL plane.

The *ReSTOR* has been extensively examined in optical and clinical studies. Near VA and spectacle independence is better in comparison with a monofocal IOL, distance VA is comparable, however, contrast sensitivity with the +4.00 *ReSTOR* is reduced (Vingolo et al., 2007; Hayashi et al., 2009b; Cionni *et al.,* 2009a). Interestingly Hayashi and colleagues (2009c) concluded that the +3.00 version of the MIOL produced similar contrast sensitivity levels in comparison with a monofocal IOL. However, de Vries and colleagues (2010) found no difference in contrast sensitivity between the +4.00 and +3.00 versions of the *ReSTOR*.

A significant limitation of the +4.00 *ReSTOR* MIOL is it's ineffectively at providing intermediate vision (Blaylock *et al.,* 2006; Pepose *et al.,* 2007). This is less of a

problem with the +3.00 D *ReSTOR* MIOL which provides a longer working distance for the patient hence improving intermediate vision (Maxwell *et al.,* 2009).
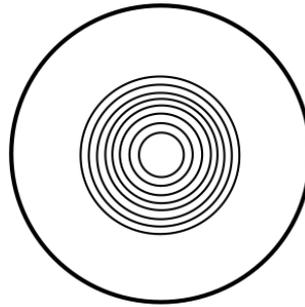
Figure 1.10 *Optic of a partially diffractive multifocal intraocular lens*

1.7.4 Pupil Size and Multifocal Intraocular Lenses

It is vital that pupil size is considered when selecting an MIOL. Pupil dependent MIOLs should not be considered with atypical pupil sizes or decentered pupil positions as their mechanism of action is interrupted. Excessively small pupil size is a contraindication to MIOL use; the splitting of light is discouraged when light propagation through the pupil is already low (Artigas *et al.,* 2007). A reduced pupil aperture results in natural increased depth of focus, so these subjects attain near vision regardless of the type of IOL (Atchison *et al.,* 1997).

1.7.5 Mixing and Matching Multifocal Intraocular Lenses

Mixing and matching refers to the implantation of two different MIOLs in contralateral eyes (Gunenc and Celik, 2008). The primary objective of mixing and matching is to extend the patient's range of clear vision (Maxwell *et al.,* 2009) whilst preserving stereopsis (Chen *et al*., 2009). There have been cases where subjects have compared vision between eyes and thus reported dissatisfaction with the unequal vision (Osher, 2009).

The binocular results of mixing and matching MIOLs have not been compared with binocular results from subjects implanted binocularly with symmetrical MIOLs. This approach requires further study to derive the viability of this type of implantation.

1.7.6 Complications of Multifocal Intraocular Lens Implantation

All MIOLs create two or more simultaneous focal points within the eye. Therefore, at any one time at least one focal point will not be convergent on the retina. This

defocused image causes a reduction in contrast and a distinctive photopic phenomenon (Dysphotopsia; Packer *et al.,* 2010; Pieh *et al.,* 2001). Many modern MIOLs incorporate an aspheric surface in an attempt to maximise optical quality, thus improving contrast sensitivity (Terwee *et al.,* 2008; Kohnen, 2009). Dysphotopsia, often described as haloes, are a common complaint with multifocal implantation, but can reduce over time as adaption to the phenomenon occurs (Dick, 2005).

Halometers have been developed to measure dysphotopsia however, the use of these instruments with MIOLs is infrequent and the results are ambiguous.

1.8 Accommodating Intraocular Lenses

1.8.1 The Mechanism of Accommodation

Accommodation is the eye's ability to change its refractive power, altering its focal length. The ability to focus over a range of distances is essential in humans although this facility to accommodate reduces with increasing age (Duane, 1922) The mechanism of accommodative action has been widely researched and is the focus of much debate (Charman, 2008).

Kepler proposed the first recorded theory of accommodation in 1611. The mechanism of action proposed by the theory is similar to the mechanism of action of a single optic accommodating IOL. With accommodative effort the crystalline lens would shift along the axial plane changing the eyes accommodative power (cited by Gilmartin, 1986).

The observations of Young in 1801 were instrumental in developing an understanding of the accommodative process. He eliminated the possibility of the cornea facilitating accommodating by observing the effect of accommodation on the first Purkinje image and by examining accommodation whilst immersing his eye in water. He proposed that a change in the eyes axial length would influence the transverse diameter and when this change was not observed deduced that accommodation was facilitated by changes in the crystalline lens shape (cited by Atchison & Charman, 2010).

The theory developed by Helmholtz (Helmholtz, 1855) is the most widely accepted model for the accommodative mechanism. It proposes that in the absence of accommodative innervation, the ciliary muscle is relaxed therefore the diameter of the

ciliary body collar is at a maximum. The resulting action is an increase in zonular fibre tension and a decrease in posterior and anterior crystalline lens curvature. Conversely, during accommodation, ciliary muscle contraction reduces the collar diameter and reduces the tension on the zonules. The lens is then free to assume its natural more spherical shape (cited by Glasser, 2006).

In contrast to Helmholtz theory, Tscherning proposed that on contraction of the ciliary muscle, the zonules would increase in tension. This action flattened the peripheral lens and increased the central thickness and curvature (Vilupuru *et al.,* 2004). Tscherning also suggested that an increase in vitreal pressure with accommodation was also responsible for changing the shape of the crystalline lens (Norn and Jensen, 2004).

Gullstrand (1909) and Fincham (1937) proposed that the elastic lens capsule was a vital component in the accommodative process. According to this theory the crystalline lens is flattened in its non-accommodative natural form. With accommodation the zonular tension decreases allowing the elastic lens capsule to manipulate the shape of the crystalline lens (cited by Gilmartin, 1986).

The Coleman theory of vitreal pressure proposes that the accommodative process is caused by differential vitreous pressure between the anterior and posterior chambers (Coleman, 1970). Based on this theory, IOLs designed to accommodate have been developed, however, this theory is contradicted by observed accommodation in subjects post vitrectomy, where the pressure differential is disrupted (Fisher, 1983).

An alternative theory proposed by Schachar suggests that with accommodative innovation, the periphery of the lens flattens and the centre of the lens steepens (Schachar *et al.,* 1996). This theory is contradicted by current *in vivo* structural examinations of the crystalline lens (Strenk *et al.,* 1999; Kasthurirangan *et al.,* 2008).

A large amount of recent *in vivo* structural investigations of the eye using ultrasound biomicroscopy (Ludwig *et al.,* 1999; Bacskulin *et al.,* 2000), Scheimpflug imaging (Koretz *et al.,* 2004), optical coherence tomography (Sheppard and Davies, 2010a) and magnetic resonance imaging (Strenk *et al.,* 2006), as well as finite image analysis and ex-vivo studies (Ehrmann *et al.,* 2008; Glasser *et al.,* 2001) support Helmholtz theory of accommodation. With accommodative innervation the ciliary muscle shifts anteriorly as well as inwards transversely (Strenk *et al.,* 2006; Sheppard and Davies,

2010a). This releases the tension on the zonular fibres attached at the anterior and equator allowing the capsule to manipulate the crystalline lens shape. The anterior lens curvature steepens as does the posterior surface (by a lesser amount); this results in a global anterior shift of the crystalline lens mass and increases the dioptric power of the eye (Glasser *et al.,* 2006; Ostrin and Glasser, 2007).

The ability to focus over a range of distances is essential in humans although this facility to accommodate reduces with increasing age (Duane, 1922) and in fact by the age of 50-55 years the capacity to accommodate is lost (Anderson *et al.,* 2008); this phenomenon is known as presbyopia. The actual cause for this loss of this mechanism is still unclear and is the focus of much debate however several factors appear to play a role in the onset of presbyopia.

Animal studies, involving Rhesus monkeys, demonstrate changes to the posterior attachment of the ciliary muscle (Tamm *et al.,* 1991), it is believed that these changes result in a reduction of ciliary motility and a eventual termination of anterior movement (Croft *et al.,* 2009). The aging human ciliary muscle undergoes a loss of muscle fibre, a reduction of ciliary muscle length, and a thickening of the anterior ciliary muscle mass. Despite these structural changes, the contractile force of the ciliary body appears to be maintained in presbyopia (Sheppard and Davies, 2010b). Structural changes of the zonule/capsular insertion are also believed to have a possible detrimental effect on accommodative ability (Farnsworth and Shyne, 1979). However, the loss of accommodative effort appears to be mainly the result of structural changes to the crystalline lens rather than changes with the ciliary muscle and zonules (Strenk *et al.,* 2005; Glasser, 2008).

The majority of current commercially available accommodative IOLs are based upon a theory known as the optic shift principal. This principal was derived from the observation of anterior shift, with accommodative effort, of a loop haptic IOL and later the shift of a silicone plate haptic IOL (Cumming, 2004). The hypothesis states that an IOL, designed to shift forwards with ciliary muscle contraction, could restore accommodation.

1.8.2   Single Optic Accommodative Intraocular Lenses

The first accommodative IOL – a single optic accommodative intraocular lens – was implanted in the UK on March 12th 1991. Single optic accommodative IOLs are based upon the optic shift principal and are designed to translate anteriorly with accommodative effort. The anterior movement increases the effective lens power at the spectacle plane, however, this resultant power is dependent on the base power: the higher the base power the more accommodative potential (Equation 1.1; McLeod *et al.,* 2003). Theoretically a maximum of 1.5 D can be achieved with a single optic translating accommodative IOL (Schor, 2009). Posterior Capsular Opacification (PCO) is the most frequent consequence of posterior chamber implantation; this occurs due to cell growth over the posterior capsule. A square truncated optic edge provides a barrier against the proliferation of cell growth over the posterior capsule and so modern IOLs are designed with this barrier in place to reduce the risks of PCO. However, accommodating IOLs are designed to be mobile within the posterior chamber and do not provide an effective barrier against the migration and proliferation of cells, thus resulting in higher levels of PCO (Hancox *et al.,* 2007).

$\Delta Dc \approx (Dm/13)\Delta s$ **Equation 1.1**

Where *ΔDc* is the change in power of the eye
Dm is the dioptric power of the lens
Δs is the change in lens position mm

1.8.2.1   BioComFold 43

The *BioComFold* (Morcher GmbH, Stuttgart, Germany) is a single-piece acrylic accommodative IOL, it has a unique haptic configuration which comprises a circular ring surrounding the optic with a series of angular connections. It was the first commercially available accommodative IOL and comprises of a 5.8 mm optic. The mechanism of action of the *BioComFold* is based upon utilising the compressive force of the ciliary body during accommodation, which compresses the outer ring forcing the optic to shift anteriorly. Legeais and colleagues (1999), using A-scan biomicroscopy, found a significant but small anterior optic displacement (0.73 ± 0.58 mm) with accommodative stimulation using pilocarpine. No studies have examined the level of accommodation achieved with the *BioComFold* or have quantified visual acuity.

1.8.2.2 1CU

The *1CU* (HumanOptics, AG, Erlangen, Germany) lens was designed using a finite element simulation model; it incorporates 4 flexible haptics, which, in principal, vaults the optic anteriorly upon the contraction of the capsular bag. Studies examining the change in anterior chamber depth have found a found a small but significant reduction in anterior chamber depth – hence an anterior displacement of the IOL. Langenbucher and colleagues (2003) found a reduction in anterior chamber depth – after instillation of pilocarpine – of 0.78 ± 0.12 mm and 0.63 ± 0.15 mm when measured using an *IOLMaster* and immersion A-scan. A lower level of anterior shift was measured using the *ACMaster* (Carl Zeiss Meditec AG, Jena, Germany) 0.220 +/- 0.169 mm (Hancox *et al.,* 2006). Wolffsohn and colleagues (2006) objectively measured an average of 0.75 D of accommodation however this reduced over time.

1.8.2.3 Crystalens AT

The *Crystalens AT* (Eyeonics/ Bausch and Lomb, Rochester, NY.) has undergone a variety of redesigns. The current generation of *Crystalens* incorporates an aberration neutral aspheric optic, 5 mm in diameter with hinged haptics. The lens is 12 mm in length and has two polyamide loops: this aids stability within the posterior capsule. The mechanism of action for the *Crystalens* is based upon the Coleman theory of vitreal pressure – a differential in pressure between the posterior and anterior chamber. When compared to the *1CU* Buratto and Meglio (2006) found a relatively large anterior shift of 1.42 ± 0.51 mm with the *Crystalens* and 1.66 ± 0.63 mm with the *1CU* measured using the *IOLMaster* following instillation of pilocarpine.
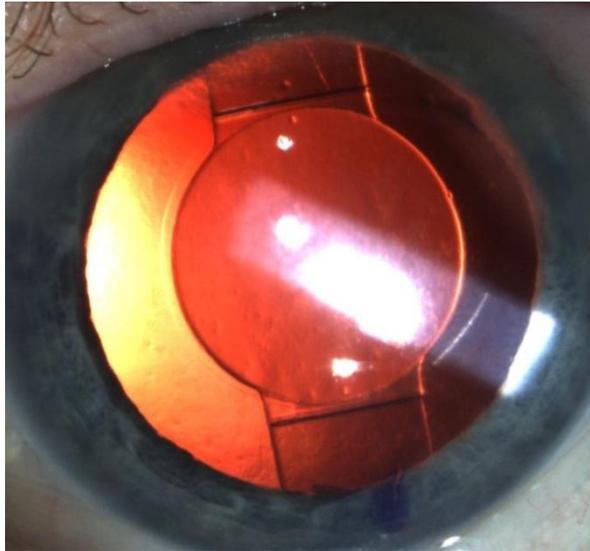
Figure 1.11 *Crystalens AT-AO*

1.8.2.4 Tetraflex

The *Tetraflex* (Lenstec, St Petersburg, Florida, USA) accommodative IOL is a one-piece hydrophilic acrylic accommodative IOL with 5.75 mm optic and closed loop haptics. The flexibility of the IOL allows implantation through a 2.5 mm incision and facilitates accommodation. The *Tetraflex* is designed to vault anteriorly with ciliary muscle compression and with a differential of pressure between the posterior and anterior chamber. In a study of 13 subjects implanted with the *Tetraflex* no anterior movement of the IOL was recorded using an anterior segment Optical Coherence Tomography system, in this study accommodation was stimulated using a proximal target rather than with pilocarpine (Wolffsohn *et al.,* 2010).

1.8.2.5 Opal-A

The *Opal-A* (Bausch and Lomb, Rochester, NY.) focus shift was a prototype single optic accommodative IOL. However, clinical examination revealed no objective accommodation with this IOL (Cleary *et al.,* 2010a).

1.8.3 Dual Optic Accommodative Intraocular Lenses

A dual optic system is designed to fill the capsular bag. These lenses have a high-powered positive anterior optic and negative posterior optic. The lens haptic attaches to both optics keeping the lenses separated. In an unaccommodated state, the capsule holds the lenses close to each other. Accommodation releases the zonules, leaving the

capsule to compress the haptics, thus moving the anterior lens forwards. The anterior lens of a dual optic has a higher power than the optic of the single lens system; this means that these lenses are able to produce higher accommodative power (McLeod *et al.,* 2007). Publications examining the effectiveness of this lens are scarce as this is still a relatively new concept. Ossma and colleagues (2007) measured defocus curves using best-case subjects (best corrected VA at least 20/20) implanted with the Synchrony duel optic lens. To demonstrate the accommodative power of the lens, defocus curves were measured and compared with a matching monofocal group. The Synchrony group maintained an increased range of focus in comparison with the monofocal group and the authors concluded that this provided evidence of the accommodative power of the IOL. However, the results need to be viewed with some scepticism; the gradients of curvature for the negative and positive slopes were similar for both IOLs. If accommodation was present then a shallower gradient of curvature should be present on the negative side.

1.9 Assessment of Presbyopic Correcting Intraocular Lenses

Objective methods for measuring accommodation have been used in subjects implanted with single optic accommodating IOLs, such methods include: photorefraction (Huber *et al.,* 2003), autorefraction (Wolffsohn *et al.,* 2006), aberrometry (Wolffsohn *et al.,* 2010), and the assessment of optic movement (Cleary *et al.,* 2010b). MIOLs do not accommodate; and, as a result, cannot be evaluated using these objective methods.

1.9.1 Defocus Curves

Defocus curves assess VA over a range of optical defocus, thus indirectly assessing VA across a range of distances. However, the technique and subsequent analysis to evaluate defocus curves are inconsistent. Gupta and colleagues (2007a) concluded that the lens sequence and presentation of letters of a LogMAR chart need to be randomised between presentations to reduce the memorisation effect; a recommendation rarely practiced.

The results of defocus curve measurements are commonly expressed as the range of focus levels where a specific visual acuity can be maintained. Gupta and colleagues (2008) proposed a specific level of acuity criteria for the assessment of accommodative

IOLs, with the aim of approximating accommodation. This criterion was adopted in a study assessing the Opal-A accommodative IOL (Cleary *et al.,* 2010). No criteria have been set for the assessment of MIOLs and the methods used to evaluate defocus curves varies between studies (Petermeier and Szurman, 2007; Toto *et al.,* 2007).

1.9.2 Assessment of Reading Ability

Reading speed is a common used test when evaluating low vision attributable to macular disease. This form of assessment has grown in popularity for the assessment of presbyopic correcting IOLs (Sanders, *et al.,* 2009; Packer *et al.,* 2010). However, as with defocus curves, there is no consensus for the methods used to evaluate the results after testing. The common metrics of critical-print size, reading acuity, and maximum reading speed are used, but the methods used to derive these values are rarely stated. Other approaches to the evaluation include the direct comparison of reading speed at each spatial frequency and recording of the spatial frequency at which reading speed is reduced below 80 words per minute. Further studies are required to determine standardised methods for evaluating reading ability with MIOLs and accommodating IOLs.

1.9.3 Subjective Perception of Vision

Subjective quality-of-life questionnaires are useful tools for understanding a subject's perception of their own vision. Questionnaires used to assess vision with presbyopic correcting IOLs are mainly bespoke and few have been validated using either classic test theory or with Rasch analysis (Appendix A3). Questionnaires should be validated on the target group for the questionnaire, however, rarely have the questionnaires been validated with presbyopic correcting IOLs.

1.9.3.1 The VF-14

The VF-14 questionnaire was validated for assessing functional impairment due to cataract. The validity of the questionnaire was examined by performing factor analysis and by correlating the results of the questionnaire with measures of VA (Steinberg *et al.,* 1994). This questionnaire has also been used to assess satisfaction after implantation of spherical (Uusitalo *et al.,* 1999) and multifocal IOLs (Cillino *et al.,* 2008). Although with multifocal subjects, the questions on the VF-14 need to be

modified to refer to vision without spectacles (Brydon *et al.,* 2000). The VF-14 is a questionnaire relating to several aspects of vision and of the 14 original questions, 7 are specific to the assessment of near vision.

Validation of the VF-14 has led to several shortened variations being developed. Numerous shortened 7-item versions of the VF exist, validated either with classic test theory (CTT) (Uusitalo *et al.,* 1999) or with Rasch analysis (Mallinson *et al.,* 2004) on subjects with cataracts.

The 10-item VF-10 was developed for a cataract population and included additional questions not present on the original VF-14 (Velozo *et al.,* 2000).

Other variations of the VF questionnaire include a 12-item version (VF-12), which excludes two questions related to driving, whilst the 9-item (VF-9; Moghimi *et al.,* 2007) and 8-item versions (VF-8R) were recently validated using Rasch analysis in pre- and post-cataract extraction patients (Gothwal *et al.,* 2010).

1.9.3.2 Cataract TyPE Specification

The Cataract TyPE Specification questionnaire is a 13-item questionnaire developed to determine functional vision and quality of life following cataract surgery. It has been validated for this purpose in monofocal and multifocal pseudophakic subjects demonstrating a high Cronbach's alpha and good correlation with visual acuity. Gothwal and colleagues (2009a) validated the questionnaire in subjects with cataracts using Rasch analysis, they reduced the questionnaire to a 12-item questionnaire, which demonstrated good measures of visual function within this group. The questions cover assessment of vision and glare; only 4 of the 13 questions are for the assessment of near vision.

1.9.3.3 The Cataract Symptom Score

The Cataract Symptom Score (CS-5 or CSS) is a 5-item questionnaire that can measure functional impairment due to cataract. It is commonly used to assess the level of impairment caused by the cataract to determine if surgery is necessary. The questionnaire has not been validated for use with presbyopic correcting IOLs but has been used in studies examining MIOLs (Sen *et al.,* 2004). Rasch analysis of this

questionnaire revealed that it was not sensitive enough to discriminate subjects with and without cataracts (Gothwal *et al.,* 2009b). The 5-items are general questions related to the satisfaction of the quality of vision and are not specific to near vision.

1.9.3.4 Catquest

The Catquest questionnaire was designed to evaluate the outcomes of cataract surgery; it is a 19-item questionnaire to be completed pre and post surgery. Repeatability and validity was analyzed for subjects undergoing cataract extraction and monofocal implantation. Subsequently Rasch validation has been conducted using Swedish and Australian populations. An abbreviated 9-item version of the Catquest (Catquest SF-9) was proposed which demonstrated a good fit to the Rasch model (Gothwal *et al.,* 2009c). The 19-item Catquest questionnaire has 9 questions specific to near vision.

1.9.3.5 The Perceived Visual Disability Questionnaire

The Perceived Visual Disability (PVD) questionnaire was designed to determine the effect of cataracts on lifestyle. The questionnaire consisted of 20 items, the results of which were correlated against measures of glare, visual acuity, and contrast sensitivity (Elliott *et al.,* 1990). The questionnaire has not been validated on pseudophakic subjects. Only 4 of the 20 questions relate specifically to near vision.

1.9.3.6 The Activities of Daily Vision Scale

The Activities of Daily Vision Scale (ADVS) is one of the most widely used questionnaires for assessing visual function pre and post cataract surgery. It has also been used to examine visual function as a consequence of glaucoma (Sherwood, 1998) and temporal cell arteritis (Kupersmith *et al.,* 2001. Validation of the instrument has been conducted using factor analysis (Mangione *et al.,* 1992) and Rasch analysis (Pesudovs *et al.,* 2003) on a monofocal IOL population. Furthermore the reliability of the questionnaire was assessed using Cronbach's alpha and retest statistics. Correlating the ADVS scores with vision loss and overall satisfaction assessed construct validity. Of the 22 original items 10 specifically relate to near vision ability.

1.9.3.7 The Visual Disability Assessment Questionnaire

The Visual Disability Assessment (VDA) questionnaire was created to measure visual disability following cataract surgery. Validation of the questionnaire was conducted using factor analysis and by correlating the results of the VDA with results from the ADVS questionnaire. Reliability testing was examined with Cronbach's alpha and with test-retest statistics. The validation was conducted in a pre and post cataract extraction with monofocal IOL implantation and advocated reducing the questionnaire from 37 to 18-items (Pesudovs & Coster, 1998). Of the original 37-items only 5 related specifically to aspects of near vision.

1.9.3.8 National Eye Institute-Refractive error Quality of Life Questionnaire

The National Eye Institute-Refractive Error Quality of Life (NEI-RQL) questionnaire is a 42-item questionnaire designed to determine the effect of refractive correction on quality of life. The questionnaire has been used to assess quality of life in subjects implanted with multifocal IOLs (Blaylock *et al.,* 2008). The validity of this questionnaire has not been examined on pseudophakic subjects although it has been assessed on a phakic population with refractive error (Nichols *et al.,* 2003) and post-laser refractive surgery (Nichols *et al.,* 2005). The NEI-RQL contains 4 questions that relate specifically to near vision, the remaining questions relate to vision throughout daily life.

1.9.3.9 Self-Perceived Quality of Vision Questionnaire

The Self-Perceived Quality of Vision Questionnaire was designed to assess vision post IOL implantation. It contains 17 questions detailing perception of satisfaction, photopic phenomenon and ability to perform visually dependent tasks. The questionnaire was validated for monofocal pseudophakic subjects using CTT and by examination of Cronbach's alpha and repeatability (Aslam *et al.,* 2004). Subsequently, the questionnaire was used to assess subjects implanted with multifocal and single optic accommodative IOLs (Harman *et al.,* 2008). Only 2 of the 17 questions relate to near vision, the remainder relate to the satisfaction with other aspects of vision.

1.9.3.10 Freedom from Glasses Value Scale

The Freedom from Glasses Value Scale (FGVS) was designed to assess the level of spectacle independence post refractive surgery and related benefits. The questionnaire was validated using CTT for use with multifocal IOLs in a study involving 304 subjects implanted bilaterally with an Apodized diffractive MIOL. The questionnaire was validated using Cronbach's alpha, and was correlated with measures of spectacle independence (Lévy *et al.,* 2010). The FGVS relate to the benefits of spectacle dependency rather than questions regarding near vision.

1.9.3.11 The Quality of Vision Questionnaire

The Quality of Vision (QoV) questionnaire was designed to measure the overall subjective perception of vision. It is a 30-item questionnaire; 9 questions are specific to dysphotopsia, 12 enquire about blurred, distorted and hazy vision and 9 are specific to focusing and depth perception. Rasch analysis was used to validate the questionnaire in a study involving 900 subjects (including correction with monofocal, multifocal and accommodative IOLs). The questionnaire is not specific to near vision, with no questions specifically relating to near vision and reading ability (McAlinden *et al.,* 2010).

1.9.3.12 The Near Activity Visual Questionnaire

The Near Activity Visual Questionnaire (NAVQ) was specifically designed to quantify the subjective perception of near visual function with spectacles and contact lenses use or following refractive surgery. The original questionnaire consists of 23 items describing near visual tasks and a further 3 questions regarding spectacle dependence, overall satisfaction, and speed of focus. Each item was assigned five possible responses on a Likert scale and an additional "not applicable" response. A pilot study was conducted to evaluate the NAVQ with subjects implanted either bilaterally or unilaterally with a single optic accommodative IOL. Rasch analysis was used to validate the questionnaire resulting in a reduced 9-item questionnaire that was internally consistent, reliable and valid with a single optic accommodative subject group (Gupta *et al.,* 2007b). However, this questionnaire has not been validated in multifocal and monofocal pseudophakic subjects.

1.9.4   Optical Bench Tests

To achieve high levels of satisfaction it is important that the optical performance of a lens does not limit vision. Optical bench testing is an important element in the design and development of MIOLs. Such testing allows verification of lens quality and provides the means for assessing the quality of the resultant retinal image.

The most common form of optical bench testing involves projecting a known resolution target through a test IOL allowing the focused image to be examined. This allows the assessment of resolution efficiency, which is a measurement of the quality of the image regardless of lens power. Resolution efficiency is expressed as a percentage of quality in comparison to a diffraction limited lens. The results of this optical bench test are dependent on the amount of positive spherical aberration of the model cornea and the negative spherical aberration of the tested IOL. The optimal resolution efficiency occurs when the level of spherical aberration of both the model cornea and IOL match (Tewee et al., 2007). There is currently no consensus on how much spherical aberration is required for the model cornea (Eppig et al., 2008) and hence this disparity has resulted in the ambiguity of results with regards to MIOLs. Gobbi and colleagues (2007) found that MIOLs resulted in reduced resolution efficiency, Christie and colleagues (1991) and Holliday and associates (1990) found comparible results with both monofocal IOLs and MIOLs, whereas the results of Tewee and colleages (2007) and Maxwell and colleagues 2009 were in favor of the MIOLs.

The method of projecting an image through the IOL can also be used to assess the contrast of resultant image by comparing the image maximum and minimum luminance. MIOLs have been shown to reduce the contrast of the image formed with respect to a monofocal IOL (Holloday et al., 1990; Lang et al., 1993; Gobbi et al., 2007). In comparison to monofocal IOLs several studies (Holloday et al., 1990; Lang et al., 1993; Gobbi et al., 2007) have reported MIOLs to demonstrate lower levels of image contrast.

An alternative optical bench test involves assessing and visualising the aberrations through an IOL. An interferometer is used to create an optical path difference (OPD). This creates a three-dimension (3-D) representation of the shape of the resultant wavefront through the optical system. Subsequently this plot can then be used to derive

several analysis functions including the point-spread function, the modulation transfer function and the Strehl Ratio.

The point spread function is a brightness cross section of the image formed from a perfect point source of light. The height and width of the peak of light gives an indication of the quality of image. The division of light from a MIOL results in a lower peak of the point spread function and the formation of two surrounding peaks of a lower intensity. The peak of a fully diffractive MIOL is approximately 58.5% of the intensity of a monofocal IOL, for a five zone refractive MIOL this peak is reduced to approximately 73.4% of the monofocal IOL (Pieh and colleagues 2002). The point spread function can also be used to examine the intensity of the surrounding halos. For the diffractive MIOL the halo was approximately 4.5% of the intensity of the main peak whilst in comparison the intensity of the refractive IOL halo was approximately 3% (Pieh and colleagues 2002).

The modulation transfer function (MTF) provides a plot of image contrast and image detail. And as such both 2d and 3d MTF functions can be depicted. Several studies have found MIOLs to have a negative impact on MTF curves in comparison with monofocal IOLs (Holliday et al., 1990; Christie et al., 1991; Pieh et al., 2002; Artigas et al., 2007).

The Strehl ratio is the area under a 3D MTF plot; it is expressed as the percentage area of a lens in comparison to the percentage area of a diffraction limited lens. The Strehl ratio is reduced in a MIOL in comparison with a monofocal IOL (Holliday et al., 1990; Christie et al., 1991; Pieh et al., 2002; Artigas et al., 2007).

A through focus curve is a plot of contrast as a function of defocus, it is created by recording MTF curves at multiple image planes (related to an equivalent defocus). The output of a through focus curve is similar to that of defocus curves measured in vivo. The through focus curve can be used to estimate position and quality of the resultant focal points (Holliday et al., 1990; Choi, et al., 2008).

Spot diagrams are used to theoretically model the imaging characteristics of a lens. A grid of rays are traced from a single object through the IOL, where they intersect the image plane spots are formed. In an ideal lens system all of the light rays would intersect a single point, abberations and multiple focal points cause rays to deviate

(Chipman, 1991). The technique also allows the theoretical modelling of the effect of tilt and decentration (Turuwhenua, 2005).

1.10 Toric Intraocular Lenses

Levels of corneal astigmatism greater than 1.50 D are prevalent in 19.0 to 22.2 per cent of the population, with astigmatism greater than 3.5 D present in 1.7 to 2.7 per cent (Hoffer, 1980; Ninn-Pedersen *et al.,* 1994; Ferrer-Blasco *et al.,* 2009).

Correcting corneal astigmatism during cataract surgery can increase spectacle independence. For the patient, this has economic benefits (Laurendeau *et al.,* 2009) as well as desirable cosmetic and practical advantages. Spectacle correction of high levels of astigmatism creates meridional magnification, which when coupled with the associated back vertex distance, produces retinal images that are asymmetrically magnified and distorted. Such images have been reported to reduce spatial perception (Guyton, 1977) and adaptation to them is particularly challenging for elderly individuals (Ogle and Madigan, 1945), in whom cataracts are more prevalent. Contrary to this, if corneal astigmatism is corrected at the corneal or IOL plane, then no significant meridional magnification is induced due to a negligible vertex distance (Novis, 2000).

The effect of clear corneal incisions (CCIs) on surgically-induced astigmatism has been extensively examined. If placed along the steep corneal axis, clear corneal incisions flatten the cornea, reducing the residual astigmatism (Khokhar *et al.,* 2006). The larger the clear corneal incision, the greater the flattening effect (Hayashi *et al.,* 1995). Studies have shown that the average surgically induced astigmatism using a 3.0 to 3.2 mm clear corneal incision is ~0.50 D (Vass and Menapace, 1994; Gross and Miller, 1996). The temporal cornea allows easy access for incisions and is the preferred site of many surgeons (Pick *et al.,* 2007); however, incisions performed on the steepest axis result in superior postoperative uncorrected vision (Jiang *et al.,* 2006). Opposite clear corneal incisions require a second clear corneal incision to be placed along the steep axis of the cornea on the opposing side of the pupil and have a greater effect than a single clear corneal incision and can correct more than one dioptre of corneal astigmatism (Ben Simon and Desatnik, 2005; Khokhar *et al.,* 2006). Limbal relaxing incisions (LRIs), otherwise known as peripheral corneal relaxing incisions, can also be used to correct

astigmatism intraoperatively. LRIs require two additional incisions placed in the peripheral cornea along the steepest meridian. To determine the required length of an LRI, a nomogram is required (Gills and Gayton, 1998). LRIs can correct higher levels of astigmatism in comparison to a single clear corneal incision and do not require a second fully penetrating incision, unlike opposite clear corneal incisions (Kaufmann *et al.,* 2005).

Alteration of corneal shape to correct astigmatism using incisions requires a predictable healing response; this is not always possible especially when high levels of astigmatic correction are involved. Toric intraocular lenses are the correction of choice with high levels of astigmatism. They promise a predictable method of astigmatic correction with minimal impact on the cornea (Amesbury and Miller, 2009); however, the effectiveness of a toric IOL is dependent on its orientation. The relationship between misalignment and resultant residual astigmatism is sinusoidal and smaller misalignments have a relatively large effect on correction than large misalignments (Ma and Tseng, 2008; Figure 1.10). If the axis of a toric IOL is misaligned by 30°, no correction of the magnitude of astigmatism occurs; however, there is a shift in the resultant astigmatic axis.

Figure 1.12 The effect of misalignment of a toric intraocular lens on residual astigmatism (Ma and Tseung, 2008)

1.10.1 Toric Intraocular Lens Design

The IOL haptic design is important when trying to prevent postoperative lens rotation. Over time, the capsular bag contracts to enclose and secure the IOL, however, before this contraction occurs there is potential for rotation (Patel *et al.,* 1999). To prevent rotation immediately after implantation, it is important to maximize the friction between the IOL haptic and the capsular bag. A polymethyl methacrylate (PMMA) IOL creates the most friction with the bag, followed by acrylic, with silicon creating the least (Oshika *et al.,* 1998). The smaller the IOL in relation to the size of the capsular bag, the less contact they have with each other, resulting in reduced friction and more risk of rotation (Chang, 2003). If the IOL is too large in relation to the capsular bag, then stretching and distortion of the capsular bag occurs (Lim *et al.,* 1998). Ideally the size of the IOL would be selected in accordance with the size of the capsular bag, however, predicting capsular bag size is difficult. Imaging techniques such as slitlamp biomicroscopy and optical coherence tomography are unsuitable due to the iris pigment blocking light (Wolffsohn and Davies, 2007). The traditional estimation of capsular bag size is the use of the white-to-white diameter (Novis, 2000), however, there are conflicting reports concerning the relationship between the corneal diameter and *in vivo* capsular tension ring derived measures of capsular bag size. Dong and Joo (2001), using a capsular tension ring demonstrated a correlation of capsular bag size with corneal diameter, however, *in vitro* studies have found no such relationship (Khng and Osher 2008). Several studies have found a relationship between axial length and capsular bag diameter (Lim *et al.,* 1998b; Vass *et al.,* 1999; Kim *et al.,* 2008) and a formula using corneal power and axial length has been derived (Vass *et al.,* 1999). These studies measured capsular bag size *in vitro* and also *in vivo* using a capsular tension ring. To develop better understanding of the relationship, direct imaging of the crystalline lens *in vivo* is required. This is possible with the development of Magnetic Resonance imaging (MRI) systems that allow visualization of the crystalline lens despite the presence of the iris, although the resolution is relatively low (Hermans *et al.,* 2009).

1.10.2 Plate Haptic Toric Intraocular Lenses

Plate haptic IOLs (Figure 1.11) demonstrate excellent long-term stability (Patel *et al.,* 1999; Jampaulo *et al.,* 2008). They have no preference in the direction of rotation, they

can be rotated both clockwise and anticlockwise within the capsular bag, this assists lens positioning. In comparison to open loop haptics, plate haptic IOLs are not as susceptible to the effects of compression from the capsular bag (Patel *et al.,* 1999). Positioning holes, present on plate haptic IOLs, allows easier and more precise placement of the IOL during implantation. Lens epithelial cells can migrate through these holes, anchoring the lens in place and improving long-term stability. The larger the holes, the more epithelial material can migrate through them, further improving fixation (Mamalis *et al.,* 1998).
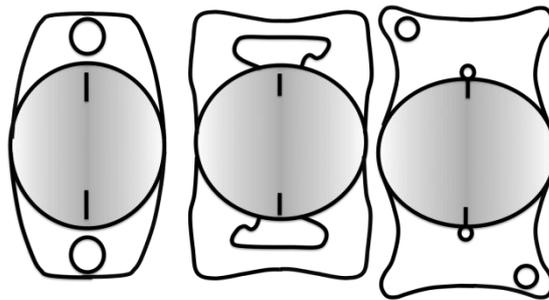
Figure 1.13 Plate haptic toric intraocular lens designs. A. STAAR toric 4304TF, B. Lentis TPlus LU 313-T, C. AT TORBI 709M

1.10.2.1 STAAR 4203TF&TL

The first commercially available toric IOL was the *STAAR 4203TF* (STAAR Surgical Company, California, USA), which achieved FDA approval in 1998. It is a biconvex silicone plate-haptic toric IOL, 10.8 mm in length, with two 1.15 mm positioning holes. The lens is available with a torus of either 2.00 or 3.50 DC, which corrects levels of corneal astigmatism between 1.50 and 3.50 DC. The lens demonstrates excellent long-term stability once fixation within the capsular bag has been established (Jampaulo *et al.,* 2008), however, in the early postoperative period, the lens demonstrates a relatively high incidence of rotation. Sun and colleagues (2000) conducted a study involving more than 100 eyes: 25 percent rotated more than 25°, seven percent more than 40° and nine percent were repositioned. Smaller studies on this lens found similar results. Ruhswurm and associates (2000) found rotation of greater than 5° in 21.6 percent and greater than 40° in 2.7 percent, with 5.2 percent requiring repositioning. Leyland and Colleagues (2001) found that 22 percent rotated more than 10° and 13.6 percent more than 20°, nine percent rotated more than 30° and were repositioned. A longer 11.2 mm version of this toric IOL was later introduced (*AA4203TL*) giving more contact with the capsular bag thus producing more stable results. In the study by Chang, (2003) 28

percent of these longer lenses rotated more than 5°, 10 percent rotated more than 10° and only two percent more than 15°. The *STAAR* toric IOL has also been used in a piggyback formation to correct high astigmatism. In these case studies, the subjects attained uncorrected distance visual acuity of 6/12 or better (Till, 2001; Gills and Van der Karr, 2002; Gills, 2003). The lenses can be sutured together through the positioning holes to reduce the chance of a single lens rotating (Gills, 2003).

1.10.2.2 AT-TORBI 709M

The *AT-TORBI* (Carl Zeiss Meditec, Berlin, Germany) (previously the Acri comfort toric IOL) is an acrylic, bi-toric, plate haptic IOL, 11 mm in length, possessing two positioning holes on the haptic. It is a microincisional lens, which can be inserted through a 1.5 mm incision. The *AT-TORBI* has a 6.0 mm optic, this can correct high levels of astigmatism, as it is available with a torus of 1.00 to 12.00 DC in 0.50 DC steps. Large-scale studies are required to demonstrate the effectiveness of this lens but early results are very promising. In a pilot study involving 21 eyes with 2.00 to 9.00 DC of corneal astigmatism, only one lens rotated more than 5° between day one and six months post-operatively, with 76.1 percent of these subjects achieving a postoperative uncorrected vision of 6/12 or better (Alió *et al.,* 2010).

1.10.2.3 Lentis TPlus LU 313-T

The *Lentis TPlus LU 313-T* (Topcon Europe, Berlin, Germany) is an acrylic, biconvex plate haptic IOL with an anterior toric surface and posterior aspheric surface. It is 11 mm in length with a 6.0 mm optic, it has two large positioning holes and incorporates a 360° square edge. An open c-loop haptic, 12 mm in length, is also available as housing for this optic (*Lentis TPlus LU312-T*). To date, no studies have been published on the rotational stability of these lenses.

1.10.3 Open Loop Haptic Toric Intraocular Lenses

Open loop haptic lenses (Figure 1.12) demonstrate excellent early rotational stability in comparison to plate haptics. The longer loop haptics ensure immediate contact between haptic and capsular bag, maximizing friction in the early post-operative period (Patel *et al.,* 1999; Chang, 2008), however, they are susceptible to late rotation caused by the compression of the capsular bag. Open loop haptics are traditionally inserted with the

haptics emerging from the optic in an anticlockwise direction and under compression the IOL optic is forced to rotate clockwise (provided that sufficient friction is present) (Figure 1.13). With insufficient friction, the loop haptics slip against the capsular bag anti-clockwise (Pärssinen *et al.,* 1998; Patel *et al.,* 1999). Open loop haptics can only be rotated clockwise when in the capsular bag. It is recommended that when positioning these lenses they should be first positioned 10° anticlockwise, with the final position established when the ophthalmic viscoelastic device (OVD) has been removed (Hyon and Yeo, 2010).
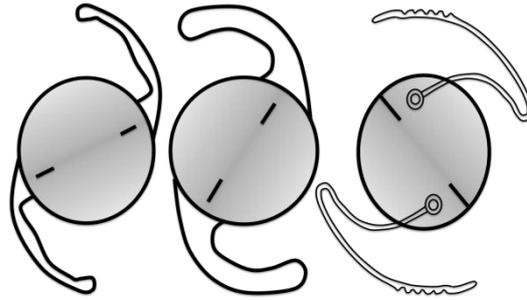
Figure 1.14 *Open Loop haptic toric intraocular lens designs. A Acrysof SN60T, B. Lentis TPlus LU312-T, C. Torica-S*
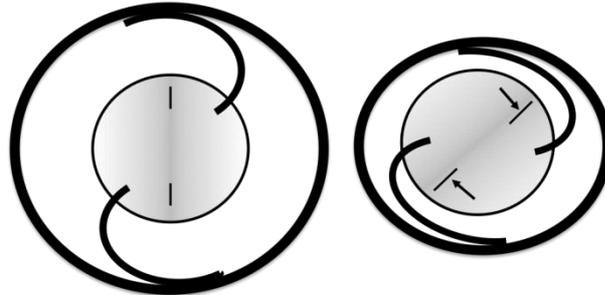
Figure 1.15 *Compression of the capsular bag forces the optic of an open loop haptic to rotate clockwise*

1.10.3.1 *AcrySof SN60T(3, 4, 5)*

The *AcrySof toric IOL* (Alcon, Fort Worth, USA) is a single-piece acrylic toric IOL with open loop L-shaped haptics. It has a posterior toric surface with three available toric powers 1.50, 2.25 and 3.00 DC. It is 13 mm in length with a 6.0 mm optic. The AcrySof toric has shown excellent rotational stability results. During its FDA trial, 81.9 per cent of lenses rotated less than 5°; only 2.9 percent rotated over 10° and only 0.8 percent were repositioned (Holland *et al.,* 2010). Two large studies involving more than 100 eyes have been conducted. Chang (2008) found that 90 percent rotated less than 5° and only one percent rotated more than 10°. A second report of experiences with 263 cases of *AcrySoft toric IOL* implantation proposed a repositioning rate of only 1.1 percent (Chang, 2009). Another study on 111 eyes found that 92.2 percent of lenses rotated less than 5°, 4.5 percent greater than 10°, 1.8 percent rotated more than 20° and two of the IOLs required repositioning (Dardzhikova *et al.,* 2009). The *AcrySof toric IOL* is more effective than opposite CCIs at reducing the level of post-operative residual astigmatism (Mendicute *et al.,* 2009).

1.10.3.2 *Torica-S*

The *Torica S* (Human Optics, Erlangen, Germany) otherwise known as the *Microcyl Toric 6116* (Human Optics), is a three piece, silicon, Z-shaped open loop haptic toric IOL. It is 11.6 mm in length with a 6.0 mm optic. The Torica S has a novel haptic design with undulations designed to increase the friction between lens and bag. It has been reported that these undulations maintain the IOL's position but make it difficult to rotate the lens within the bag (de Silva *et al.,* 2006). To prevent the haptic undulations from causing trauma when rotating the lens, it is recommended that they are compressed against the optic and held away from the capsular bag until the lens is in the required position (de Silva *et al.,* 2006). In a study of 21 eyes (14 subjects) no lens rotated more than 5° (de Silva *et al.,* 2006). In a multicentre study of 68 eyes of 48 subjects, 85 percent of lenses showed rotation of no more than 5° and only 1.5 percent rotated more than 20°. The mean astigmatic error of the 68 eyes reduced from 4.60 ± 2.30 DC to 1.12 ± 0.90 DC (Dick *et al.,* 2006). Several studies have used these lenses for correcting astigmatism after keratoplasty to good effect – the wide choice of toric powers making these lenses a viable solution for correcting the high astigmatism that can result after keratoplasty (Frohn *et al.,* 1999; Tehrani *et al.,* 2003; Buchwald and Lang, 2004; McMullan *et al.,* 2007).

1.10.4 Closed Loop Haptic Toric Intraocular Lens

Closed loop haptics (Figure 1.14) are a relatively new addition to the toric IOL market. These lenses are typically longer than the plate haptics which should give good initial friction. The loops have a second insertion on the IOL that may resist capsular compression. Details regarding the rotational stability of this design are sparse and more research is required to prove their effectiveness.
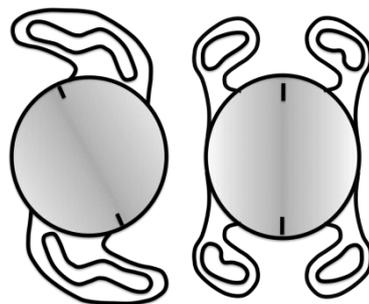
***Figure 1.16** Closed loop haptics. A. T-flex 573T & 623, B Akreos toric intraocular lens*

1.10.4.1 T-flex Toric Intraocular Lenses 573T and 623T

The *T-flex toric* (Rayner, Hove, UK) is a single-piece, acrylic, closed loop haptic with anti-vaulting haptic technology. It is available in two sizes; the *573T* has a 5.75 mm optic and 12 mm haptics, and the *623T* has a 6.25 mm optic and 12.5 mm haptic. The anterior surface of the optic houses the toric surface, which is available with a torus of one to 11 DC. The anti-vaulting haptic technology is designed to reduce the effect of compression using a lock and key system. Compression will push the outside of the haptic against the inner haptic, locking it into place. It has been reported that in a group of 10 subjects no lens rotated more than 5° between one week and two years after implantation (Narendran *et al.,* 2009). In a case report involving a post-keratoplasty aphakic patient, with high levels of astigmatism, the *T-flex* was implanted and successfully trans-sclerally fixated. This reduced the level of astigmatism from 11.00 to 2.00 D (Borkenstein *et al.,* 2009).

1.10.4.2 *Akreos toric IOL*

The *Akreos* (Bausch & Lomb, Rochester, USA) aspheric platform is a single piece acrylic, closed loop haptic IOL. It has a 6.0 mm optic and is 11 mm in length with a 360° square edge. Studies are required to assess the rotational stability of this lens platform and its suitability to house a toric design.

1.10.5 Use Of Toric Intraocular Lenses in Keratoconus and Post-Keratoplasty

Irregular astigmatism creates many challenges for the surgeon. Manual and automated keratometers measure corneal power over the central area; however with irregular astigmatism, the power over the central cornea is not always representative of the peripheral cornea. Videokeratoscopy provides analysis of the corneal power across the peripheral cornea and is a more suitable technique for assessing the true power profile of the cornea (Borkenstein *et al.,* 2009). Studies fitting toric IOLs to patients with irregular astigmatism demonstrate a large reduction in residual astigmatic error and improved visual acuity (Frohn *et al.,* 1999; Tehrani *et al.,* 2003; Buchwald and Lang, 2004; McMullan *et al.,* 2007; Navas and Suárez, 2009; Borderie *et al.,* 1999). Toric IOLs cannot fully correct irregular astigmatism but they can reduce overall levels of residual astigmatism (Kersey *et al.,* 2007).

1.10.6 Intraocular Lens Repositioning

Post-operative ocular trauma can result in IOL rotation. If the trauma results in wound leakage, then the risk of significant rotation is higher (Pereira *et al.,* 2010). The entrapment of the IOL after capsular contraction is complete after approximately two weeks, therefore, in the early period it is important for the patient to avoid excessive movement and the risk of trauma. A post-operative check to assess misalignment should be completed within this two-week period, as repositioning of the lens is vital before fusion between the capsular bag and IOL is complete. For repositioning surgery, reference markers are necessary to aid accurate alignment (Chang, 2009). Formulae have been developed to determine the optimum rotation of a misaligned IOL, this requires the known cylindrical power of the IOL, its current orientation, and the resultant residual astigmatism and axis (Tseng and Ma, 2008). If fusion between bag and IOL is complete, repositioning may not be possible. The resultant cylinder can be corrected via several methods, including spectacles, corneal refractive surgery or by implantation of a second toric IOL. Jin and colleagues (2010) reported on a case where a toric IOL could not be realigned, leaving a residual refraction of +2.25/-5.00 × 45. A second toric IOL was implanted in the sulcus with an obliquely crossed cylindrical axis to the original IOL. The resultant post-operative refraction after the second implantation was +0.84/-1.70 × 47.

1.10.7 Methods of Assessing Rotation

When determining the degree of postoperative rotation, accounting for the difference in eye rotation at each visit is essential. Many factors contribute to this rotation including cyclotorsion, head rotation, Bell's phenomenon and supine position (Werblin *et al.,* 1995). A study by Viestenz and associates (2005) used image analysis of retinal photographs taken over a six-month period to compare rotation of the eye between visits. The average rotation was 2.5° with a maximum rotation of 11.5°. Most studies examining IOL rotation have been subjective, using either a slitlamp eyepiece graticule or slit beam protractor. These methods do not account for head rotation and are accurate to only 5° (Sun et al, 2000; Ruhswurm *et al.,* 2000). With digital imaging more objectivity can be applied to the analysis of rotation. Original studies using image analysis compared the axis of the IOL with the horizontal but did not account for eye rotation (Patel *et al.,* 1999; Nguyen and Miller, 2000; Becker et al., 2004). Weinland

and colleagues (2007) used conjunctival blood vessels as a reference but found that only 17 of 40 eyes could be analysed due to image quality. Shah and co-workers (2009) overlaid a radial axis grid over the centre of the IOL to ascertain the angle of the toric markings to the nearest 0.1°. A line connecting the centre of the IOL with a single episcleral vessel was used to compensate for eye rotation. This method is accurate if the centration of the IOL is constant; errors will occur with the positional movement of the IOL.

1.11 Conclusion

Since the advent of the first intraocular lens significant research has been undertaken to improve the post-operative visual outcomes. Despite the rapid increase of new intraocular lens designs, there has been little change in the way the lenses are evaluated.

Assessment of vision with MIOLs is generally limited to the use of visual acuity charts (often not LogMAR) and non-validated questionnaires. Where defocus curves are used there is no standardisation in the methodology used or the analysis performed on the results. Therefore it is difficult to determine differences between MIOL designs with the current methodologies. Assessment of dysphotopsia is largely reliant on questionnaires or the spontaneous reporting of photopic phenomenon. Claims of reduced dysphotopsia are anecdotal rather than based on scientific evidence and methods to assess this specific problem of dysphotopsia are vital for understanding the phenomenon.

Assessment of reading ability with presbyopic correcting IOLs has undergone a surge due to the introduction of this measure into the recommended ISO standards in IOL evaluation. It is clear from the research into low vision that this is a valuable asset in the assessment of vision; however, there are inconsistencies in the approach taken for analysing the results when used in IOL studies.

Mixing and matching MIOL designs has the theoretical benefit of increasing the range of vision. However, no studies have been conducted which compare bilateral implantation with *mixing and matching* of these MIOLs. Also sectorial refractive MIOLs have not been evaluated *in vivo*.

Toric IOLs are an effective tool for reducing post-operative levels of astigmatism; however, the outcomes are dependent on the orientation of the IOL matching that of the corneal astigmatism. The majority of studies examining the rotational stability of toric IOLs have used subjective methods. Most image analysis studies have not compensated for eye torsion. Those, which compensated for eye torsion, used methodologies vulnerable to lens decentration or blighted by poor image quality. A valid, repeatable method is required for the assessment of lens orientation.

Therefore the aims of the thesis are:

- to develop a new defocus curve metric for the assessment of MIOLs, and to evaluate the range of vision provided by a selection of MIOL designs
- to validate a specific near vision questionnaire for the assessment of presbyopic correcting IOLs
- to assess the reading ability of a range of presbyopic correcting IOLs using a metric correlated with the subjective perspective of near vision
- to validate a new ocular biometry device based upon time domain interferometry
- to develop a valid repeatable method for the assessment of toric IOL rotation
- to assess the rotational and centrational stability of a closed loop haptic IOL
- to establish the orientation of a closed loop haptic IOL in respect to the targeted axis as determined by ocular biometry.

1.12 Supporting Publications

Buckhurst, P.J., Wolffsohn, J.S., Davies, L.N. & Naroo, S.A. (2010). Surgical correction of astigmatism during cataract surgery. *Clin Exp Optom.* **93,** 409-18.

Buckhurst, P.J., Naroo, S.A. & Shah, S. (2010). Advanced Intraocular Lens Designs. *European Ophthalmic Review.* **4,** 82-86.

Chapter 2 Assessment of Multifocal Intraocular Lenses Using Defocus Curves

2.1 Introduction

Multifocal Intraocular lenses (MIOLs) use the principal of simultaneous vision and produce two or more focal points to extend the clear range of vision: The implication of this is that popular objective methods used to assess accommodation *in vivo* (such as dynamic aberrometry (Wolffsohn *et al.,* 2010) and dynamic autorefraction (Wolffsohn *et al.,* 2006; Cleary *et al.,* 2010) are inappropriate as they do not provide information regarding the near performance of these lenses.

Previous *in vivo* studies have examined the visual range of provided by MIOLs using measurements of visual acuity (VA) either at varying distances (Schmidinger *et al.,* 2006; Hayashi *et al.,* 2009c; Maxwell *et al.,* 2009) or through different levels of spectacle lens defocus (Steinert *et al.,* 1992; Cillino *et al.,* 2008; Alfonso *et al.,* 2009b). However, there is variability in what methods are used to assess VA at variable distances; where a LogMAR chart is involved often the distance at which VA is measured is not adjusted according to the standardized logarithmic progression, and thus not appropriate for the chart (Alfonso *et al.,* 2007; Alfonso *et al.,* 2010). Often only a limited range of distances are examined and the randomisation of letters is either restricted or not discussed (Blaylock *et al.,* 2009). An alternative to measuring VA at multiple distances is to measure VA at a set distance under varying levels of spectacle lens defocus. When viewing a distance object (assumed infinity) the vergence of light entering the eye is approximately zero. The light from a near object has a negative vergence at the eye, which drives the accommodation system of the eye to create a more positively powered crystalline lens that is, if the accommodation apparatus is still functional. Negative spectacle lenses optically create this negative vergence of light and thus simulate the desired clear object distance depending on their dioptric power (Equation 2.1; Rabbetts, 2007).

$$F = \frac{-1}{f}$$ **Equation 2.1**

F is the spectacle lens power
f is the image distance in (m)

Measuring VA through a range of spectacle lenses creates a profile of VA over a range of focal demands – equivalent to estimating VA over a range of distances – this profile is known as a defocus curve. Previous studies have shown that VA measured using this method provides an underestimation of the true VA at corresponding distance. This underestimation is due to the minimising effects of concave lenses (although this can be compensated for mathematically; Gupta *et al.,* 2008) and the lack of the near triad response (if measured monocularly; Pieh *et al.,* 2002).

The two focal points created by a MIOL result in a distinctive defocus curve profile with two peaks of acuity (Maxwell *et al.,* 2009). These peaks correspond with the MIOL near- and distance-focal points. The dioptric distance between the peaks is determined by the equivalent addition of the lens at the spectacle plane. The distance between the peaks and the gradient of each peak can be used to evaluate the position and quality of each focal point. (Hansen *et al.,* 1990)

Depth-of-focus refers to the range of optical defocus at the retina that can be tolerated without a reduction in VA. On a defocus curve, a large depth-of-focus would result in the maintenance of VA through a large range of dioptric defocus. It is, therefore, important to consider the factors that can influence the depth-of-focus when performing studies using defocus curves (Atchison *et al.,* 1997).

2.1.1 Pupil Size and Defocus Curves

Pupil size has an effect on depth-of-focus and, therefore, the profile of a defocus curve. A miosed pupil increases the depth-of-focus by acting as a pinhole, reducing the blur circle on the retina (Day, 2009). Interestingly, a large pupil can also increase the depth of focus as more peripheral light rays enter though the large pupil. These rays are refracted by the peripheral cornea, which increases in positive spherical aberration towards the limbus. Positive spherical aberration results in a multifocal effect as peripheral rays are refracted more than central rays, creating a small positive addition (Atchison *et al.,* 1997; Marcos *et al.,* 1999). This effect is limited by a combination of the Stiles Crawford Effect and an increased blur circle (Legge *et al.,* 1987; Atchison *et al.,* 1997; Marcos *et al.,* 1999). Spherical IOLs compound the effect of the spherical aberration of the cornea and can potentially increase the depth-of-focus. However, this has not been demonstrated *in vivo*. Aberration control aspheric IOLs are designed to compensate for the positive spherical aberration of the cornea by inducing negative

spherical aberration (Wang *et al.,* 2010). This has the potential to reduce the overall levels of spherical aberration in the eye thus reducing the depth-of-focus.

The influence of pupil size on MIOLs has been assessed extensively *in vitro* using optical bench tests (Kawamorita and Uozato, 2005; Schwiegerling, 2007; Artigas *et al.,* 2007). *In vivo* defocus curve studies conducted in the early 90s used separate subject groups divided according to their pupil sizes, however group numbers were low and details of randomisation was not stated (Knorz *et al.,* 1993). *In vivo* studies of the effects of pupil size on defocus curves are absent in the current generation of MIOLs.

2.1.2   Other Influences on Depth-of-Focus

Depth-of-focus has been shown to increase with:

- reduced VA (Tucker and Charman, 1975; Legge *et al.,* 1987, Marcos *et al.,* 1999).
- decreasing spatial frequency (Tucker and Charman, 1975; Legge *et al.,* 1987; Marcos *et al.,* 1999).
- decreasing contrast (Atchison *et al.,* 1997).
- decreasing luminance (Tucker and Charman, 1986).
- increased retinal eccentricity (Wang and Ciuffreda, 2004).
- increased age (Green *et al.,* 1980).

Ambiguity surrounds the effect of refractive error on depth-of-focus as it has been proposed that both myopic (Jiang and Morse, 1999) and hypermetropic (Green *et al.,* 1980) eyes have increased depth of focus in comparison with emmetropes.

2.1.3   Defocus Curve Methodology

Standardisation of measurements should ensure comparisons between studies and hence several considerations need examining to ensure accuracy of measurement. Defocus curves measurements in MIOL subjects are performed with a full distance correction in place, ensuring that manifest refraction does not influence defocus curve results. Both LogMAR and Snellen charts are frequently used for measurement of VA, however the LogMAR system has several advantages over the Snellen system. The LogMAR chart expresses VA according to the logarithm of the minimum angle of resolution (MAR). The progression of letter size per line is by 0.1 LogMAR intervals; equating to a ratio of 1.2599. The spacing between each letter is equal to one letter

71

width and the spacing between each line is equal to the height of the previous row with 5 letters on each line (Bailey and Lovie, 1976). Each letter using the LogMAR system contributes to the overall visual acuity and has a value of 0.02 LogMAR, thus allowing sub-line accuracy (Hazel and Elliot, 2002).

Gupta and colleagues (2007) advocated that to increase accuracy and to minimise memorisation effects, both the lenses used and the letters read should be randomised between VA measurements when quantifying defocus curves. This can be easily achieved using a computerised test chart where letters can be randomised. Randomisation of letters has not been used with MIOL assessment and in these studies the order of lenses is either not stated or is in a specific order from high to low power (Table 2.1 and Table 2.2).

The back vertex distance (BVD) of the additional lens should also be stated as this has an influence on the magnification caused by the spectacle lens and the effective power of the lens. The BVD can be used to correct for the magnification effects; this correction has been applied with previous multifocal contact lens studies (Gupta *et al.,* 2009), although it has not been implemented in MIOLs investigations.

2.1.4 Analysing Defocus Curves

Defocus curves in studies of MIOLs have been used to compare the range of vision between different types of IOLs: MIOLs and monofocal IOLs; different MIOL designs; MIOLs and accommodating IOLs; Different accommodating IOLs.

Two methods are currently employed to analyse the defocus curves:

- **Direct comparison method** - this compares the means of each VA for each level of defocus (Table 2.1).
- **Depth-of-focus method** - that compares the depth-of-focus according to specific criteria (Table 2.2).

The direct comparison analysis method provides a detailed breakdown of VA at each level of defocus by comparing the mean VA at each level. It requires at least two IOL types for comparison and is susceptible to type 1 statistical error unless repeated-measure analysis of variance or a correction factor such as Bonferroni is used. A variety of *post hoc* tests have been used ranging from the Tukeys *post hoc* test, which

only provides moderate protection against type 1 error to the Scheffe's *post hoc* test, which offers a high level of protection. However, the majority of studies provide no details regarding the protection against a type 1 error (Table 2.1).

First Author	Subjects and IOL design (Subjects)	Chart type	Defocus range (step size)	Statistical test (details of protection)	Randomization		Results	
					Letters	Lenses	Level of defocus	Visual acuity
Olsen 1990	Diffractive +3.50 D n=19(19) Monofocal n=19(19)	Peli-Robson	-7.00 to +7.00 D (0.50 D)	t-test (no details)	X	X	0.00D	Monofocal group better
							-7.00 to -2.00 D	Diffractive multifocal group better
Percival 1991	Diffractive +3.50 D n=47(47) Refractive +4.00 D n=40(40) Refractive +3.50 D n=24(24)	Snellen	-2.50 to 0.00 D (1.25 D)	Fisher's exact test (no details)	X	X	0.00 D	Refractive +3.50 D better than refractive +4.00 D
							-2.50 D	Refractive +4.00 D better than refractive +3.50 D and diffractive +3.50 D
Percival 1993	Refractive +3.50 D n=25(25) Monofocal n=25(25)	Snellen	0.00 to -2.50 D (1.25 D)	Fisher's exact two tail test (no details)	X	X	-2.50 to -1.25 D	Refractive +3.50 D multifocal better
Hunold 1993	Diffractive +3.50 D n=50(35) Monofocal n=?	Snellen	-5.00 to +5.00 D (1.00 D)	Wilcoxan rank test (no details)	X	X	-4.00 to -1.00 D	Diffractive +3.50 D better than Monofocal
Auffarth 1993	Diffractive +3.50 D n=50(35)	Snellen	-5.00 to +5.00 D (1.00D)	Wilcoxan rank test (no details)	X	X	-5.00 to -2.00 D	Diffractive +3.50 D better than monofocal
Walkow 1997	Diffractive +4.00 D n=40(40) Refractive +3.50 D n=40(40)	Snellen	-5.00 to +5.00 D (0.50 & 1.00 D)	t-test (no details)	X	X	-1.50D	Refractive +3.50 D better than diffractive +4.00 D
							-5.00 to -2.50 D	Diffractive +4.00 D better than diffractive +4.00 D

First Author	Subjects and IOL design (Subjects)	Chart type	Defocus range (step size)	Statistical test (details of protection)	Randomization		Results	
					Letters	Lenses	Level of defocus	Visual acuity
Vaquero-Ruano 1998	Refractive +3.50 D n = 50 Monofocal n = 50 (total 78 subjects)	Snellen	-4.00 to +3.00 D (1.00 D)	t-test (No protection)	X	X	-1.00 to -4.00 D	Refractive +3.50 D better than monofocal
Liekfeld 1998	Diffractive +4.00 D n=26(26) Refractive +3.50 D n=24(24)	Snellen	-5.00 to +5.00 D (0.50 D)	t-test (no details)	X	X	-1.50 D	Refractive +3.50 D better than diffractive +4.00 D
							-3.00 to -4.50 D	Diffractive +4.00 D better than Refractive +3.50 D
Weghaupt 1998	Diffractive +3.50 D n=10(9) Refractive +3.50 D n=13(9)	Snellen	-6.00 to +3.00 D (0.50 D)	t-test (no details)	X	-ve to +ve	-2.00 to -4.00 D	Diffractive +3.50 D better than Refractive +3.50 D
Brydon 2000	Refractive +3.50 D n=15(15) Monofocal n=13(13)	Snellen	0.00 to -2.50 D (1.25 D)	No details	X	X	-2.50 D	Refractive +3.50 D better than monofocal
Toto 2007	Diffractive +4.00 D n=14(14) Apodized Diffractive +4.00 D n=14(14)	LogMAR	-5.00 to +2.00 D (0.50 D)	Mann-Whitney U (bonferroni correction)	X	X	-4.00, -3.50 & -1.00 D	Apodized diffractive +4.00 D better than diffractive +4.00 D
							-3.00 & -2.00 D	Diffractive +4.00 D better than Apodized diffractive +4.00 D

First Author	Subjects and IOL design (Subjects)	Chart type	Defocus range (step size)	Statistical test (details of protection)	Randomization		Results	
					Letters	Lenses	Level of defocus	Visual acuity
Gunenc 2008	Diffractive +4.00 D n=10* Refractive +3.50 D n=10* 'Mix and match' n=10(10) Contralateral eye study*	Snellen	-5.00 to +3.00 D (0.50 D)	Mann Whitney U test (no details)	?	?	-1.50 to -0.50 D	Refractive +3.50 D and 'Mix and match' group better than Diffractive +4.00 D
							-3.50 to -2.50 D	Diffractive +4.00 D and 'Mix and match' group better than Refractive +3.50 D
							-5.00 to -3.50 D	'Mix and Match' group better than Refractive +3.50 D
Cillino 2008	Refractive +3.50 D n=16 2nd Refractive +3.50 D n=15 Diffractive +4.00 D n=16	LogMAR	-5.00 to +2.00 D (1.00 D)	ANOVA (Tukeys post hoc)	X	X	-3.00 D	All multifocal groups better than the monofocal group Diffractive +4.00 D better than both refractive +3.50 D groups
Alfonso 2008	Apodized Diffractive +4.00 D n=22(12) Refractive/ Diffractive +3.75 D n=26(18) Monofocal n=32(16)	LogMAR	-5.00 in +2.00 D (0.50 D)	t-test (no details)	X	+ve to −ve	-1.00 to -3.00 D	Refractive/diffractive +3.75 D better than apodized diffractive +4.00 D
							-3.50 D	Apodized diffractive +4.00 D better than Refractive/diffractive +3.75 D
Alfonso 2009	Apodized Diffractive +4.00 D n=36(18) Refractive/Diffractive +3.75 D n=40(20)	LogMAR	-5.00 to +2.00 D (0.50 D)	t-test (No protection)	X	+ve to −ve		No significant difference between groups

First Author	Subjects and IOL design (Subjects)	Chart type	Defocus range (step size)	Statistical test (details of protection)	Randomization		Results	
					Letters	Lenses	Level of defocus	Visual acuity
Petermeier 2009	Apodized Diffractive n=10(5) 5 eyes amblyopic	Snellen	-5.00 to +3.00 D (0.50 D)	No details	X	X		Defocus curve profiles similar but suppressed in the amblyopic eye
Maxwell 2009	Apodized Diffractive +4.00 D n=282 (141) Apodized Diffractive +3.00 D n=276 (138)	LogMAR	-5.00 to +2.00 D (0.50 D)	ANOVA (bonferroni correction)	X	-ve to +ve & +ve to –ve	-2.00 to -1.00 D	Apodized diffractive +3.00 D better than Apodized diffractive +4.00 D
							-3.00 to	Apodized diffractive +4.00 D better than Apodized diffractive +3.00 D
Alfonso 2010	Apodized Diffractive +4.00 D n=20 (10) Aspheric Apodized Diffractive +4.00 D n= 20 (10) Apodized diffractive +3.00 D n=20 (10) Refractive/ Diffractive +3.75 D n=20 (10)	LogMAR	-5.00 to +2.00 D (0.50 D)	ANOVA (Scheffe test)	X	X	-2.50 to -2.00 D	Apodized diffractive +3.00 D better than all other multifocal groups
							-4.00 to -3.00 D	All other multifocal groups better than Apodized diffractive +3.00 D

Table 2.1 *Table of defocus curve results and methodology using the direct analysis method*

2.1.5 Depth-of-Focus Metrics

Depth-of-focus metrics provide a general overview of the performance of a lens. This is the dioptric range over which the subjects can sustain a specific level of VA. There is no consensus for the level of acuity considered to be the limit for depth-of-focus and often the criteria are not stated, preventing comparison between studies (Table 2.2).

The criteria can be absolute or relative. A relative criterion determines its VA cut-off relative to the best-attained level of VA. Relative criteria have not been used in multifocal studies, but have been used with the assessment of accommodating IOLs (Cleary *et al.,* 2010). A relative criterion of 'best VA + 0.04 LogMAR' was found to best approximate objective accommodation (Gupta *et al.,* 2008). With an absolute criterion the limits of VA are independent of best VA. The limit of 0.3 LogMAR is the most common criterion used with multifocal IOL studies and matches the level of VA defined as the driving standard in Europe (Coeckelbergh *et al.,* 2002).

In eyes with no ability to accommodate, a drop in VA occurs when introducing both positive and negative defocus lenses. Where accommodation is possible the VA can be maintained with the introduction of negative lenses but still drops when introducing positive lenses. The dioptric range over which VA can be maintained with negative lenses is related to the amount of accommodation, but can also be affected by those factors influencing depth of focus. MIOLs work on the principal of simultaneous vision rather than accommodation and consequently the introduction of positive and negative lenses has a detrimental effect on VA outside the depth of focus. However, a relative or absolute depth of focus criterion is difficult to apply to MIOL defocus curves due to the double peaked curve. Theoretically, a criterion designed to approximate objective accommodation should provide equal values for a MIOL and a monofocal IOL. This is assuming that the VA from the second peak does not reach that of the first distance peak. The defocus curve of a MIOL can pass the depth of focus criterion line several times. In all previous studies on using depth of focus criteria, it has not been stated whether the values not meeting the criteria between the max and min values for defocus are included or not (Table 2.2).

First Author	Subjects and IOL design	Chart type	Defocus range (step size)	Randomization		Depth of Focus criteria	Range of focus
				Letters	Lenses		
Hansen 1990	Diffractive +3.50 D n=53(52)	Snellen	-5.00 to +5.00 D (0.50 D)	X	X	'Excellent vision' - not quantified	Diffractive +3.50 D = 4.00 to 5.00 D
Post 1991	Diffractive +3.50D n=16 Monofocal n = 22	Snellen	-6.00 to +6.00 D (0.50 D)	X	X	Absolute 0.3 LogMAR	Diffractive +3.50 D = 3.8 D Monofocal = 1.80 D
Steinert 1992	Refractive +3.50 D n = 32 Monofocal n = 30	Regan chart	-6.00 to +6.00 D (0.25 to 1.00 D)	X	X	Absolute 0.4 LogMAR	Refractive +3.50 D = 4.75 D Monofocal = 2.75 D

Bellucci 1993	Diffractive +3.50 D n = 52 (52 eyes) Monofocal n = 20 (20 eyes)	Snellen
		
		Jaeger (33cm)
			-5.00 to +2.50 D (0.50 D) -2.50 to +4.50 D (0.50 D)	X	X	Distance: Absolute 0.4 LogMAR Near: Absolute J2	Diffractive +3.50 D: Distance = 5.00 D
							                                 Near = 4.25 D
							Monofocal: Distance = 2.75 D
							                                 Near = 1.25 D

First Author	Subjects and IOL design	Chart type	Defocus range (step size)	Randomization		Depth of Focus criteria	Range of focus
				Letters	Lenses		
Knorz 1993	Refractive +4.00 D n = 25 (14 monocular) Diffractive +3.50 D n = 10 Refractive Sectorial n = 9	Snellen 10 ft-c & 1000 ft-c	-5.00 to +1.00 D (0.50 D)	X	X	Absolute 0.4 LogMAR	Monofocal : 10ft-c = 2.00 D 1000ft-c = 2.00 D Refractive +4.00 D: 10ft-c = 3.00 D 1000ft-c = 4.00 D Diffractive +3.50 D: 10ft-c = 4.50 D 1000ft-c = 4.50 D Refractive sectorial: 10ft-c = 3.00 D 1000ft-c = 3.00 D
Jacobi 1995	Refractive +3.50 D n=31(25)	Snellen	-6.00 to +3.00 D (0.25 to 0.50 D)	X	X	Absolute 0.4 LogMAR	Refractive +3.50 D 71±7 years (n=18) = 2.50 D 46±6 years (n=13) = 6.25 D Astigmatism <1.25 D Astigmatism ≥ 1.25 D
Negishi 1996	Refractive +3.50 D n=48(30)	Snellen	-6.00 to +4.00 D (0.25 to 1.00 D)	X	X	Absolute 0.5 logMAR Negative only	Refractive +3.50 D = 4.00 D
Weghaupt 1998	Diffractive +3.50 D n=10(9) Refractive +3.50 D n=13(9)	Snellen	-6.00 to +3.00 D (0.50 D)	X	-ve to positive	Absolute 0.40 LogMAR	Diffractive +3.50 D = 5.00 D Refractive +3.50 D = 4.50 D Including Curve under line
Arens 1999	Refractive +3.50 D n=21 Monofocal n=15	Snellen	-5.00 to +3.00 D (0.50 D)	X	X	Absolute 0.40 LogMAR	Refractive +3.50 D = 4.00 D Monofocal = 2.00 D

First Author	Subjects and IOL design	Chart type (distance)	Defocus range (step size)	Randomization		Depth of Focus criteria	Range of focus
				Letters	Lenses		
Kamlesh 2001	Refractive +5.00 D n =20 Monofocal n = 20	Not stated	-5.00 to +5.00 D (0.50 D)	X	X	Absolute 0.40 LogMAR	Refractive +5.00 D = 3.10 D Monofocal = 1.65 D
Kaushik 2002	Refractive +5.00 D n=20 Monofocal n=20	Not stated	-5.00 to +5.00 D (0.50 D)	X	X	Absolute 0.40 LogMAR	Refractive +5.00 D = 3.00 D Monofocal = 1.60 D
Bi 2004	Refractive +3.50 D n=36(30) monofocal n=40(32)	Snellen	-4.00 to +4.00 D (0.50 D)	X	X	Absolute 0.4 LogMAR	Refractive +3.50 D = 4.50 D Monofocal = 2.00 D
Petermeier 2007	Apodized diffractive +4.00 D n=55(32) Monofocal n=38	LogMAR chart	-5.00 to +3.00 D (0.50 D)	X	X	Absolute 0.4 LogMAR	Apodized diffractive +4.00 D has an additional 3.00 D range of focus over the monofocal IOL
Toto 2007	Diffractive +4.00 D n=14 Apodized diffractive +4.00 D n=14	LogMAR	-5.00 to +2.00 D (0.50 D)	X	X	Absolute 0.3 LogMAR negative range	Diffractive +4.00 D = 4.5 D Apodized diffractive +4.00 D = 4.00 D
Kaymak 2007	Refractive/ Diffractive +3.75 D n=20	LogMAR	-5.00 to +3.00 D (0.50 D)	X	X	Absolute 0.3 LogMAR	Refractive/ Diffractive +3.75 D = 5.50 D

First Author	Subjects and IOL design	Chart type (distance)	Defocus range (step size)	Randomization		Depth of Focus criteria	Range of focus
				Letters	Lenses		
Bi 2008	Apodized diffractive +4.00 D n=20 Monofocal n=18	Not stated	Not stated	?	?	Not stated	Apodized diffractive +4.00 D = 4.87 ± 1.09 D Monofocal = 2.08±0.69 D
Gunenc 2008	Monocular Diffractive +4.00 D n=10 Monocular Refractive +3.50 D n=10 Binocular Mix and match n=10	Snellen	-5.00 to +3.00 D (0.50 D)	?	?	Absolute 0.3 LogMAR	Monocular Diffractive = 5.80 D Monocular refractive = 5.60 D Binocular mix and match = 5.85 D
Harman 2008	Refractive +3.50 D n=24 Single optic accommodating n=21 Monofocal n=19	LogMAR	-5.00 to +3.00 D (0.50 D)	X	X	Absolute 0.3 LogMAR Negative range	Single optic accommodating: 3 mth = 2.24 ± 0.61 D, 18 mth = 2.47 ± 0.80 D Refractive +3.50 D: 3 mth = 2.98 ± 0.91 D, 18 mth = 3.38 ± 1.14 D Monofocal: 3 mth = 1.77 ± 0.53 D, 18 mth = 2.15 ± 0.77 D
Liekfeld 2010	Refractive/ Diffractive toric n=4(4)	LogMAR	-5.00 to +2.00 D (0.50 D)	X	X	Absolute 0.3 LogMAR	Refractive/ Diffractive toric = 5.50 D

First Author	Subjects and IOL design	Chart type (distance)	Defocus range (step size)	Randomization Letters	Lenses	Depth of Focus criteria	Range of focus
Packer 2010	Diffractive +4.00 D n=244(125) Monofocal n=245(123)	LogMAR	-5.00 to 0.00 D (0.50 D)	X	X	Absolute 0.3 LogMAR negative range	Diffractive +4.00 D = 4.00 D Monofocal = 1.50 D

Table 2.2 *Table of defocus curve methodology and results from depth of focus analysis*

Despite the inconsistency in measurement and in data analysis the prior investigations support the theory that VA with a MIOL is superior in comparison to a monofocal IOL over a wider range of negative defocus.

The depth-of-focus method, gives no clear indication of differences between MIOLs. Studies using the direct comparison method, have found a higher second VA peak for a diffractive MIOL in comparison to a refractive MIOL. However, it is unclear if this peak is over a smaller range. It has also been proposed that a lower addition IOL has less of an impact on intermediate VA.

2.1.6 Mesopic Conditions and Defocus Curves

The human visual system is able to adapt to a change in illumination by more than a factor of 10^{11} using a combination of two types of photoreceptors: rods and cones (Stockman and Sharpe, 2006). Scotopic conditions describe the situation where light levels are insufficient to activate the cone photoreceptors, thus vision is achieved solely by the response of the rod photoreceptors. Photopic conditions describe the situation where the rod photoreceptors have been fully saturated and so only the cone photoreceptors can deliver an interpretable signal (Stockman and Sharpe, 2006). A common definition of photopic conditions is a luminance level greater than 10 cdm^2 (Uvijls *et al.,* 2001) and scotopic levels are commonly described as below 0.001 cdm^2.

The most common description for mesopic levels is between 0.001 and 3 cdm^2 (Commission Internationale de l'Eclairage, 1989; He *et al.,* 1997) although alternative levels described in Lux (0.05 to 50 Lux) have also been proposed (Colvard, 2003).

An overview of the methodology used from 1993 to assess mesopic vision in multifocal IOL subjects can be seen in Appendix A2. The most common illumination level used to simulate mesopic conditions is 3 cdm^2, this falls within the Commission Internationale de l'Eclairage recommended range. An adaption time of 5 minutes is also used before measuring vision. European directives on driving recommend that testing vision in twilight conditions requires an adaption time of at least 5 minutes (Uvijls *et al.,* 2001) as mesopic vision can change depending on the adaption time (Stockman and Sharpe, 2006).

Defocus curves have not been assessed in mesopic conditions where the VA at each defocus level is likely to be lower than that in photopic conditions. The mesopic conditions will also result in an increase in pupil size (Yang *et al.,* 2002), thus changing the depth of focus and the IOL optics within the pupil area.

2.2 Study Aim

This was a prospective study designed to assess the range of clear vision provided by numerous MIOL designs by measuring and analysing defocus curves in photopic conditions. Secondary aims were to assess the visual performance of these lenses in mesopic conditions and to examine the relationship between VA through defocus and VA at the corresponding distance.

2.2.1 Subjects

Seventy-five subjects (27 males, 48 females) of mean age 61.2 ± 8.9 years planning to undergo bilateral cataract surgery or electing for bilateral clear lens extraction were recruited from Solihull Hospital (Solihull, U.K.) and the Midland Eye Institute (Solihull U.K.). The principal investigator of the study (PB) recruited all participating subjects. The inclusion criteria for the study were as follows:

- Requiring bilateral cataract surgery or electing for bilateral clear lens extraction
- A likely postoperative best corrected distance visual acuity of at least 0.1 LogMAR
- The absence of any ocular pathology and previous surgery
- Corneal astigmatism less that 1.50 D
- Aged between 40 and 70 years
- Suitable for MIOL implantation
- Willing to have MIOL implantation
- Willing to participate in the study
- Able to achieve reliable partial coherence interferometry results
- Willing to attend an extra post-operative aftercare visit
- Absence of post-operative capsular opacification, corneal refractive surgery, and capsulotomy

The 75 recruited subjects were implanted with five combinations of IOLs. The subjects were strictly divided into one of five groups based on their operation date for their first eye. Each group was assigned a type of IOL:

- The first 15 subjects were bilaterally implanted using mix and match strategy; a *ReZoom* MIOL (Abbott Medical Optics, Inc.) was implanted in the right eye and a *Tecnis ZM900* MIOL (Abbott Medical Optics, Inc.) was implanted in the left.
- The second 15 subjects were implanted bilaterally with the *ReZoom* MIOL.
- The third 15 subjects were implanted bilaterally with the *Tecnis ZM900* MIOL.
- The fourth 15 subjects were implanted bilaterally with the *Lentis Mplus* MIOL (Topcon Europe).
- The remaining 15 subjects were implanted bilaterally with the *Softec 1* monofocal IOL (Lenstec, St Petersburg, Fl, USA).

The implications of MIOL implantation were discussed with each subject by the principal investigator and consultant Ophthalmologist performing the surgery; the final decision to operate was made by the consultant Ophthalmologist.

Pre-operatively an *IOLMaster* (Carl Zeiss Meditec AG) running v5 analysis software and NIDEK *OPD-Scan II* (Optical Path Difference Scanning System II; NIDEK Co Ltd, Gamagori, Japan) Wavefront Aberrometer were used to determine axial length and corneal power. To determine IOL power, the Hoffer Q IOL formula was used for short axial lengths, (<22 mm; College of Ophthalmologists' Guidelines) and the SRK/T was used for all other axial lengths; emmetropia was the target in all cases.

All operations were performed by one of three surgeons using topical or local anaesthetic. A 2.85 mm clear corneal incision (widening to 3.2 mm before the insertion of the IOL) was placed on the steepest corneal axis to reduce residual levels of postoperative astigmatism. Phacoemulsification, aspiration, and irrigation were performed through a 5.5 mm capsulorhexis using the *Millennium phacoemulsification system* (Bausch and Lomb, Rochester, N.Y., USA.). All IOLs were implanted into the capsular bag.

Four subjects were later excluded from the study due to post operative complications: two from the *Lentis Mplus* group (one developed cystoid macular oedema and one

required neodymium-doped yttrium aluminium garnet (Nd:YAG) Laser capsulotomy), one from the bilateral *Tecnis ZM900* group (required post operative laser-assisted *in situ* keratomileusis) and one from the bilateral *Mix and Match* group (underwent post operative Nd:YAG capsulotomy). An additional four subjects were recruited to replace those who were excluded. The final patient demographics are detailed in Table 2.3.

	Bilateral *Softec 1*	**Bilateral** *ReZoom*	**Bilateral** *Tecnis ZM900*	*Mix and Match*	**Bilateral** *Lentis MPlus*
Age Mean±SD (years)	62.1 ± 6.8	62.3 ± 8.4	60.7 ± 11.0	58.5 ± 9.2	62.3 ± 9.0
Gender	3 Male, 12 Female	7 Male, 8 female	4 male, 11 female	7 male, 8 female	7 male, 8 female

***Table 2.3** Subject demographics*

The National Health Service (NHS) Local Research Ethics Committee of Solihull approved this study and informed consent was obtained from each subject. The consequences and details of the study were explained to each patient. The study was conducted in accordance with the tenets of the Declaration of Helsinki.

2.2.2 Methods

All subjects were examined 3-6 months post-operatively by the principal investigator. During this visit the following tests were performed:

2.2.2.1 Full Refraction

A combination of several techniques were used to establish the full refraction: Retinoscopy using the Keeler *Professional Retinoscope* (Keeler Ltd, Windsor, UK) and autorefraction using the *Shin-Nippon NVision-K 5001* (Ajinomoto Trading, Inc., Tokyo, Japan) were performed followed by a full subjective refraction at 6 m using the *Thomson Test Chart 2000* (Thomson Software Solutions, Hatfield, Herts., UK.). The *Shin-Nippon NVision-K 5001* autorefractor (Ajinomoto Trading, Inc., Tokyo, Japan) provides valid and repeatable measures of pseudophakic eye refraction in monofocal and accommodating IOLs (Wolffsohn *et al.,* 2010b). Autorefraction is also a valid starting point with diffractive MIOLs (Bissen-Miyajma *et al.,* 2010); however, with refractive concentric MIOLs, autorefraction results overestimate the levels of spherical myopia present in the eye (Muñoz *et al.,* 2007). The distance focal point was the target with all subjects.

2.2.3 Monocular and Binocular Intermediate (80 cm) and Near (40 cm) Visual Acuity

The Early Treatment of Diabetic Retinopathy Study (ETDRS) Near LogMAR Chart 2000 (Precision VisionTM, La Salle, IL., USA) was used to measure VA for intermediate and near. The *ETDRS* chart is a LogMAR chart and therefore uses the standard logarithmic progression of letter sizes; a factor of 1.259. It is designed for use at 40 cm but can also be used at a distance of 79.8 cm ($40*1.259^3$). Near and intermediate LogMAR VA was calculated using the M notation for letter size and working distance (Holladay 1997; Equation 2.2). As several measurements of near and intermediate vision were required for the study, 4 EDTRS charts were cycled to prevent memorisation of letters.

$$VA(LogMAR) = -\log\left(\frac{D}{M}\right)$$

Equation 2.2

VA = Visual Acuity
D = working distance
M = letter size (M notation)

2.2.4 Monocular Defocus Curves in Photopic Conditions and Binocular Defocus Curves in Photopic and Mesopic Conditions

In total 4 best distance corrected defocus curves were measured per subject. *The Thomson test chart 2000* (Thomson Software Solutions, Hatfield, Herts., UK.), positioned at 6 m, was used to measure the VA with each defocus lens. These were placed in a random order over the range of +1.50 to −5.00 D in 0.50 D steps and the letters on the *Thomson test chart 2000* were randomised between measures. An *Oculus Universal Trial Frame* (Keeler Ltd, Windsor, UK) was used to house the manifest refraction and each additional defocus lens; it was adjusted to ensure a 12 mm Back Vertex Distance. For each measurement of VA subjects were prompted once using the phrase "can you read any more letters on the line below?" according to the methodology described by Gupta and colleagues (2008).

In photopic conditions the defocus curves were measured monocularly and binocularly and in mesopic conditions the defocus curves were measured binocularly. Light levels were strictly controlled to a constant luminance of 120 cdm^2 and illuminance of 100 lux for photopic conditions, for mesopic conditions the luminance was a constant 3 cdm^2

and illuminance 10 lux; the *Minolta LS-110 luminance meter* (Konica Minolta Photo Imaging Inc., Mahwah, NJ, USA) was used to measure luminance. Illumination was measured using a light meter at the position of the subjects' eyes. To achieve 3 cdm^2 the room lights were lowered, the screen brightness was reduced and a neutral density screen filter was placed over the computer monitor. Neutral density filters have been used previously to reduce the brightness of a screen to mesopic levels (Walkey *et al.,* 2006). Each subject was allowed five minutes to adapt to the transition between photopic and mesopic conditions prior to the resumption of measurements.

2.2.5   Subjective Assessment of Near and Intermediate Vision

Each subject was requested to rate their intermediate and near vision on a scale of 0 (completely satisfied) to 5 (completely unsatisfied) by completing a short questionnaire of two questions:

- How satisfied are you with the near visual ability that you have?
- How satisfied are you with the intermediate visual ability that you have?

2.2.6   Measurement of Pupil Size

Monocular pupil size were measured in both photopic and mesopic conditions using a validated portable infrared pupillography device (Murray *et al.,* 1991; Scheffel *et al.,* 2010); the *Pupilscan II infrared pupillometer* (Keeler Ltd, Windsor, UK).

2.3   Statistical Analysis

2.3.1   Assumption of Normality

The one-sample Kolmogrov-Smirnov test was used to determine if results from each measurement followed a normal distribution. Where the data followed a normal distribution parametric analysis was performed, whilst non-parametric statistical analysis were utilised for non-normally distributed data. In all cases, a p value less than 0.05 was considered statistically significant.

2.3.2   Comparison of Eyes

A two-way repeated measures ANOVA was conducted to determine any significant difference between the right and left eyes of symmetrically implanted subjects. The same analysis was conducted to determine if there was a significant difference between

the right eye of the bilaterally implanted *Tecnis ZM900* group and the eye implanted with the *Tecnis ZM900* in the *Mix and Match* group. This was also determined for the right eye of the bilateral *ReZoom* group and the *ReZoom* eye of the *Mix and Match* group.

2.3.3 Correction of Effective Power and Magnification of the Defocus Curves

Any refractive lens placed in front of the eye has a magnifying effect on the retinal image; the level of magnification is dependent on: the vertex distance between eye and lens, the shape of the spectacle lens and its refractive index (Gupta *et al.,* 2008; Equation 2.3). In reduced aperture lenses, the lens thickness is assumed to be zero. This correction was applied to every VA measured in the defocus curve.

$$SM = \frac{1}{\left(1 - \frac{t}{n}F1\right) * \left(1 - dFs\right)}$$ **Equation 2.3**

SM = Spectacle Magnification
t = Lens thickness
n = Refractive index
F1 = Front surface power
d = Back Vertex Distance
Fs = Lens power

The back vertex distance of a lens also influences its effective power at the ocular plane. To determine the actual amount of defocus at the ocular plane a correction needs to be used for each lens in accordance with its back vertex distance (Equation 2.4). This second correction was not applied to the data as conventionally the effective addition of the MIOL is expressed in respect to its power at the spectacle plane rather than at the ocular plane.

$$\text{Ocular Defocus} = \frac{Fs}{\left(1 - dFs\right)}$$ **Equation 2.4**

Fs = Lens power
d = Back Vertex Distance

2.3.4 Curve Fitting

For each photopic monocular and binocular defocus curve a best-fit polynomial regression curve was fitted to the data points using *SigmaPlot 2000* (SPSS Inc.,

Chicago, IL., USA). Each data set was fitted with a 4th, 5th, 6th, 7th, 8th, 9th, 10th 11th and 12th order polynomial. The curve fitting process was limited to 200 iterations for each curve. For each data set the coefficent of determination (r^2) and standard error of estimate was calculated. Increasing the order of the polynomial results in a higher r^2 and decreases the standard error of estimate up until a 9th order polynomial; fitting polynomials of 10th order using *SigmaPlot 2000* displayed more variability in the standard error of estimation as valid curves could not be fitted to all data sets within the iteration limit (Table 2.4).

	r2	Standard Error of Estimate
4th Order	0.8197 ± 0.1404	0.0964 ± 0.0410
5th order	0.8458 ± 0.1317	0.0928 ± 0.0410
6th order	0.9250 ± 0.0652	0.0705 ± 0.0301
7th order	0.9507 ± 0.0444	0.0601 ± 0.0253
8th order	0.9635 ± 0.0371	0.0555 ± 0.0222
9th order	0.9768 ± 0.0243	0.0493 ± 0.0208
10th order	0.9315 ± 0.2166	0.1548 ± 0.4906

Table 2.4 *Coefficient of determination r^2 and standard error of estimate with increasing order of polynomial*

The 9th order polynomial function (Equation 2.5) was used for all further analysis as it was the lowest order polynomial which provided a universal best fit to all data sets.

$$y = a + bx + cx^2 + dx^3 + ex^4 + fx^5 + gx^6 + hx^7 + ix^8 + jx^9 \qquad \textbf{Equation 2.5}$$

2.3.5 Comparison of Defocus Curve Measurement with Physical Visual Acuity Measurement

The polynomial equation was used to predict the VA for a defocus of -1.25 D, corresponding to a distance of 80 cm (Equation 2.6).

$$VA = a + b(-1.25) + c(-1.25)^2 + d(-1.25)^3 + e(-1.25)^4 + f(-1.25)^5 \\ + g(-1.25)^6 + h(-1.25)^7 + i(-1.25)^8 + j(-1.25)^9 \qquad \textbf{Equation 2.6}$$

VA at 40 cm, measured using the near EDTRS chart, was compared with the VA with a defocus lens of –2.50 D using Pearson's product moment correlation (PPMC). The Bland and Altman limits of agreement were used to calculate the difference between the two measures of VA along with the average difference. This analysis was performed with *SPSS v15.0* (SPSS Inc., Chicago, IL., USA). The same tests were used to compare the VA at 80 cm measured using the EDTRS chart with the VA as determined by Equation 2.6.

2.3.6 Calculation of the Subjective Amplitude of Accommodation and Range-of-Focus

The subjective amplitude of accommodation and range of focus were calculated for each subject binocularly and monocularly using the fitted 9th order polynomials. Using Equation 2.5 and the table of corresponding x and y values, produced by *SigmaPlot 2000*, a "trial and error" determination of the range of x when y equals the amplitude of accommodation (AOA) criteria (best VA +0.04 LogMAR) was determined as described by Gupta and colleagues (2008). If the second multifocal peak (corresponding with the near focal point) met the AOA criteria the range of x values meeting the criteria for both focal points were summated.

The absolute criteria of 0.30 LogMAR was used to calculate depth of focus, the Newton-Raphson method (Ypma, 1995) was used to calculate x when $y = 0.3$. The Newton-Raphson method is used to find the roots of a function, by adjusting the polynomial function by 0.3 to find x when $y = 0.3$ (Equation 2.7). The table of corresponding x and y values produced by *Sigmaplot 2000* was used to determine the initial approximation x_0.

$$x_1 = x_0 - \frac{f(x_0)}{f'(x_0)} = x_0 - \frac{(a-0.3)+bx_0+cx_0^2+dx_0^3+ex_0^4+Fx_0^5+gx_0^6+hx_0^7+ix_0^8+jx_0^9}{b+2cx_0+3dx_0^2+4ex_0^3+5Fx_0^4+6gx_0^5+7hx_0^6+8ix_0^7+9jx_0^8}$$

Equation 2.7

The resultant x_1 from Equation 2.7 is a better approximation of x when $y=0.3$ however for increased accuracy this process is repeated by taking the resultant x_1 to be x_n and putting this value through Equation 2.8 until the % error is reduced to 0 (Equation 2.9).

$$x_{n+1} = x_n - \frac{f(x_n)}{f'(x_n)} = x_n - \frac{(a-0.3) + bx_n + cx_n^2 + dx_n^3 + ex_n^4 + fx_n^5 + gx_n^6 + hx_n^7 + ix_n^8 + jx_n^9}{b + 2cx_n + 3dx_n^2 + 4ex_n^3 + 5fx_n^4 + 6gx_n^5 + 7hx_n^6 + 8ix_n^7 + 9jx_n^8}$$

Equation 2.8

$$\%error = \frac{(x_{n+1} - x_n)}{\left(\frac{x_{n+1} + x_n}{2}\right)}$$

Equation 2.9

The Newton-Raphson method was used to determine each intersection of the curve at 0.3 LogMAR. The range of focus was calculated as the dioptric distance over which VA was better than 0.3 LogMAR.

2.3.7 Calculation of Defocus Areas

Defocus curves can be used to subjectively calculate depth-of-focus defined as the dioptric range where a subject can sustain VA according to a specific minimum VA; although there is no consensus on the actual VA criteria that should be used. Some studies have used an absolute criterion where the minimum level of acuity is independent of the subject's maximum VA, others propose a minimum criterion adjusted according to the maximum VA attained by the subject.

Furthermore subjects implanted with a MIOL do not accommodate and therefore these metrics are unsuitable for describing the acuity profiles these lenses generate. Instead the polynomial equations for each curve were integrated so that a new "Area of Defocus" metric (LogMAR*m^{-1}) could be derived. The most common criteria used to define the upper limit for depth-of-focus is 0.3 LogMAR, this corresponds to a VA of 6/12. 6/12 corresponds with the minimum binocular visual acuity required for a group 1 driving licence in the European Union (Coeckelbergh *et al.,* 2002).

The integral of the 9th order polynomial equation was used to calculate the area of defocus (Equation 2.10).

$$\int_{a_1}^{a_0} ax + bx^2 + cx^3 + dx^4 + ex^5 + Fx^6 + gx^7 + hx^8 + ix^9 + jx^{10}$$ **Equation 2.10**

The defocus curves were divided into distance, intermediate and near zones. The near zone was defined as between -2.00 and -4.00 D, corresponding with a 50 to 25 cm

range; commonly referred to as the range of near vision (Millodot, 2002b). The intermediate zone was defined as -2.00 to -0.50 D, from 50 cm (arms length) to 2 m. Beyond this, the distance zone was defined as the distances between -0.50 to +0.50 D. These zones were used to define the limits of integration (Figure 2.1).
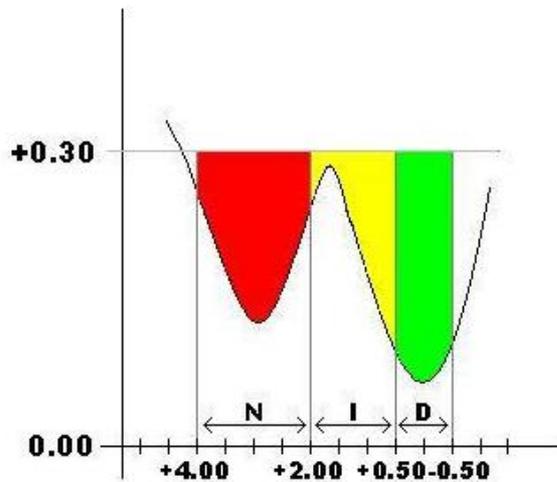
Figure 2.1 *Defocus range divided into near, intermediate and distance zones*

Integration derives the area, bound by the limits, between the function and the *x*-axis. To determine the area of defocus, the area calculated from integration (a) was subtracted from the rectangular area (bound in red) calculated as the distance between the integration limits on the *x*-axis (1&2) and the distance between 0 and 0.3 on the *y*-axis.
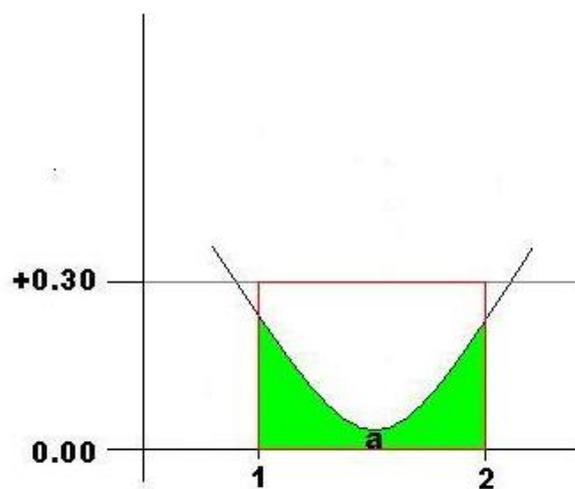
Figure 2.2 *Area of defocus defined as the area between the curve function and upper limit of y=0.3*

Where the function crosses the *x*-axis the area sign becomes negative, therefore when subtracting this value from the rectangular area it increases the area value as desired rather than decreasing the area value.

The upper area limit defined as 0.3 LogMAR bounds the area of defocus. To calculate the *x*-values when *y*=0.3 the Newton-Raphson method was used as described in Section 2.4.4. Where the upper limit was reached before reaching the limits of integration then the x values at the upper limit replaced the limits of integration. (Figure 2.3)
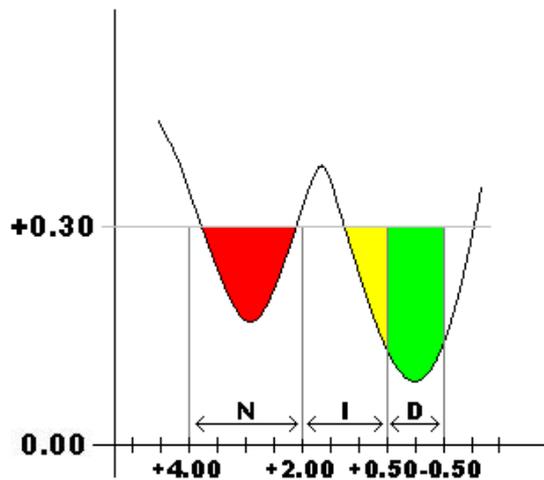
Figure 2.3 *The curve function intersects y=0.3 within the near, intermediate and distance zones. Therefore x when y=0.3 is taken as the new zone limit*

A two-way repeated measures ANOVA was used to determine if there was any statistically significant difference in the areas of defocus between lenses. If a significant difference was found then a one-way ANOVA was used to examine differences for each area. Where significant differences were identified a Bonnferoni *post hoc* test was performed to determine pair-wise differences.

2.3.8 Direct Comparisons of Defocus Curves

A two-way repeated measures ANOVA was used to determine if there was a significant difference in the defocus curves between eyes. The same two-way ANOVA was used to determine if there was an overall difference in the binocular and monocular curves between lens groups. If a difference was found then a one-way ANOVA was applied to the data. The Bonferroni *post hoc* was used to identify the pair-wise differences between the lenses.

Each VA measurement for the mesopic curve was adjusted by the difference in VA at zero defocus. A two-way repeated ANOVA was then applied to the adjusted data to assess if the defocus curve shape profile changed between conditions.

2.3.9 Correlation Between Subjective Ratings of Vision and Measurements of Vision

The subjective rating of intermediate vision was correlated with the intermediate VA at 80 cm measured with the *EDTRS* chart and the intermediate area of defocus using the Spearman's rank correlation co-efficient. The subjective rating of near vision was correlated with the near VA at 40 cm measured with the *EDTRS* chart and near area of defocus using the Spearman's rank correlation co-efficient.

2.4 Results

Ages were similar between groups (F_4=0.370, p=0.829). No significant difference in the right eye pupil size of each group was found in both photopic (F_4=0.267, p=0.898) and mesopic conditions (F_4=0.460, p=0.765). Pupil size increased on average by 1.22±1.02 from photopic to mesopic conditions (Table 2.6).

No significant difference was found between the right and left eyes of those subjects implanted with symmetrical IOLs (*Softec 1*, $F_{1,28}$=0.200, p= 0.658; *ReZoom* $F_{1,28}$ = 0.1726, p=0.681; *Tecnis ZM900*, $F_{1,28}$ = 0.1088, p = 0.744; *Lentis Mplus*, $F_{1,28}$=1.206, p=0.272; Table 2.7 and Table 2.6). No significant difference was found between the right eye of the binocular *Tecnis ZM900* group and the *Tecnis ZM900* eye of the *mix and match* group ($F_{1,28}$=1.310, p=0.204). Similarly no difference was found between the right eye of the binocular *ReZoom* group and the *ReZoom* eye of the *mix and match* group ($F_{1,28}$=1.311, p=0.204; Table 2.9). All further monocular analysis were performed on the right eye of the symmetrically implanted groups.

	Softec 1		ReZoom		Tecnis ZM900		Mix and match		Lentis MPlus	
	R	**L**	**R**	**L**	**R**	**L**	*Tecnis*	*ReZoom*	**R**	**L**
Photopic mean±SD (mm)	4.23 ±0.74	4.27 ±0.78	4.09 ±0.71	4.06 ±0.69	4.16 ±0.62	4.16 ±0.61	4.18 ±0.76	4.19 ±0.77	3.95 ±0.69	3.94 ±0.70
Mesopic mean±SD (mm)	5.65 ±0.78	5.69 ±0.79	5.40 ±0.76	5.35 ±0.73	5.62 ±0.80	5.60 ±0.83	5.48 ±0.76	5.49 ±0.78	5.20 ±0.79	5.19 ±0.79

Table 2.6 *Average pupil size in photopic and mesopic conditions.*

	+1.50	**+1.00**	**+0.50**	**Plano**	**-0.50**	**-1.00**	**-1.50**	**-2.00**	**-2.50**	**-3.00**	**-3.50**	**-4.00**	**-4.50**	**-5.00**
Softec 1 mean±SD (LogMAR)	0.49 ±0.15	0.27 ±0.12	0.08± 0.07	-0.09 ±0.07	0.09± 0.06	0.22 ±0.09	0.36 ±0.11	0.50 ±0.14	0.60 ±0.13	0.67 ±0.14	0.72 ±0.14	0.79 ±0.15	0.86 ±0.13	0.94 ±0.11
ReZoom mean±SD (LogMAR)	0.37 ±0.16	0.22 ±0.16	0.08 ±0.13	-0.02 ±0.09	0.09 ±0.10	0.24 ±0.13	0.35 ±0.13	0.31 ±0.12	0.23 ±0.12	0.21 ±0.12	0.31 ±0.14	0.47 ±0.14	0.58 ±0.16	0.70 ±0.16
Tecnis mean±SD (LogMAR)	0.54 ±0.15	0.36 ±0.13	0.16 ±0.10	0.00 ±0.11	0.13 ±0.09	0.31 ±0.10	0.48 ±0.16	0.41 ±0.14	0.19 ±0.13	0.10 ±0.10	0.17 ±0.10	0.30 ±0.17	0.44 ±0.18	0.58 ±0.16
Lentis Mplus mean±SD (LogMAR)	0.39 ±0.15	0.20 ±0.14	0.06 ±0.10	-0.07 ±0.08	0.04 ±0.08	0.18 ±0.09	0.21 ±0.08	0.14 ±0.12	0.04 ±0.10	0.15 ±0.09	0.24 ±0.11	0.32 ±0.13	0.45 ±0.11	0.55 ±0.11

Table 2.7 *Monocular defocus curve results for the right eyes of subjects implanted symmetrically.*

	+1.50	+1.00	+0.50	Plano	-0.50	-1.00	-1.50	-2.00	-2.50	-3.00	-3.50	-4.00	-4.50	-5.00
Softec 1 mean±SD (LogMAR)	0.46 ±0.12	0.26 ±0.10	0.08± 0.08	-0.03 ±0.06	0.07± 0.06	0.21 ±0.06	0.39 ±0.12	0.51 ±0.10	0.61 ±0.11	0.69 ±0.12	0.76 ±0.12	0.83 ±0.12	0.92 ±0.09	0.99 ±0.10
ReZoom mean±SD (LogMAR)	0.35 ±0.15	0.20 ±0.12	0.09 ±0.12	-0.05 ±0.10	0.05 ±0.10	0.17 ±0.13	0.29 ±0.14	0.30 ±0.13	0.25 ±0.13	0.22 ±0.12	0.36 ±0.11	0.49 ±0.15	0.61 ±0.17	0.74 ±0.19
Tecnis mean±SD (LogMAR)	0.55 ±0.14	0.35 ±0.12	0.15 ±0.10	0.01 ±0.08	0.17 ±0.12	0.35 ±0.17	0.47 ±0.18	0.38 ±0.12	0.21 ±0.12	0.11 ±0.13	0.17 ±0.11	0.28 ±0.13	0.53 ±0.16	0.60 ±0.15
Lentis Mplus mean±SD (LogMAR)	0.44 ±0.16	0.23 ±0.10	0.06 ±0.05	-0.05 ±0.08	0.05 ±0.05	0.18 ±0.07	0.22 ±0.11	0.14 ±0.13	0.10 ±0.15	0.19 ±0.13	0.31 ±0.13	0.44 ±0.15	0.54 ±0.13	0.63 ±0.12

***Table 2.8** Monocular defocus curve results for the left eyes of subjects implanted symmetrically*

	+1.50	+1.00	+0.50	Plano	-0.50	-1.00	-1.50	-2.00	-2.50	-3.00	-3.50	-4.00	-4.50	-5.00
Tecnis **eye** mean±SD (LogMAR)	0.53 ±0.15	0.33 ±0.14	0.11± 0.11	0.00 ±0.12	0.16± 0.08	0.37 ±0.12	0.50 ±0.16	0.35 ±0.07	0.16 ±0.09	0.10 ±0.12	0.21 ±0.11	0.37 ±0.11	0.50 ±0.12	0.64 ±0.14
ReZoom **eye** mean±SD (LogMAR)	0.35 ±0.15	0.20 ±0.12	0.09 ±0.12	-0.05 ±0.10	0.05 ±0.10	0.17 ±0.13	0.29 ±0.14	0.30 ±0.13	0.25 ±0.13	0.22 ±0.12	0.36 ±0.11	0.49 ±0.15	0.61 ±0.17	0.74 ±0.19

***Table 2.9** Monocular results for the mix and match group*

2.4.1 Direct Comparison of Defocus Curves

Comparisons of the monocular defocus curves revealed a significant difference in curve profiles between lens groups ($F_{3,56}$=24.659, p<0.001; Figure 2.4). The monocular *ReZoom* eyes had better VAs in comparison to the monocular *Softec 1* eyes between -2.00 D and -5.00 D. Whilst for the *Tecnis ZM900* eyes this range was between -2.50 and -5.00 D, whereas for the *Lentis MPlus* eyes the range was between -1.50 and -5.00 D. The *ReZoom* group achieved a higher level of VA in comparison with the *Tecnis ZM900* group with a defocus of +1.50, +1.00 and -1.50 D but lower levels of VA between -3.00 and -4.00 D. The *Lentis MPlus* provided better VA in comparison with the ReZoom at -2.00, -2.50 and -5.00 D. In comparison with the *Tecnis ZM900* the *Lentis MPlus* produced better VA between -0.50 and -2.50 D and at +1.00 and 1.50 D.

There was a significant difference in curve profiles between each group binocularly ($F_{4,70}$=24.441, p<0.001; Figure 2.5). The binocular *Tecnis ZM900*, binocular *ReZoom* and *Mix and Match* groups all achieved significantly higher VAs over the range of −2.00 to −5.00 D in comparison with the binocular *Softec 1* group. The bilateral *Lentis Mplus* group had higher VAs in comparison with the *Softec 1* group over the range of −1.50 to −5.00 D. The binocular *ReZoom* performed better at +1.00, -1.00 and −1.50 D in comparison with the binocular *Tecnis ZM900* group but significantly worse from −3.00 to −4.00 D and at −5.00 D. The 'mix and match group showed no significant difference in comparison to the binocular *ReZoom* group and the binocular *Tecnis ZM900* group. The binocular *Lentis Mplus* was significantly better than the binocular *ReZoom* group at −2.00 D, −2.50 D and at −5.00D. It was also significantly superior than the binocular *Tecnis ZM900* group over the range of −0.50 to −2.50 D and in contrast to the *Mix and Match* group, was significantly better at −1.50 D and −2.00 D.
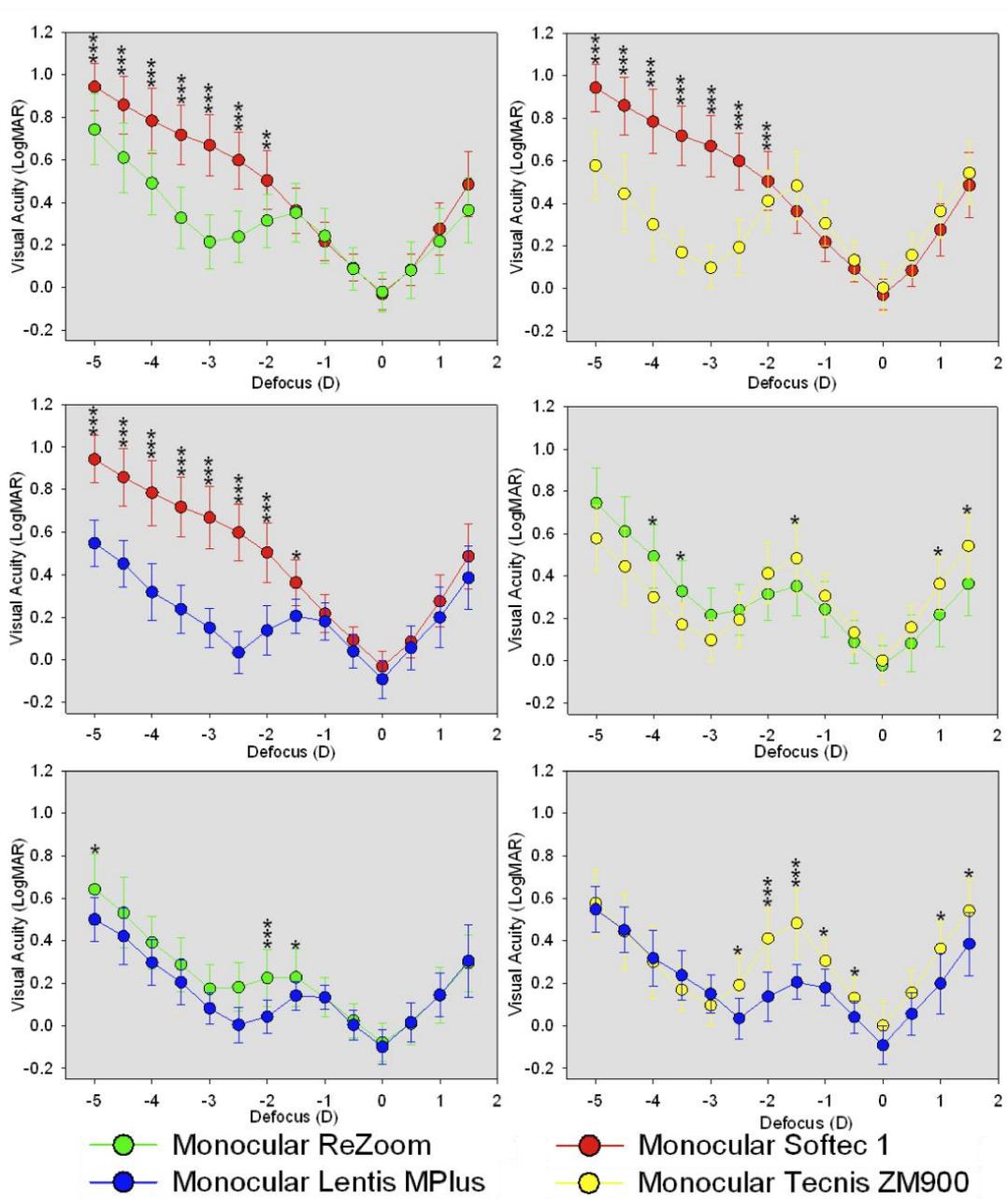
Figure 2.4 *Comparison between monocular defocus curves*

* denotes significance at the p<0.05 level; ** at p<0.01; *** at p<0.001.
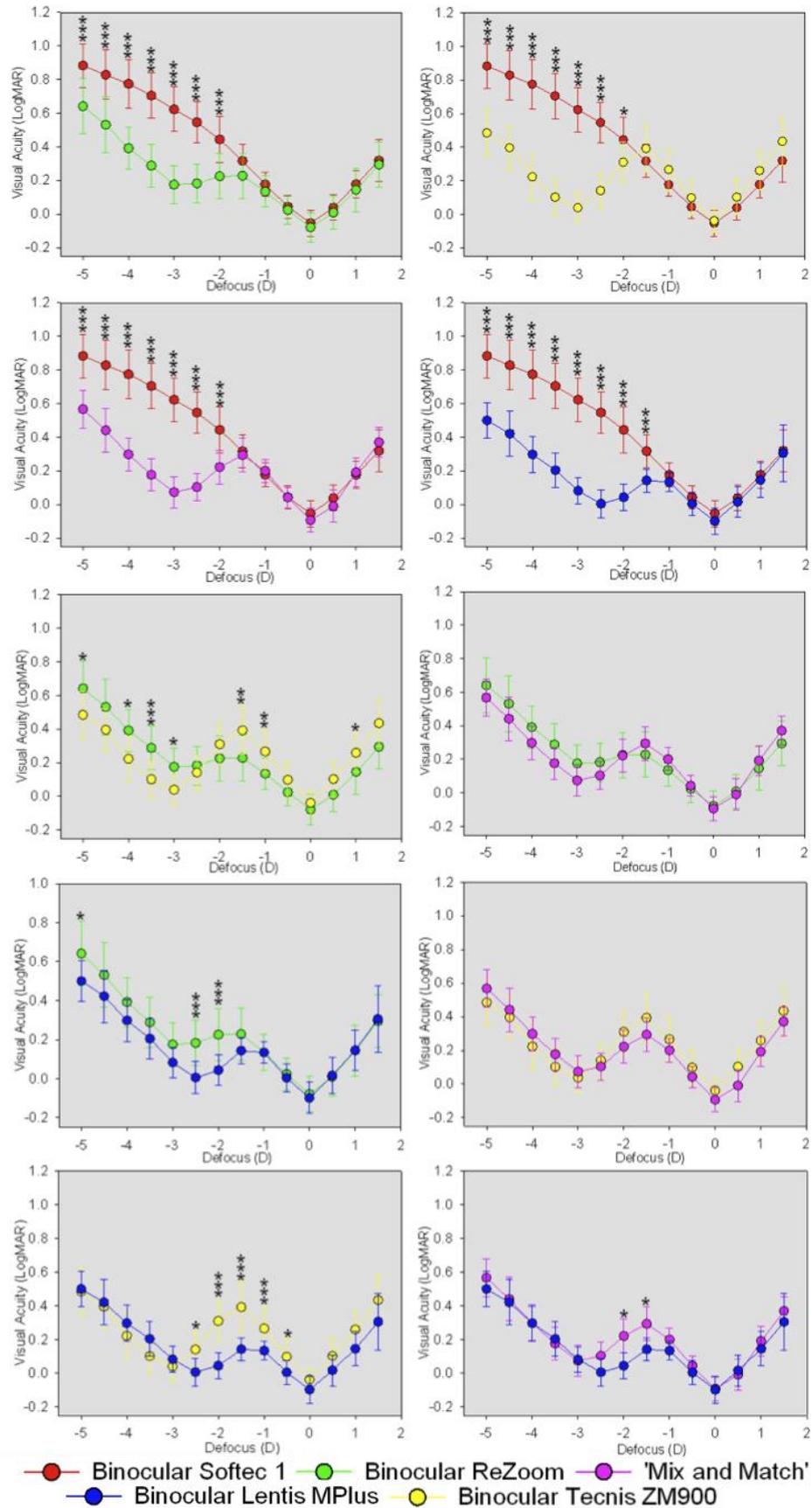
Figure 2.5 *Comparison of binocular defocus curves in photopic conditions*

*** denotes significance at the p<0.01 level; ** at p=0.01; * at p<0.05

There was a significant difference between the photopic and mesopic binocular defocus curves for each of the MIOL groups (*ReZoom*: $F_{1,28}=12.727$, p=0.001; *Tecnis ZM900*: $F_{1,28}=14.399$, p=0.001; *Mix and match*: $F_{1,28}=24.284$, p<0.001; *Lentis Mplus*: $F_{1,28}=18.906$, p=0.001; Figure 2.6).

Each VA measurement for the mesopic curve was adjusted by the difference in VA at zero defocus; this assessed if the defocus curve shape profile changed between conditions. No significant difference was found between the adjusted mesopic defocus curves and photopic defocus curves (*ReZoom*: $F_{1,28}=0.278$, p=0.602; *Tecnis ZM900*: $F_{1,28}=0.0003$, p = 0.986; *Mix and match*: $F_{1,28}=0.384$, p=0.974; *Lentis Mplus*: $F_{1,28}=0.931$, p=0.343).
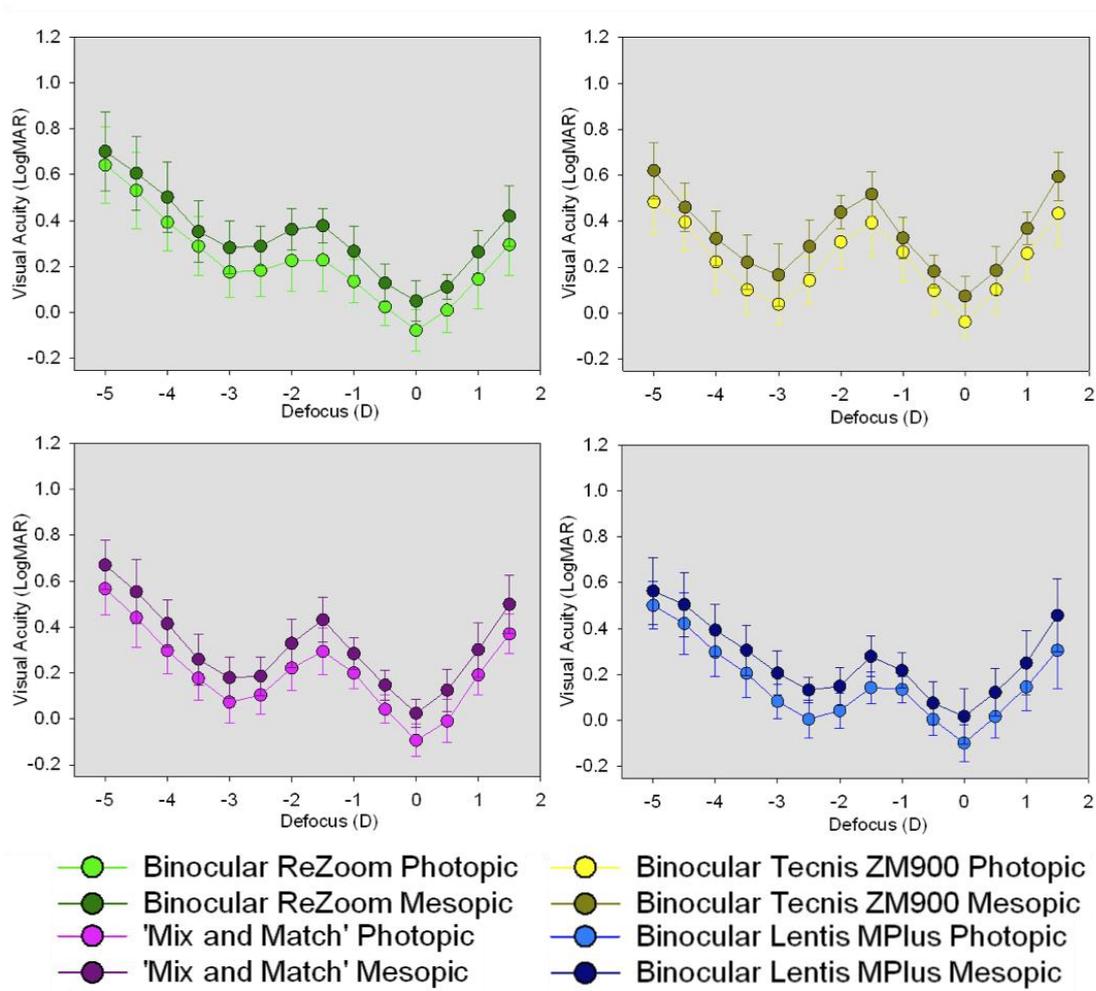
Figure 2.6 *Binocular defocus curves in mesopic and photopic conditions.*

2.4.2 Comparison of Visual Acuities Measured with the *EDTRS* Chart.

Examination of monocular and binocular NVA (40 cm) showed a significant difference between the groups (monocular: $F_3=44.162$, $p<0.001$; binocular: $F_4 = 52.663$, $p<0.001$; Table 2.10 and Table 2.11). All multifocal groups had improved monocular and binocular near VA in comparison with the monofocal groups ($p<0.001$). Near VA was significantly higher with the *Lentis MPlus* group than the *ReZoom* group binocularly ($p=0.002$) and monocularly ($p=0.002$). No other significant differences were found ($p>0.05$).

	Monocular *Softec 1*	**Monocular** *ReZoom*	**Monocular** *Tecnis ZM900*	**Monocular** *Lentis Mplus*
40 cm mean±SD (LogMAR)	+0.63±0.12	+0.34±0.12	+0.24±0.12	+0.18±0.09
80 cm mean±SD (LogMAR)	+0.32±0.08	+0.24±0.24	+0.31±0.15	+0.26±0.10

Table 2.10 *Monocular intermediate and near visual acuity*

	Binocular *Softec 1*	**Binocular** *ReZoom*	**Binocular** *Tecnis ZM900*	*Mix and match*	**Binocular** *Lentis Mplus*
40 cm mean±SD (LogMAR)	+0.57±0.09	+0.26±0.10	+0.17±0.11	+0.18±0.10	+0.12±0.08
80 cm mean±SD (LogMAR)	+0.28±0.09	+0.17±0.10	+0.28±0.14	+0.19±0.08	+0.19±0.08

Table 2.11 *Binocular intermediate and near visual acuity*

There was no significant difference in the monocular intermediate VA between the groups ($F_3=1.751$, $p=0.167$; table 2.10 and Table 2.11); however, there was a significant difference when measured binocularly ($F_4=4.569$, $p=0.002$). The binocular *ReZoom* group achieved higher levels of intermediate VA when compared to both the binocular *Softec 1* ($p=0.019$) and binocular *Tecnis ZM900* ($p=0.024$) groups.

2.4.3 Correlation of Visual Acuity Metrics

The average monocular best-distance corrected NVA was +0.35±0.21 LogMAR and the VA measured with a defocus lens of –2.50 D was +0.23±0.20 LogMAR. The mean difference (95% confidence interval) was 0.12 (±0.290) LogMAR (Figure 2.7). The results from both methods were highly correlated ($r = 0.734$, $p < 0.001$).
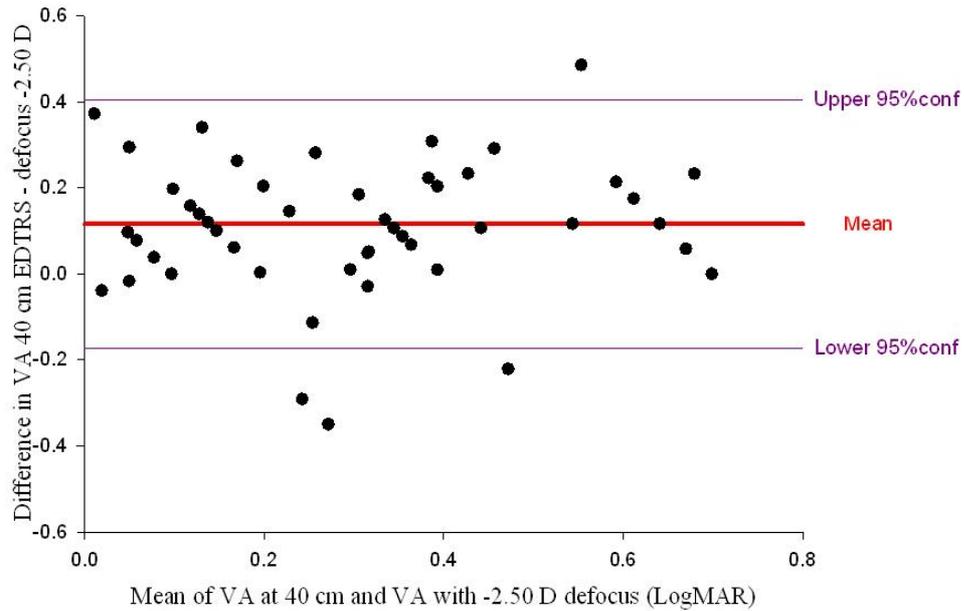
Figure 2.7 *Bland and Altman plot comparing near visual acuity with visual acuity with a –2.50 D defocus lens*

The average monocular best-distance corrected IVA was +0.28±0.11 LogMAR, the VA as determined by Equation 2.5 was +0.32±0.13 LogMAR. The mean difference (95% confidence interval) was -0.04 (±0.27) LogMAR (Figure 2.8) and the results from both methods were moderately correlated (r=0.370, p=0.004).
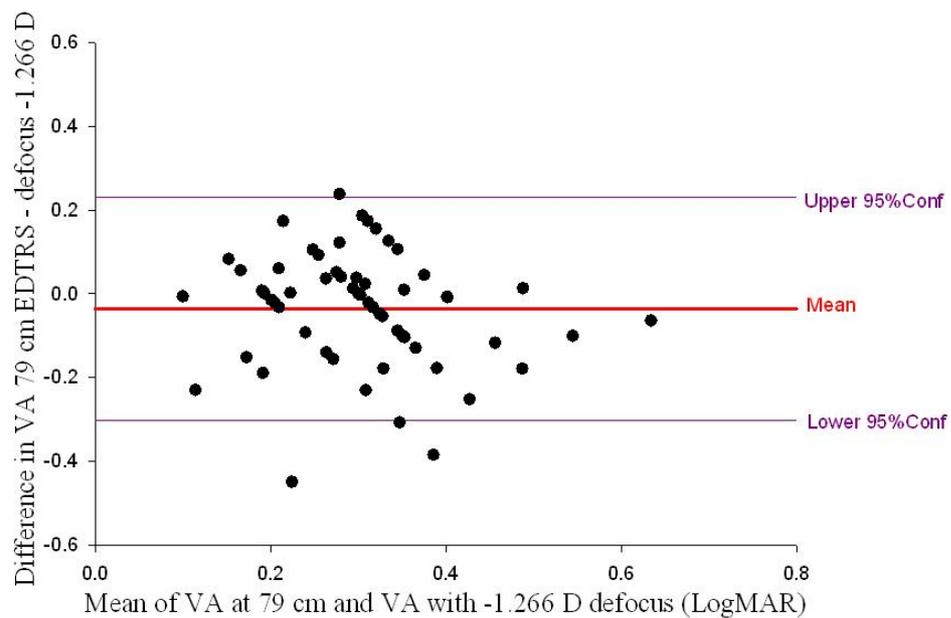
Figure 2.8 *Bland and Altman plot comparing monocular intermediate visual acuity with visual acuity as determined by Equation 2.5*

The mean binocular best-distance corrected NVA was +0.26±0.19 LogMAR and the VA with a –2.50 D defocus lens was +0.20± 0.21. The mean difference (95% confidence interval) was 0.062 (±0.195) LogMAR (Figure 2.9) the results from both methods were significantly correlated (r = 0.882, p < 0.001).
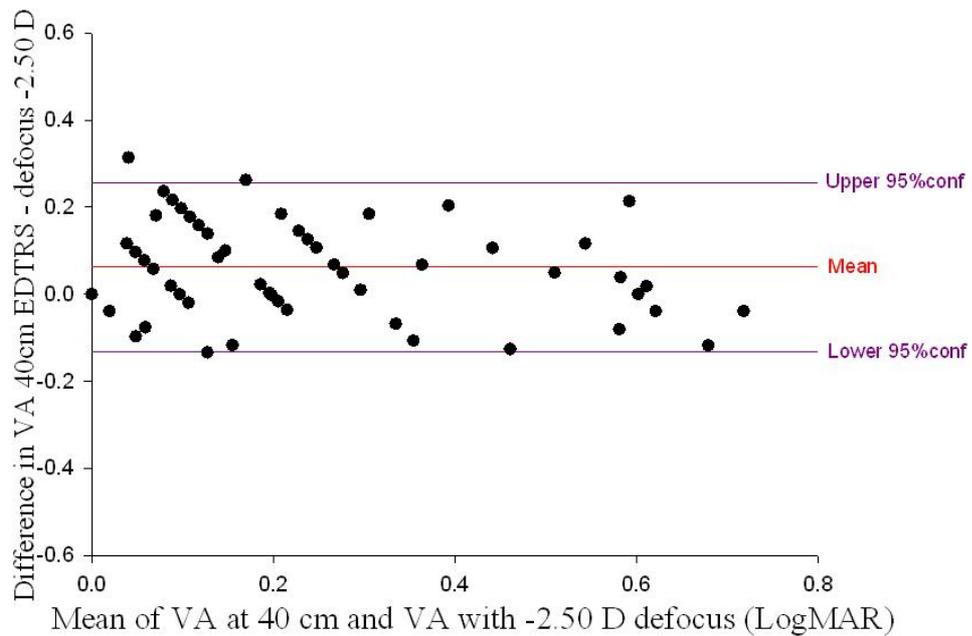
Figure 2.9 *Bland and Altman plot comparing mean binocular near visual acuity with visual acuity using a –2.50 D defocus lens*

The mean binocular best-distance corrected VA at 79 cm measured with the EDTRS chart was 0.22±0.11 LogMAR and the mean y-value on the defocus curve when x = -1.266 was 0.25±0.12 LogMAR. The mean difference (95% confidence interval) was -0.028 (±0.208) LogMAR (Figure 2.10) the results from both methods were significantly correlated (r = 0.565, p < 0.001).
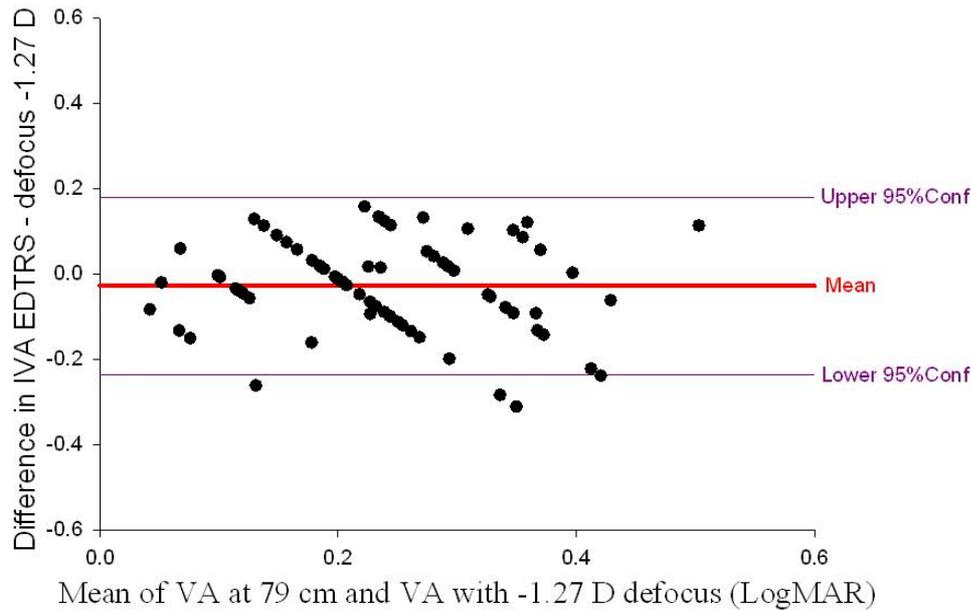
Figure 2.10 *Bland and Altman plot comparing binocular intermediate visual acuity with visual acuity as determined by Equation 2.6*

2.4.4   Amplitude of Accommodation and Range-of-Focus

There was no significant difference in monocular AOA ($F_3 = 0.600$, p = 0.617) and binocular AOA ($F_4 = 2.180$, p=0.080) between groups (Figure 2.11).
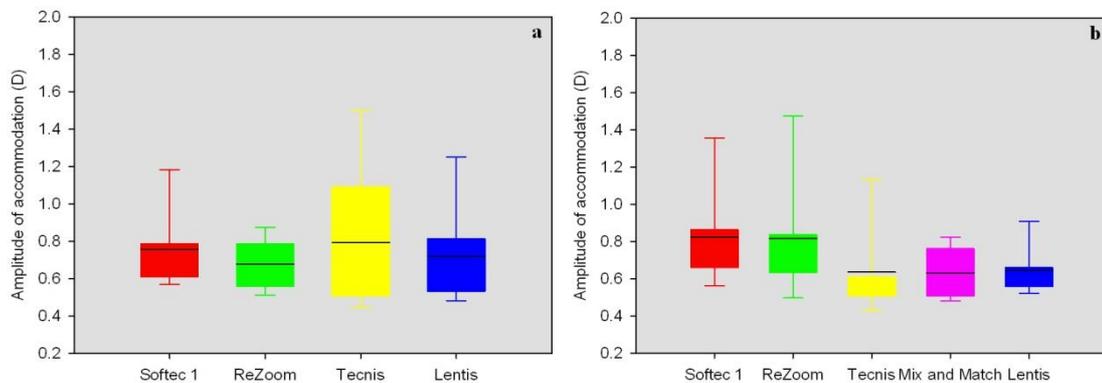
Figure 2.11 *Amplitude of accommodation of different multifocal intraocular lenses; a) monocular b) binocular*

There was a significant difference in the monocular ($F_3 = 24.6853$, p <0.001) and binocular ($F_4 = 10.1034$, p <0.001) range-of-focus between groups (Figure 2.12). All multifocal groups achieved a wider range of focus monocularly in comparison to the monofocal group (p<0.001). The *Lentis MPlus* eye had an increased monocular range of focus in comparison to the *ReZoom* (p<0.001) and *Tecnis ZM900* (p=0.007) eyes.

106

Binocularly all multifocal groups had a wider range-of-focus in comparison to the monofocal group ($p<0.001$), the binocular range-of-focus was similar in all multifocal groups ($p=1.000$).
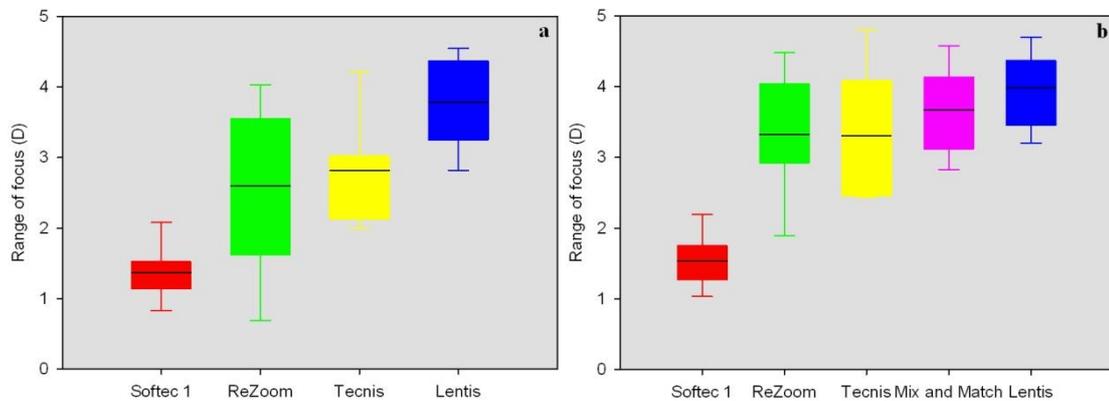
Figure 2.12 *Range-of-focus of different multifocal intraocular lenses; a) monocular b) Binocular*

2.4.5   Area-of-Defocus

There was no significant difference in the distance monocular ($F_3=2.229$, $p=0.095$) and binocular ($F_4=2.475$, $p=0.052$) area of defocus between groups (Figure 2.13).
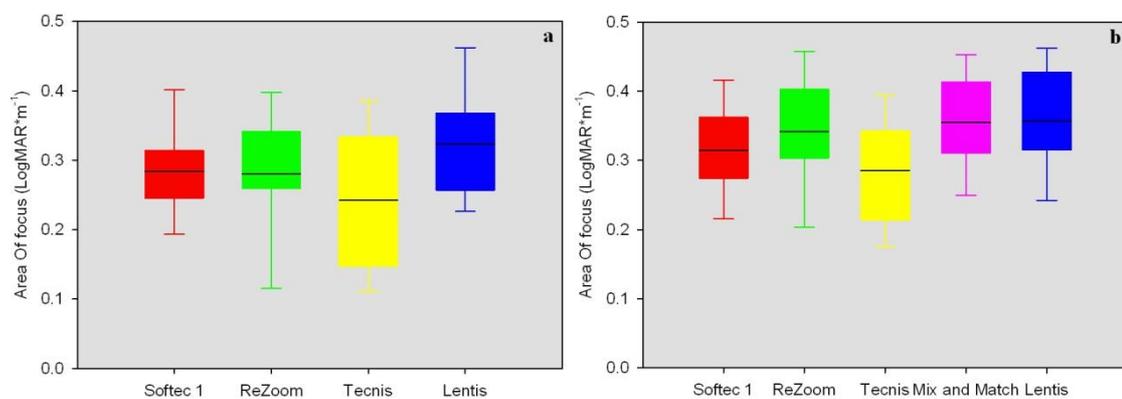
Figure 2.13 *Distance 'Area of defocus' of different multifocal intraocular lenses; a) monocular b) binocular*

An overall significant difference in monocular ($F_3=11.364$, $p<0.001$) and binocular ($F_4=10.342$, $p<0.001$) intermediate Area of defocus was found between groups (Figure 2.14).

Monocularly the *Lentis Mplus* eye had a larger area of defocus in comparison to all other IOL types ($p<0.05$). Comparison of the binocular area of defocus revealed that

107

the bilateral *Lentis Mplus* provided a greater area of defocus than the *Softec 1* (p < 0.001), *Tecnis ZM900* (p < 0.001) and *Mix and match* (p<0.001) group. The *ReZoom* group had a larger intermediate area than the *Tecnis ZM900* group (p = 0.006).
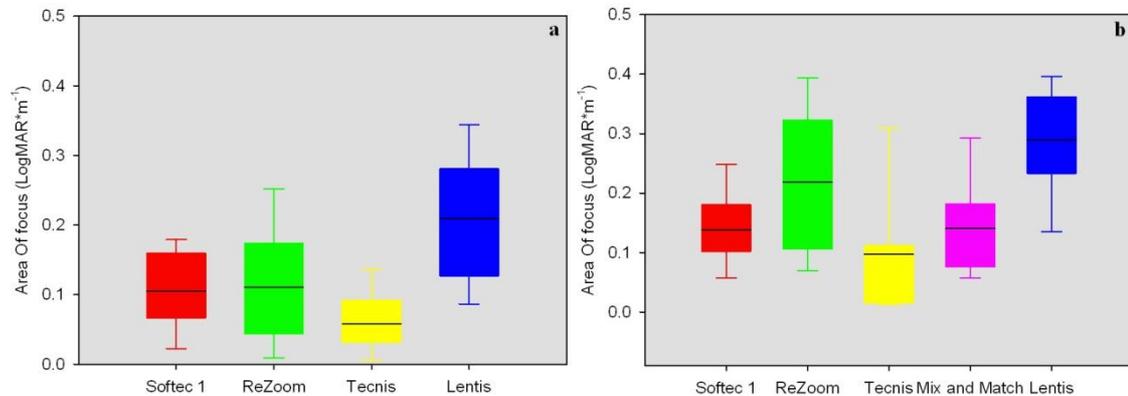
Figure 2.14 *Intermediate area of defocus of different multifocal intraocular lenses; a) monocular b) binocular*

There was an overall difference in near area of defocus monocularly (F_4=21.057, p<0.001) and binocularly (F_4=26.674, p<0.001; Figure 2.15). Monocularly and binocularly the near area of defocus was larger in the multifocal eyes in comparison to the monofocal eyes (p=0.05). The monocular near area was greater with the *Lentis Mplus* eye than the *ReZoom* eye (p=0.001). The near area was greater in the binocular *Lentis Mplus* and binocular *Tecnis ZM900* group than the binocular *ReZoom* group (p<0.05).
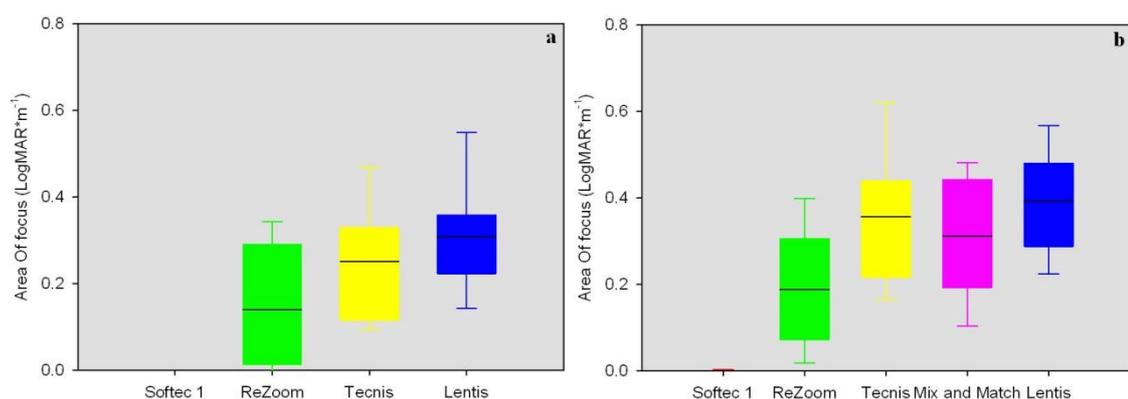
Figure 2.15 *Intermediate area of defocus of different multifocal intraocular lenses; a) monocular b) binocular*

2.4.6   Subjective Rating of Intermediate and Near Visual Acuity

The average subjective responses for near and intermediate areas are displayed in Table 2.12. The binocular intermediate area of defocus was moderately correlated to the subjective rating of intermediate vision (r_s=-0.294, p=0.010; Figure 2.16) while the binocular IVA was not significantly correlated to the subjective ratings (r_s=0.148, p=0.204; Figure 2.17). The subjective rating for near vision was moderately correlated to both NVA (r_s=0.438, p<0.001; Figure 2.18) and near 'Area of Focus' (r_s=-0.385, p=0.001; Figure 2.19).

	Softec 1	*ReZoom*	*Tecnis ZM900*	*Mix & match*	*Lentis Mplus*
Intermediate Median ± interquartile range	3.0±1.0	1.0±1.0	2.0±2.0	1.0±1.5	1.0±1.5
Near Median ± interquartile range	4.0±3.0	1.0±2.0	1.0±0.5	1.0±2.0	1.0±1.0

Table 2.12 *Subjective rating of intermediate and near vision with different multifocal intraocular lenses*
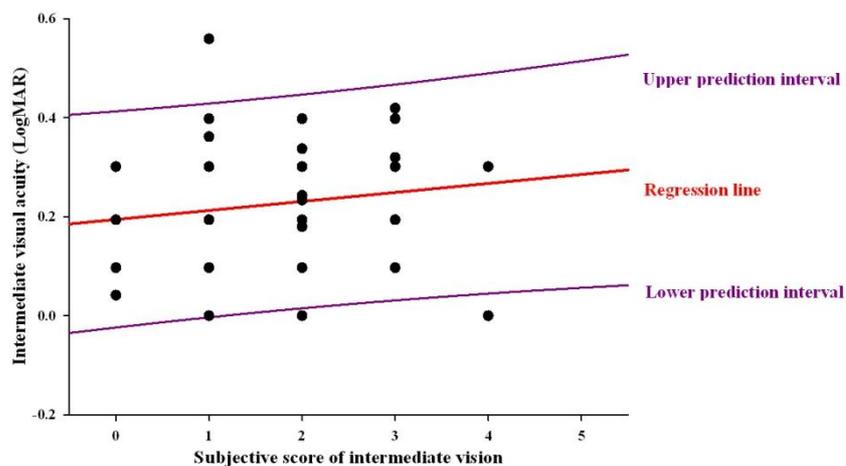
Figure 2.16 *Comparison of the subjective perception of intermediate vision and visual acuity at 80 cm.*
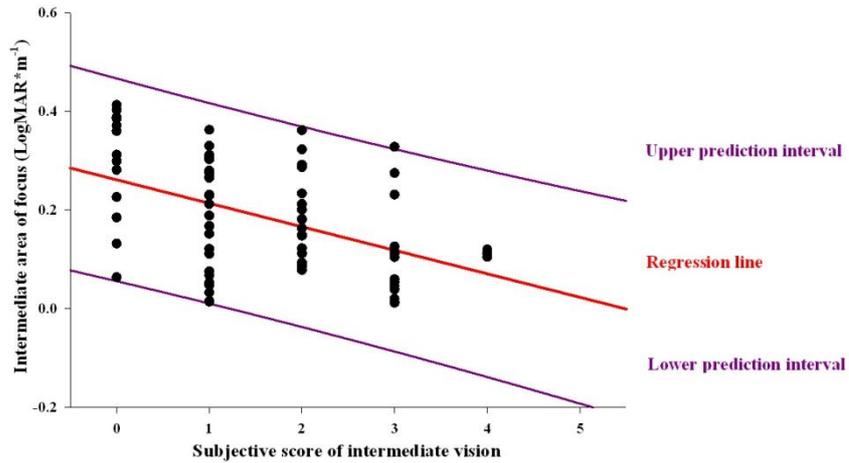
Figure 2.17 *Comparison of the subjective perception of intermediate vision and the*

intermediate area of focus.
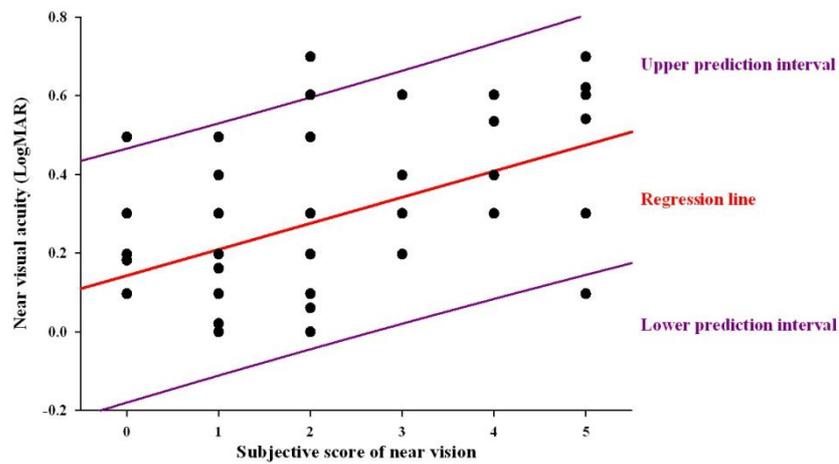
Figure 2.18 *Comparison of the subjective perception of near vision and visual acuity at*

40 cm.
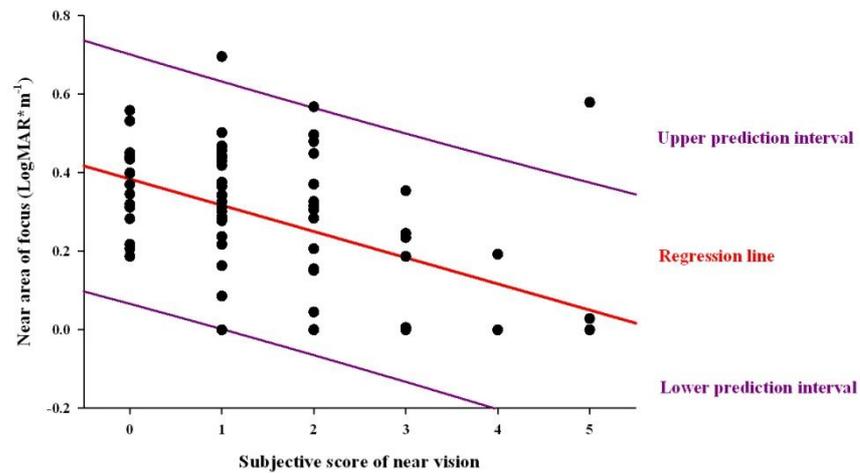
Figure 2.19 *Comparison of the subjective perception of near vision and the near area*

of focus.

2.5 Discussion

This study examined the effective range of vision provided by the implantation of different MIOL designs. Furthermore the investigation provides a useful insight into the use of defocus curves to determine the influence of lens design on visual outcomes. The *Tecnis ZM900* is a concentric diffractive MIOL with a +4.00 addition. Maximum VA was achieved at the distance focal point corresponding with 0.00 D defocus, and at the near focal point positioned at -3.00 D. The second focal point achieves a high level of VA, as the split between the distance and near focal point is equal. The *ReZoom* multifocal IOL is a concentric refractive design with a +3.50 D addition corresponding with a spectacle defocus between -2.50 and -3.00 D. In comparison to the *Tecnis ZM900* this peak was lower. The *Tecnis ZM900* IOL achieved higher VA values between -3.00 and -4.00 D binocularly and between –3.50 and –4.00D monocularly. Intermediate VA (-1.50 D) was better with the *ReZoom* MIOL. This could be attributed to the lower addition and the fact that a refractive MIOL does not create as precise a near focal point as a diffractive design. It is possible that this provides a greater spread of light along the longitudinal axis (Terwee *et al.,* 2008). The *Lentis Mplus* is a sectorial refractive multifocal design with a +3.00 D addition. This design of IOL achieves optimal VA with a spectacle defocus of -2.50 D. In comparison with the diffractive MIOL (*Tecnis ZM900*), the *Lentis MPlus* achieves significantly higher VA throughout the intermediate range and into the near focal range (between -0.50 to -2.50 D). The larger intermediate range is particularly notable with the lower +3.00 D addition. In comparison with the *ReZoom* multifocal the *Lentis MPlus* performs better between a -2.00 and -2.50 D focal range. The higher second peak and slightly lower reading addition of the *Lentis MPlus* MIOL is responsible for this difference in acuity.

Although the concept of mixing and matching refractive and diffractive MIOLs has been in practice since the introduction of the *CeeOn 811E* and *Array SA40N* (Gunenc and Celik 2008), this is the first study examining defocus curve profiles of subjects implanted binocularly with the ReZoom or Tecnis MIOL and comparing them with subjects implanted with a mixture of both MIOLs. This study demonstrates the benefits of mixing and matching MIOLs, whereby a combination of lenses achieves a compromise defocus curve profile: the intermediate visual acuity is not significantly reduced in comparison to the *ReZoom* group and near vision is not significantly reduced in comparison to the *Tecnis ZM900* group. The defocus curve profile of the

mix and match group provides a closest match to that of the *Lentis MPlus* with a difference just at -1.50 and -2.00 D.

Direct comparisons of defocus curves provide a detailed comparison of VA at every level of defocus. However, metrics for providing a global overview of the performance of a lens is important to allow standardised comparisons between studies. Depth-of-focus and AOA are the two most common metrics used with defocus curves. The criteria used to define AOA, as refined by Gupta and associates (2008), does not effectively describe the visual outcomes of MIOLs as these lenses do not accommodate. In this study no differences in AOA were found between the MIOL and monofocal designs despite the presence of the second focal point. The most commonly utilised method for analysing defocus curves is the absolute criteria of 0.3 LogMAR used to define the depth-of-focus (Table 2.2). Although this methodology is able to detect a difference in the range of focus between a monofocal and multifocal lens it was not sensitive enough to ascertain differences between multifocal lens types implanted binocularly. Similarly it does not give any indication of where the range of vision is located as it is clear that the multifocal designs perform differently over particular focal ranges.

This study has therefore proposed a new metric area of focus, providing an overview of the visual range separately for distance, near and intermediate. By using area it also includes the level of VA within the range as well as the range itself. The area metric identifies the increased level of VA within the intermediate range of a lower addition MIOL in comparison to a high addition lens. Using the area metric, differences between the MIOL groups can be identified as well as the difference between a monofocal IOL and MIOL. Binocularly the *Lentis MPlus* group had a greater area in the intermediate range when compared to all other multifocal groups. It is also evident that the *ReZoom* area was greater than the *Tecnis ZM900* area within this range. Examination of the near areas reveals that the *Tecnis ZM900* and *Lentis MPlus* groups provided a greater area in comparison to the *ReZoom* group. There were no differences in the areas of the *mix and match* group in comparison to the binocular *Tencis ZM900* and *ReZoom* groups. The area metric provides an overview of results that can be standardised across studies.

A potential source of error occurs when fitting polynomial curves to each data set. This study has concluded that when using a 14-point data set between +1.50 and -5.00 D a ninth order polynomial is most appropriate. Fitting polynomials of a high order creates oscillation of the fitted curve known as the Runge phenomenon (Runge, 1901). This oscillation occurs mostly at the edges of a dataset between the first and last values. To account for this phenomenon the chosen defocus curve range was 1.00 D either side of the required range for measurement of the area of focus. Therefore when using a 9th order polynomial it is important to retain the full range of defocus curve between +1.50 and -5.00 D despite the area metric only using the area between +0.50 and -4.00 D. For future studies the possibility of using spline curves will be investigated. Spline curves piece together polynomial functions preventing the occurrence of Runge's phenomenon. These have the potential to reduce the number of data points required to those within +0.50 and -4.00 D. The repeatability of VA measurements using LogMAR charts has previously been examined and so was not assessed in this study (Raasch *et al.*, 1998).

In comparison to the defocus curves measured in photopic conditions those measured in mesopic conditions demonstrated a uniform suppression of the defocus curve across the measured range of focus. Comparison of the mesopic and photopic defocus curve indicates that all IOL designs tested exhibited pupil independent characteristics. The pupil size increased by an average of 1.1 mm in mesopic conditions. With a pupil dependent lens, a non-uniform change would be expected in the defocus curve profile due to the increased pupil size. However in this study the defocus curves of all groups changed uniformly across the defocus range. This result was expected in the *Tecnis ZM900* group and *Lentis MPlus* groups as these lenses are designed as pupil independent. However the *ReZoom* MIOL is a pupil dependent lens, and *in vitro* studies have shown the near focal point not appearing until a pupil size of 3.5 mm was achieved (Artigas *et al.,* 2007). This study did not find such a change and the lens exhibited the same curve profile despite a change in pupil size of 1.2 mm. With *in vitro* studies the simulated pupil aperture is placed over the centre of the IOL, this may explain the difference in our findings as even with small pupils if the lens is decentred the near zones can appear within the resultant pupil aperture. The group size involved in this study was not large enough to divide the group into large and small pupils within

a standard illumination. It is important that further investigation of the effect of pupil size on the visual performance of a zonal refractive MIOL is conducted.

Each measure of VA along a defocus curve corresponds with a specific working distance. Pieh *et al.,* (2002) found that VA as measured using the defocus curves underestimate the VA in pseudophakic subjects. In contrast the current study found good agreement between the VA results attained with the near chart via the defocus curve method. There are several differences in the methodology implemented between studies which may explain these differences: the previous study by Peih and colleagues (2002) utilised a single LogMAR chart for the defocus curve measurements and another for measurement at each distance, this is susceptible to memorisation effects as the letters were not randomised between measures, similarly the order of spectacle lenses were not randomised.

Near VA is the most common method used to determine the effectiveness of a MIOL. In the current study VA was measured at 80 cm and at 40 cm. At 80 cm the *ReZoom* group demonstrated better binocular VA than both the *Tecnis ZM900* and *Softec 1* group. At 40 cm all MIOL groups achieved a better VA in comparison with the monocular group and the *Lentis MPlus* group achieved a higher VA in comparison with *ReZoom* MIOL. The intermediate area of focus had a higher correlation with the subjective rating of near vision in comparison to intermediate VA. Near VA and the near area of focus were both moderately correlated to the subjective rating of near vision. Intermediate area of focus assesses vision over a wide focal range as opposed to intermediate VA, which only measures VA at one distance. This may explain why the subjective ratings have a higher correlation with the area of focus in comparison to VA. Measurement of vision using defocus curves is a lengthy process, however it is more sensitive to differences between MIOL designs in comparison to levels of VA measured at one intermediate and near distance and is therefore a useful tool for the evaluation of these IOLs.

The methodology we have used in this investigation has highlighted the differences between MIOL designs and demonstrated that by mixing and matching diffractive and refractive IOLs a compromise between the two lens profiles is attained. The defocus curve profile obtained using the +3.00 D sectorial MIOL was better within the intermediate range than with the other two IOLs incorporating a higher addition.

Mixing and matching IOLs is a useful method for customising vision depending on the range of focus required by the patient. A +1.50 addition sectorial refractive multifocal has become available and the results of a group of twenty subjects implanted with a combination of the +1.50 and +3.00 D are currently under evaluation using the same defocus curve methodology used in this study.

2.6 Limitations of the Study

Measurement of VA, although highly repeatable (Raasch et al. 1998), is a subjective measure. In this study the time taken to measure all four defocus curves may have had a fatiguing effect as 56 measurements of distance VA were performed per subject as well as extra measurements of VA at intermediate and near distances. Further error may have occurred when fitting a polynomial curve to each data set. In future studies the use of spline curves will be investigated as this will reduce the incidence of Runges phenomenon and will allow a lower number of visual acuity measurements. However the use of spline curves will increase the complexity of the area of focus measurement. The current study compared VA measured using the defocus curves with that measured at the corresponding distance, however, intermediate VA was compared with a predicted VA measurement at -1.25 D according to the defocus curve function. Future studies comparing these measures would benefit with additional measures of VA across a wide range of distances.

In this study the performance of a range of MIOLs was assessed in mesopic and photopic conditions. All lenses exhibited the same curve shape suggesting a level of pupil size independency. However, a drop in illumination levels has been shown to increase the depth-of-focus as well as suppressing VA. To examine the effect of pupil sizes larger group sizes are needed where subjects can be divided by their respective pupil size under specific illumination levels.

It is important to compare subjective *in vivo* results with objective methods. Studies currently in progress aim to compare the results from these defocus curves with optical bench tests designed to predict the optical performance of each lens.

2.7 Conclusion

Defocus curves are an important assessment tool allowing evaluation of multifocal IOLs. This study has highlighted the potential for *mixing and matching* multifocal

IOLs. It also highlights the advantage of using the relatively lower +3.00 D reading addition IOL. A MIOL with a +4.00 D addition does not provide sufficient VA across a wide range of intermediate and near distances and so needs to be used in combination with a lower powered MIOL or selected if that level of near vision is required by the patient.

Defocus curve methodology and analysis needs to be standardised so that results can be compared between studies. The direct method of assessment is important as it can determine differences between lenses at each level of focus. However the results attained from this method need to be viewed with caution as the number of statistical tests required to analyse a defocus curve leaves it vulnerable to type 1 errors. Alternatively this study has proposed an area of focus metric. Obtaining the three areas (for distance, intermediate and near) does not require an extensive knowledge of mathematics and is easily obtained using the following steps provided that the defocus curve is measured over the range of +1.50 to -5.00 D in 0.50 D steps:

- Each data set is fitted with a 9th order polynomial (Equation 2.5)
- x is calculated when $y=0$ by imputing an approximation of x into Equation 2.7. The output from this equation is inputted into Equation 2.8 and 2.9 and repeated until 0 error exists.
- The area is calculated using Equation 2.10 and setting the limits of integration to either the upper and lower limit of the near (-0.50 and +0.50D), intermediate (-2.00 and -0.50D) and near (-4.00 and -2.00D) or if the curve intersects $y=0.30$ then the x value is the new limit.

Defocus curves describe the VA threshold, at a high contrast, over a range of optical defocus. This measure therefore provides an indication of the level of vision attained at specific distances. More information is required to attain a better understanding of the visual capacity of a subject after implantation of IOLs. In Chapter 3 the use of reading ability and the perception of near vision is explored in subjects following monofocal, multifocal and accommodative IOL implantation.

Chapter 3 Assessment of Reading Ability and Near Vision Satisfaction

3.1 Introduction

Reduction in visual quality can have a negative impact on an individual's independence and impinge on all aspects of life (Scott *et al.,* 1999). Chapter 2 detailed the use of defocus curves for assessing high contrast acuity at a range of focal lengths. However, day-to-day task performance is not purely dependent on high contrast VA. Subjective quality-of-life questionnaires are valuable tools for understanding the perception of vision and allow quantification of a patient's visual satisfaction throughout everyday life. Similarly, assessment of reading vision is another important method of determining the impact of low vision in the real world, often the main motivation for electing for cataract surgery is the desire to improve reading (Mönestam and Wachtmeister, 1997). Reading tests were initially developed for the assessment of low vision (Legge *et al.,* 1989) but have subsequently increased in popularity for the assessment of pseudophakic correction.

3.1.1 Reading Ability Tests

Measurement of reading ability provides greater detail regarding visual ability in non-clinical situations. Spot or survival reading: approximately 40 words per minute (WPM), occurs when the size of print approaches the threshold visual acuity. Fluent reading: approximately 160 WPM, occurs when the print size is large enough to provide an optimal reading speed. Acuity reserve refers to the difference between the threshold print size and the actual print size. Sufficient reserve is required before fluent reading is possible. Reduced visual acuity has a negative impact on the acuity reserve, thus larger print sizes are required before fluent reading is possible (Whittaker and Lovie-Kitchin, 1993).

Measurement of near visual acuity allows the determination of acuity threshold and thus provides information on spot reading. Reading ability tests are designed to assess reading speed across a range of print sizes from which details of spot reading, fluent reading and the acuity reserve can be derived. Visual factors such as the extent of visual field (Virgili *et al.,* 2004), contrast of print (Legge *et al.,* 1987b), and pursuit and

saccadic eye movements (Braswell and Rine, 2006), impact on reading ability. It is important to remember, however, that reading is an advanced cognitive process requiring comprehension and intellectual capacity (Friedman *et al.,* 1999). Reading is a process that develops until adulthood and again reduces with a loss of cognitive function in old age (Hartley *et al.,* 1994).

Both the *Radner* (Radner, 1998) and *Minesota Near* reading charts (*MNRead*; Lighthouse International, New York, USA) have superseded previous reading charts such as the *Pepper Visual Skills for Reading Test* (Baldasare *et al.,* 1986). The popularity of these charts can be attributed to their ease of implementation and the standardisation of the text used for each line of writing (Stelmack *et al.,* 1987).

3.1.2   The Minesota Near Reading Chart

The original *MNRead* was developed for the assessment of low vision patients using the drifting text method: this measures dynamic reading speed by moving sentences across a computer screen at increasing speeds (Legge *et al.,* 1989). In comparison, the static text method presents stationary sentences and examines the time taken to read these sentences. The two methods produce similar results, however, the drifting text method is relatively difficult to administer (Rice *et al.,* 2005). Therefore a static printed text version of the MNRead was developed; the current printed card format uses a regular 0.1 LogMAR progression with print sizes ranging from 1.30 to -0.60 LogMAR. There are 60 characters and 10 words per sentence. Each subject starts at the largest print size and is encouraged to read each paragraph at the fastest speed comfortable to them. The time taken to read each paragraph is recorded. This continues until the patient can no longer resolve the print (Mansfield *et al.,* 1993).

Reading speed, in words per minute, is then calculated for each paragraph using Equation 3.1, the results of which can be used to plot a graph of acuity versus reading speed. From this graph several metrics can be derived to describe reading ability (http://gandalf.psych.umn.edu/groups/gellab/MNREAD/speed.html accessed 20/01/11).

$$reading\,speed\,(wpm) = \frac{(60 \times (10 - e))}{t}$$
Equation 3.1

e is the number of mistakes
t is the time taken to read each paragraph

118

3.1.2.1 Reading Acuity

Reading acuity (RA) is the smallest print size that can be resolved and is independent of reading speed. Each sentence comprises of ten six character words and the metric regards each word as having a value of 0.01 Log Units. RA is calculated using Equation 3.2 (http://gandalf.psych.umn.edu/groups/gellab/MNREAD/speed.html accessed 20/01/11).

$$Reading\ Acuity\ (logMAR) = 1.4 - (s \times 0.1) + (e \times 0.01) \qquad \textbf{Equation 3.2}$$

s is the number of paragraphs read
e is the number of mistakes

3.1.2.2 Maximum Reading speed

Maximum reading speed (MRS) is the quickest reading speed where print size is not a limiting factor. Visual inspection is the most common method used to determine reading speed; this involves a subjective judgement of where the peak of the graph exists. The median reading speed of the first three sentences on the *MNRead* equates to the visual inspection method and can be used as a valid alternative (Rice *et al.,* 2005). The metric MRS is designed to be independent of visual acuity and instead is more sensitive to reading ability. MRS takes a long time to reach adult levels and can change depending on whether reading is required for comprehension or to skim (Chung *et al.,* 1998).

3.1.2.3 Critical Print Size

Critical print size (CPS) is the smallest print size where maximum reading speed can be maintained. It can be calculated through visual inspection of the graph; the CPS is recorded as the point at which the reading speed first starts to drop. This technique may be prone to error as reading speed measurements around the CPS limit can be noisy and difficult to gauge subjectively (Cheung *et al.,* 2008a).

Asymptopic curves can be reliably fitted to *MNRead* data. Asymptotic curves are commonly used on drug dose response curves where a stronger response is found from a higher dosage of drug until saturation occurs and the maximum response has been found (Ozawa *et al.,* 1989); this same response can be found with reading speed. As the size of print increases the reading speed increases until saturation occurs and the patient

has reached their maximum reading speed. The asymptotic curve (Equation 3.3) increases from the value a-b until it approaches the maximum value *a* otherwise known as the asymptote. The value *c* describes the rate of growth of the curve.

$$Y = a - b \exp^{-cx}$$ **Equation 3.3**

Where asymptotic curves have been used the maximum reading speed has been described as the metric *a* in the equation and CPS was described as the print size at percentage of the asymptote. Chung and colleagues (2008a) proposed that the percentage of the asymptote chosen for the critical print size could be modified depending on the task to be achieved. The study found that CPS was equivalent to reading speed at 80% or 90% of the fitted curve asymptote. Where missing data is present non-linear mixed effects modelling can be used and individual data sets can then be estimated from this model (Cheung *et al.,* 2008a).

Nygaard and colleagues (2008) successfully fitted Weibull functions to *MNRead* results of subjects with age related macular degeneration (AMD). CPS in this study was regarded as the lower confidence interval of the asymptote of the curve.

These metrics fail to describe the reading profile across a range of spatial frequency and several descriptions are required to gain an understanding of reading vision. The Reading Ability Score (RAS) metric has been described as a value, which describes reading vision over a range of spatial frequencies. RAS is calculated as the sum of the Logarithmic reading speed between 0.0 LogMAR and 1.0 LogMAR, which is then divided by the average value across the range for a group of normally sighted young healthy patients (ages 19-23). This metric provides a quantifiable measure of the improvement in reading ability gained when a subject with AMD uses a hand magnifier (Cheong *et al.,* 2008b).

3.1.3 The Radner reading test

The *Radner reading test* was developed as a static printed reading acuity chart with standardized sentence construction. Each sentence contains three lines, fourteen words and eighty-two to eighty-four characters; the first and second line has five words and the third line has four words. The construction of the sentences has been standardised to ensure that syllables, nouns and verbs are positioned across each sentence

consistently. The reading speed measurements attained with the *Radner reading test* correlate well with long text paragraphs and the measurements of reading speed are highly repeatable. Reading acuity is expressed as the smallest distinguishable print size and is expressed in logRADs. Reading speed is calculated using Equation 3.4; from this MRS and critical print size can be calculated (Radner *et al.,* 1998).

$$\text{Re} adingSpeed = \frac{14 \times 60}{t} \qquad \textbf{Equation 3.4}$$

Each paragraph consists of 20 syllables, and equates to 0.1 logRAD. To calculate reading acuity the number of paragraphs read is counted along with the number of errors. Any incorrectly identified syllables are accounted for with each having a value of 0.005 logRAD (Equation 3.5; Maaijwee *et al.,* 2008).

$$\textit{Reading acuity (logRAD)} = 1 - (s \times 0.1) - (e_s \times 0.005) \qquad \textbf{Equation 3.5}$$

s is the number of paragraphs read
e_s is the number of incorrectly identified syllables

3.1.4   Reading ability with Multifocal and Accommodative Intraocular Lenses

Reading charts are gaining popularity as a method for assessing and comparing the performance of multifocal and accommodative IOLs (Table 3.1); this trend has been assisted by the American national standards institute who, in their guidelines of the assessment of multifocal and accommodative IOLs (ANSI Z80.12-2007), require the assessment of functional reading vision to meet their requirements. RA, CPS and MRS are common metrics used in the calculation of reading ability; however, how these metrics are calculated is rarely discussed in the literature. A common alternative is to compare reading ability of subjects implanted with different IOLs by comparing the average reading speeds for each print size (Brown *et al.,* 2009).

First Author	Lenses assessed (number of eyes)	Reading chart (distance)	Metrics assessed	Results
Akutsu 1992	+3.50 D Diffractive n=7 Monofocal (BCNVA) n=7	Computerized MNRead (20 cm)	Reading speed as a function of contrast and size	Monofocal better than +3.50 D diffractive with small low contrast print sizes.
Richter-Muecksch 2002	+4.00 D Diffractive n=20(40). +3.50 D refractive n=30(40) Monofocal (BCNVA) n=20(40)	Radner charts (50, 40, 30 & 25 cm)	Maximum reading Speed: No details of how metric determined	No difference
			Critical print size: No details of how metric determined.	Monofocal better than diffractive and refractive. Diffractive better than refractive.
			Reading speed for print sizes between 0.7 and 0.30 logRAD: Multiple t-tests used (no significance correction)	Monofocal and Diffractive better than refractive.
			Reading acuity: Smallest print read	Monofocal and Diffractive better than refractive.
			Reading distance: Distance required for smallest reading acuity	Refractive = 40 cm Diffractive = 30 cm
Hutz 2006	Refractive +3.5 D n=20 Diffractive +4 D n=20 Apodized diffractive +4 D n=20	Radner Reading Cards (Unknown)	Reading acuity: Smallest print read	Diffractive better than refractive and Apodized diffractive
			Reading speed at 0.4 logRAD	Diffractive better than refractive and Apodized diffractive
Souza 2006	Apodized Diffractive +4 D n=15 Monofocal n=15 (best near correction in monofocal group).	MNRead Portuguese (30 to 40 cm)	Reading acuity: Smallest print read.	No difference
			Critical print size: No details of how metric determined.	No difference
Cumming 2006	Single optic accommodating n=263 Monofocal n=64	MNRead (40 & 81 cm)	Reading acuity: Smallest print read	Single optic accommodating better than monofocal
Hancox 2006	Single optic accommodating /Monofocal n=30	MNRead (40 cm)	Smallest print size with a reading speed greater than 80 wpm	No difference

First Author	Lenses assessed (number of eyes)	Reading chart (distance)	Metrics assessed	Results
Pepose 2007	Single optic accommodating n=14 Refractive +3.5 D n=12 Apodized diffractive +4 D n=14	MNRead (40 & 81 cm)	Reading acuity: Smallest print read	81 cm- Single optic accommodating better than refractive and Apodized diffractive. Refractive better than Apodized diffractive. 40 cm- Apodized diffractive better than single optic accommodating and Refractive
Hütz 2008	Refractive +3.5 D n=20 Diffractive +4 D n=20 Apodized diffractive +4 D n=20	Radner reading cards (40, 60 & 80 cm)	Reading acuity: Smallest print read	Single Optic accommodating provided best intermediate vision
			Reading speed at 0.4 LogRAD	Apodized diffractive provided best near vision.
Harman 2008	Single Optic accommodative n=21 Refractive +3.5 D n=24 Monofocal n=19	MNRead cards (40 cm)	Maximum reading speed: No details of how determined	No difference
			Critical print size: No details of how determined	Refractive and single optic accommodating better than monofocal.
Ito 2009	Monofocal monovision n=38 Refractive +3.5 D n=22	MNRead Japanese (30 cm)	Maximum reading speed: No details of how determined	Maximum reading speed – No difference
			Critical print size: No details of how determined	Critical print size – Monovision better than Refractive
			Reading acuity: Smallest print read	Reading acuity – Monovision better than refractive
			Direct comparison of reading speed for each print size: Mann Witney U test (no significance correction)	Reading speed from 0.3 to 0.1 LogMAR print size better with the monovision group.

First Author	Lenses assessed (number of eyes)	Reading chart (distance)	Metrics assessed	Results
Brown 2009	Single optic accommodative (a) n=96 Single optic accommodative (b) n=55	MNRead (40 cm)	Direct comparison of reading speed for each print size: Mann Witney U test (Bonferroni correction)	Single optic accommodative (a) better than single optic accommodative (b)
			Smallest print size with a reading speed greater than 80 wpm	Single optic accommodative (a) better than single optic accommodative (b)
Chen 2009	Refractive +3.5 D/ Diffractive +4 D combination n=15 Mono n=16	Radner Chinese reading cards (25 cm)	Reading acuity: Smallest print read	Multifocal combination better than monofocal
			Reading speed: No details of how determined.	Multifocal combination better than monofocal
Sanders 2010	Single optic accommodative n=255 Monofocal n=101	MNRead (40 cm)	Direct comparison of reading speed for each print size. Mann Witney U test (Bonferroni correction)	Single optic accommodative better than monofocal
			Smallest print size with a reading speed greater than 80 wpm	Single optic accommodative better than monofocal
Hütz 2010a	Refractive +3.5 D / diffractive +4 D combination n=20	Radner (40, 60 & 80 cm)	Reading speed at 0.4 LogRAD	No comparisons made
Packer 2010	Diffractive +4 D n=125 (244) Monofocal n=123 (245)	MNRead (40 cm)	Reading acuity: Smallest print read	Diffractive better than monofocal
			Critical print size: No details of how determined	Diffractive better than monofocal
Hütz 2010b	Diffractive +4 D silicone/acrylic combination n=21 (42)	Radner (40 cm)	Reading speed: No details of how determined.	No difference

Table 3.1 *Summary of studies examining the reading ability of subjects implanted with a multifocal and accommodating intraocular lens*

3.1.5 Questionnaires used to Determine Patient Satisfaction Following Cataract Surgery

Quality of life questionnaires can be targeted to assess a person's perceived ability to perform a particular task or to self rate a particular characteristic.

Subjective questionnaires have been used extensively to assess the quality of vision and their impact on the ability to perform daily tasks following implantation with multifocal and accommodating IOLs. However, the majority of these questionnaires are bespoke and have rarely been validated with a pseudophakic subject group (Chapter 1.9.3; Appendix A3; de Boer *et al.,* 2004). Many of these questionnaires have required modification to make the questions relevant for the specific subject groups (Brydon *et al.,* 2000).

Typically quality of life questionnaires use a Likert scales category response. These involve a limited selection of responses per question and the summation of scores from these responses gives a final total (Likert, 1932).

Methods used to validate and create the questionnaire need to be considered. Traditional classic test theory has been superseded by the more complex Item response theory, which has been used to revalidate questionnaires previously.

3.1.6 Classic Test Theory and Item Response Models

Classic Test Theory (CTT) and Item Response Models (IRM) are both used to assist the development of the questionnaire and to check its reliability and validity. CTT is based on the assumption that the observed score X is composed of both the true score and the error (Equation 3.6).

$$X=T+E \qquad\qquad \textbf{Equation 3.6}$$

This model assesses the sum of total responses and does not assume different levels of difficulty for each item. This theory also regards raw scores as a linear response. Techniques based upon CTT include Factor analysis, correlations between item measures and Cronbach's alpha

Rasch analysis is a form of IRT developed by George Rasch (Rasch, 1961). It assumes each response is a product of the difficulty of the item and the ability of the person to

perform the task. This creates a model where items are scaled according to difficulty and subjects ranked according to ability. While CTT assumes a linear relationship between raw scores, Rasch analysis uses the principal of additive scoring whereby scores are positioned on an interval rather than ordinal scale. This process is referred to as item calibration where items are scores along a scale, measured in Log-odd units (logits). An increase of 1 logit corresponds with an increase of the effect occurring by a factor of 2.718 (Tennant *et al.,* 2004). The Rasch model is designed to measure one characteristic; this is known as a unidimentional model. Accuracy of fit statistics are calculated to ensure that each item is measuring the desired characteristic (Prieto *et al.,* 2003).

3.1.7   Validation of Current Visual Quality of Life Questionnaire

It is important that quality-of-life questionnaires are examined for validity and that the questionnaire has been validated for use on the intended subject group. Due to the inherent advantages IRT has over CTT; the popularity of Rasch analysis has increased it is now considered the standard technique for validating questionnaires (de Boer *et al.,* 2004).

3.2   Study Aim

This was a prospective study involving subjects implanted bilaterally with monofocal, multifocal and single optic accommodative IOLs. The purpose of the study was to validate a visual related quality-of-life questionnaire for use with these subjects and to assess the most appropriate metric for assessing reading ability.

3.2.1   Subjects

One hundred and ten subjects (45 males, 65 females) of mean age 62.8 ± 9.2 years were recruited from Solihull Hospital (Solihull, UK) and the Midland Eye Institute (Solihull, UK). The principal investigator of the study (PB) recruited ninety of the subjects for the study; three co-investigators trained by the principal investigator recruited the remaining twenty. The inclusion criteria for the study was as follows:

- requiring bilateral cataract surgery or electing for bilateral clear lens extraction
- a likely postoperative best corrected distance visual acuity of at least 0.1 logMAR
- the absence of any ocular pathology and previous surgery

- corneal astigmatism less that 1.50 D

- aged between 40 and 70 years

- absence of immuno-suppressant conditions

- suitable for multifocal IOL implantation

- willing to have multifocal IOL implantation

- willing to participate in the study

- willing to attend an extra post-operative aftercare visit

- absence of post-operative capsular opacification, corneal refractive surgery, and YAG capsulotomy

The 110 recruited subjects were implanted with 6 combinations of IOLs. The subjects were strictly divided into one of five groups based on their operation date for their first eye. Each group was assigned a type of IOL:

- The first 15 subjects were bilaterally implanted with a *mix and match* strategy; a *ReZoom* MIOL (Abbott Medical Optics Inc.) was implanted in the right eye and a *Tecnis ZM900* MIOL (Abbott Medical Optics Inc.) was implanted in the left.

- The second 15 subjects were implanted bilaterally with a *ReZoom* MIOL.

- The third 15 Subjects were implanted bilaterally with the *Tecnis ZM900* MIOL.

- The fourth 15 subjects were implanted bilaterally with the *Lentis Mplus* MIOL (Topcon Europe BV).

- The next 20 subjects were implanted bilaterally with the *Softec 1* monofocal IOL (Lenstec).

- The remaining 30 subjects were implanted bilaterally with the *Tetraflex* single optic accommodating IOL (Lenstec, St Petersburg, Florida, USA).

The implications of multifocal and single optic accommodating IOL implantation were discussed with each subject by the principal investigator and consultant Ophthalmologist performing the surgery. Ultimately the decision to operate was made by the consultant ophthalmologist.

Pre-operatively an *IOLMaster* (Carl Zeiss Meditec AG) running v5 analysis software and *NIDEK OPD-Scan II* (Optical Path Difference Scanning System II; NIDEK Co Ltd) Wavefront Aberrometer were used to determine axial length and corneal power. To determine IOL power, the Hoffer Q IOL formula was used for short axial lengths,

(<22 mm; College of Ophthalmologist's Guidelines) and the SRK/T was used for all other axial lengths; emmetropia was the target in all cases.

All operations were performed by one of three surgeons using topical or local anaesthetic. A 2.85 mm clear corneal incision, widening to 3.2 mm after injection, was placed on the steepest corneal axis to reduce residual levels of postoperative astigmatism. Phacoemulsification, aspiration and irrigation were performed through a 5.5 mm capsularhexis using the *Millennium phacoemulsification system* (Bausch and Lomb). All IOLs were implanted into the capsular bag.

Six subjects were later excluded from the study due to post operative complications: two from the *Lentis Mplus* MIOL group (one cystoid macular oedema and one requiring Yag Laser), one from the Bilateral *Tecnis ZM900* MIOL group (Post operative LASIK), one from the *Mix and Match* group (post operative YAG capsulotomy) and two from the Tetraflex group (post-operative YAG Capsulotomy). An additional six subjects were recruited to replace those who were excluded. The final patient demographics are detailed in Table 3.3.

	Bilateral *Softec 1*	Bilateral *ReZoom*	Bilateral Tecnis ZM900	*Mix and Match*	Bilateral Lentis MPlus	Bilateral *Tetraflex*
Ages Years (mean±SD)	63.6±6.6	62.3±8.4	60.7±11.0	58.5±9.2	62.3±9.0	65.8±9.8
Gender	6 Male, 14 Female	7 Male, 8 female	4 male, 11 female	7 male, 8 female	7 male, 8 female	14 male, 16 female

***Table 3.2** Subject demographics*

The NHS Local Research Ethics Committee of Solihull approved this study and informed consent was acquired prior to the start of the study for each subject. The consequences and details of the study were explained to each patient. The study was conducted in accordance with the tenets of the Declaration of Helsinki.

3.2.2 Methods

All subjects were examined 3-6 months post-operatively by the principal investigator. During this visit the following tests were performed:

3.2.2.1 Full Refraction

A full refraction was preformed utilising the same methodology detailed in Chapter 2. A Humphrey's binocular balancing technique was employed at the end of refraction to ensure a maximum plus refraction was achieved in the *Tetraflex* group

3.2.2.2 Subjective Assessment of Near and Intermediate Vision

All subjects were required to complete the initial unreduced NAVQ at this three-month post-operative visit. The NAVQ was selected for validation, as it is a specific near vision questionnaire, designed for different methods of presbyopic correction, including multifocal and accommodating IOLs. The questions did not require modification for use with these subjects. All subjects completed the questionnaire unassisted but were reminded to provide answers best describing their vision without the use of spectacles.

One and a half weeks following the appointment all subjects were posted the questionnaire and were instructed to return it completed within a two-week period. Failure to return the questionnaires within two weeks resulted in exclusion of both sets of results from the repitition analysis.

3.2.2.3 Assessment of Reading Ability

The *MNRead* chart was used to measure binocular reading speed over a variety of print sizes, at a distance of 40 cm, with full distance refraction in place. Each subject was instructed to read each paragraph as fast but as comfortably as possible. A card was used to obscure each line of text until required. The time taken to read each line of text was measured with a stopwatch to the nearest 0.1-second. A strict constant illumination of 500 Lux (120 cdm^2) was maintained for all *MNRead* measurements. A practice session was not used as previous studies have shown this as unnecessary (Subramanian and Pardhan, 2009). The *MNRead* has had extensive repeatability studies showing high repeatability in the assessment of children (Virgili *et al.,* 2004b), pre-presbyopic subjects (Subramanian and Pardhan, 2006), low vision subjects (Subramanian and Pardhan, 2009) and with pseudophakic subjects with presbyopic correction (Brown *et al.,* 2009; Sanders and Sanders, 2009). Therefore assessment of the repeatability of the *MNRead* was deemed unnecessary for this study.

3.3 Statistical analysis

3.3.1 Assumption of Normality

The one-sample Kolmogrov-Smirnov test was used to determine if results from each measurement followed a normal distribution. Where the data followed a normal distribution parametric analysis was used; non-parametric statistical analysis was used for non-normally distributed data.

3.3.2 Subject Demographics

A one-way ANOVA was used to determine if there was a statistical difference between group ages and refractive outcomes.

3.3.3 Analysis of the *Minnesota Near Reading Chart*

3.3.3.1 Asymptotic Curve Fitting

For each individual subject's data set, reading speed (y) in words per minute (WPM) was plotted against print size (x) in LogMAR. An asymptotic curve was then fitted to the data (Equation 3.7) using the least squared non-linear regression function of *Statistica* version 9 (Statsoft Inc., Tulsa, OK, USA). The logarithm of the reading speed was calculated and was then plotted against the print size (x); asymptotic curves were again plotted for each resultant dataset.

$$y = a - b\exp^{-cx}$$ **Equation 3.7**

3.3.3.2 Calculation of Reading Acuity

Reading acuity was defined as the smallest print size that can be resolved regardless of speed. This metric regards each word as having a value of 0.01 Log Units. Reading acuity was calculated using Equation 3.2. A one-way ANOVA was conducted to determine group differences; where significant differences were found the Games-Howells *post hoc* test was performed to determine the pair-wise differences.

3.3.3.3 Calculation of Maximum Reading Speed

Maximum reading speed was calculated in two ways: First, it was calculated using the median reading speed of the first three paragraphs. Second, it was calculated and recorded as the asymptote 'a' of the asymptotic curve function. To assess the difference

between these two measures of maximum reading speed, difference versus mean plots were evaluated (Bland and Altman, 1986). Furthermore a one-way ANOVA was used to determine the difference between each IOL group with both metrics.

3.3.3.4 Calculation of Critical Print Size

Critical print size was measured through visual inspection and asymptotic curve fitting:

3.3.3.4.1 Visual Inspection

A scatter plot of *MNRead* scores was drawn on *Sigmaplot* (SPSS Inc, Chicago, IL, USA) from which the CPS was determined subjectively by two examiners. The first examiner was the principal investigator of the study who was familiar with the analysis of the *MNRead*. The second examiner was a UK trained optometrist who was provided with the scatter plots and instructions to determine CPS attained from the website http://gandalf.psych.umn.edu/groups/gellab/MNREAD/speed.html (accessed 27/09/2010).

3.3.3.4.2 Asymptotic Curve Fitting

CPS was calculated as x when $y = 80\%$, 90%, 95% and 99% of the asymptote (a) using Equation 3.8.

$$x = \frac{-\ln\left(\frac{a-y}{b}\right)}{c}$$
      Equation 3.8

Difference versus mean plots was used to examine the differences between the 5 metrics. One-way ANOVAs with Games-Howells *post hoc* testing was used to assess differences between the IOL groups.

3.3.3.4.3 Reading Performance Index

A single metric – the reading performance index (RPI) – was calculated, incorporating reading speed over a wide range of print sizes the area under the graph was calculated using the integral of the asymptotic function (Equation 3.9). The lower limit for integration was the x value when $y=0$ and the upper limit of x was defined as 1.0 LogMAR (Figure 3.1).

$$\int_{a_1}^{a_0} ax + \left(\frac{b}{c}\exp^{-cx}\right) + d \qquad \textbf{Equation 3.9}$$

Where $d = d_1 + d_2$
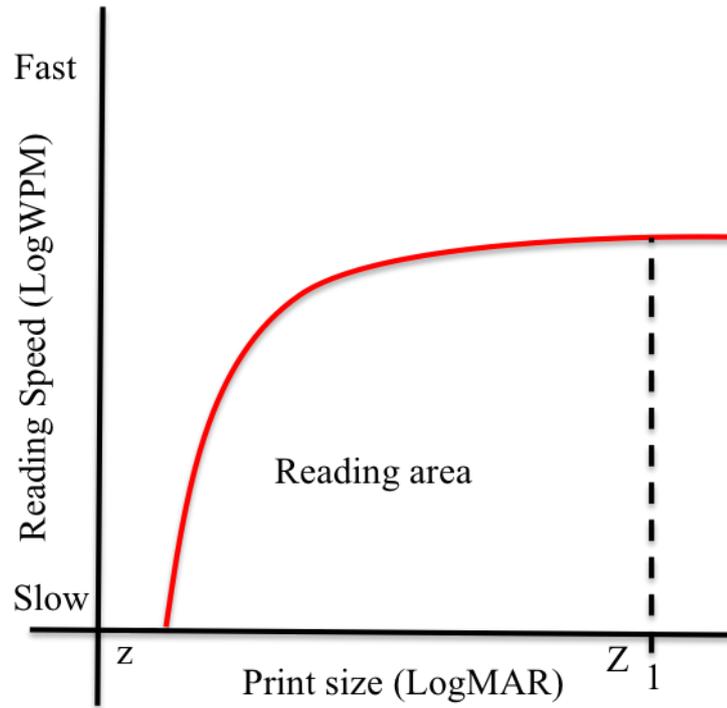
Figure 3.1 *The reading perception index is calculated as the area under the curve between 1.0 LogMAR and the value of x when y = 0*

A third data set was created to normalise for individual differences in maximum reading speed (adjusted RPI). The asymptote of the curve (*a*) was calculated for each curve. The average value of the asymptote was calculated for the entire data set, then each data set was normalised to this average value by multiplying all data points in the series for each subject by the ratio of difference. The result gave an equal asymptote value for each subject. The area under each curve was recalculated with the adjusted datasets to attain normalised reading areas accounting for individual differences in reading speed.

Differences in reading area were examined using a one-way ANOVA with Games-Howells *post hoc* tests.

3.3.4 Near Activity Vision Questionnaire Analysis

Rasch analysis was used to reduce questions to those relevant for measuring near vision ability and to reduce the rating scale for each question. The results of the first 23-items were required to fit both category function statistics (this helps refine the rating scale) and item fit statistics (to determine the appropriate questions). The last 3-items were calculated to fit the category function.

3.3.4.1 Assessment of the Item Response Scales

A category function table was used to refine the response scale to ensure that all item responses were relevant to the final Rasch score for both the first 23-question items and for the final 3-questions. The criteria used to determine suitability was as follows.

- Structure calibration and category measure values were required to increase in number with each response category.
- The outfit mean square was required to fall within the value of 0.6 to 1.4
- The probability of response would be at approximately 50%

If the criteria were not met the responses would be combined with adjacent categories until all statistics met the requirements.

3.3.4.2 Item Fit Categories

Item fit statistics were used to remove inappropriate questions from the NAVQ questionnaire. All question items were required to match the criteria of four specific Item fit tests:

3.3.4.2.1 Item Fit Statistics

Item fit statistics refer to how precise the data set item scores match predicted scores determined by the Rasch model. The values provided by both the infit and outfit mean square (MNSQ) provide a description of how well the results of a particular item fit the Rasch model. The Outfit mean square (MNSQ) is susceptible to the influence of outlying data whilst the infit MNSQ is influenced by general trends in scores. The values of Output MNSQ and Input MNSQ should fall within the range of $0.6 - 1.4$ as below 0.6 and the item responses are deemed too predictable and above 1.4 is deemed too variable (Wright and Linacre, 1994).

3.3.4.2.2 Item Targeting

Item targeting is conducted using the Persons map of Items*:* this displays on a vertical scale the extent of scores from the subjects and items. The higher on the scale the person or item score, the higher the overall Rasch score. The mean and standard deviations are shown for both and the aim is to achieve provide similar means. Items furthest away from the mean line fit the model the least and so require elimination. Large gaps between items indicate a gap in the response category and thus would indicate that additional items need to be added (Stelmack *et al.,* 2004).

3.3.4.2.3 Frequency of Endorsement

Frequency of endorsement describes the percentage of subjects that select each response category per item. If the proportion of subjects that select a particular category response is high then the suggestion is that the item is too predictable and measurement of this attribute is unnecessary. 65% and 80% has been proposed as suitable criteria for frequency of endorsement (Streiner and Norman, 1995; Wolffsohn and Cochrane, 2000).

3.3.4.2.4 Skew and Kurtosis

If data is skewed then it does not form a symmetrical frequency distribution, this would result in a prevalence of high scores with positive skew or low scores with negative skew for the particular item. The level of kurtosis corresponds to the height of the frequency distribution peak; a high kurtosis value represents a uniform spread of answers. Values greater than 2 for both skew and kurtosis suggest that the item is not appropriate for the instrument (Streiner and Norman, 1995).

Items are ranked by suitability to the 4-criteria; the poorest fitting items are removed one at a time with the statistics recalculated after removal. Determining the order of item reduction and item fit statistics, are regarded as the most important criterion followed by item targeting, frequency of endorsement, and skew and kurtosis. Removal of items continues until all items fit the statistics or until the separation index drops below 2; although this results in a loss of instrument sensitivity (Gupta *et al.,* 2007b).

3.3.4.3 Reliability Statistics

Assessment of internal consistency was determined using Cronbach's alpha coefficient; this examines the internal consistency of the questionnaire. Repeatability of results was evaluated by performing intraclass correlation coefficient (ICC). The ICC used was based around a two-way mixed ANOVA model with a 95% confidence interval. Single value absolute agreement ICCs were calculated as the questionnaire is designed to be examiner independent.

Furthermore a receiver operating characteristic (ROC) curve was constructed, the results of the non-reduced general satisfaction scale (Item-26) was used to categorize subjects as having good near vision (categories 0-2) or poor near vision (categories 3-6). It has been suggested that an area under the curve of greater than 0.6 indicates a high level of discriminative ability (Gupta *et al.,* 2007b).

A one-way ANOVA with a Games-Howells *post hoc* testing was used to determine the differences between the subjective scores for each of the groups.

3.3.5 Comparison of Metrics

Pearson's product moment correlation coefficient was used to determine the correlation between the NAVQ scores and the resultant *MNRead* statistics. A stepwise linear regression coefficient was calculated to determine the relationship of the *MNRead* metrics with the NAVQ scores.

3.4 Results

The ages of the 110 subjects were similar between groups ($F_5=1.526$, p=0.188).

3.4.1 *Minnesota Near Reading Chart* analysis

3.4.1.1 Determining Maximum Reading Speed

The results of the two MRS metrics are displayed in Table 3.4. The mean difference (95% confidence interval) in reading speed between the metrics was 1.72 (± 17.16; graph 3.2).

The maximum reading speed was similar for each of the intraocular lens groups when measured as the median of print sizes from 1.3 to 1.1 LogMAR ($F_5=1.136$, $p=0.348$) and when measured as the asymptote of the curve ($F_5=1.266$, $p=0.286$).

	Maximum reading speed Mean±SD (Words Per Minute)	
	Median of print sizes 1.3 to 1.1 LogMAR	**Denoted by the asymptote of a curve**
Bilateral *Softec 1*	163.71 ± 10.63	163.03 ± 11.90
Bilateral *ReZoom*	163.33 ± 21.64	162.98 ± 18.87
Bilateral *Tecnis ZM900*	161.66 ± 16.81	159.03 ± 18.93
Mix and Match	170.57 ± 15.81	169.21 ± 17.62
Bilateral *Lentis Mplus*	164.60 ± 23.26	161.46 ± 22.19
Bilateral *Tetraflex*	154.06 ± 24.48	151.92 ± 25.25
Total	162.99 ± 19.46	161.27 ± 19.71

Table 3.3 Mean values of maximum reading speed calculated as the Median of the print sizes between 1.3 to 1.1 logMAR and as denoted by the asymptote of the curve
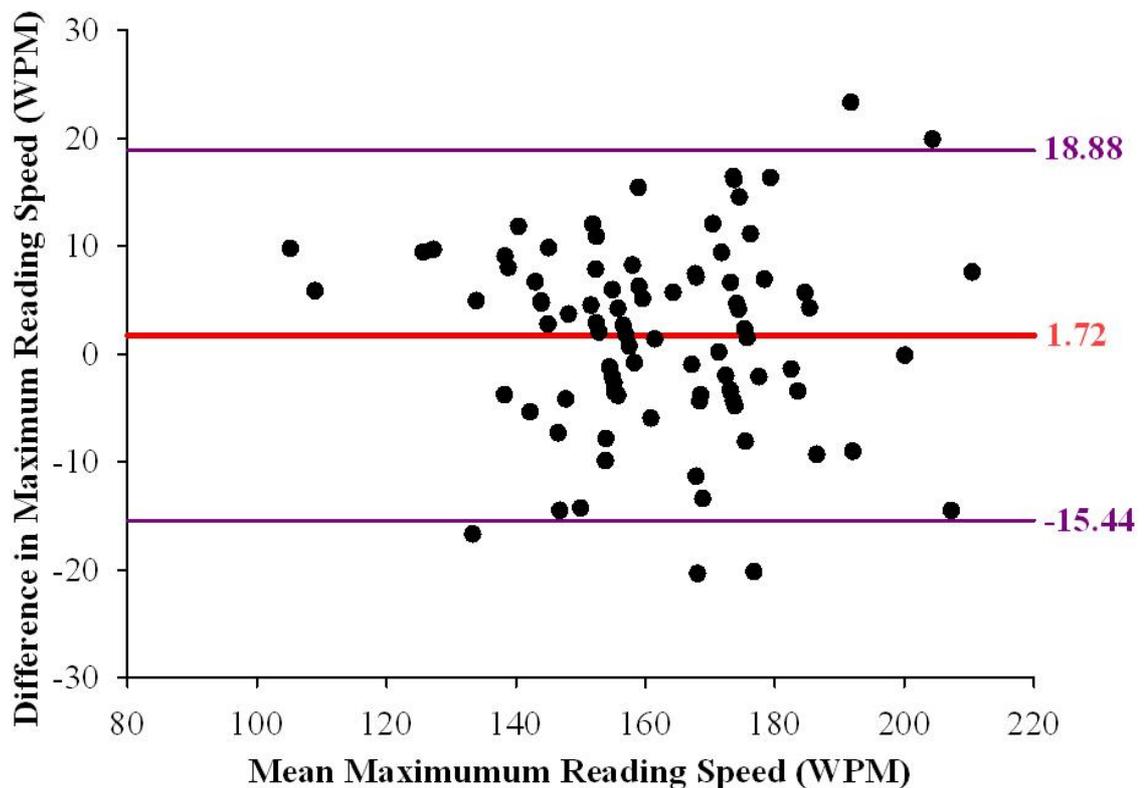
Figure 3.2 Bland and Altman plot comparing maximum reading speed as calculated using the median reading speed of the first three Minnesota Near Reading Chart paragraphs and as calculated using the value a from the asymptotic curve

3.4.1.2 Critical Print Size

The results of the five CPS metrics are displayed in Table 3.5. The mean difference (95% confidence interval) in CPS when measured using the visual inspection method and 80% of the asymptote was 0.1887 (±0.2421) LogMAR. The difference was 0.1470 (±0.2497) logMAR when the visual inspection method was compared with 90% (of the asymptote), 0.1053 (±0.2617) logMAR when compared with 95% and 0.0083(±0.3032) LogMAR when compared with 99% (Figure 3.3).

	Critical print size Mean±SD (logMAR)				
	Visual inspection	x when y=80% of the asymptote	x when y=90% of the asymptote	x when y=95% of the asymptote	x when y=99% of the asymptote
Bilateral *Softec 1*	0.60±0.08	0.41±0.06	0.45±0.06	0.49±0.06	0.59±0.09
Bilateral *ReZoom*	0.37±0.14	0.20±0.12	0.25±0.12	0.29±0.16	0.40±0.11
Bilateral *Tecnis*	0.37±0.18	0.16±0.17	0.21±0.18	0.25±0.20	0.36±0.23
Mix and Match	0.34±0.20	0.12±0.19	0.17±0.19	0.22±0.19	0.33±0.20
Bilateral *Lentis Mplus*	0.19±0.12	0.05±0.11	0.08±0.11	0.12±0.11	0.20±0.12
Tetraflex	0.54±0.15	0.34±0.11	0.37±0.11	0.41±0.11	0.50±0.12
Total	0.40±0.20	0.21±0.18	0.26±0.18	0.30±0.18	0.39±0.20

Table 3.4 *The main values of the 5 values used to calculate critical print size*
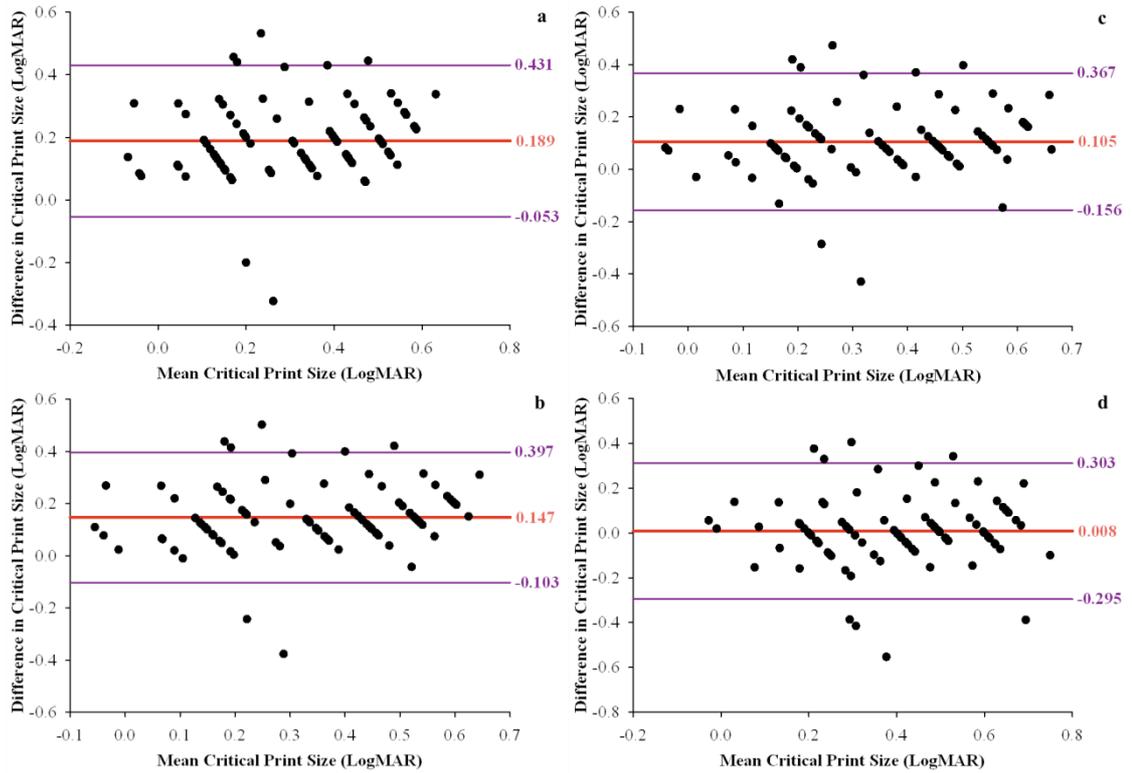
Figure 3.3 Bland and Altman plots comparing critical print size as calculated using the visual inspection method and with 80% (a), 90% (b), 95% (c) and 99% (d) of the asymptote

A significant difference in critical print size between the IOL groups was found regardless of the metric used to calculate CPS (Visual inspection; $F_5=14.227$, $p<0.001$, 80% of the asymptote; $F_5=15.557$, $p<0.001$, 90% of the asymptote; $F_5=15.557$, $p<0.001$, 95% of the asymptote; $F_5=14.390$, $p<0.001$ and 99% of the asymptote; $F_5=11.711$, $p<0.001$). According to all of the metrics the multifocal groups achieved a better CPS than the *Softec 1* group; additionally the *Lentis Mplus* group achieved a higher CPS score in comparison to the *ReZoom* multifocal, and the 'mix and match' group and *Lentis MPLus* group provided significantly greater CPS scores in comparison with the *Tetraflex* group. The visual inspection metric showed better CPS scores with the *ReZoom* group in comparison with the *Tetraflex* group, and with the *Lentis MPLus* group in comparison with the *Tecnis ZM900*. However the other metrics did not show this difference (Table 3.6).

		Metric used to assess critical print size				
IOLs compared		**Visual Inspection**	**% of the asymptote**			
1	**2**		**80**	**90**	**95**	**99**
Softec 1	*ReZoom*	**p=0.001**	**p=0.001**	**p=0.001**	**p=0.002**	**p=0.011**
Softec 1	*Tecnis ZM900*	**p=0.001**	**p<0.001**	**p<0.001**	**p<0.001**	**p=0.001**
Softec 1	Mix and match	**p<0.001**	**p<0.001**	**p<0.001**	**p<0.001**	**p<0.001**
Softec 1	*Lentis Mplus*	**p<0.001**	**p<0.001**	**p<0.001**	**p<0.001**	**p<0.001**
Softec 1	*Tetraflex*	p=0.883	p=0.674	p=0.615	p=0.573	p=0.540
ReZoom	*Tecnis ZM900*	p=1.000	p=0.964	p=0.966	p=0.971	p=0.983
ReZoom	Mix and Match	p=0.990	p=0.591	p=0.647	p=0.714	p=0.864
ReZoom	*Lentis Mplus*	**p=0.018**	**p=0.023**	**p=0.014**	**p=0.010**	**p=0.009**
ReZoom	*Tetraflex*	**p=0.037**	p=0.074	p=0.117	p=0.189	p=0.490
Tecnis ZM900	Mix and Match	P=0.990	p=0.967	p=0.978	p=0.987	p=0.998
Tecnis ZM900	*Lentis Mplus*	**p=0.018**	p=0.172	p=0.172	p=0.086	p=0.062
Tecnis ZM900	*Tetraflex*	**P=0.037**	**p=0.007**	**p=0.014**	**p=0.029**	p=0.150
Mix and Match	*Lentis Mplus*	p=0.092	p=0.608	p=0.446	p=0.323	p=0.175
Mix and Match	*Tetraflex*	**p=0.006**	**p<0.001**	**p=0.001**	**p=0.004**	p=0.051
Lentis Mplus	*Tetraflex*	**p<0.001**	**p<0.001**	**p<0.001**	**p<0.001**	**p<0.001**

Table 3.5 *Games Howells post-hoc examinations of the differences between the intraocular lens designs*

The mean difference in CPS scores as measured by visual inspection was 0.03 (±0.25; figure 3.4) LogMAR when measured by two different examiners and the ICC was 0.761.
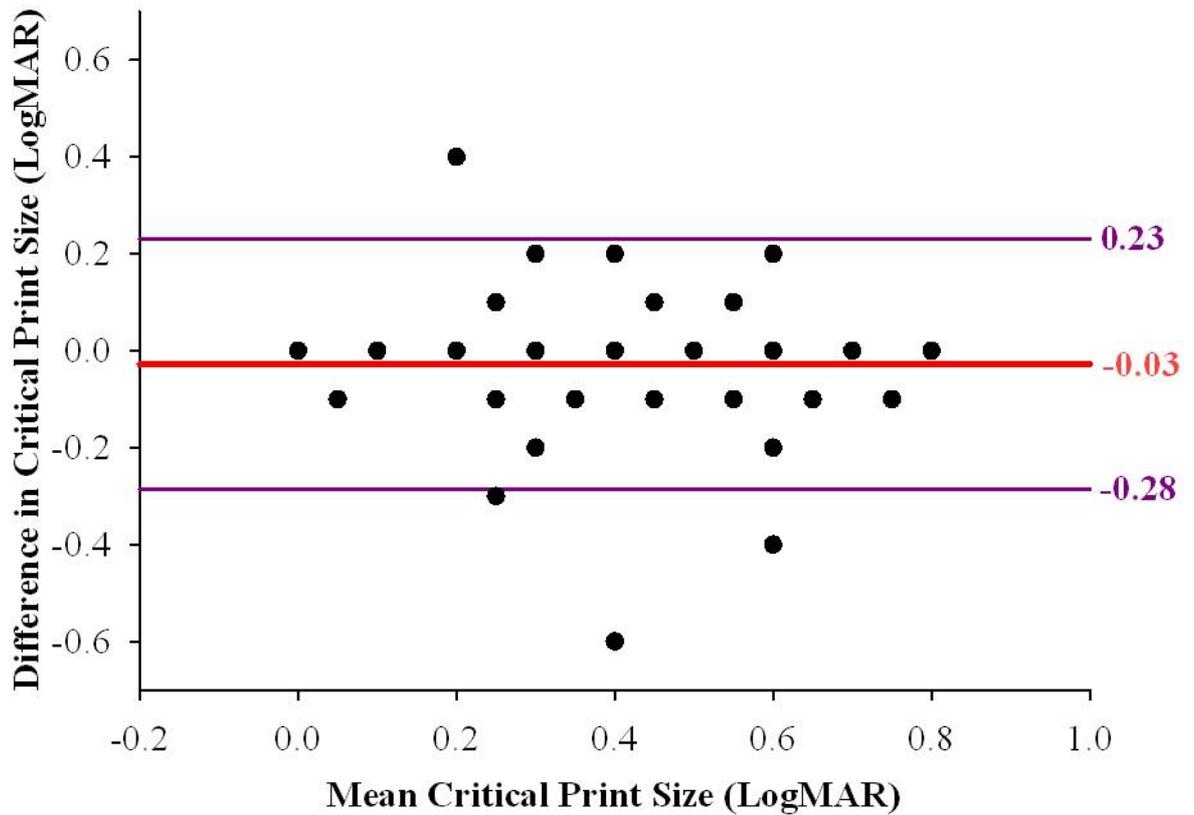
Figure 3.4 *Bland and Altman plot comparing critical print size as measured by the two examiners.*

3.4.1.3 Reading Acuity

Overall there was a significant difference in reading acuities between the different IOL groups (F_5=14.911, p<0.001; Table 3.7). The reading acuity with each of the multifocal groups was similar, as was the reading acuity of the *Softec 1* and *Tetraflex* groups. However, the multifocal groups all achieved better reading acuity scores in comparison with the *Softec 1* and *Tetraflex* groups (Table 3.8).

	Softec 1	ReZoom	Tecnis ZM900	Mix and Match	Lentis MPlus	Tetraflex
Reading acuity mean±SD (LogMAR)	0.41±0.08	0.20±0.14	0.16±0.15	0.11±0.21	0.07±0.12	0.36±0.11

Table 3.6 *Reading acuity of each of the IOL groups*

	Softec 1	ReZoom	Tencis ZM900	Mix and Match	Lentis MPlus
ReZoom	p = 0.001				
Tecnis ZM900	p < 0.001	p = 1.000			
Mix and Match	p < 0.001	p = 1.000	p = 1.000		
Lentis MPlus	p < 0.001	p = 0.153	p = 1.000	p = 1.000	
Tetraflex	p = 1.000	p = 0.033	p = 0.002	p < 0.001	p < 0.001

Table 3.7 *Games Howells post hoc testing results for the intraocular lens groups*

3.4.1.4   Reading Performance Index

The adjusted and non-adjusted reading performance index for each group is shown in Figure 3.5. The mean difference (95% confidence interval) in reading area between the adjusted and non-adjusted values was –0.002 (±0.099) LogWPM*LogMAR. There was a significant difference in the adjusted and non-adjusted reading areas between the 6 groups (adjusted; F_5=15.232, p<0.001, non-adjusted; F_5=15.394, p<0.001). The adjusted and non-adjusted reading area was greater with the MIOLs than with both the monofocal and accommodating IOLs. The *Lentis Mplus* group provided a greater adjusted and non-adjusted RPI than the *ReZoom* group (Table 3.9).
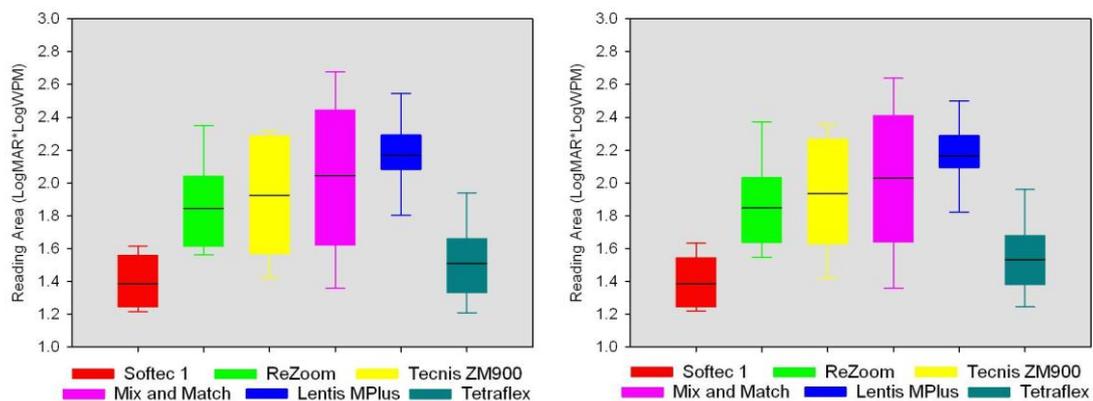
Figure 3.5 *Adjusted (right diagram) and non-adjusted (left diagram) reading performance index results for each group*

	Softec 1	ReZoom	Tencis ZM900	Mix and Match	Lentis MPlus
Post-hoc results for the non-adjusted RPI					
ReZoom	p = 0.001				
Tencis ZM900	p < 0.001	p = 0.980			
Mix and Match	p < 0.001	p = 0.477	p = 0.889		
Lentis MPlus	p < 0.001	p = 0.049	p = 0.250	p = 0.872	
Tetraflex	p = 0.862	p = 0.038	p = 0.005	p < 0.001	p < 0.001
Post-hoc results for the adjusted RPI					
ReZoom	p = 0.001				
Tencis ZM900	p < 0.001	p = 0.963			
Mix and Match	p < 0.001	p = 0.554	p =0.956		
Lentis MPlus	p < 0.001	p = 0.044	p = 0.284	p = 0.798	
Tetraflex	p = 0.734	p = 0.052	p = 0.005	p < 0.001	p < 0.001

Table 3.8 *Games Howells post hoc testing results for the intraocular lens groups*

3.4.2   Near Activity Visual Questionnaire Analysis

3.4.2.1   Results of Category and Item Reduction

The item and category reduction procedure resulted in a final 9-item questionnaire, each with a 4-response category scale (plus an additional not applicable response). The resultant Rasch separation index and reliability index was 2.78 and 0.89. The final 3 questions were reduced to having a 5-response scale (Appendix A4).

3.4.2.2   Near Activity Visual Questionnaire with Presbyopic Correcting Intraocular Lenses

The results of the reduced NAVQ are displayed in Table 3.10. There was a significant difference between the groups $F_5=33.156$, p<0.001. Post hoc testing revealed a difference between the *Softec 1* group and all other groups. Similarly the *Tecnis*

ZM900, Mix and match and the *Lentis Mplus* groups achieved significantly higher NAVQ results in comparison with the *Tetraflex* group (Table 3.11).

	Softec 1	*ReZoom*	*Tecnis ZM900*	**Mix and Match**	*Lentis MPlus*	*Tetraflex*
NAVQ results Mean±SD Logits	55.07 ± 7.99	19.62 ± 13.40	11.39 ±10.96	16.39 ± 11.99	16.14 ± 15.05	29.21 ± 11.73

Table 3.9 *Result of the Near Activity Visual Questionnaire for each intraocular lens group*

	Softec 1	**ReZoom**	**Tencis ZM900**	**Mix and Match**	**Lentis Mplus**
ReZoom	p < 0.001				
Tencis ZM900	p < 0.001	p = 0.355			
Mix and Match	p < 0.001	p = 0.932	p = 0.857		
Lentis MPlus	p < 0.001	p = 0.942	p = 0.931	p = 1.000	
Tetraflex	p < 0.001	p = 0.196	p < 0.001	p = 0.009	p = 0.034

Table 3.10 *Games Howells post hoc testing results for the intraocular lens groups*

3.4.3 Correlation Between the Minnesota Near Reading Chart Metrics and the Near Activity Visual Questionnaire results

All of the MNRead metrics displayed a moderate correlation with the results of the NAVQ except for the two MRS metrics (Table 3.12)

	Correlation of MNRead metrics with the reduced NAVQ results									
	Critical print size					Maximum reading speed		RPI		Reading acuity
	Visual inspection	80%	90%	95%	99%	*a*	Median of three	Adjusted	Non-adjusted	
rs	0.562	0.545	0.527	0.506	0.464	0.006	-0.080	-0.548	-0.566	0.558
Sig	P<0.001	P<0.001	P<0.001	P<0.001	P<0.001	0.933	0.452	P<0.001	P<0.001	P<0.001

Table 3.11 *Correlation of Minnesota near reading metrics with the Near Activity visual Questionnaire results*

The average NAVQ scores from the 75 subjects who completed the questionnaire both on the day of assessment and again within one month of examination was: 27.01 ± 18.11 and 29.03 ± 20.20 Logits respectively. The test retest reliability ICC was calculated as 0.715.

The multiple linear regression model showed that the unadjusted reading area metric accounted for 57% of the reduced NAVQ results. A further 2% could be accounted for by including the CPS calculated by visual inspection (Equation 3.10). MRS and RA did not contribute to subjective rated near performance.

NAVQ scores = 6.664 + (29.227xReading area) + (28.293 x CPS visual inspection)

Equation 3.10

3.5 Discussion

Maximum Reading Speed (MRS) was similar for all of the IOL groups; this highlights the fact that MRS is related more to cognitive factors rather than visual acuity. Previous literature has highlighted the importance of age matching each subject group as MRS can be linked with age. Therefore MRS is not a useful tool for evaluating determining differences between IOL groups. However, it is a useful metric for ensuring that the reading ability of each subject group, independent of vision, is the same.

The traditional measurement of CPS is to visually inspect a scatter plot and subjectively determine the smallest print size for which MRS is maintained. Using asymptotic curve functions to determine CPS allows an objective measurement. In the study by Cheung and colleagues (2008) CPS in subjects with AMD was defined as 80% of the MRS as determined by an asymptotic curve. In this study CPS defined by visual inspection was compared with CPS defined as a percentage of the MRS. The average CPS scores were closest when 99% of the MRS was used. However, this percentage score showed the least levels of correlation with the resultant NAVQ score and was least likely to detect a difference between IOL groups. 80% of the MRS proved to be the most discriminatory and correlated the best with the NAVQ scores however the average score displayed the highest disparity in comparison with CPS by visual inspection. In contrast the 90% and 95% values proved to be a compromise between the two results. The visual inspection method correlated highest with the

NAVQ results however the analysis of results demonstrated a relatively high level of inter-observer variability

The reading performance index (RPI) metric proposed by this study describes reading ability over a wide range of print sizes. The non-adjusted reading area had a slightly higher correlation with the NAVQ results in comparison with the adjusted area, but both proved to be similarly discriminative. The MRS was similar for each group; this explains the relatively small impact the adjustment of the asymptote had on the RPI.

As expected there was no correlation between the NAVQ results and MRS. The CPS, reading acuity and RPI all demonstrated a similar moderate correlation with the NAVQ results. Multiple linear regression revealed that the RPI accounted for the largest proportion of the NAVQ results. This highlights the value of the RPI metric but suggests that evaluation of the CPS using curve fitting metrics does not illuminate additional detail regarding reading vision. This suggests that RPI is the most appropriate single metric used to describe reading ability with pseudophakic presbyopic correction, especially since CPS through visual inspection is susceptible to inter-observer error.

In the present study reading speed was measured at 40 cm with the *MNread*, which corresponds with an effective reading addition of +2.50. The results show that RPI was greater with the *Lentis Mplus* than the *ReZoom* group. In support of these findings a similar result was attained from the defocus curve measurements in Chapter 2, where the binocular *Lentis MPlus* group achieved a higher VA with a -2.50 D in comparison to the binocular *ReZoom* group at the $p<0.001$ level. The defocus curves highlighted a difference between the *Tecnis ZM900* and *Lentis MPlus* groups at the $p<0.05$ level; this difference was not found using any of the *MNRead* metrics. No other differences between multifocal groups were present either with the defocus curves or with the reading area. For comparison of MIOLs, it is important to consider the distance at which the *MNRead* is measured, as the reading addition of the IOL will determine which distance will provide favourable results. As the *MNRead* uses a standardized logarithmic scaling of letter size, it can be used at several distances provided that the distances are changed by the corresponding logarithmic progression; this is an important consideration if MIOLs with different reading additions are compared.

No significant difference in the adjusted and non-adjusted RPI was found between the *Softec 1* and *Tetraflex* groups. In a previous study involving 255 subjects implanted with the *Tetraflex* IOL and 101 subjects implanted with a monofocal IOL; reading ability was higher with the accommodating IOL. This prior study utilised a direct comparison method where reading speed, at every print size, was compared using the Wilcoxon Mann-Whitney U statistical test with Bonferroni correction (Packer *et al.,* 2010). Research shows that single optic accommodative IOLs provide a low level of accommodation; these levels appear to be too small to be measured consistently using reading charts.

The reduced NAVQ was deemed reliable and valid for use with accommodative and multifocal IOL subjects and achieved high test-retest reliability. This study has used a short three-week post evaluation limit for the return of the repeated NAVQ, to reduce the chances of adverse complications influencing the results.

The usefulness of Cronbach's alpha has been questioned as increasing subject numbers increase the coefficient value. The coefficient for the reduced 9-item NAVQ was higher (0.95) suggesting that all items were well correlated and so contributed towards the assessment of near visual ability.

The separation index for the NAVQ was 2.78 which shows that the questionnaire is able to discriminate between subjects with and without near vision difficulties. This conclusion is supported by the ROC curve where the area under the curve was 0.941.

The correlation between the *MNRead* results and NAVQ results demonstrates good construct validity. The small disparity between the methods may be explained by the inclusion of detailed questions regarding computer use and looking at the details on a wristwatch face. Typically these tasks are performed at a distance further than the 40 cm as detailed by the *MNRead*.

3.6 Limitations of the Study

For the assessment of reading ability the *MNRead* was placed at a single set distance (40 cm). This is an important factor as it biases the measurement of reading ability to favour MIOLs with an effective addition of +2.50 D. However, as the *MNRead* uses a logarithmic progression, it is important that the distance is standardized. Ideally

measurement of reading ability should be preformed at several distances to cover distances corresponding with the effective additions of each lens. However, this would require several reading charts as randomization would be required to reduce the memorization effect (Gupta *et al.,* 2007). The *Radner* reading charts may be ideal for this purpose, as Multiple *Radner* charts exist, each with a consistent and standardized sentence construction.

Validation of questionnaires require a large subject base, the power of this study could be improved by the inclusion of additional groups such as duel-optic accommodating IOLs, partially diffractive multifocal IOLs and monofocal IOLs implanted according to a monovision strategy.

3.7 Conclusion

The present study proposes two new techniques for the assessment of pseudophakic correction of presbyopia. The first concerns the analysis of reading ability by using the metric; reading performance index (RPI). The following steps are required to calculate RPI.

- The time taken to read each paragraph is converted to reading speed (WPM), correcting for errors.
- The reading speed is converted to a logarithmic scale (logWPM).
- A asymptotic function is then fitted to the data with print Size (logMAR) on the x-axis and Log reading speed (logWPM) on the y-axis.
- The integral of the function is then used to calculate reading area with the limits of integration being 1 and where y=0.

For future studies examining the subjective assessment of near vision in presbyopic correcting IOLs the shortened 9-item NAVQ should be used with the additional 3 independent items (Appendix A4). The 9 main items all use the full 5-category scale. The raw scores can then be adjusted by the conversion chart to provide a linear 0-100 Logits scale (Appendix A4). The 3 additional items can be used and provide a evaluation as to the speed of accommodative change, spectacle independence and overall satisfaction of vision, these items are assessed on a 5-category scale.

Defocus curves, reading ability and the subjective perception of near vision have all demonstrated that without a near addition the MIOLs provided a high level of near vision. Despite the increased range of clear vision, the improvement in reading ability and the greater subjective perception of near vision; there is still dissatisfaction post MIOL implantation. Dysphotopsia and residual refractive error constitute the majority of cases of MIOL dissatisfaction. In Chapter 4 a Halometer is designed and used to assess the extent of Dysphotopsia post MIOL implantation.

Chapter 4 Assessment of Dysphotopsia in Pseudophakic Subjects with Multifocal Intraocular Lenses

4.1 Introduction

Multifocal IOLs create two or more images within the eye; these images are focused at different planes. For distance viewing, the distance focal point will be in focus with the near focal point creating an out of focus blur circle on the retina. As a consequence contrast sensitivity is reduced and the secondary image causes unusual photopic phenomenon often described as haloes (Buznego and Trattler, 2009). The photopic phenomenon, often referred to as dysphotopsia in the literature, is a major cause of multifocal dissatisfaction (Woodward *et al.,* 2009) and is responsible for a relatively high frequency of MIOL explanations (Mamalis *et al.,* 2008).

4.1.1 Examination of Dysphotopsia

Understanding dysphotopsia is vital in achieving successful multifocal IOL implantation. The current literature shows that implantation of a multifocal rather than a monofocal IOL can lead to unwanted dysphotopsia (Leyland & Zinicola, 2003). However, the literature comparing IOLs is equivocal, due to the lack of objective methods for assessing dysphotopsia. The majority of studies use various subjective questionnaires in the form of; verbal interviews (Jacobi *et al.,* 2003), bespoke questionnaires (Kohnen *et al.,* 2006), validated questionnaires (Harman *et al.,* 2008) or through subject-initiated complaints (Shoji, 1996). An alternative method is to use graphics depicting visual demonstrations of different types of dysphotopsia allowing the subject to indicate which is most representative of what they perceive (Hunkeler *et al.,* 2002).

Instruments designed to measure the effects of disability glare are commonly used in MIOL studies. Disability glare is the reduction of vision from a glare source present within the visual field. This glare is due to the spread of light across the retina known as straylight (Vos, 1984). The majority of instruments, used to assess disability glare, are composed of a central target of diminishing spatial frequency or contrast sensitivity surrounded by a glare source. The intensity of the ambient light and glare source is changed to determine the effect this has on visual acuity or contrast sensitivity. Examples of this technique can be found in the form of the *Brightness Acuity Tester*

(BAT; Marco, Florida, USA), *Mesoptometer II* (Oculus Optikgeräte GmbH, Wetzlar-Dutenhofen, Germany) or Digital View-in visual testing units, such as the *Optec 6500* (Stereo Optical Co Inc, Chicago, Illinois). Several custom built glare testing units have also been developed (Bailey and Bullimore 1991). However, these testing units do not quantify the extent of dysphotopsia and the literature shows variable results. Similar studies involving the *C-Quant* (Oculus Optikgeräte GmbH, Wetzlar-Dutenhofen, Germany), an instrument for evaluating the quantity of ocular straylight, have failed to determine a difference between multifocal and monofocal IOLs. This disparity between reported dysphotopsia and the results recorded with glare testing units may be due to the optical properties of MIOLs. Dysphotopsia due to MIOLs is the result of a second out of focus image being present on the retina rather than diffuse straylight over the retinal surface (Hofmann *et al.,* 2009). Spherical refractive error results in an out of focus blur circle being present on the retina. MIOLs are designed so that one focal point produces a spot image and the second focal point produces the surrounding blur. This surrounding blur results in the retinal image having less contrast against its background and also results in the halo phenomenon. Table 4.1 presents a summary of the methodology used to measure dysphotopsia in MIOLs.

Author	IOL designs	Type of glare test	Results
Keates 1987	Refractive +4 D n=38(46)	Mentor Brightness acuity tester	No decrease in VA with the BAT
Keates 1989	Refractive +4 D n=10(?)	Mentor Brightness acuity tester	No decrease in VA with the BAT
Percival 1989	Diffractive +3.5 D n=55(55) Monofocal n=55(55)	Questionnaire	No difference with photopic phenomenon
Hansen 1990	Diffractive +3.5 D n=53(55)	Subject interview	No photopic phenomenon
Percival 1990	Diffractive +3.5 D n=55(55) monofocal n=55(55)	Questionnaire	No difference with photopic phenomenon
Percival 1991	Diffractive +3.5 D n=47(47) Refractive +4 D n=40(40) Refractive +3.5 D n=24(24)	Subject interview	Diffractive +3.5 D subjects noticed most photopic phenomenon refractive +3.5 D the least
Vanderschueren 1991	Diffractive +3.5 D n=16(12) Monofocal n=16(?)	Mentor Brightness acuity tester	Diffractive +3.5D slight decrease in VA for the first 8 weeks after not difference not tested with monofocal group
Gimbel 1991	Diffractive +3.5 D n=149(298) Monofocal n=131(262)	Questionnaire	Diffractive +3.5D higher prevalence of halos rings flare/glare.
Goes 1991	Diffractive +3.5 D n=?(269)	Subject interview	Glare diminished over time. No conclusive results
Steinert 1992	Refractive +3.5 D n=32(64) Monofocal n=30(60)	Questionnaire	No difference with photopic phenomenon
Namiki 1993	Phakic n=12(12) Monofocal a n=6(6) Monofocal b n=6(6) Monofocal c n=6(6) Monofocal d n=6(6) Diffractive +3.5 D n=6(6)	Perimetry halometer	Diffractive +3.5D slightly more glare not statistically significant
Winther-Nielsen 1993	Diffractive +3.5 D n=25(50) Monofocal n=23(46)	MCT 8000	Diffractive +3.5 D experienced reduction in CS when in twilight conditions with glare

Author	IOL designs	Type of glare test	Results
Akutsu 1993	Diffractive +3.5 D n=7(7) Monofocal n=7(7) Phakic n=7(7) Young phakic n=7(7)	Custom glare test	Pseudophakic more glare than phakic multifocal more glare than monofocal.
Auffarth 1993	Diffractive +3.5 D n=40(80) Monofocal n=40(80)	Mesoptometer II	Glare reduces CS more with diffractive +3.5 D group than with the monofocal group
Rüther 1993	Diffractive +3.50 D n=10(10) Monofocal n=10(10)	Custom glare test	No differences between groups
Rossetti 1994	Diffractive +3.5 D n=42(42) Monofocal n=38(38)	Questionnaire	Diffractive +3.5 D experienced more haloes than monofocal group
Wiemer 1994	Diffractive +3.5 D a n=35(?) Diffractive +3.5 D b n=50(?) Diffractive +4 D n=62(?) Monofocal n=50(?)	Mentor Brightness acuity tester	No significant difference in glare between groups
Schmidt 1994	Refractive +3.5 D n=35(?)	Mentor Brightness acuity tester	No comparative group
Hessemer 1994	Diffractive +3.5 D n=28(56) Monofocal n=28(56) Phakic n=28(56)	Ocutrast	Mesopic VA with glare worse with Diffractive +3.5 D group
Teping 1994	Refractive +4 D n=20(20) Refractive +3.5 D n=14(14)	Mesoptometer II –	No difference between groups
Winther-Nielsen 1995	Diffractive +3.5 D n=58(116) Monofocal n=63(126)	MCT 8000 Questionnaire	CS lower in diffractive +3.5 D group in twilight conditions with glare Reported difficulty with night driving
Weghaupt 1996	Refractive +3.5 D n=9(14) Monofocal n=?(13) Phakic n=?(16)	Mentor Brightness acuity tester	CS with glare lower in refractive group than other groups
Negishi 1996	Refractive +3.5 D n=30(48)	Titmus glare tester	Glare within normal limits

Author	IOL designs	Type of glare test	Results
Eisenmann 1996	Refractive +3.5 D n=27(?) Diffractive +3.5 D n=23(?) Monofocal n=25(?) Phakic cataract n=25(?)	Glare and Halo test	No difference between pseudophakic groups Greater glare in phakic subjects with cataract
Allen 1996	Diffractive +4 D n=79 Monofocal n=70	Questionnaire	Higher prevalence of glare and haloes
Shoji 1996	Refractive n=19(29) Refractive b n=?(33) Monofocal n=?	Subject reported symptoms	Prevalence of haloes
Vaquero 1996	Refractive +3.5 D n=42(?) Monofocal n=28 Phakic n=42	Mentor Brightness acuity tester	Similar glare results
Javitt 1997	Refractive +3.5 D n=100 Monofocal n=103	Modified cataract TyPE specification questionnaire	Driving towards headlights worse with multifocal
Negishi 1997	Refractive +3.5 D n=22(36) Monofocal n=31(52)	Questionnaire	Refractive +3.5D difficulty with night driving
Walkow 1997	Refractive +3.5 D n=40(80) Diffractive +4 D n=40(80)	Questionnaire	No difference in glare or haloes between groups
Vaquero-Ruano 1998	Refractive +3.5 D n=?(50) Monofocal n=?(50)	Questionnaire	Glare reduced past 2 months
Pieh 1998	Refractive +3.5 D n=25(29) Diffractive +3.5 D n=8(12)	Mentor Brightness acuity tester	CS with Glare worse with diffractive than refractive
Grosskopf 1998	Refractive +3.5 D n=50 Monofocal n=85 Phakic cataract n=41	Mesoptometer II	Both monofocal and multifocal groups significant levels of glare sensitivity
Arens 1999	Refractive +3.5 D n=21(42) Monofocal n=15(30)	Mentor Brightness acuity tester	No difference between groups
Steinert 1999	Refractive +3.5 D n=123 Monofocal n=123	Questionnaire	Higher reporting of glare and haloes in MIOL group

Author	IOL designs	Type of glare test	Results
Dick 1999	Refractive +3.5 D n=28(28) Monofocal n=28(28)	Questionnaire Glare and Halo test Straylightmeter	No significant difference between monofocal and multifocal group
Lesueur 2000	Refractive +3.5 D n=24(24) Refractive +4 D n=22(22)	Questionnaire	No difference in prevalence of haloes
Sasaki 2000	Refractive +3.5 D n=31(58)	Miller-Nadler glare tester	Night time CS with central glare was reduced
Javitt 2000	Refractive +3.5 D n=64(128) Monofocal n=60	Modified cataract TyPE specification questionnaire	Multifocal group more likely to report glare and haloes
Schmitz 2000	Refractive +3.5 D n=28(28) Monofocal n=28(28)	CSV1000 +HGT	No difference in CS in the presence of glare
Häring 2001	Refractive +3.5 D n=161(?) Monofocal n=123(?)	Questionnaire	Significantly more photopic phenomenon in refractive +3.5 D group in comparison with the monofocal group
Kamlesh 2001	Refractive +5 D n=20(20) Monofocal n=20(20)	Questionnaire	Prevalence of photopic phenomenon similar in each group.
Pieh 2001a	Refractive +3.5 D	Glare and Halo test Questionnaire	Size of halo similar when focused with distance or near focal point
Pieh 2001b	Refractive +3.5 D n=14(15) Monofocal n=10(11)	Mentor Brightness acuity tester	CS better with monofocal
Walkow 2001	Diffractive +4 D n=50(69)	Questionnaire	Low levels of glare and haloes
Dick 2002	Refractive +3.5 D n=25(50)	Questionnaire	Glare and haloes reported
Kaushik 2002	Refractive +5 D n=20(20 Monofocal n=20(20)	Questionnaire	NO difference between groups
Jacobi 2002	Refractive +3.5 D n=54(54) Monofocal n=40(41)	Questionnaire	Multifocal more photopic phenomenon than monofocal
Hunkeler 2002	Refractive +3.5 D n=22(?)	Gross estimation Halometer Visual categorization of dysphotopsia	Examined characteristics of halos

Author	IOL designs	Type of glare test	Results
Leyland 2002	Refractive +3.5 D n=29(58) Refractive +4 D n=15(30) Monofocal n=16(32)	Modified Cataract TyPE questionnaire Mentor Brightness acuity tester	Subjective symptoms worse in Refractive +3.5 D group than monofocal group. No difference between refractive + and monofocal CS showed no significant drop with any group with glare.
Sedgewick 2002	Refractive +3.5 D n=17(34) Monofocal n=15(30)	Verbal interview	Photopic phenomenon more significant with multifocal IOL
Rau 2003	Refractive +4 D N=40(80)	Questionnaire	Reporting on levels of photopic phenomenon
Jacobi 2003	Refractive +3.5 D n=29(29) Monofocal n=22	Questionnaire	Photopic phenomenon more prevalent in Refractive +3.5 D group than in the monofocal group
Aralikatti 2004	Refractive +3.5 D n=15(15)	Questionnaire	Prevalence of glare
Baïkoff 2004	Phakic refractive +2.5 D n=33(55)	Verbal interview	Prevalence of glare
Nijkamp 2004	Refractive +3.5 D n=68 Monofocal n=69	Modified CS5 questionnaire	Photopic phenomenon more prevalent in refractive +3.5 D group than in the monofocal group
Sen 2004	Refractive +3.5 D n=35(53) Monofocal n=40(67)	Modified CS5 questionnaire	Photopic phenomenon more common in refractive +3.5 D group
Alió 2004	Refractive +3.5 D n=16(32) Asymmetrical Diffractive +4 D n=12(24) Single Optic Accommodative n=12(24)	Questionnaire	Photopic phenomenon more common in refractive and diffractive group in comparison to the single optic accommodative.
Lee 2005	Refractive +3.5 D n=199(224)	Questionnaire	No differences in halos with refractive error
Mester 2005	Refractive +3.5 D n=14(28) Asymmetrical diffractive n=16(32)	Verbal interview	Prevalence of photopic phenomenon with both IOL types
Wang 2005	Refractive +3.5 D n=27(45)	Verbal interview Modified Cataract TyPE specification	Prevalence of photopic phenomenon
Elgohary 2006	Refractive +3.5 D n=17 Monofocal n=10	Questionnaire	Higher prevalence of photopic phenomenon with multifocal group

Author	IOL designs	Type of glare test	Results
Kohnen 2006	Appodized diffractive +4 D n=117(234)	Questionnaire	Prevalence of photopic phenomenon
Chiam 2006	Apodized diffractive +4 D n=40(80) Monofocal n=40(80)	Verbal interview	Prevalence phenomenon more common in multifocal group in comparison to monofocal
Renieri 2006	Refractive +3.5 D n=18(18) Apodized diffractive +4 D n=18(18)	CSV 1000 HGT Questionnaire	No difference in CS levels between groups. More subjective photopic phenomenon with diffractive group
Salati 2007	Refractive +3.0 D n=62(124)	Questionnaire	Halos more prevalent with large pupils
Zeng 2007	Refractive +3.5 D n=10(20) Aspheric n=10(20) Monofocal n=10(20)	CSV 1000 HGT Modified Cataract TyPE specification questionnaire	CS worse both with and without glare
Lubiński 2007	Refractive +3.5 D n=20(40)	CSV 1000 HGT Modified Cataract TyPE specification questionnaire	Prevalence of Photopic phenomenon
Petermeier 2007	Apodized diffractive n=32(55)	Questionnaire FACT CS chart with glare	Halo prevalence
Zhang 2007	Apodized diffractive n=30(34) Monofocal n=30(34)	Questionnaire	Glare more prevalent with diffractive group in comparison with monofocal IOL
Mester 2007	Diffractive +4 D n=25(50) Refractive +3.5 D n=25(50)	Questionnaire	Photopic phenomenon more prevalent in refractive group than in diffractive group
Vingolo 2007	Apodized diffractive +4 D n=50(100) Monofocal n=20(40)	Questionnaire	Photopic phenomenon more prevalent in diffractive group in comparison with monofocal
Alfonso 2007b	Apodized diffractive +4 D n=325(650) Blue filter Apodized diffractive +4 D n=335(670)	Questionnaire	Photopic phenomenon prevalent in multifocal group
Pepose 2007	Single Optic accommodating n=14 Appodized Diffractive +4 D n=12 Refractive +3.5 D n=14 Diffractive accommodative combination n=6 Refractive accommodative combination n=3	FACT CS chart with glare Questionnaire	CS with glare better with single optic accommodative than with multfocal groups. CS with glare better with refractive than with diffractive Photopic phenomenon less prevalent in single optic accommodative group

Author	IOL designs	Type of glare test	Results
Kaymak 2007	Diffractive/refractive +3.75 D n=20(40)	Visual categorization of dysphotopsia	Presence of halos
Chiam 2007	Refractive +3.5 D n=50(100) Apodized diffractive +4 D n=50(100)	Questionnaire	No significant difference
Bi 2008	Apodized diffractive +4 D n=20(40) Monofocal n=18(36)	Takaci-CGT-1000 glare tester	No significant difference
Blaylock 2008	Apodized diffractive +4 D n=30(60)	SIFIMAV Vision Tester with glare	No significant reduction of CS with glare
Goes 2008b	Diffractive +4D n=30(59)	Questionnaire	Prevalence of glare
Cerviño 2008	Refractive +3.5 D n=(?)13 Apodized diffractive +4 D n=(?)22 Monofocal a n=(?)20 Monofocal b n=(?)12	C-Quant	No significant difference
Palmer 2008	Refractive +3.5 D n=32(64) Diffractive +4 D n=26(52) Asymetrical Diffractive +4 D n=32(64) Monofocal n=24(48)	Questionnaire FACT chart with glare	Higher prevalence of glare with the Diffractive +4 D group in comparison to other groups CS worse with and without glare in diffractive groups followed by refractive and then monofocal
Goes 2008a	Refractive +3.5 D Diffractive +4D combination n=20(40)	Questionnaire	Prevalence of photopic phenomenon
Harman 2008	Refractive +3.5 D n=30(60) Single Optic Accommodative n=30(60) Monofocal n=30(60)	Questionnaire Mentor Brightness acuity tester	Photopic phenomenon more prevalent in refractive +3.5 D No difference in glare score
Chang 2008b	Refractive +3.5 D n=15(30) Apodized diffractive +4 D n=15(30)	CSV 1000 HGT Questionnaire	Photopic phenomenon more sever with the refractive +3.5 D CS better with Refractive +3.5 D
Alió 2008a	Refractive/Diffractive +3.75 D n=52(69)	Verbal interview	Prevalence of photopic phenomenon

Author	IOL designs	Type of glare test	Results
Vries 2008a	Apodized diffractive +4 D n=32(60) Monofocal n=23(44) Phakic n=?	C-Quant	No difference between diffractive and monofocal. Both pesudophakic groups more straylight than phakic
Vries 2008b	Apodized diffractive +4 D n=22(44)	Questionnaire	Prevalence of photopic phenomenon
Alió 2008b	Refractive/diffractive +3.75 Da n=(?)54 Refractive/diffractive +3.75 Db n=(?)40	Questionnaire	Prevalence of photopic phenomenon
Mayer 2008	Monofocal/ Apodized diffractive multifocal +4 D combination n=13(26)	Questionnaire	Prevalence of photopic phenomenon
Cillino 2008	Refractive a +3.5 D n=16(32) Refractive b +3.5 D n=15(30) Diffractive +4 D n=16(32) Monofocal n=15(30)	VF7 questionnaire	Photopic phenomenon more common in refractive groups
Barisić 2008	Refractive +3.5 D n=50(100) Diffractive +4 D n=50(100)	Questionnaire	Photopic phenomenon more common with refractive group
Alfonso 2008	Apodized diffractive +4 D n=12(22) Refractive/diffractive +3.75 D n=18(26)	FACT chart with Glare	CS with glare less with refractive/diffractive +3.75D
Lacmanović-Loncar 2008	Refractive +3.5 D Apodized diffractive combination n=10(20)	Questionnaire	Prevalence of photopic phenomenon
Forte 2009	Refractive +3.5 D n=35(55)	Questionnaire	Prevalence of photopic phenomenon
Bautista 2009	Diffraction +4 D n=137(250)	Questionnaire	Prevalence of photopic phenomenon
Lubiński 2009	Refractive +3.5 D n=20(40)	CSV-1000 HGT Verbal interview	CS with glare and photopic phenomenon improved over 9 months
Blaylock 2009	Apodized diffractive +4 D n=32(64)	Questionnaire	Photopic phenomenon better after surgery
Lan 2009	Apodized diffractive +4 D n=41(50) Monofocal n=24(30)	Questionnaire	No difference between groups
Allen 2009	Refractive +3.5 D n=20(20) Monofocal n=29(29)	Subjective illustration halometer Questionnaire	No significant difference in straylight meter, Halometer and Questionnaire
Hayashi 2009a	Refractive +3 D n=22(44) Monofocal n=22(44)	Contrast Sensitivity acuity Tester (CAT-2000) Verbal questionnaire	No difference in CS with glare Prevalence of halos reported

Author	IOL designs	Type of glare test	Results
Alfonso 2009b	Apodized diffractive +4 D n=20(40)	Questionnaire FACT with glare	Prevalence of photopic phenomenon
Hofmann 2009	Apodized diffractive +4 D n=20(40) Monofocal n=20(40)	C-quant Questionnaire	Photopic phenomenon more prevalent in diffractive group No significant difference in straylight
Cionni 2009b	Apodized diffractive +4 D n=15(30) Apodized diffractive +4 D monofocal combination n=20(40) Apodized diffractive +4 D phakic combination n=32(64)	CSV-1000 HGT Questionnaire	No significant difference
He 2009	Diffractive +4 D n=57(57) Monofocal n=57(57)	Questionnaire	Photopic phenomenon similar
Cionni 2009c	Apodized diffractive +4 D n=72(144) Monofocal n=51(102)	CSV-1000 With glare Questionnaire	Photopic phenomenon more prevalent with diffractive group CS with glare reduced in Multifocal group
Petermeier 2009	Apodized diffractive +4 D n=3(6)	FACT with glare Subject interview	No Photopic phenomenon reported
Zhao 2009	Apodized diffractive +4 D n=41(54)	CSV-1000 With glare	No Difference in CS with or without glare
Kohnen 2009	Apodized diffractive +3 D 84(168)	Questionnaire	Photopic phenomenon returned to pre-operative levels by six months post-operative
Hayashi 2009c	Apodized diffractive +3 D n=32(64) Monofocal n=32(64)	CAT-2000 with Glare	No significant different
Maxwell 2009	Apodized diffractive +3 D n=141(282) Apodized diffractive +4 D n=138(276)	Questionnaire	No difference
Gierek-Ciaciura 2010	Refractive +3.5 D n=10(20) Diffractive +4 D n=10(20) Apodized diffractive +4 D n=10(20)	Verbal interview	Photopic phenomenon

Table 4.1 Summary of dysphotopsia assessment in multifocal intraocular lens studies

4.1.2 Measurement of Glare and Haloes

To measure the surrounding retinal blur circle or halo, several instruments often referred to as halometers have been created. These devices measure the size of a photopic scotoma created by a central glare source. Early methods for the assessment of halos involved drawing the outline of the halo created from a candle at a set distance (Elliot, 1924). The first halometer, described in the literature, consisted of a tungston lamp mounted on a wooden box with a slide rule radiating away from the light. Subjects were required to move the slide rule to the outer rim of the halo to provide a measure of the photopic scotoma surrounding the light source (Elliot, 1924).

4.1.2.1 Gross Estimation Halometer

Gross estimation halometery was described by Hunkeler and colleagues (2002). The technique involved a central light source with an overlaying neutral density filter being placed 3 m from the subject. The subjective method required placing the examiner's hands on either side of the light source, subject verbally manipulated the examiners hands until they intersected with the outer rim of the photopic phenomenon being experienced by the subject. The distance between the examiner's hands was taken as the representation of the size of the photopic scotoma. The technique failed to identify any differences between a MIOL and monofocal IOL; no validation studies have been conducted using this technique.

4.1.2.2 Perimetry Halometer

Namiki and Tagami (1993) attached a glare source within an *OCTOPUS 500E* (Haag-Streit, Koeniz, Switzerland) automated perimeter to determine the extent of visual field loss surrounding a central glare source. With this technique there was no significant difference in glare between a monofocal and multifocal group.

4.1.2.3 Subjective Illustration Halometery

The halometers created by Allen and associates (2009) and by Lee and colleagues (2006) both used similar principals for measuring glare. Both are computer programs, which present a central glare source requiring the subject to circle the perceived photopic phenomenon. The central glare sources differ with each test: Allen and colleagues (2009) used a red cross within a white ring as the central light source, Lee and associates (2006) utilised a single white spot. These halometers have been used to

examine dysphotopsia following MIOL implantation (Allen *et al.,* 2009), post LASIK (Lee *et al.,* 2006) and to examine the effectivity of Brimonidine tartrate 0.2% (Lee *et al.,* 2008). Lee and colleagues (2008) found good repeatability with this type of Halometery instrument, however, the design used for examining MIOLs was not assessed for repeatability and was found to show similar results with both multifocal and monofocal IOLs.

4.1.2.4 Glare & Halo Test

The *Glare & Halo test* (Tomey, AG, Erlangen) is a standardized commercially available computerised test used to measure the size of photopic phenomenon. A central white target 15 mm in size is displayed on screen and the subject is required to place a mark at the boundary of the photopic phenomenon for 12 equidistant orientations separated by 30 degrees surrounding the glare source. The central glare area in degrees is then calculated in accordance with the working distance of the subject. The *Glare & Halo* test has been used in three studies examining the difference in halo sizes between a monofocal IOL and the *Array* refractive MIOL; Pieh and colleges (2001) found a significant difference in dysphotopsia between the two types of pseudophakic correction, however, two further studies did not find a significant difference (Eisenmann *et al.,* 1996, Dick *et al.,* 1999). The *Glare & Halo* test has also been used to assess photopic phenomenon in post LASIK subjects (Lackner *et al.,* 2003). Repeatability studies have not been conducted using this instrument.

4.1.2.5 Halometer DG

The Halometer DG has a central light source with a variable intensity control. A luminous optotype of a set size and brightness is moved horizontally towards and away from the glare source until it is just distinguishable. The working distance is set as 30 cm and the distance between the optotype and the glare source are recorded. The Halometer DG was validated on phakic subjects with and without cataracts (Babizhayev, 2009).

4.1.2.6 Gutiérrez and Colleagues Halometer for Measuring Haloes

The halometer described by Gutiérrez and colleagues (2003) was designed to measure dysphotopsia in subject's post-LASIK. The halometer comprises a board with a central hole through which a light emitting diode (LED) is placed to provide the glare source.

To create the targets, a series of holes radiating away from the central light also have LEDs shining through them. These LEDs flash in sequence, similar to a visual field screening test allowing the area of photopic scotoma to be mapped. No repeatability studies have been conducted using this instrument.

Despite several attempts at devising an instrument for clinically quantifying dysphotopsia; a technique has not been developed and validated for this use with MIOL subjects. A new halometer is required for use with these subjects implanted with MIOLs to assess this phenomenon of dysphotopsia.

4.2 Development of a New Halometer

4.2.1 Conceptual Design

The initial design for the halometer consisted of a display screen presenting a series of dots, of varying contrasts, radiating away from a central LED which was controlled by a single battery. This design was inspired by the design of Gutiérrez and colleagues (2003). Subjects would be requested to count the number of dots seen in each direction. Subsequently, the dot targets were changed to letters as keeping track of the number of dots observed with the centralised glare was found to be difficult (Figure 4.2). It became apparent that, in its current form, results would be unreliable and not sensitive enough to detect differences in glare profiles. Also the output of the light source was not stable enough to provide a consistent glare source for multiple examinations.
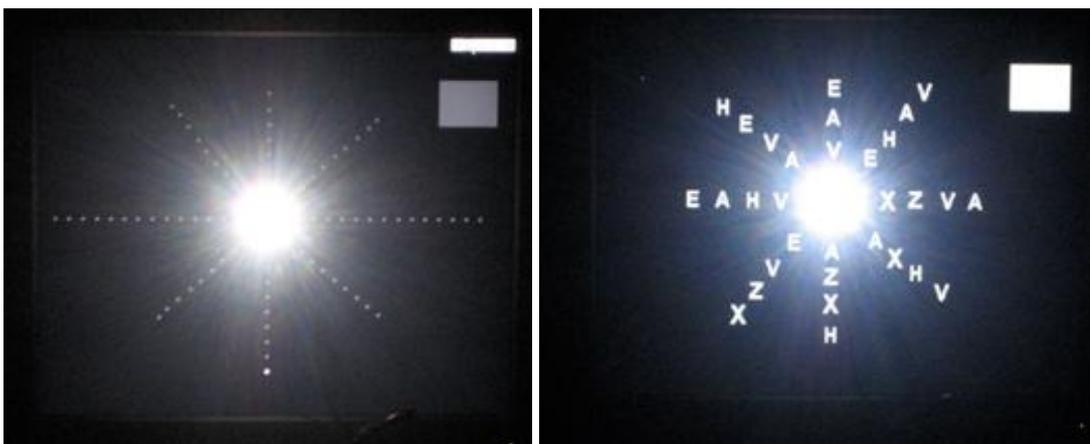
Figure 4.1 *Early halometer prototypes viewed through a 0.8 Bangerter foil*

Instead of a using a static display, a computer program was developed that would allow a changing letter to move away and towards the glare source in meridians separated by

45 degrees. The letter targets were designed to have multiple contrast levels. A glare source was then developed that would provide a stable output.

4.2.2 Design of the Target

The principal investigator for the study (PB) created a computer program using *Liberty BASIC* (Shoptalk Systems, Framingham, Massachusetts, USA) that could move a letter target of variable contrast across a black screen. The font "Arial bold" was chosen as it is non-serif and approximates the 5x4 letters stipulated with the British Standard BS 4274. The letters were also chosen according to this standard and were limited to 'D', 'E', 'F', 'H', 'N', 'U', 'V', 'Z'. These letters were selected due to their similar legibility (Bailey, 1998). Pixel size – in degrees subtending at the subjects' eye – was calculated according to the screen resolution, the screen height and the subject working distance (Equation 4.1).

$$Pixel size = \left(\frac{ArcTan\left(\frac{\frac{h}{2}}{wd} \right)}{\frac{p}{2}} \right)$$

Equation 4.1

h is the height of the screen
wd is the working distance of the screen to the subject
p is the number of pixels across the vertical portion of the monitor

The program was designed so that the letter size and its position on the screen were controllable. The letter size was displayed in degrees subtended at the eye and displayed in the corner of the screen. The program was based around a turtle graphics design; the left/right arrow keys moved the letter towards or away from the centre of the screen 0.05° at a time. At each key press the letter would move and change (in a random order), while simultaneously the distance, in degrees subtended at the eye, between the centre of the screen and the centre of the letter would be displayed. The program was designed to enable the letter to move in 8 directions separated by 45°.

The computer program was designed to display the letter at 4 contrast levels against a dark screen. A luminance meter (*Luminance Meter LS-110*; Minolta, Osaka, Japan) was

mounted parallel to a dell flat screen monitor in order to determine the screens luminance while varying the pixel grey intensity. Weber's contrast equation (Legge, 2007; Equation 4.2) was used to calculate and define the 4 letter contrast levels; 1000, 500, 100 and 25 Weber contrast units (C_w).

$$C_{Weber} = \left(\frac{L_t - L_b}{L_b} \right)$$
Equation 4.2

L_t is the luminance of the letter target
L_b is the luminance of the background
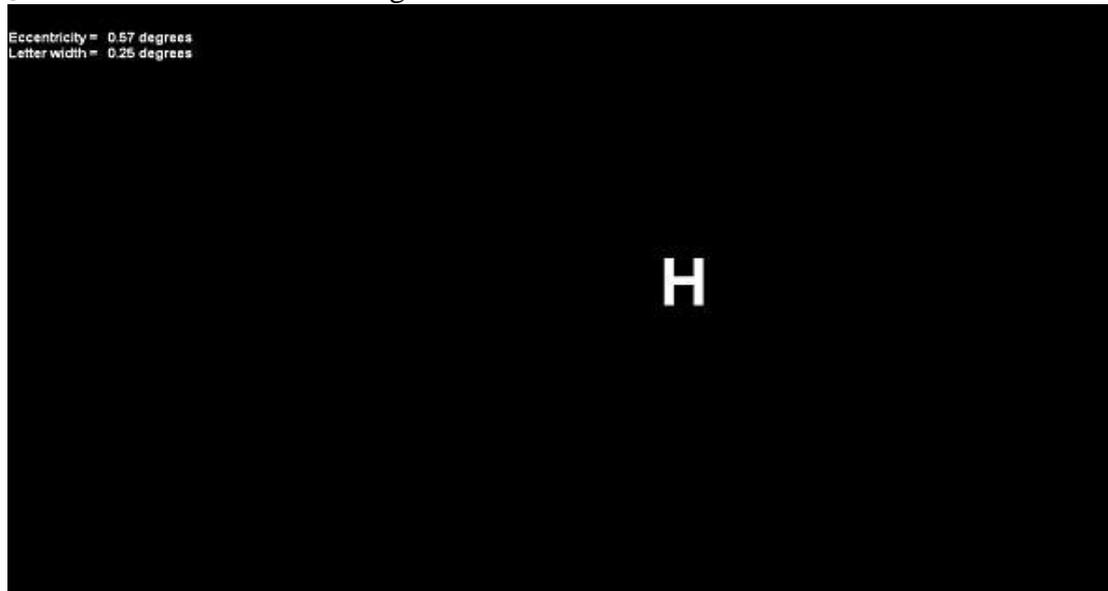
Figure 4.2 *Snapshot of the computer screen display for the BD Halometer with a 1000 C_w contrast letter*

4.2.3 Design of the Glare Source

To ensure the repeatability and validity of the test, it was important to ensure that the glare source retained a constant brightness. A *Warm White Luxeon Emitter white Star LED LXHL-BW03* (Lumeds Lighting LL, San Jose, USA) was mounted at the end of a telescopic arm. This LED has a Correlated colour Temperature (CCT) of 3200K, whilst maintaining 70% lumen over 50,000 hours of operation. The telescopic arm was shrink-wrapped in a black matt plastic to ensure non-reflectance. The Mark 1 Buckhurst and Drew (BD) Halometer was connected to three lithium ion batteries through a *CH1030 Project 18 pin board* (Revolution Education Ltd., Bath, UK), designed to provide protection against a drop in output by running the current through 10K, 4K7, 100R and 22K resisters. Subsequently the Mark 2 BD Halometer was

developed where the 18-pin board was connected to a mains output with a consistent voltage, the current was limited to 5V and 100 mA (full load 1 W).
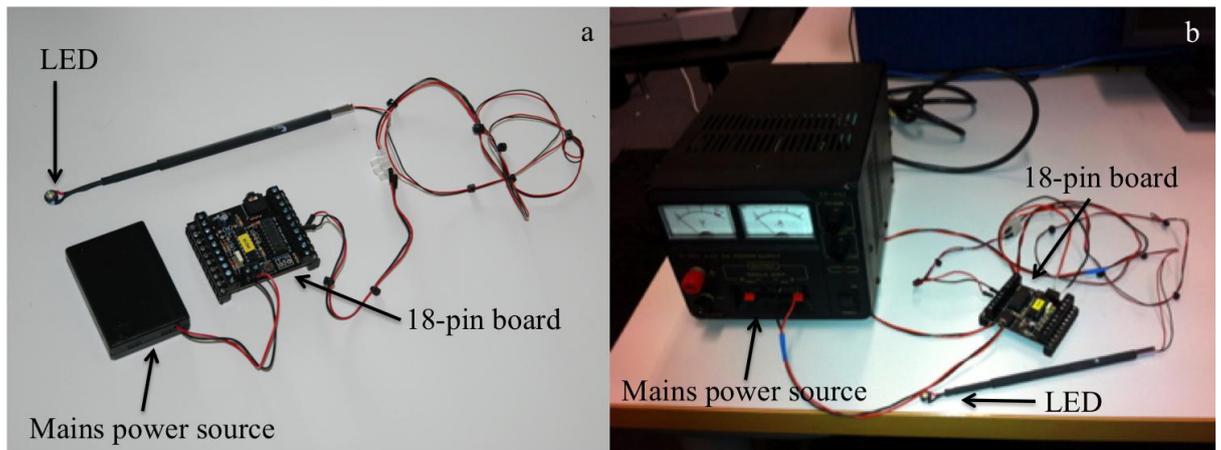
Figure 4.3 *The BD Halometer glare sources for the mark 1 BD Halometer (a) and the mark 2 BD Halometer (b)*

The glare source was mounted 4 mm above the *S130C laser power Meter* (Thorlabs, Munich, Germany) the power output of the Mark 1 and the Mark 2 BD Halometer was assessed over a 49 minute time period.
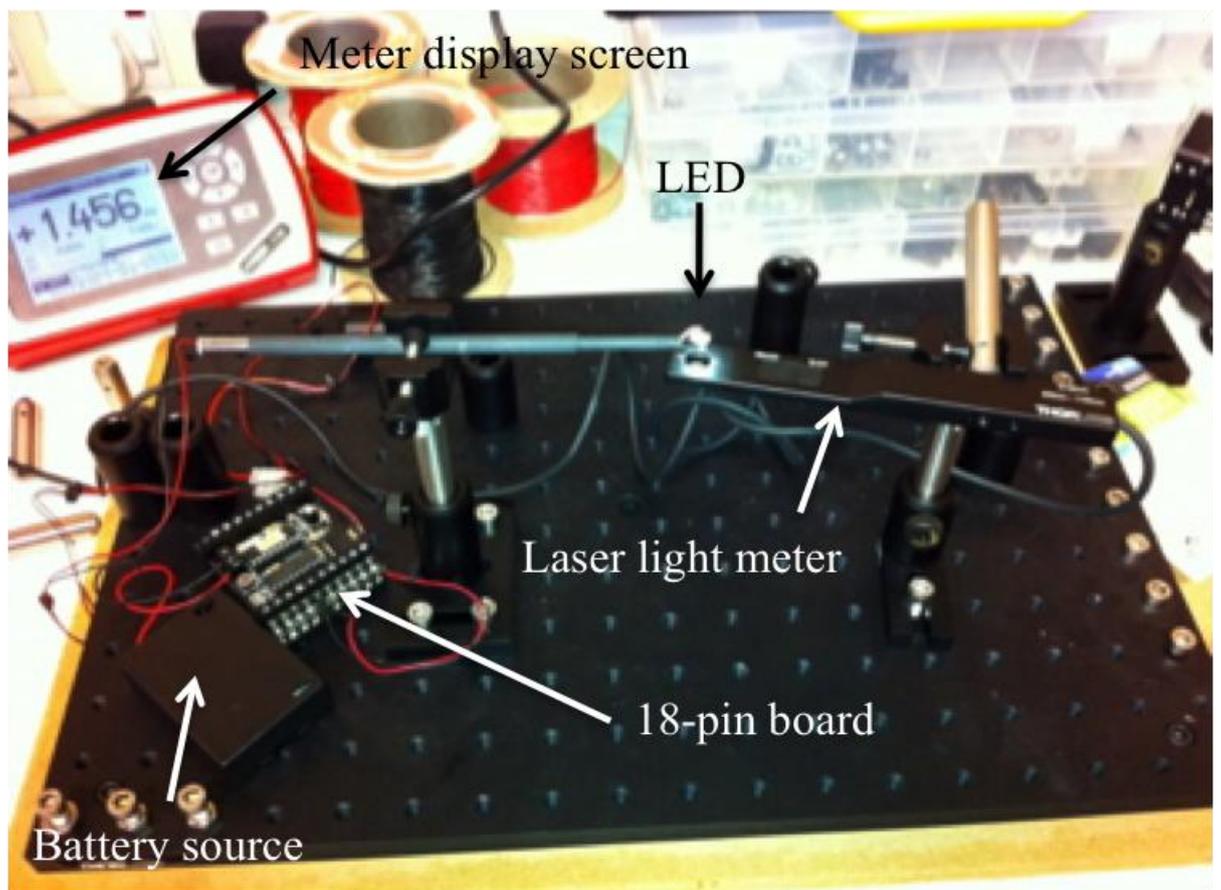
Figure 4.4 *Halometer glare source mounted 5 mm from a laser power meter*

The output of the Mark 1 BD Halometer deteriorated by 11% over the first 5 minutes of use, the output over the following 45 minutes by less than 8%. The output of the Mark 2 BD Halometer remained consistent over the 50 minutes (Figure 4.6)
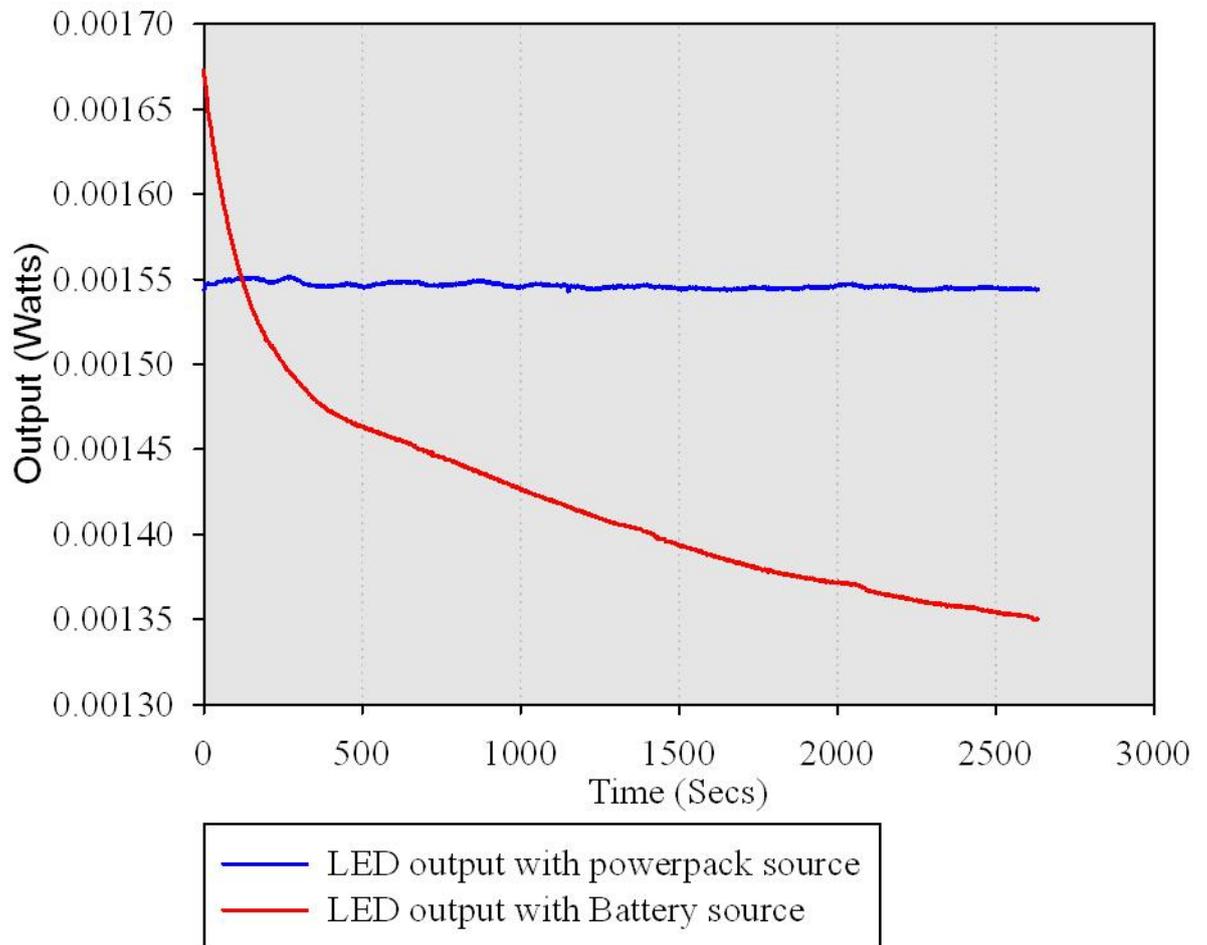
Figure 4.5 *Output of glare sources over time (red mark 1 blue mark 2)*

4.2.4   Set up of the Halometer

A flat-screen monitor was used to display the BD Halometer program; the light source arm was attached to the edge of the computer screen allowing the LED to be positioned in the centre of the screen corresponding to the 0° position on the glare test screen. Subjects need to be positioned with their eyes incident with the light path as the radiation pattern of the LED is unidirectional with the highest intensity of light at 0° of alignment.
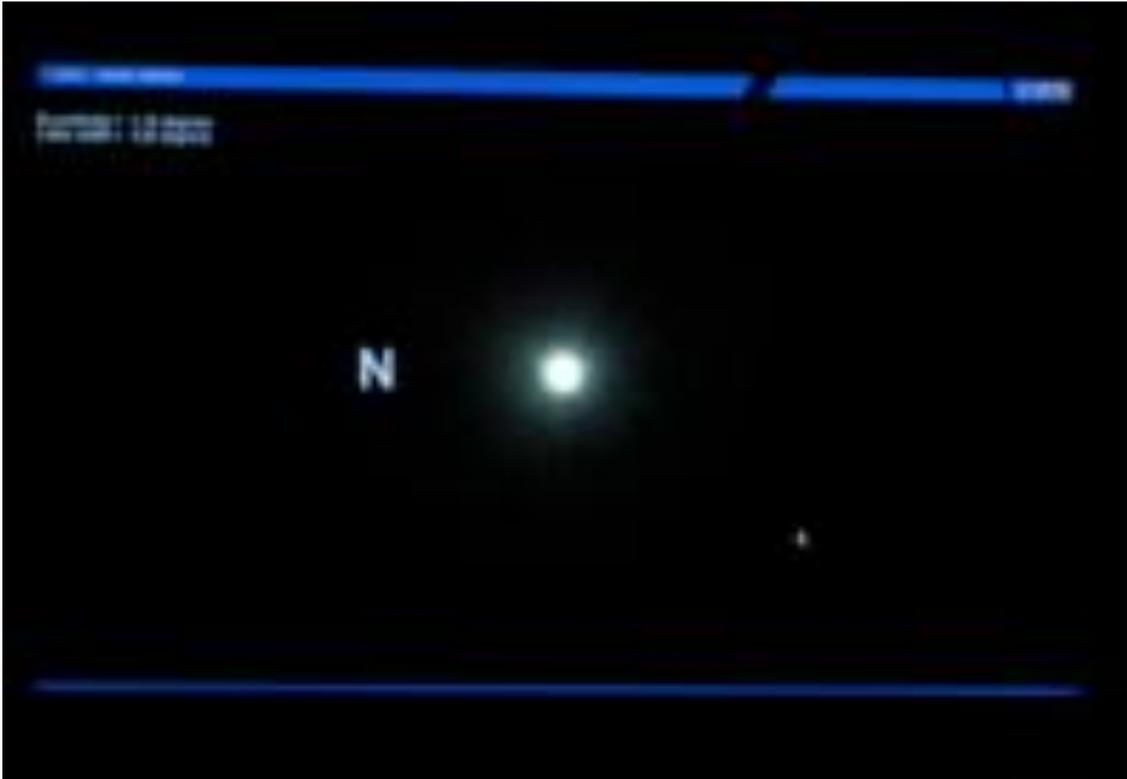
Figure 4.6 *Image of the BD Halometer*

4.3 Study Aim

Implantation of MIOLs is known to result in dysphotopsia; however, there is a shortage of studies examining the extent of the photopic phenomenon. Two studies were conducted using the custom developed BD Halometer. The first study involved young phakic subjects to determine the inter-observer and intra-observer variability of the instrument. This first study also measured the effect of *Bangerter foils* (Haag-Streit, Koeniz, Switzerland) on the measurement of dysphotopsia and Straylight. The second study was preformed on three groups of subjects implanted with a concentric fully diffractive multifocal, sectorial refractive multifocal and monofocal IOL.

4.3.1 Subjects

Twenty subjects (10 males, and 10 females) of mean age 27.65 ± 3.13 years were recruited by the primary investigator of the study (PB). The inclusion criteria for the study were as follows:

- Uncorrected VA of at least 0.10 LogMAR in each eye
- Mean spherical error within -0.75 D to +0.75 D
- Spectacle astigmatism less than 0.75 D
- The absence of any ocular pathology and previous surgery

168

- Aged between 18 and 40 years

A further forty-five subjects (14 males, 31 females) of mean age 61.8 ± 8.9 years were recruited from Solihull Hospital (Solihull, UK) and the Midland Eye Institute (Solihull UK). The inclusion criteria for the study were as follows:

- Requiring bilateral cataract surgery or electing for bilateral clear lens extraction
- A likely postoperative best corrected distance visual acuity of at least 0.1 LogMAR
- The absence of any ocular pathology and previous surgery
- Corneal astigmatism less that 1.50 D
- Aged between 40 and 70 years
- Suitable for multifocal IOL implantation
- Willing to have multifocal IOL implantation
- Willing to participate in the study
- Able to achieve reliable partial coherence interferometry results
- Willing to attend an extra post-operative aftercare visit
- Absence of capsular opacification, LASIK and YAG capsulotomy

The 45 recruited subjects were implanted with 3 combinations of 3 different IOLs. The lenses were implanted in order depending on the date of the first eye surgery:

- The first 15 subjects were implanted bilaterally with the *Tecnis ZM900* (Abbott Medical Optics Inc.).
- The second 15 subjects were implanted bilaterally with the *Lentis Mplus* (Topcon Europe BV)
- The remaining 15 subjects were implanted bilaterally with the *Softec 1 monofocal IOL* (Lenstec).

The implications of multifocal IOL implantation were discussed with each subject by the principal investigator and consultant Ophthalmologist performing the surgery; the final decision to operate was made by the consultant Ophthalmologist.

Pre-operatively an *IOLMaster* (Carl Zeiss Meditec AG) running v5.2 analysis software and a NIDEK *OPD-Scan II* (Optical Path Difference Scanning System II; NIDEK Co Ltd) Wavefront Aberrometer were used to determine axial length and corneal power. To determine IOL power, the Hoffer Q IOL formula was used for short axial lengths,

(<22 mm; College of Ophthalmologist's Guidelines) and the SRK/T was used for all other axial lengths; emmetropia was the target in all cases.

All operations were performed by one of three surgeons (SS, AK & MB) under topical or local anaesthetic. A 2.85 mm clear corneal incision, widening to 3.2 mm after injection, was placed on the steepest corneal axis to reduce residual levels of postoperative astigmatism. Phacoemulsification, aspiration and irrigation were performed through a 5.5 mm capsularhexis using the *Millennium phacoemulsification system* (Bausch and Lomb). All IOLs were implanted into the capsular bag.

Three subjects were later excluded from the study due to postoperative complications: two from the *Lentis Mplus* group (one cystoid macular oedema and one requiring YAG Laser) and one from the Bilateral *Tecnis ZM900* group (Post operative LASIK). An additional three subjects were recruited to replace those excluded. The final patient demographics are detailed in Table 4.

	Bilateral *Softec 1*	Bilateral *Tecnis ZM900*	Bilateral *Lentis MPlus*
Age mean±SD (years)	62.1 ± 6.8	60.7 ± 11.0	62.3 ± 9.0
Gender	3 Male, 12 Female	4 male, 11 female	7 male, 8 female

Table 4.2 Pseudophakic Subjects' Demographics

The NHS Local Research Ethics Committee of Solihull approved this study and informed consent was obtained from each subject. The consequences and details of the study were explained to each patient. The study was conducted in accordance with the tenets of the Declaration of Helsinki.

4.3.2   Phakic Evaluation

All subjects were examined during two separate visits separated by at least two hours and by no more than 2 weeks. During the visits the following tests were conducted:

4.3.2.1   Full Refraction

Retinoscopy using the *Keeler Professional Retinoscope* (Keeler Ltd, Windsor, UK) followed by a full subjective refraction at 6 m using the *Thompson Test Chart 2000*

(Thomson Software Solutions, Hatfield, Herts. UK) was performed to assess post-surgical residual refractive error.

4.3.2.2   Measurement of Straylight using the C-Quant

The *C-Quant* provides a measure of the level of straylight over the retina. Straylight originates from the scattering of light and creates a veil over the eye and is known to increase with age, ocular pathology and with surgery. Increased straylight is regarded as disability glare and has a detrimental effect on night driving. The *C-Quant* measures straylight using the compensation comparison method: the central target stimulus is separated into two hemi-spheres surrounded by a neutral ring which itself is surrounded by the circular straylight stimulus (Figure 4.8). At each presentation one of the two target hemi-spheres flashes along with the surrounding straylight stimulus. The resultant effect is that one hemisphere flashes with the intensity of its self-generated stimulus along with the straylight stimulus and the other hemisphere flashes according to the intensity of the straylight stimulus only. The subject is asked to respond to which hemi-sphere flashes greatest. The program determines the point at which the straylight created by the background stimulus prevents the observer from determining the correct flashing hemisphere (Franssen *et al.,* 2006).

Aston University

Illustration removed for copyright restrictions

Figure 4.7 *Internal display for the C-Quant Straylight meter; a, Right test stimulus. b, left test stimulus. c, Neutral zone. d, Straylight stimulus (Franssen et al., 2006)*

With the *C-Quant* three repeats are necessary to achieve an accurate measurement of straylight and measurement of straylight was considered reliable if the estimated standard deviation (ESD) was below 0.8 and the quality factor for the psychometric sampling (Q) was above 1.00 (Cerviño *et al.,* 2008b).

To simulate glare conditions *Bangerter foils* were inserted into the eyepiece of the *C-Quant*, these lenses are used for optical penalisation therapy. The foils are designed to reduce vision in standardised steps from 1 to 0.1. The point spread function of the 0.6, 0.4 and 0.3 foils are similar and reduce visual acuity by equal amounts. The 0.8 foil spreads light by a lesser degree and so has a reduced affect on visual acuity. Each lens has a series of micro-bubbles; the density of which determines the spread the light (Pérez *et al.,* 2010).

Figure 4.8 *0.8 Bangerter foil (right) and 0.6 Bangerter foil (left) mounted within a trial lens housing*

For the current study the 0.8 and 0.6 *Bangerter foils* were used to simulate different levels of light spread on the retina. These two foils were secured within a trial lens plastic housing (replacing the previous lens in place) and a third clear lens with no refractive power was used as a control. Ocular straylight was measured with each of the *Bangerter foils*; these were placed within the lens holder of the *C-Quant* and to ensure repeatability all lenses were placed at the same orientation for each measurement. Three measurements were taken per lens giving a total of 9 measurements; the order of presentation was randomised. Straylight repeatability was assessed at the second subject visit.

4.3.2.3   Measurement of Halos

The bespoke Mark 1 BD Halometer was used to measure dysphotopsia in the phakic subjects with the three lens types (Control lens, 0.8 *Bangerter foil* and 0.6 *Bangerter foil*). Each subject was positioned 3 meters from the instrument; a reference marking was used to align the subject's eyes to a constant position incident to the LED light source. For a period of 5-minutes before examination the mark 1 BD Halometer was switched on allowing sufficient 'warm up' time for the output to stabilise. BD Halometery was conducted in a dark room with the Halometer as the only light source. During this period the subjects became adapted to the lighting conditions. The three *Bangerter foils* were placed in the trial frame in random order in front of the right eye with the contralateral eye occluded. The photopic scotoma was measured in all 8 positions for each of the 4 contrast levels using a letter height of 0.21°. This height approximates a 6/15 letter. A 6/15 letter height best approximates the geometrical angle a number plate letter (79 mm) subtends the eye at a distance of 20.5 m; the minimum driving requirement for the UK (Keil *et al.*, 2003). The testing of each position and contrast level occurred in a random order and at each position the target letter was moved inwards from a peripheral area of seeing towards the glare source. The last point at which the letter could be correctly identified was recorded, if a letter was incorrectly identified, then the letter was changed. Two incorrect answers were regarded as a negative response and then the last positive response in degrees was noted. During the first visit the principal investigator conducted Halometery, for the second visit, Halometery was repeated by the primary investigator and then repeated by a co-investigator (a UK registered Optometrist; HP) blind to the results of the primary investigator.

4.3.3   Pseudophakic Evaluation

All subjects were examined at two separate visits; separated by at least two hours and by no more than 2 weeks. During the visits the following tests were conducted:

4.3.3.1   Full Refraction

A full refraction was conducted using the same technique detailed in Chapters 2 and 3. Utilising retinoscopy, auto-refraction and subjective refraction, subjects were corrected for distance vision.

4.3.3.2 Subjective Assessment of Dysphotopsia

All subjects were asked to evaluate their experience of photopic phenomenon post-IOL implantation. The same question was asked to each subject: "Please can you rate your experience of glare or unusual phenomenon around lights such as halos on a scale of 0 to 10. Zero meaning no experience of glare 10 meaning it is the worst possible". Each subject's 0-10 grade was recorded.

4.3.3.3 Subjective Categorization of Dysphotopsia

Each subject was shown a set of dysphotopsia illustrations as depicted on the *EVP Eyevispod program* (PGB, Milan, Italy). Subjects were instructed to indicate the illustration which best represented their experience of dysphotopsia.

Aston University

Illustration removed for copyright restrictions

Figure 4.9 *The EVP EyeVisPods' (PGB, Milan, Italy) graphical illustration depicting dysphotopsia*

4.3.3.4 Measurement of Straylight using the *C-Quant*

Retinal straylight was measured on each subject using the *C-Quant*. The average of three readings was taken as the measurement of straylight. It was measured at both the first and second visit.

4.3.3.5 Measurement of Halos

Dysphotopsia was measured using the Mark 2 BD Halometer. Glare was measured at the 8 orientations, in a random order, using only the 500 C_w contrast target letters 0.21° in size (Section 4.6). The glare was measured both monocularly and binocularly. This was measured at both the first and second visit.

4.4 Statistical Analysis

4.4.1 Assumption of Normality

The one-sample Kolmogrov-Smirnov test was used to determine if results from each measurement followed a normal distribution. Where the data followed a normal distribution parametric analysis was used, non-parametric statistical analysis was used for non-normally distributed data.

4.4.2 Comparison of Demographics and Eyes

A one-way ANOVA was conducted to examine the mean ages of the IOL groups. For each IOL group a paired student t-test was conducted to compare the results of the right and left eyes for the *C-Quant.* Furthermore a mixed-repeated measures ANOVA was conducted to compare the right and left eye results of the BD Halometer.

4.4.3 Calculation of Glare Area

The co-ordinates of two adjacent tested meridians coupled with the central 0 point conforms to a triangular configuration. The area of glare was calculated as the sum of the individual triangular areas. To calculate areas, first, the x and y co-ordinates of the oblique meridians were calculated using trigonometry equations (Equation 4.3; Figure 4.11)

$Y=h*sin(45)$ **Equation 4.3**

$Cos(45) = Sin(45)$ therefore y=x

175
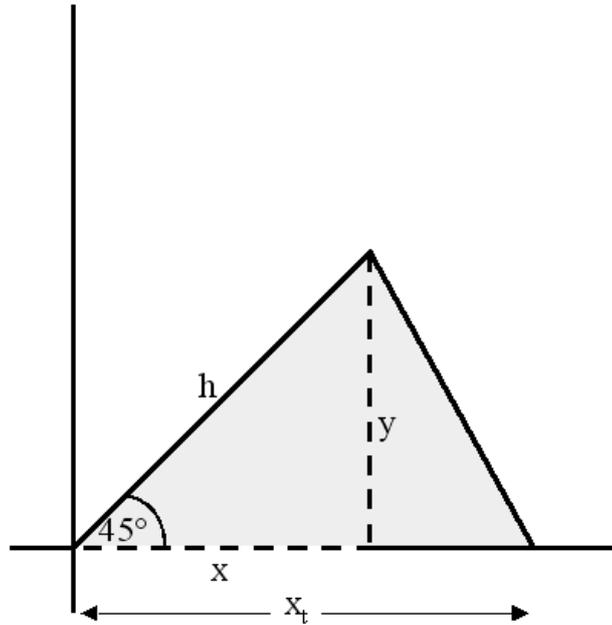
Figure 4.10 *The co-ordinates link to make a triangle, from this the area between the tested meridians is calculated*

Then the area between the two meridians was calculated (Equation 4.4, Figure 4.11) and the total area was calculated as the sum of all of the individual areas (Figure 4.12).

$$area = \frac{1}{2} \times X_t \times y$$

Equation 4.4
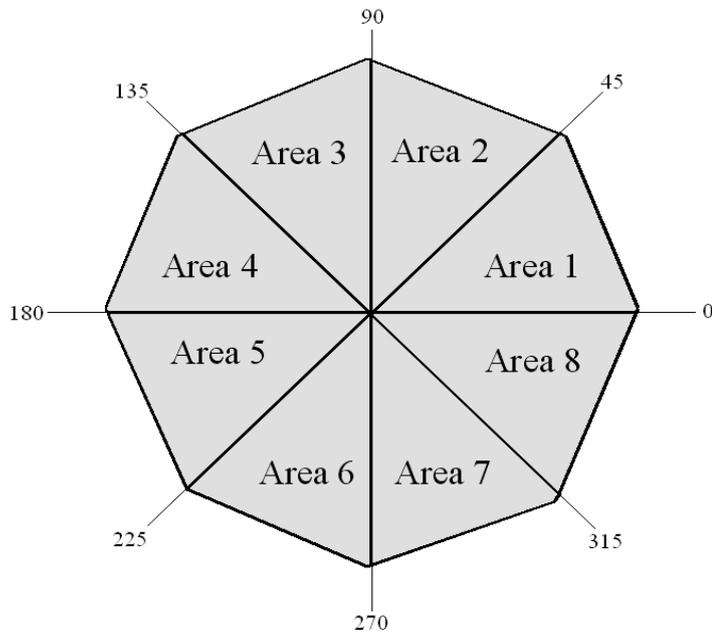
Figure 4.11 *Total glare area is the sum of all of the 8 areas*

4.4.4 Repeatability of Straylight and Halometry Scores

Intra-observer variability of the *C-Quant* measurements, on the phakic subjects, was tested for each *Bangerter foil* separately using intraclass correlation co-efficient (ICC) based on a two-way mixed ANOVA model with a 95% confidence interval. As Straylight was calculated as the average of three measurements, the average repeatability value statistics was calculated. The same ICC calculation was performed on the pseudophakic group responses at the two visits. Intra-observer and inter-observer variability of the Halometer scotoma area results were calculated using the ICC separately for each *Bangerter foil* at each contrast level in the phakic group. The same two-way mixed ANOVA model was used but the single value statistics were recorded. ICCs were also calculated for the pseudophakic group for each meridian separately.

4.4.5 Phakic Group Analysis

Assessment of the influence of the *Bangerter foils* with the measurement of straylight was calculated using a one-way repeated measures ANOVA; where significant differences were found pair-wise differences were determined using the Bonferonni *post hoc* test.

The one-way repeated measures ANOVA was also calculated for the areas of photopic scotoma for each of the Bangerter foils.

4.4.6 Pseudophakic Analysis

4.4.6.1 Subjective Scoring and Categorization of Dysphotopsia

The subjective perception of photopic phenomenon was assessed using the Kruskal-Wallis test; where significance was found multiple Mann-Whitney tests were performed with a Bonferroni correction ($p < 0.017$). A Chi-Squared analysis was conducted to determine if the prevalence of each category of glare for each IOL matched the expected result. The expected null hypothesis was that all 15 subjects would identify the clear category.

4.4.6.2 Comparison of Straylight and Repeatability

Straylight was compared using a one-way ANOVA; where significance was found the Tukey's *post hoc* test was used to examine the interactions of the groups.

4.4.6.3 Comparison of Photopic Phenomenon

A two-way repeated measures ANOVA was used to determine any significant difference in the defocus curves between eyes. The same two-way ANOVA was used to determine if there was an overall difference in the binocular and monocular curves between lens groups. If a difference was found then multiple one-way ANOVAs were applied to the data. The Bonferroni *post hoc* was used to detail the individual differences between the lenses.

4.4.7 Correlation Between Subjective Ratings of Vision, Straylight and Measurement of Photopic Phenomenon

The subjective rating of dysphotopsia was correlated with both measurement of Straylight and measurement from the BD Halometer using the Spearman's rank correlation co-efficient.

4.5 Results

4.5.1 Comparison of Demographics and Eyes

The ages were similar for each IOL group (F_2=0.177, p=0.838). There was no significant difference in Straylight results between the right and left eye for each of the IOL groups (*Softec 1*, p=0.902; *Tecnis ZM900,* p=0.430, *Lentis Mplus,* p=0.513).

4.5.2 Repeatability

4.5.2.1 Phakic Group Analysis

Intra-observer variability for the *C-quant* was 0.875 (ICC) with no lens in place, 0.871 with a 0.8 *Bangerter foil* and 0.883 with the 0.6 *Bangerter foil*. For the Halometer, intra-observer variability can be seen in Table 4.3 and inter-observer variability is displayed in Table 4.4.

	Contrast of the Optotype target			
	1000 C$_w$	**500 C$_w$**	**100 C$_w$**	**25 C$_w$**
Control lens	0.876	0.843	0.775	0.806
0.8 *Bangerter foil*	0.979	0.929	0.874	
0.6 *Bangerter foil*	0.929	0.840		

Table 4.3 *Intra-observer variability of the BD Halometer with each Bangerter foil and at each contrast level (n=20)*

	Contrast of the Optotype target			
	1000 C$_w$	**500 C$_w$**	**100 C$_w$**	**25 C$_w$**
Control lens	0.776	0.729	0.632	0.675
0.8 *Bangerter foil*	0.696	0.675	0.532	
0.6 *Bangerter foil*	0.576	0.529		

Table 4.4 *Inter-observer variability of the BD Halometer with each Bangerter foil and at each contrast level (n=20)*

4.5.2.2 Pseudophakic Group Analysis

Intra-observer variability for the *C-Quant* was 0.765. The intra-observer variability of the Halometer for each meridian (at the 500 C$_w$) can be seen in Table 4.5.

	0	**45**	**90**	**135**	**180**	**225**	**270**	**315**
ICC	0.890	0.895	0.907	0.877	0.840	0.916	0.906	0.910

Table 4.5 *Intra-observer variability of the BD Halometer at each meridian with the pseudophakic group (n=45)*

4.5.3 Phakic Results

4.5.3.1 Levels of Straylight for Each *Bangerter Foil*

There was a significant difference between groups ($F_{1.551}=80.655$, p<0.001) [$F_2=80.655$, p < 0.001]. The control lens exhibited the lowest level of Straylight

followed by the 0.8 *Bangerter foil* with the 0.6 *Bangerter foil* having the highest Straylight value (all pairwise comparisons; p<0.001 level, Figure 4.13).
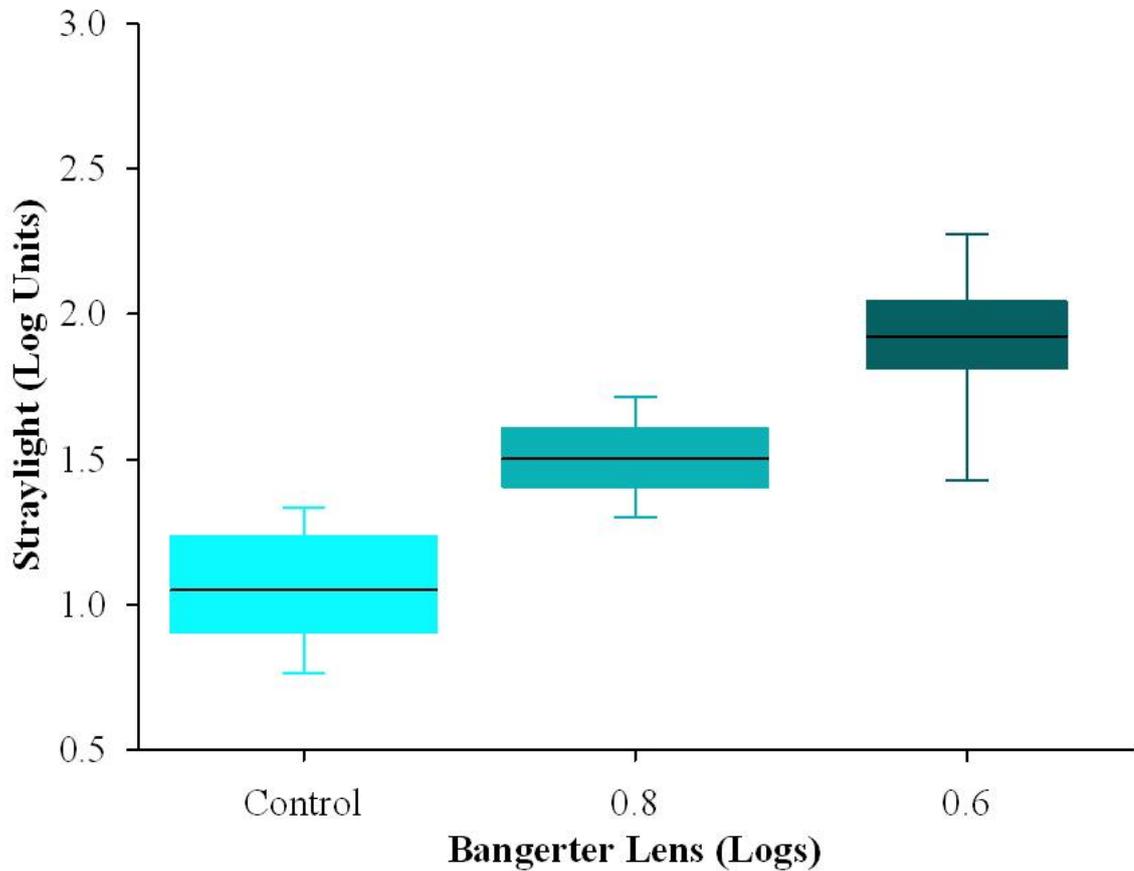
Figure 4.12 *Straylight values for each Bangerter foil (n=20)*

4.5.3.2   Levels of Photopic Phenomenon for Each *Bangerter Foil*

There was a significant difference in the size of halos measured using the different *Bangerter foils* and target contrasts ($F_{1.799}$=29.564, p<0.001). Table 4.6 and Figure 4.13 show the individual differences between each *Bangerter foil* and tested contrast level.
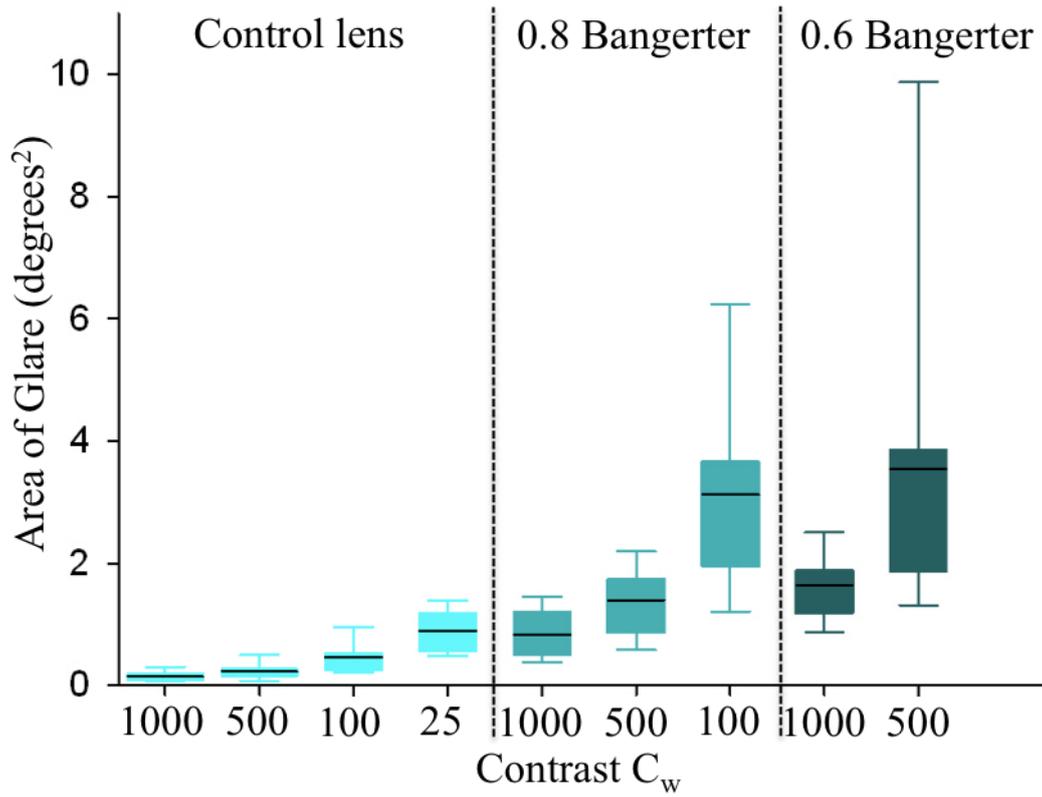
Figure 4.13 *Area of photopic scotoma for each Bangerter foil at each contrast level (n=20)*

		Control lens			0.8 *Bangerter*			0.6 *Bangerter*	
		500 C$_w$	**100 C$_w$**	**25 C$_w$**	**1000 C$_w$**	**500 C$_w$**	**100 C$_w$**	**1000 C$_w$**	**500 C$_w$**
Control lens	**1000 C$_w$**	p < 0.001	p < 0.001	p < 0.001	P < 0.001	p < 0.001	p < 0.001	p < 0.001	p < 0.001
	500 C$_w$		p < 0.001	p < 0.001	P < 0.001	p < 0.001	p < 0.001	p < 0.001	p = 0.001
	100 C$_w$			p < 0.001	P = 0.072	p < 0.001	p < 0.001	p < 0.001	p = 0.001
	25 C$_w$				P = 1.000	p = 0.170	p < 0.001	p = 0.001	p = 0.005
0.8 *Bangerter*	**1000 C$_w$**					p = 0.002	p < 0.001	p = 0.001	p = 0.006
	500 C$_w$						p = 0.001	p = 1.000	p = 0.450
	100 C$_w$							p = 0.010	p = 1.000
0.8 *Bangerter*	**1000 C$_w$**								p = 0.30

Table 4.6 *Differences between each BD Bangerter foil and contrast level (n=20)*

4.5.3.3 Correlation Between Straylight Results and the Area of Glare

Correlation between the straylight results and the area of photopic scotoma was only significant with the 500 C$_w$ contrast glare test target and with a 0.8 *Bangerter foil*. All other comparisons revealed poor correlation.

Bangerter foil used		Contrast of glare test target			
		1000 C_w	500 C_w	100 C_w	25 C_w
Control	Pearson correlation	r=-0.28, p=0.908	r=-0.122, p=0.609	r=-0.640, p=0.788	r=0.299, p=0.200
0.8	Pearson correlation	r=0.116, p=0.625	r=0.514 p=0.020	r=0.374 p=0.104	
0.6	Pearson correlation	r=-0.26 p=0.914	r=-0.004 p=0.987		

Table 4.7 *Correlation between the straylight results and the photopic scotoma areas (n=20)*

4.5.4 Pseudophakic Results

4.5.4.1 Subjective Scores

A significant difference in subjectively rated glare was found between the three groups (H2=12.359, p=0.002). No significant difference was found between the *Softec 1* and *Lentis Mplus* groups (Z=0.187) or between the *Softec 1* group and the *Tecnis ZM900* group (Z=0.29). However there was a significant difference between the *Tecnis ZM900* and the *Lentis Mplus* group (Z<0.001).
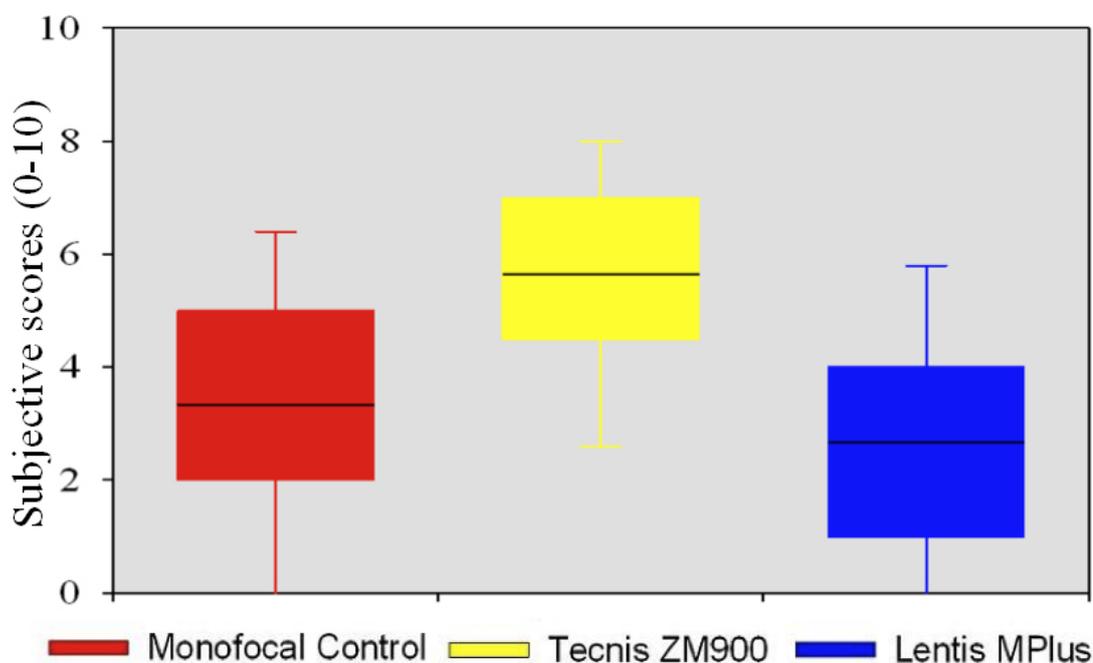
Figure 4.14 *Box plots of subjective 0-10 dysphotopsia scores (n=15x3)*

4.5.4.2 Categorization of Dysphotopsia

The observed frequencies of the Softec 1 (χ^2_5=3.267, p=0.659) and the Lentis MPlus (χ^2_5=6.667, p=0.247) did not significantly deviate from the expected model frequencies. There was a significant difference between the observed and expected frequencies for the Tecnis ZM900 (χ^2_5=15.000, p=0.010). Dysphotopsia categorisation is summarised in Figure 4.15 for each of the IOL groups.
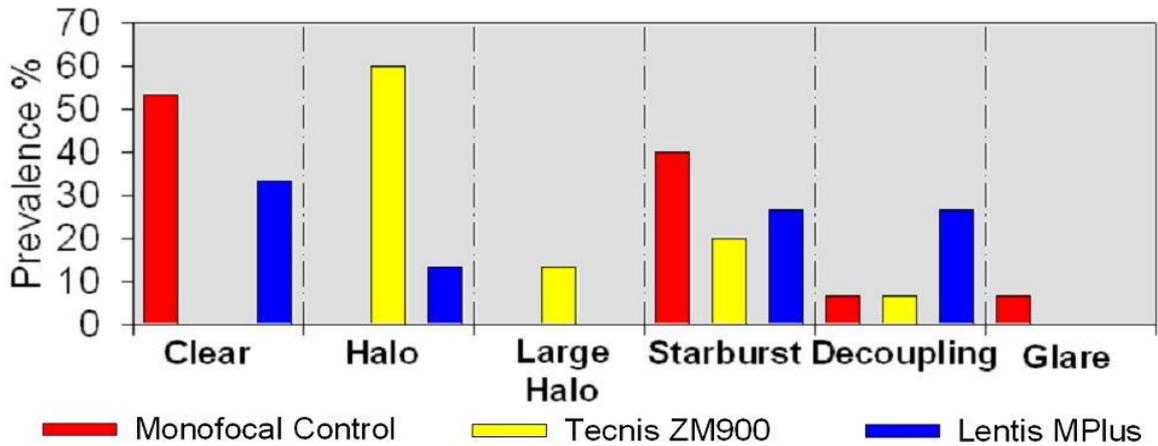
Figure 4.15 *Prevalence of the types of dysphotopsia (n=15x3)*

4.5.4.3 Straylight as Measured with the *C-Quant*

The level of Straylight present in the right eyes of each group is displayed in Figure 4.16; all IOL groups demonstrated a similar amount of straylight (F_2=0.414, p=0.664).
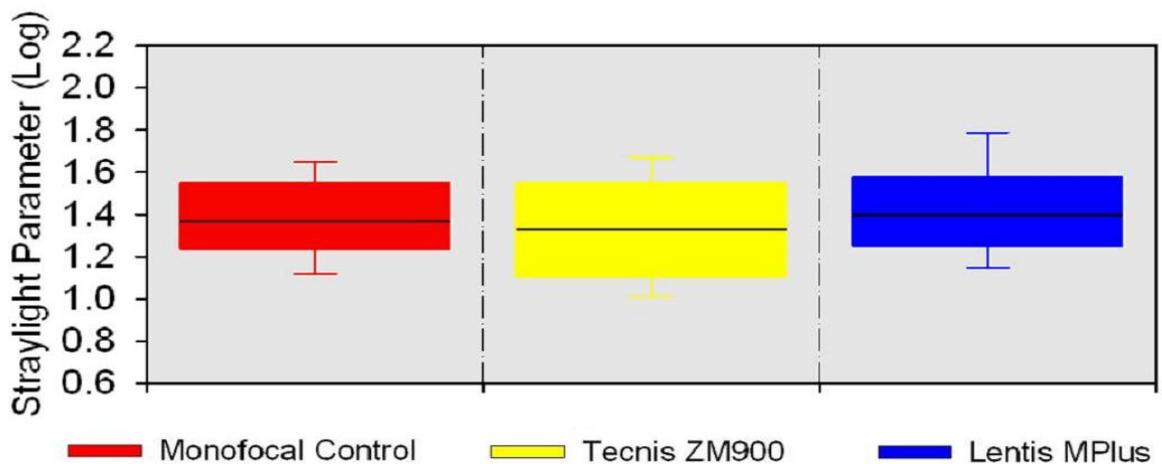
Figure 4.16 *Level of straylight for each IOL group (n=15x3)*

4.5.4.4 Comparison of Photopic Phenomenon

4.5.4.4.1 Monocular Comparison

There was a significant difference in the size of halos when comparing the photopic phenomena in the right eyes ($F_{2,42}=11.288$ p<0.001). Pair size differences between the groups can be seen in Table 4.8 (Figure 4.17).
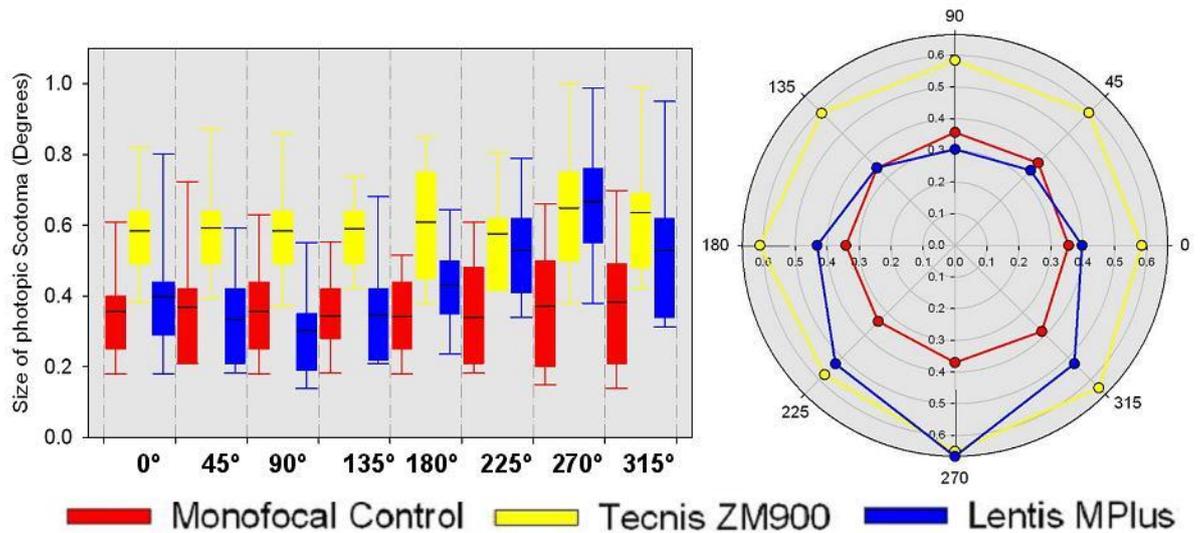
Figure 4.17 *Monocular results of the BD Halometer for each of the IOL groups. Right box plots, left Polar plot (n=15x3)*

Position Measured	IOL design	Monofocal control	Tecnis ZM900
0	*Tecnis ZM900*	p = 0.001	
	Lentis Mplus	p = 1.000	p = 0.011
45	*Tecnis ZM900*	p = 0.001	
	Lentis Mplus	p = 1.000	p < 0.001
90	*Tecnis ZM900*	p < 0.001	
	Lentis Mplus	p = 0.989	p < 0.001
135	*Tecnis ZM900*	p < 0.001	
	Lentis Mplus	p = 1.000	p < 0.001
180	*Tecnis ZM900*	p < 0.001	
	Lentis Mplus	p = 0.258	p = 0.003
225	*Tecnis ZM900*	p < 0.001	
	Lentis Mplus	p = 0.005	p = 1.000
270	*Tecnis ZM900*	p = 0.001	
	Lentis Mplus	p = 0.001	p = 1.000
315	*Tecnis ZM900*	p = 0.010	
	Lentis Mplus	p = 0.247	p = 0.567

Table 4.8 *Comparison of monocular BD Halometery results for each of the IOLs at each meridian (n=15x3)*

Examination of the binocular glare areas revealed a significant difference between the groups (F_2=8.163, p=0.001). The area of glare was significantly greater in the *Tecnis ZM900* group than the monofocal (p=0.001) and *Lentis Mplus* (p=0.034) group. Glare areas for the *Lentis Mplus* and monofocal groups were similar (p=0.578).

4.5.4.4.2 Binocular Comparison

There was a significant difference in the size of halos when comparing the photopic phenomenon binocularly ($F_{2,42}=19.525$, $p<0.001$). Differences between groups can be seen in Table 4.9 and Figure 4.18.
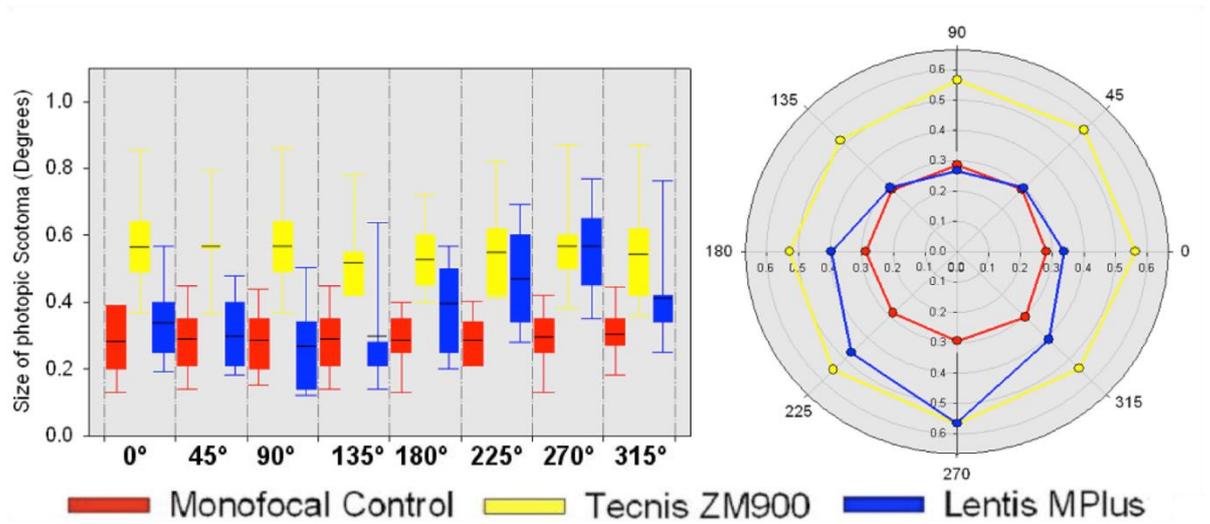
Figure 4.18 *Binocular results of the BD Halometer for each of the IOL groups. Right box plots, left Polar plot (n=15x3)*

Position Measured	IOL design	Monofocal control	*Tecnis ZM900*
0	*Tecnis ZM900*	p < 0.001	
	Lentis Mplus	p = 0.899	p < 0.001
45	*Tecnis ZM900*	p < 0.001	
	Lentis Mplus	p = 1.000	p < 0.001
90	*Tecnis ZM900*	p < 0.001	
	Lentis Mplus	p = 1.000	p < 0.001
135	*Tecnis ZM900*	p < 0.001	
	Lentis Mplus	p = 1.000	p < 0.001
180	*Tecnis ZM900*	p < 0.001	
	Lentis Mplus	p = 0.024	p = 0.005
225	*Tecnis ZM900*	p < 0.001	
	Lentis Mplus	p = 0.001	p = 0.282
270	*Tecnis ZM900*	p < 0.001	
	Lentis Mplus	p < 0.001	p = 1.000
315	*Tecnis ZM900*	p < 0.001	
	Lentis Mplus	p = 0.194	p = 0.065

Table 4.9 *Comparison of the binocular BD Halometery results for each of the IOLs at each meridian (n=15x3)*

Examination of the binocular glare areas revealed a significant difference between the groups (F_2=14.453, p<0.001). The area of glare was significantly greater in the *Tecnis ZM900* group than in the monofocal (p<0.001) and the *Lentis Mplus* (p=0.001) group. Glare areas for the *Lentis Mplus* and monofocal groups were similar (p=0.554).

4.5.4.5 Correlation Between Subjective Scores, Straylight and Photopic Phenomenon Measurement

There was no significant correlation between the subjective scores and the Straylight scores (r_s = -0.103, p = 0.503; Figure 4.19). Similarly no significant correlation was found between the subjective scores and the monocular (r_s=0.246, p = 0.103; Figure 4.20) and binocular (r_s = 0.241, p = 0.111; Figure 4.21) Halometery scores.

No significant correlation was found between the Straylight scores and the Halometer scores both monocular (r = 0.051, p=0.739) and binocular (r = 0.153, p = 0.315).
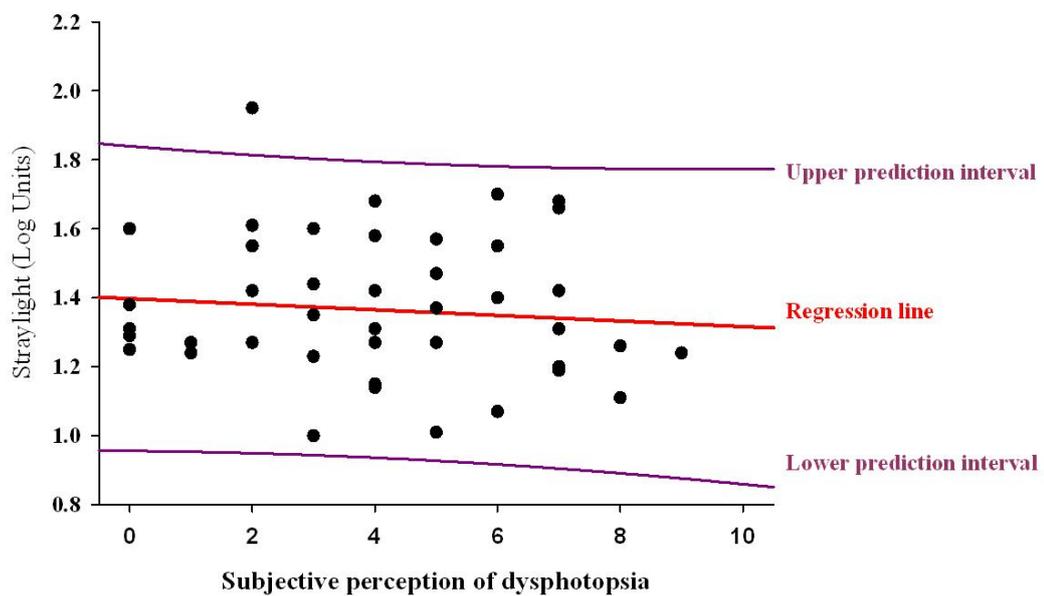
Figure 4.19 *Comparison of the subjective perception of dysphotopsia and straylight scores.*
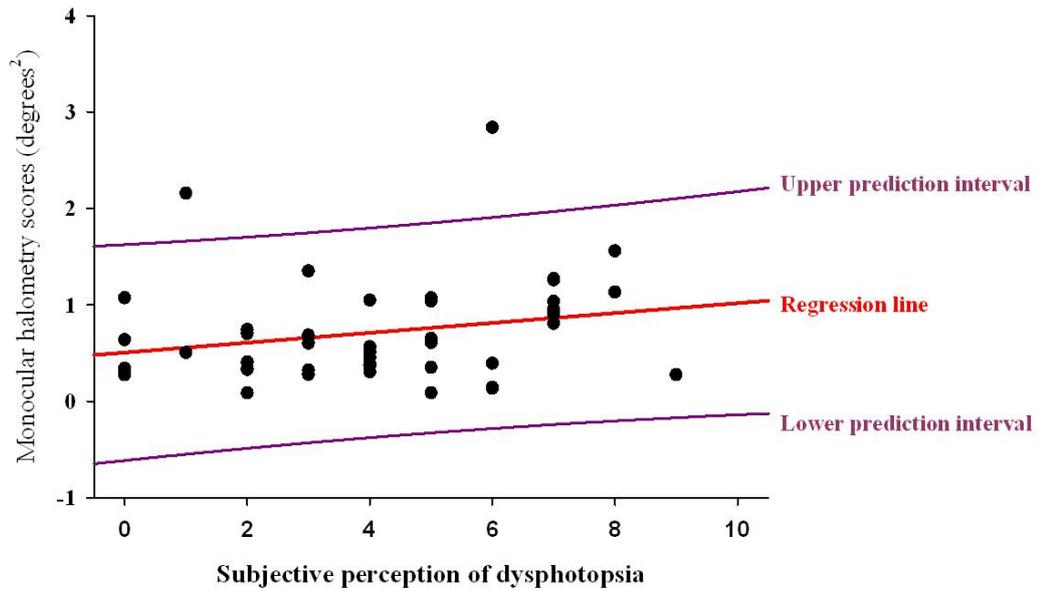
Figure 4.20 Comparison of the subjective perception of dysphotopsia and the monocular halometery scores.
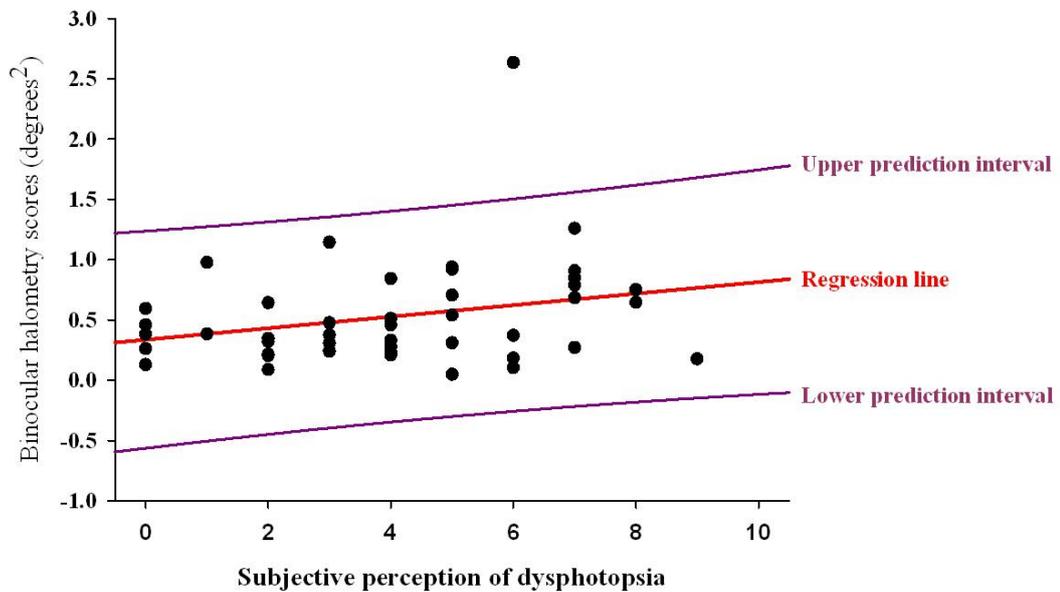
Figure 4.21 Comparison of the subjective perception of dysphotopsia and the binocular halometery scores.

4.6 Discussion

The use of Halometery in studies examining MIOLs has been limited to gross estimation Halometery, perimetry Halometery, subjective illustration Halometery, and the Glare & Halo test. All of these Halometers (with the exception of perimetry Halometery) require the subject to indicate subjectively the boundaries of their

photopic scotoma. Of the six studies that have used a Halometer to examine dysphotopsia with MIOL subjects five failed to demonstrate an increase in dysphotopsia with MIOL implantation (Hunkeler *et al.,* 2002; Namiki & Tagami, 1993; Allen *et al.,* 2009; Eisenmann *et al.,* 1996; Dick *et al.,* 1999). The Halometer described by Gutiérrez and Colleagues (2003) measured the area of scotoma at 12 meridians using a visual field style presentation program with dot light sources as the target. The Halometer DG uses a moveable optotype target to determine the size of the scotoma caused by a central glare source. However, this Halometer only measures dysphotopsia in one meridian and assumes that it is uniform in all positions around the glare source. The BD Halometer also uses Optotype targets, however it is able to map out the extent of scotoma in 8 meridians surrounding the light source, therefore assessing the uniformity and extent of scotoma.

This study shows that the BD Halometer is a valid and repeatable method for the assessment of dysphotopsia. The letter size of 6/15 enabled all subjects to identify the letter at the 500 C_w contrast level. The effects of dysphotopsia appear compounded during night driving and therefore a level of acuity matching that of the geometric angle size of a United Kingdom number plate was deemed an appropriate size target for the Halometer. For the phakic study several contrast levels were assessed. At maximum contrast a ceiling effect occurred where the target was visible at the minimum distance between letter and glare source. At the 100 C_w and 25 C_w contrast level, the letter was not visible with the 0.6 and 0.8 *Bangerter foil* due to the reduced visual acuity with these lenses. Therefore, for the pseudophakic assessment, a contrast level of 500 C_w was chosen to ensure the visibility of the target and minimising examination time, whilst minimising the ceiling effect.

Bangerter foils are an effective tool for increasing light scatter, as they have a detrimental effect on the point spread function (Pérez *et al.,* 2010). An increase in the density of the *Bangerter foils* increased the amount of Straylight and the photopic scotoma area. However, results from the C-Quant and BD Halometer did not correlate in both the phakic subjects and the pseudophakic subjects; this demonstrates that the instruments measure different aspects of vision. This is highlighted by the results in the pseudophakic group where the *C-Quant* detected no significant differences in the level of Straylight regardless of the implanted IOL. This concurs with previous studies and

suggests that measures of Straylight are not inferred measures of dysphotopsia caused by MIOLs.

The repeatability of the BD Halometer was higher in the pseudophakic study compared with the phakic study; this can be largely attributed to the change in light source between the mark1 and mark 2 versions of the BD Halometer. The mark 1 Halometer was attached to lithium Ion batteries, which showed a consistent, although small, decay in output over time. In contrast the mark 2 Halometer displayed a more consistent output therefore providing a higher standardization of glare between measurements.

At each meridian the *Tecnis ZM900* displayed a larger amount of photopic scotoma in comparison with the *Softec 1*. This is in keeping with the known descriptions of halos caused by MIOLs. The *Lentis Mplus* did not demonstrate the same appearance; superiorly the photopic scotoma region was similar to the monofocal IOL, however in the inferior portion of the visual field (270°) there was a greater amount of scotoma similar to the levels exhibited by the *Tecnis ZM900*. This can be explained by the location of the reading portion of the lens. In all subjects the *Lentis Mplus* IOL was implanted with the reading portion inferiorly, resulting in the defocused rays from the second focal point falling on the superior portion of the retina, responsible for the inferior visual field. As well as in the 270° position the levels of photopic scotoma with the *Lentis MPlus* was greater in the 180° and 225° positions binocularly and in the 225° position monocularly. This may be explained by the nature of the haptics used to hold the *Lentis MPlus* in place: IOLs that use an open C-loop haptic are known to rotate clockwise under capsular compression. This rotation could explain the increase in glare at the 225° and 180° positions. It would also explain the increased standard deviation in the inferior regions. However, dilated slit-lamp photography would be required to prove this hypothesis. These results raise important questions regarding the best orientation of the sectorial multifocal. Currently the surgical recommendation is to implant all lenses inferiorly however studies need to be conducted to determine the effect on vision of atypical segment placement.

The subjective categorisation of dysphotopsia supports the Halometery results; approximately 73% of the *Tecnis ZM900* subjects associated their dysphotopsia with either the small or large halo images, in comparison only 13% of the *Lentis MPlus* group associated their vision with the halo illustration, with 53% of this group reporting

either the starburst or decoupling image. The decoupling image is of interest as it depicts a ghost image inferiorly to the light sources on screen. Despite this difference, dysphotopsia ratings were similar for the *Lentis MPlus* group and the *Softec 1* group, and between the *Softec 1* group and the *Tecnis ZM900* group. There was no correlation between the subjective scores and the Straylight and Halometery results. These findings highlight the variability found with subjective rating scales and a need for an objective method of testing for quantifying haloes and glare. Adaption and tolerance to dysphotopsia are additional factors that need to be considered and may further explain the disparity between test methods.

Type A personality traits are regarded as a risk factor for multifocal IOL implantation as this group is widely regarded as intolerant to dysphotopsia (Fine and Hoffman, 2000; Koch and Wang, 2007). Standardised Halometery may be useful in determining other risk factors for MIOL rejection.

4.7 Limitations of the Study

A limitation of the study is the assumption that the *Lentis Mplus* retained its inferior position post implantation. Future studies warrant dilated digital slit lamp examination or aberrometry. It can be assumed that the lenses are reasonably stable as they are a hydrophobic acrylic material, 12 mm in length, ensuring a high level of friction between capsular bag and IOL (Chapter 7). In view of the present findings, the expected clockwise rotation of c-loop haptics may explain the increase in glare profile in the lower left portion of the subjects visual field.

The limitations of the Mark 1 Halometer are clear; new lithium Ion batteries were required for each examination and a 5-minute 'warm up' period was required before the glare source reached a stable output. The Mark 2 Halometer reduced this limitation and further work is required to achieve a glare source where the peak emission can be matched to varying wavelengths within the visual spectrum. Future studies will explore alternative power sources to achieve a stable glare source with USB power.

The use of the Arial Bold font was not ideal, but sufficient, as the purpose of the Halometer was to determine the extent of photopic scotoma rather than visual acuity. However, further refinements of the target would involve standardizing the Optotype to that employed in current LogMAR test charts.

4.8 Conclusions

The Halometer BD demonstrates good inter- and intra-repeatability for the measurement of Dysphotopsia in subjects implanted with MIOLs. The fully diffractive MIOL demonstrated a uniform increase in dysphotopsia in comparison with the monofocal IOL as measured with the Halometer. The Sectorial refractive MIOL demonstrates a localised increase in dysphotopsia over the inferior visual field. These findings were not demonstrated with the C-Quant; the level of straylight was similar with each IOL group.

As well as increased dysphotopsia, uncorrected refractive error remains a cause of post-surgical dissatisfaction. Improving the accuracy of ocular biometry and of IOL calculation formulae has the potential for reducing post-operative residual refractive error. Chapter 5 examines the accuracy of a new optical biometry device, designed to assist in IOL power calculations.

Chapter 5 A New Optical Low Coherence Reflectometry Device for Ocular Biometry in Cataract Patients

5.1 Introduction

The accurate measurement of ocular biometry is critical in optimizing post-operative refractive outcomes (Norrby, 2008). Ultrasound is the traditional technique for measuring anterior chamber depth (ACD) and axial length (AL) but is generally limited to a resolution of about ±0.15 mm (Butcher and O'Brien, 1991; Raj *et al.,* 1998). Partial coherence interferometry has subsequently been developed as an ocular biometry technique (Hitzenberger, 1991; Hitzenberger *et al.,* 1993). Since the advent of the first commercial device in 2001 the *IOLMaster* (Carl Zeiss Jena GmbH) this has become the technique of choice for ocular Biometry. It is non-contact in nature, avoiding the risk of corneal abrasion and contamination. It also provides significantly higher resolution measurements of axial length (about ±0.02 mm; equivalent to 0.05 D) and is less susceptible to examiner error (Hill *et al.,* 2008). The *IOLMaster* has been shown to be accurate and repeatable in both cataract biometry assessment (Packer *et al.,* 2002; Nemeth *et al.,* 2003) and in the study of refractive error (Vogel *et al.,* 2001; Santodomingo-Rubido *et al.,* 2002). The *IOLMaster* thus improved the refractive outcome results of cataract surgery (Eleftheriadis, 2003; Rose and Moshegov, 2003) and by 2002 was used in over a third of hospital eye units in the UK (Gale *et al.,* 2004).

The IOL master uses the effect of time domain interferometric – or coherent superposition of light waves – to measure ocular lengths of the eye in a technique similar to one-dimensional optical coherence tomography. The *IOLMaster* uses a 780 um diode laser. The beam is split: one half reflects off a fixed mirror and the other a moving mirror. The two beams are reflected by structures within the eye back to the signal detector. Axial length is determined when a specific interference signal is attained (Figure 5.1).
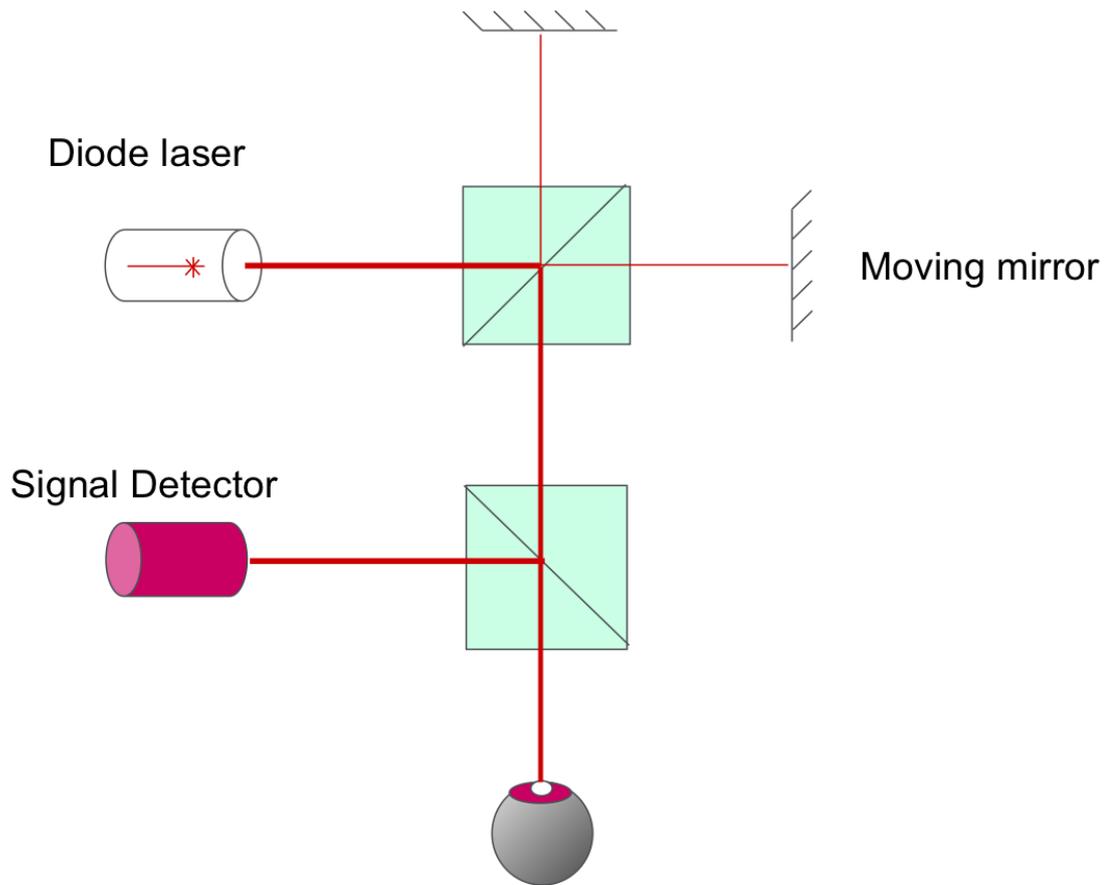
Figure 5.1 *Schematic diagram of the IOLMaster*

The *IOLMaster* uses Partial Coherence Interferometry (PCI) to measure AL. Measurements of corneal curvature, horizontal iris width (white-to-white), and ACD are assessed using other imaging techniques. The instrument does not have the facility to assess corneal, crystalline lens or retinal thickness (Santodomingo-Rubido *et al.,* 2002). Each of the *IOLMaster's* three assessments also requires realignment of the device with the visual axis of the eye. It fails to measure in up to 20% of eyes with dense opacities and macular disease (Nemeth *et al.,* 2003; Tehrani *et al.,* 2003; Freeman and Pesudovs, 2005), although this can be reduced to less than 10% with more advanced analysis of the interference waveform (Hill *et al.,* 2008). Ultrasound measurements are not affected by lens opacities and macular disease. Only eyes filled with silicone oil are unsuitable for ultrasound. In these patients PCI is a valid technique (Tehrani *et al.,* 2003; Parravano *et al.,* 2007).

The largest source of error with IOL power predictions is from the estimation of the post-operative IOL position. A new ocular biometry device jointly developed by Haag-Streit (*LenStar LS900,* by Haag-Streit, Koeniz, Switzerland) and Wavelight (*Allegro*

Biograph, by Wavelight, Erlangen, Germany), has recently become commercially available and uses optical low coherence reflectometry (OLCR) to measure corneal thickness, ACD, crystalline or intraocular lens thickness, and AL. The technique was developed in the late 1980s for reflection measurement in telecommunication devices with micrometer resolution. It was first applied to *in-vivo* biological tissue (the eye) by Fercher and colleagues (1988). The *LenStar LS900* uses other imaging technique simultaneously for assessing central corneal curvature, horizontal iris width (white-to-white), pupil size, and pupil and visual axis decentration. These additional parameters may assist in improving the calculation of the predicted post-operative IOL position

The *LenStar LS900* also uses the effect of time domain interferometry, or coherent superposition of light waves, to measure ocular lengths of the eye. However, the *LenStar LS900* uses a superluminescent diode with a Gaussian-shaped spectrum allowing higher axial resolution; hence the name: optical low coherence reflectometry (OLCR). In OLCR, an 820 μm beam is split into a reference beam and sample beam. The sample beam enters the eye, reflecting from the structures as in PCI. The reference beam enters a spinning glass cube; this reflects the light while continuously changing the optical path length. Both beams return to a signal detector and where the interference pattern is analyzed. The distance between the interference peaks define the optical distance between structures. Dividing this optical distance by the refractive index of the medium it travels through gives the geometric distance (Figure 5.2).
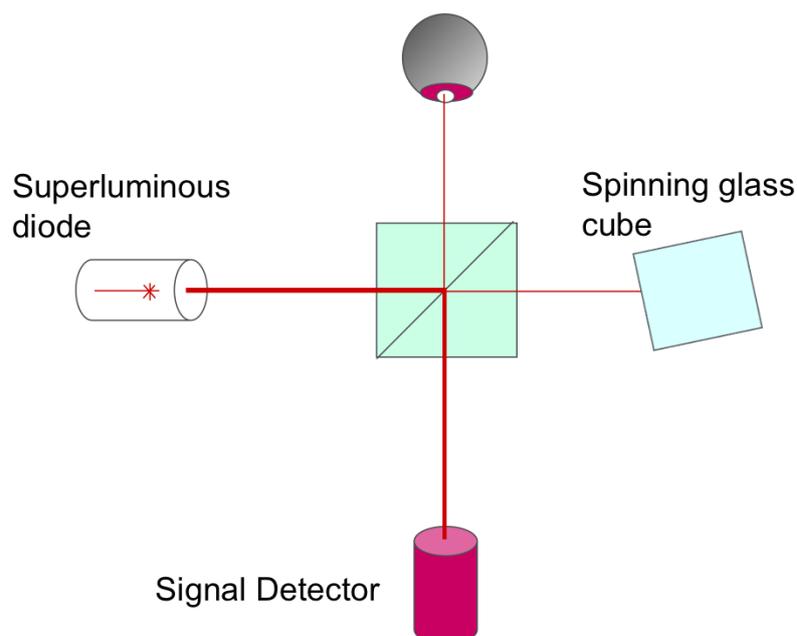
Figure 5.2 *Schematic diagram of the LenStar LS900*

5.2 Study Aim

This study evaluated the validity of the *LenStar LS900* when compared with the *IOLMaster* and A-scan applanation ultrasonograph. It also examined the accuracy of *LenStar LS900* measurements with IOL calculation formulae and assessed the relationship between pre-operative crystalline lens position and post-operative IOL position.

5.2.1 Subjects

One-hundred and twelve patients (36 male and 76 female), with a mean age of 76.4 ± 9.1 years (range from 41 to 96 years), listed for cataract surgery were recruited by a single clinician (PB) and participated in the study. The inclusion criteria were as follows:

- Clinically significant cataract requiring Phacoemulsification and IOL implantation.
- The absence of corneal disease and previous ocular surgery
- Aged over 18
- Willing to participate in the study

For each subject the *IOLMaster* was used to determine axial length and corneal power. For IOL power, the Hoffer Q IOL formula was used for short axial lengths, (<22 mm; College of Ophthalmologist's Guidelines) and the SRK/T was used for all other axial lengths; the target refraction was chosen according to the subjects' visual requirements. A *Softec 1* (Lenstec) monofocal IOL was implanted in all subjects.

All operations were performed by one of three surgeons using topical or local anaesthetic. A 2.85 mm clear corneal incision, widening to 3.20 mm after injection, was placed on the temporal cornea. Phacoemulsification, aspiration and irrigation were performed through a 5.50 mm capsulorhexis using the *Millennium phacoemulsification system* (Bausch and Lomb). All IOLs were implanted into the capsular bag.

The study was approved by the National Research Ethics Committee and conformed to the Declaration of Helsinki (2008).

5.2.2   Methods

The *LenStar LS900* was focused and aligned using the image of the eye on the computer monitor while the patient fixated on a flashing red light. The eyes were in focus when the instrument head was approximately 6.8 cm away from the subject's eyes. Subjects were asked to perform a complete blink just before measurements were taken in order to spread an optically smooth tear film over the cornea. The instrument takes 16 consecutive scans per measurement without the need for realignment, and five measurements were taken (as recommended) to test intrasession repeatability. The device uses OLCR to measure corneal thickness, ACD, crystalline or intraocular lens thickness and AL using the 820 μm superluminescent diode. The retinal thickness can also be determined from the scans, but this requires subjective alignment of a cursor and was not assessed in this study. The *LenStar LS900* also uses a 950 μm light to assess by image analysis:

- *central corneal topography* – using two rings of diameter 1.65 mm and 2.30 mm (for an eye of radius 7.8 mm) of 16 light spot each, reflected off the air/tear interface.
- *horizontal iris width (white-to-white)* – fitting the best circle with the lowest error square to the detected edge and pupil size using the same method.
- *pupil and visual axis decentration* – Comparison of the visual axis in respect to the centre of the cornea and pupil as circumscribed by the limbus.

The *IOLMaster* – running Advanced Technology version 5 software (Hill *et al.,* 2008) – was used to make the same assessments. The subject viewed the instrument's internal illuminated targets while the eyes were focused and aligned on the computer monitor. The eyes were in focus when the instrument head was approximately 5.5 cm away. Subjects were asked to perform a complete blink just before measurements were taken in order to spread an optically smooth tear film over the cornea. AL was measured by partial coherence interferometry (laser diode infrared light of wavelength 780 μm). ACD was determined by analyzing the image of an optic section, measuring the distance between the anterior corneal pole and the anterior surface of the crystalline lens. Corneal curvature was captured by measuring an image of light spots reflected from the tear film interface. The light spots are arranged in a 2.3 mm diameter

hexagonal pattern; the separations between the opposite spot reflections are used to determine corneal curvature (Santodomingo-Rubido *et al.,* 2002). Five separate measurements were averaged for both AL and corneal curvature, whereas a single shot automatically generated and averaged five measurements of ACD.

A-scan applanation ultrasound (*OcuScan*; Alcon Surgical, Irvine, California, USA) was performed on a subgroup of 21 patients (5 male and 16 female), with a mean age 78.1 ± 8.1 years (range 70 to 90 years, median 77.5 years). The A-scan applanation device – using the time taken for ultrasound waves to reflect back to its receiver from an optical surface (Story and Rabie, 1983) – calculated ACD, crystalline lens thickness, and AL. One drop of topical anaesthetic, benoxinate HCl 0.4% (Minims, Chauvin Pharmaceuticals, Romford, UK), was instilled in the patient's eye 2 min before ultrasound measurement. Care was taken in aligning the transducer probe along the optical axis and to exert minimal corneal pressure. Ten measurements were taken for each eye and the mean calculated.

The intersession repeatability of the *LenStar LS900* was examined by repeating the measurement again in a second session on the same day on 32 of the patients (nine male and 23 female), with a mean age of 73.7 ± 9.3 years (range from 41 to 87 years, median 74.5 years).

Twenty-five subjects returned for a one-year post-operative assessment (mean age 73.5 ± 7.4, range 55 to 80, median 74.4). The *Lenstar LS900* and *Pentacam* (Oculus, Optikgera te GmbH, Germany) were used to measure the distance between the anterior surface of the IOL and the posterior surface of the cornea. Following dilation using 1% Tropicamide (Minims, Chauvin Pharmaceuticals, Romford, UK), 5 measurements were taken using a *Lenstar LS900* and 3 measurements using a *Pentacam*. The *Pentacam* is a commercially available Scheimpflug system; it can image the anterior segment by analyzing the results of 25 or 50 scans at different meridians. The accuracy of the automatic measurement of anterior depth in pseudophakic subjects is variable due to limitations in the software's edge detection algorithms when examining a pseudophakic eye (de Castro *et al.,* 2007). Instead of using the automatic measurement, the distance between the anterior IOL surface at the centre of the pupil and the posterior corneal surface at the centre of the cornea was measured manually in the 90° and 180° scans using the callipers and images present in the software. For each of the three

measurements the IOL position at the 90° and 180° degree positions were measured and the average of all of the measurements were recorded.

The automated anterior chamber depth measurement from the *Lenstar LS900* is the distance between the anterior IOL and posterior corneal surface. This distance was also calculated manually using the *Lenstar LS900* scan images with software callipers. A valid measurement required two interference peaks to be detected at the anterior and posterior surface of the IOL; any measurements failing to detect both edges were rejected. The average of 5 measurements was recorded.

5.3 Statistical Analysis

The bias between measurements (the mean difference and 95% confidence interval) was calculated and presented graphically (Bland and Altman, 1986). The level of agreement between biometry measurements was tested using the Pearson product moment correlation coefficient. Comparisons between measurements were performed using paired two-tailed t tests. Corneal curvatures were analyzed in the steepest and flattest meridian in dioptres, using the refractive index 1.332. The *IOLMaster* and ultrasonograph determine ACD from the front corneal surface, whereas the *LenStar LS900* measures ACD from the posterior corneal surface. Therefore corneal thickness, calculated by the *LenStar LS900,* was added to its anterior chamber measurement for comparison.

The position of the back surface, and middle of the IOL, was calculated by adding the known IOL thickness, and half of the IOL thickness, to the distance between the posterior cornea and anterior IOL surface respectively . Pearson's product moment correlation coefficient was used to determine the relationship between the front, middle and back surface of the crystalline lens and the front, middle and back surface of the IOL.

5.4 Results

The mean, 95% confidence interval, and range of each of the parameters assessed by the *LenStar LS900* and *IOLMaster* in this patient population are presented in table 5.1.

	Instrument	
Biometry	*LenStar LS900*	*IOLMaster*
Pupil size (mm)	5.11 (2.77), 2.43–7.26	–
White-to-white (mm)	12.08 (0.86), 11.20 to 12.80	12.15 (0.95), 11.06 to 12.91
Corneal curvature (D) flat meridian	42.78 (2.83), 38.58 to 46.54	42.82 (2.83), 39.20 to 46.77
Corneal curvature (D) steep median	43.88 (2.74), 39.87 to 47.36	43.93 (2.82), 39.90 to 47.37
Corneal thickness (mm)	0.55 (0.04), 0.47 to 0.64	–
Anterior chamber depth (mm)	3.19 (0.93), 2.05 to 4.45	3.09 (1.02), 2.10 to 5.28
Crystalline lens thickness (mm)	4.41 (0.50), 2.49 to 5.56	–
Axial length (mm)	23.25 (2.21), 20.93 to 26.60	23.24 (2.19), 20.94 to 26.50
Failed measurement (%)	9	10

Table 5.1 *Average (95% confidence interval), followed by range, of biometry measurements as assessed by the LenStar LS900 and IOLMaster Failed measurement refers to coherence interferometry measurements; n=112. A dash indicates that these could not be measured with the instrument*

Coherence interferometry measurements with the *LenStar LS900* failed for 9 patients with dense cataracts. The *IOLMaster* could not take partial coherence interferometry measurements in these same patients, plus one additional patient. The difference between the *LenStar LS900* and *IOLMaster* (or ultrasound measurements) for each individual patient was compared with the mean and plotted for each biometry component. The measurement of the white-to-white corneal measurement was similar for the *LenStar LS900* and *IOLMaster* (Table 5.2; Figure 5.3). The *LenStar LS900* read as much as 0.72 mm above and 0.60 mm below the *IOLMaster* for the white-to-white diameter.

Biometry	Instrument	
	IOLMaster	Ultrasound
White-to-white (mm)	0.06 (0.33) p = 0.305, r = 0.74	
Corneal curvature (D) flat meridian	-0.03 (0.31) p = 0.305, r = 0.98	
Corneal curvature (D) steep median	-0.05 (0.32) p = 0.130, r = 0.97	
Anterior chamber depth (mm)	0.10 (0.40) p = 0.014, r = 0.68	0.32 (0.62) p = 0.028, r = 0.36
Crystalline lens thickness (mm)		0.16 (0.83) p = 0.382, r = 0.03
Axial length (mm)	0.01 (0.02) p < 0.001, r = 0.99	-0.14 (0.15) p<0.001, r = 0.99

Table 5.2 *Mean difference (95% confidence interval), significance (p value) and correlation (r) of IOLMaster (n=101) and ultrasonography (n=21) with the LenStar LS900 biometry measurements*
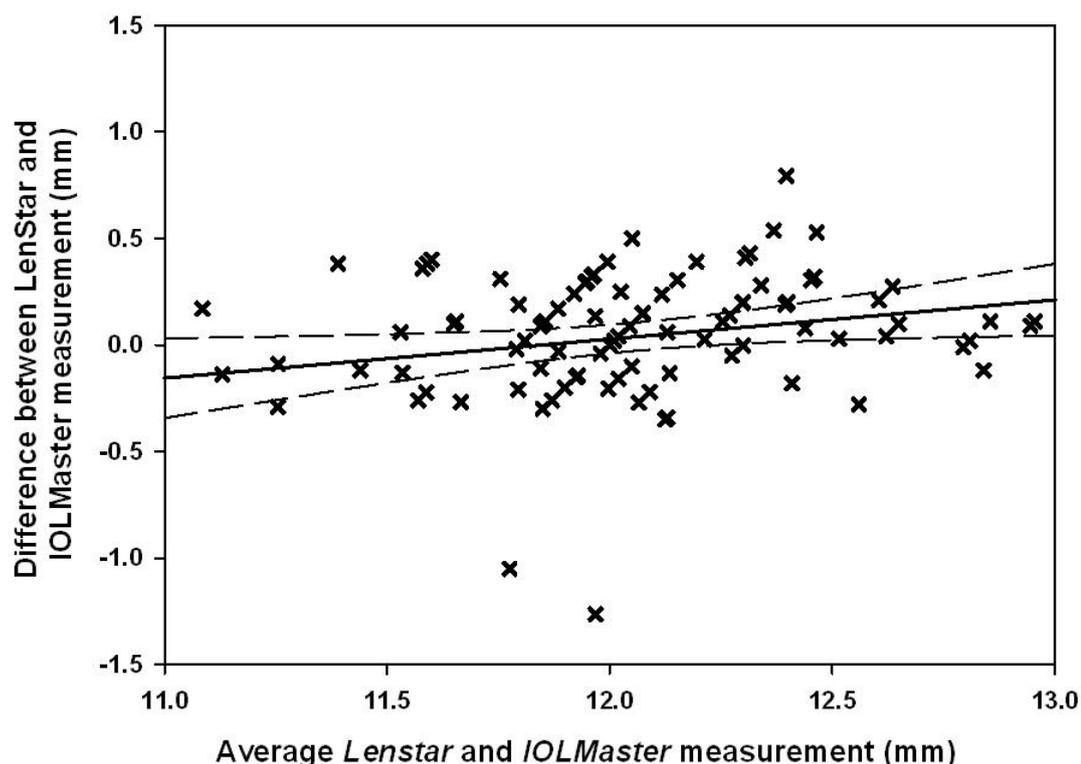
Figure 5.3 *White-to-white: difference between LenStar LS900 and IOLMaster. The solid line denotes mean and dashed lines 95% confidence intervals. n=112 eyes*

Corneal curvature measurements from the *LenStar LS900* were similar to those from the *IOLMaster* (Table 5.2; Figure 5.4). The *LenStar LS900* read as much as 0.58 D

above and 0.68 D below the *IOLMaster* for corneal curvature. For comparison of the mean spherical and vector power between the *LenStar LS900* and *IOLMaster* see Appendix A5.
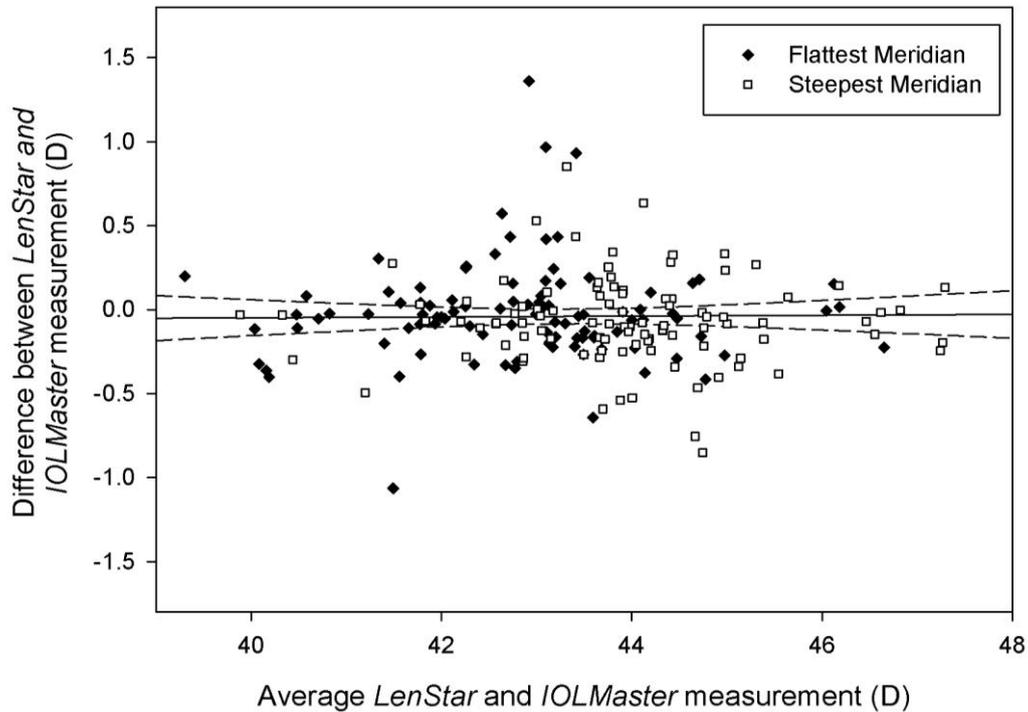
Figure 5.4 Corneal curvature: difference between LenStar and IOLMaster in the flattest and steepest meridians. The solid line denotes the mean and dashed lines 95% confidence intervals of the average curvature. n=112 eyes

ACD, as measured by the *LenStar LS900*, was significantly greater than both the *IOLMaster* and ultrasound assessment (Table 5.2; Figure 5.5). However, there was no apparent bias with the magnitude of the ACD. The *LenStar LS900* read as much as 0.88 mm above and 0.68 mm below the *IOLMaster*. It read as much as 1.53 mm above and 0.89 mm below applanation ultrasound for ACD.
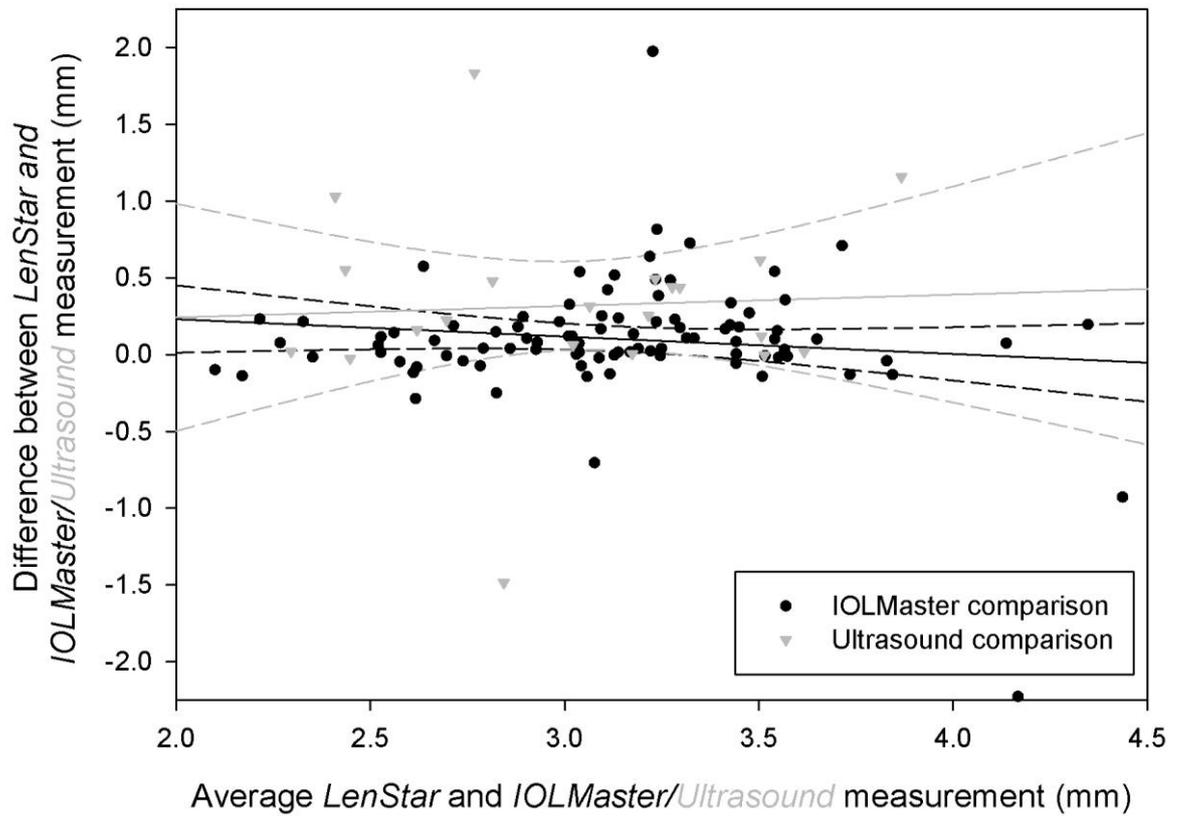
Figure 5.5 *Anterior chamber depth: difference between LenStar LS900 and*

IOLMaster/ A-Scan ultrasonography. The solid line denotes the mean and dashed lines

95% confidence intervals. n=112/21 eyes

Crystalline lens thickness measured by the *LenStar LS900* was similar to the ultrasound

measurements (Table 5.2; Figure 5.6). However, the variability was high: the *LenStar*

LS900 read as much as 1.79 mm above and 1.46 mm below ultrasound measurements.
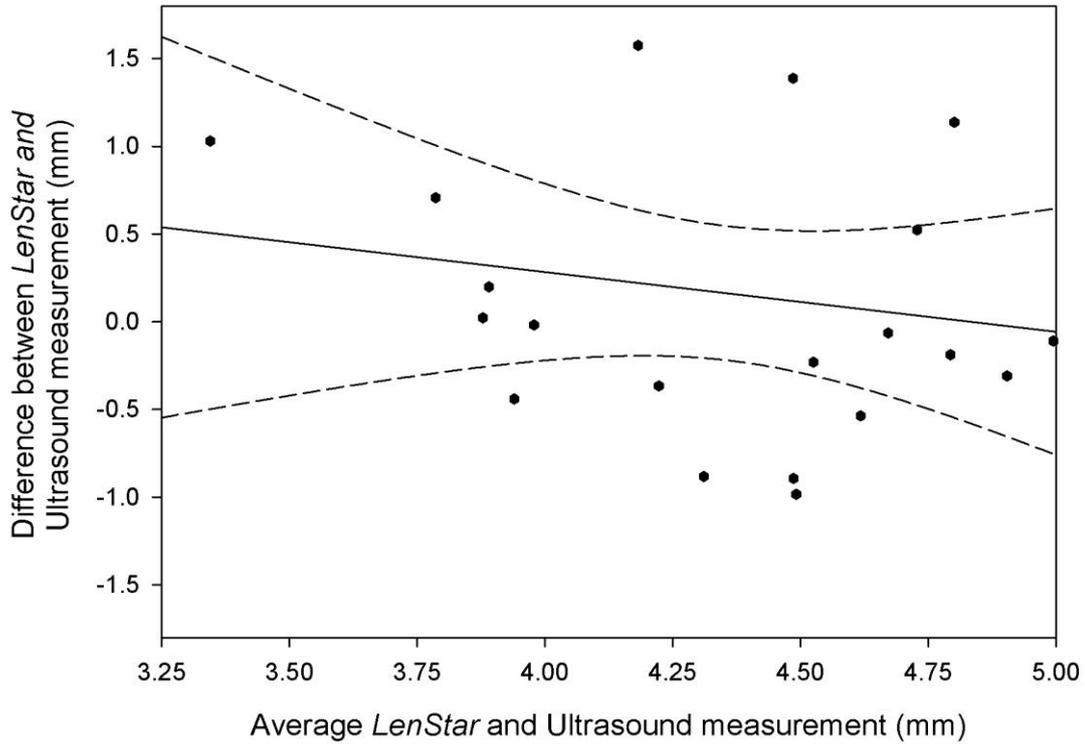
Figure 5.6 *Crystalline lens thickness: difference between LenStar LS900 and A-scan ultrasonography. The solid line denotes the mean and dashed lines 95% confidence intervals. n=21 eyes.*

AL, as measured by the *LenStar LS900*, was longer than the *IOLMaster* measurement, however, this measurement was not clinically significant. The *LenStar LS900* AL measurements were shorter than the ultrasound measurements, and there was a bias towards a greater disparity with increasing AL (Table 5.2; Figure 5.7). The *LenStar LS900* could be expected to read as much as 0.06 mm above to 0.04 mm below the *IOLMaster* and 0.16 mm above to 0.44 mm below applanation ultrasound for AL.
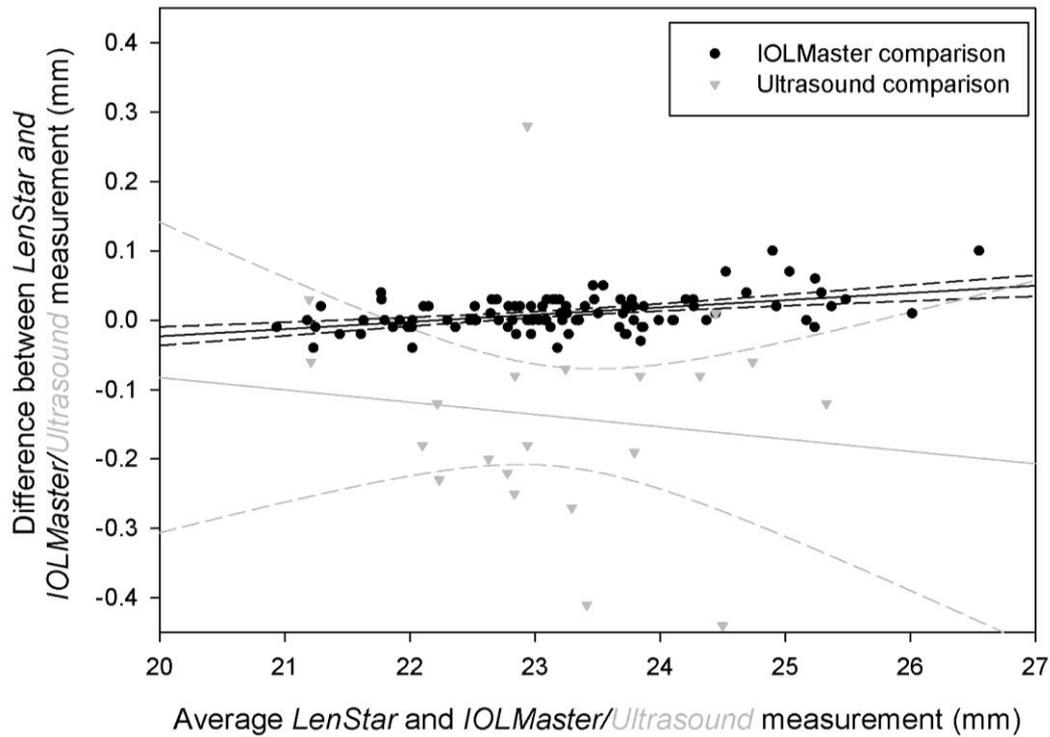
Figure 5.7 *Axial length: difference between LenStar LS900 and IOLMaster/A-scan ultrasonography. The solid line denotes the mean and dashed lines 95% confidence intervals. n=111/21 eyes*

The *LenStar LS900* intrasession and intersession variability was small. Intersession variability of the average reading was consistently smaller than the intrasession variability for the measurements of OLCR and corneal curvature (Table 5.3). The intrasession repeatability could be improved by using the *LenStar LS900* software functionality—for example, ACD variability halved to ±0.024 mm by excluding the most aberrant value of the five measurements.

Biometry	Intra-session	Inter-session
Pupil size (mm)	0.079	0.112
White-to-white diameter (mm)	0.077	0.073
Corneal curvature (D) flat meridian	0.14	0.09
Corneal curvature (D) steep median	0.14	0.07
Corneal thickness (mm)	0.003	0.001
Anterior chamber depth (mm)	0.051	0.013
Crystalline lens thickness (mm)	0.089	0.024
Axial length (mm)	0.016	0.006

***Table 5.3** Intrasession (five repeats; n=112) and intersession (two sessions; n=32) average standard deviation of repeated measurements with the LenStar LS900*

The *LenStar LS900* was able to detect the front and back surface of the IOL in only one subject. It was able to detect one of the surfaces in ten subjects and failed to detect either surface in the remaining 14 subjects. Both surfaces needed to be detected to provide a valid measure, the position of the posterior or anterior lens surface cannot be determined if only a single surface is detected as there are no details regarding which surface was detected and displayed by the interference pattern. As the post operative IOL position could only be established in one subject using the *LenStar LS900*; all Post-operative IOL position results have been taken using the *Pentacam.*

The pre-operative crystalline lens position (measured with the *LenStar LS900*) and the one-year post-operative IOL position (measured with the *Pentacam)* are shown in figure 5.8. The correlation of the pre-operative crystalline lens position and post-operative IOL positions are as follows:

- Anterior crystalline lens surface position correlated poorly with the post-operative front ($r = 0.306$, $p=0.190$), middle ($r = 0.285$, $p = 0.223$), and back ($r = 0.266$, $p = 0.257$) positions of the IOL.
- The middle of crystalline lens had a moderate correlation with the front ($r = 0.472$, $p = 0.036$) and central ($r = 0.494$, $p = 0.027$) post-operative position of the IOL but a poor correlation with the back surface position ($r = 0.385$, $p = 0.093$).

- The back surface of the crystalline lens had a moderate correlation with the anterior surface of the IOL (r=0.453, p=0.045), but a poorer correlation with the middle (r = 0.436, p = 0.426) or back surface of the IOL(r = 0.371, p = 0.108).
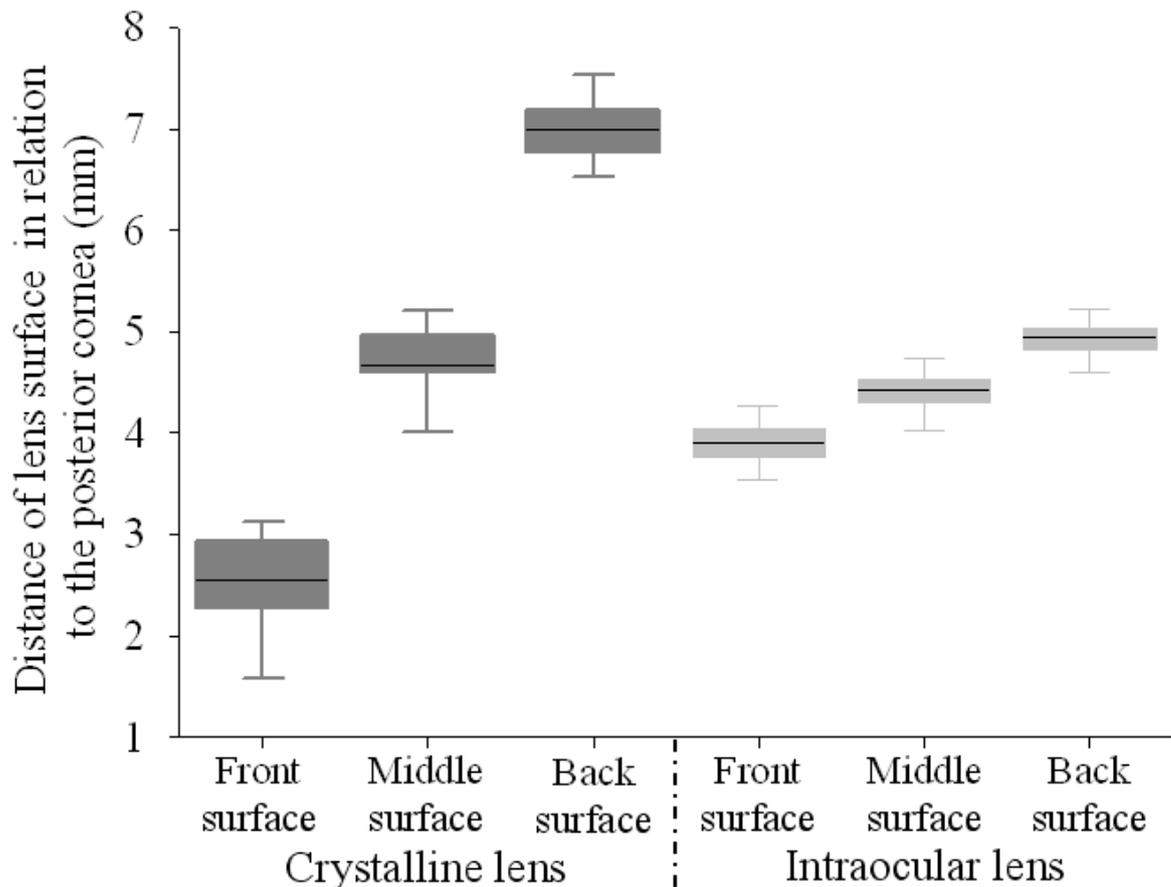
Figure 5.8 *Position of the pre-operative crystalline lens and post-operative intraocular lens in relation to the posterior corneal surface*

5.5 Discussion

This study shows the validity, repeatability, and clinical utility of OLCR for ocular biometry assessment in comparison with current instrumentation used in clinical practice. Only 9% of patients could not be measured using the *LenStar LS900*, which was similar to the proportion of failed measurements with the *IOLMaster,* and similar to a previous study (Hill *et al.,* 2008). In general, measurements of length/thickness were larger when measured by the *LenStar LS900* and compared to the *IOLMaster*. However, the clinical significance of this variation is minor with the 0.01 mm difference in axial length equating to 0.03 D (Hill *et al.,* 2008). The greater variability

when comparing the device to applanation ultrasound is in part due to the lower resolution of the ultrasound technique (Butcher and O'Brien, 1991; Raj *et al.,* 1998), and because laser light is reflected from the retinal pigment epithelium (in contrast to ultrasound waves which are reflected from the internal limiting membrane; Storey and Rabie, 1983).

The *IOLMaster* does not use coherent interferometry to measure ACD. Instead it analyses an image of an optic section (comprising a 0.7 mm width slit beam at 38° to the visual axis) to determine the distance between the anterior surface of the cornea and crystalline lens (Santodomingo-Rubido *et al.,* 2002). The OLCR waveform produces interference peaks at the anterior and posterior corneal surfaces as well as at the anterior crystalline lens surface, The *LenStar LS900* analyses this waveform to determine the anterior chamber depth and corneal thickness. These need to be combined for comparison with the IOLMaster AC depth. The disparity between ACD measurements performed by ultrasonography and *IOLMaster* has previously been reported (Reddy *et al.,* 2004).

The *LenStar LS900* and *IOLMaster* were found to measure equivalent values for white-to-white and corneal curvature using image analysis. Caution must be taken when using a dioptric representation of corneal curvature, as differences in the assumed corneal refractive index (n=1.3375 (*IOLMaster*) and n=1.332 (*LenStar LS900*)) would result in a clinically significant difference in average curvature for both medians − equivalent to 0.76 (0.21) D (p < 0.001) in this study population. The *LenStar LS900* measurements of crystalline lens thickness were not correlated to those recorded by ultrasonography. The larger intra-session variability (±0.33 vs ±0.09 mm) and range of values (2.83 to 5.06 vs 3.72 to 5.38 mm) with ultrasound compared with the *LenStar LS900* suggest that optical low coherence reflectometry may be the better technique to assess crystalline lens thickness.

Using the recommended intraocular lens power calculation formulae − incorporating many of the discussed biometry measurements − the difference between the *LenStar LS900* and *IOLMaster* was 0.01 (0.30) D (96% within 0.5 D) for SRK II, 0.16 (0.30) D (87% within 0.5 D) for Hagis (which uses anterior chamber depth, hence the greater difference) and 0.04 (0.24) D (95% within 0.5 D) for Hoffer Q.6 Hence, despite some

statistical differences between the ocular biometry measurements the *LenStar LS900* measurements clinically matched current techniques.

The coefficient of repeatability for intra- and intersession repeatability using the *LenStar LS900* are impressive (≤2% of the average value for each biometric measure) and at least comparable with the *IOLMaster* (Lam *et al.,* 2001; Santodomingo-Rubido *et al.,* 2002) and ultrasound (Butcher and O'Brien, 1991; Raj *et al.,* 1998). As expected, using the average of repeated measurements decreases the variability, and this can be further improved by excluding the most divergent of the results as allowed by the functionality of the *LenStar LS900* software.

Examination of the post-operative IOL position relative to the pre-operative crystalline lens position has some interesting implications. The Post-operative position of the centre of the IOL is on average 0.25 ± 0.52 mm anterior to the pre-operative crystalline lens centre position. The Hoffer Q and Hagis formulas use anterior chamber depth in the calculations to predict the post-operative IOL position; however, the results from this study suggest that anterior chamber depth alone is a poor measurement for the prediction of IOL position and that the size of the crystalline lens is an important measurement to include in IOL calculations. The Holladay 2 formula includes the measurement of lens thickness however the calculation of this variable prior to the launch of the *LenStar LS900* was limited to measurements with A-Scan, which this study has demonstrated can vary.

Subsequent to the completion of this study several validation investigations have been published on the *LenStar LS900*. Both Holzer and colleagues (2009) and Rohrer and associates (2010) found excellent correlation between the *LenStar LS900* and *IOLMaster* results for corneal curvature and AL and a good (but lower) correlation of the ACD. These two studies found no significant difference between the measurements of both machines. However, both Cruysberg and associates (2010) and Hoffer and associates (2010) found that the *LenStar LS900* produced significantly longer AL measurement in comparison with the *IOLMaster* and three studies found a shorter anterior chamber depth measurement and flatter corneal curvature measurement with the *LenStar LS900* (Cruysberg *et al.,* 2009; Hoffer *et al.,* 2010; Rabsilber *et al,* 2010). These results are in support of the present findings where the AL and ACD measurements of the *LenStar LS900* were found to be significantly longer than those of

the *IOLMaster*. In the present study corneal curvature was also found to be flatter however this finding was not significant (Appendix A5).

Compared with currently used clinical instrumentation, the *LenStar LS900* provides a comprehensive range of ocular biometry measurements required by newer, more accurate intraocular lens power calculation formulae (Fenzl *et al.,* 1998). In addition, it allows measurements such as corneal thickness (including the functionality of measurement while the patient views internal off-axis illuminated targets at 2 mm and 2.7 mm eccentricity separated by 22.5°), retinal thickness, and the decentration between the visual axis and the centre of the cornea. Some of these measurements may improve the accuracy of intraocular lens power prediction or may be useful in assessing the development of refractive error (Santodomingo-Rubido *et al.,* 2002). It is therefore envisaged that the *LenStar LS900* will be well received in both the clinical and research environment due to its high resolution, good validity and repeatability compared with currently used instrumentation, single alignment requirement and non-contact measurement.

5.6   Limitations of the Study

The *LenStar LS900* was used to determine the post-operative IOL position, however, it failed to determine lens position in all but one of the subjects. Instead post-operative IOL position was determined using the *Pentacam*. The *Pentacam* software also failed to determine the anterior IOL position using its automated settings. Therefore IOL position was measured manually using the software callipers, which is likely to have increased the measurement variability compared to an automated technique. Often the boundary of the anterior cornea and posterior cornea can be difficult to determine. The *LenStar LS900* measures along the visual axis; in comparison, the measurement using the *Pentacam* was from the centre of the posterior corneal surface to the IOL at the centre of the pupil. To improve the objectivity of the test an automatic edge detection program could be developed to analyze the *Pentacam* images.

5.7   Conclusions

The *LenStar LS900* has shown to provide valid and repeatable measures of axial length, crystalline lens thickness, anterior chamber depth and corneal thickness using OLCR. It

is also able to measure corneal power, corneal diameter, pupil diameter and the position of the visual axis. This has the potential for increasing the accuracy of IOL calculations; thus reducing postoperative refractive error. Levels of corneal astigmatism greater than 1.50 D was present in 21% of the subjects assessed during this study. The implication of this is high levels of postoperative levels of astigmatism can be expected in these subjects; increasing spectacle dependency. Following MIOL implantation postoperative astigmatism compromises visual acuity at all distances (Hayashi *et al.,* 2010). Corneal astigmatism can be corrected on the cornea or by using a toric IOL optic. The reduction of astigmatism using a toric IOL is dependent on its orientation matching the axis of astigmatism on the cornea. In Chapter 6 a new method used for assessing the rotational stability of a toric IOL is described and in Chapter 7 this technique is used to assess the orientational stability of a closed loop haptic aspheric and toric IOL.

5.8 Supporting Publications

Buckhurst, P.J., Wolffsohn, J.S., Shah, S., Naroo, S.A., Davies, L.N. & Berrow, E.J. (2009). A new optical low coherence reflectometry device for ocular biometry in cataract patients. *Br J Ophthalmol.* **93,** 949-53.

Chapter 6 Rotational Analysis of a Toric Intraocular Lens

6.1   Introduction

IOL rotation is most commonly measured subjectively using a slitlamp bio-microscope (Viestenz *et al.,* 2005), eyepiece graticule (Ruhswurm *et al.,* 2000) or slit-beam protractor (De Silva *et al.,* 2006). However, methods used for determining rotations are not always specified (Chang, 2003). These subjective techniques rely on the patient maintaining a stable and vertical head position at each assessment and rotation is estimated to the nearest 1 to 5 degrees.

Digital imaging has been applied to toric IOL rotation assessment. Original studies used generic (Nguyen and Miller, 2000, Becker *et al.,* 2004) or custom image-analysis software (Bender *et al*., 2004) to assess the rotation of a line drawn to join features on the IOL, however, this axis was compared with the image horizontal plane, ignoring the effect of head or eye rotation between assessments. Viestenz and colleagues (2005) evaluated the eye's rotational stability during photography over a period of at least 6 months using fundus image analysis. The findings indicated changes of eye rotation, on average, by 2.5 degrees between visits, however the change was as high as 11.5 degrees, being greater in women, older patients, and those with worse visual acuity or higher astigmatism. The author noted that the deviation in the measured orientation of the eye between visits resulted from a combination of cyclotorsion, head rotation, and autorotation during fixation of the positioning light. The study also estimated relatively large errors from the mounting of the camera and framing and projection of slides: this is less of an issue with cameras integrated into slitlamps. The latter usually has an external light source as well as the slit beam to allow illumination of the iris and bulbar conjunctiva at the same time as the retro-illumination. Viestenz and colleagues (2005) recommend a digital overlay technique that uses conjunctival vessels, Axenfeld loops, or iris structure as references to account for these intrinsic rotations. Weinand and associates (2007) used this technique in 17 of 40 eyes to compare rotation immediately after implantation, then at 6 months after implantation of a single-piece acrylic IOL. The other images could not be analysed due to insufficient dilation (IOL orientation required visibility of both haptic–optic junctions) and poor image quality. In addition, a different camera was used on each occasion and repeatability of analysis and image capture was not assessed. Patel and colleagues (1999) also compensated for head and

eye rotation by rotating the retro-illuminated image to align preoperatively made corneal ink markings on a surgical video frame at the 6 o'clock position. This technique had an intra-observer variability of 2.3 to 3.1 degrees. More recently, Shah and associates (2009) calculated the centre of the IOL as the centre of a rectangle with toric IOL marks as the opposite corners. A radial grid was overlaid on the centre of the IOL to assess the axis of a line joining the toric marks to 0.1-degree precision. The axis of a line joining the centre of the IOL to a single prominent episcleral vessel was used to compensate for eye and head rotation. However, this complex method is susceptible to error if the IOL changes centration. Although blood vessels have been used as reference points it has been proposed that iris features are a more stable alternative, as they are not susceptible to the effects of phenylepherine (Osher, 2010). Table 6.1 compiles a list of toric IOL studies and the methodologies used to measure rotation.

Study (first Author)	Name of IOL	Eyes (Px)	Follow up period (months)	Analysis	Rotation ±(SD)	Rotation description
Shimizu, 1994	Nidek Nt-98B	47 (47)	Not stated to 3 Rotation	Image analysis no correction for head tilt	Unknown	21% > 30°
Grabow, 1997	STAAR 4203TF	81 (Unknown)	6+	Unknown	Unknown	5% ≥ 40°
Ruhswurm, 2000	STAAR 4203TF	37 (30)	20±17	Slit-lamp protractor	Unknown	21.6% >5° 2.7% ≥ 40°
Sun, 2000	STAAR 4203TF	130 (99)	3 (106 eyes)	Unknown	Unknown	25% ≥ 20 7% > 40°
Leyland, 2001	STAAR 4203TF	22 (16)	4	Slit lamp protractor	8.9° ± 11.6°	22% >10° 13.6%>20° 9% >30°
Till, 2002	Mixed STAAR 4203TF & TL	TF 63 TL 37 (81 altogether)	23±17 (weeks)	Not stated	Unknown	14% >15°
Chang, 2003	STAAR 4203TF & 4203TL	TF 6 (4) TL 50 (37)	1	Slit lamp protractor	Unknown	TF group 50% ≥ 30° TL group 28% > 5° 10% >10° 2% > 15°
Jampaulo, 2008	STAAR 4203TF and 4203TL	25 (19)	0.5 to 26.2 (Rotation)	Image analysis no correction for head tilt	1.4 ± 1.9°	100% ≤ 5°
Chang, 2008	STAAR 4203TF and 4203TL AcrySof SN60T	TL 80(80) TF 10 (10) 100 (100)	1	Slit lamp protractor	5.6 ± 8.5 3.4 ± 3.4	27% > 5 9% > 10 3% > 15 3.3% repositioned 10% >5 1% > 10
Weinand, 2007	AcrySof SN60T	17 (Unknown)	Surgery and 6 (rotation)	Image analysis with correction for head tilt	0.7 range 0.1 to 1.8	0% > 5
Bauer, 2008	AcrySof SN60T	53 (43)	4	Slit lamp protractor	3.5 ± 1.9	Unknown
Olaru, 2008	AcrySof SN60T	32 (30)	2	Unknown	Unknown	9% > 5 3% > 30
(Mendicute *et al.*, 2008)	AcrySof SN60T	30 (15)	3	Slit lamp protractor	3.6 ± 3.1	19% > 5 3% > 10

Study (first Author)	Name of IOL	Eyes (Px)	Follow up period (months)	Analysis	Rotation ±(SD)	Rotation description
Zuberbuhler, 2008	AcrySof SN60T	44 (33)	Between 1 week and 3 months	Slit lamp integrated eye piece with axis graticule	2.2 ± 2.2	5% > 5
Dardzhikova, 2009	AcrySof SN60T	111 (70)	6	Unknown	Unknown	7.8% > 5 4.5% > 10 1.8% > 20 2 repositions
Mendicute, 2009	AcrySof SN60T	20	3	Slit lamp integrated eyepiece with axis graticule	3.53 ± 1.97	5% > 5
Ruíz-Mesa, 2009	AcrySof SN60T	32 (19)	6	Slit lamp integrated eyepiece with axis graticule	0.91 ± 1.77	3% > 5
Correia, 2009	AcrySof SN60T	20 (13)	2	Slit lamp protractor	$3.2 \pm$ Unknown	20% > 5 5% > 10
Tsinopoulos, 2010	AcrySof SN60T	29(19)	Surgery to 2 (Rotation)	Image analysis no correction for head tilt	2.7 ± 1.5	10% > 5
Holland, 2010	AcrySof SN60T	244	6	Slit lamp integrated eye piece with axis graticule	3.4 ± 3.0	18.9% > 5 2.9% > 10 0.4% repositioned
de Silva, 2006	MicroSIl 6116TU	21 (14)	1 day to 6 months Rotation	Slit lamp protractor	$5 \pm ?$	0% > 5
Dick, 2006	MicroSIl 6116TU	68 (48)	3	Unknown	Unknown	15% > 5 1.5% >20
(Gerten *at al.*, 2001)	Custom IOL (600TW) Dr Schmidt	26 (24)	12-48	Slit lamp protractor	Unknown	46% > 5 23% > 10
Shimizu, 1994	Nidek Nt-98B	47 (47)	? to3 Rotation	Image analysis no correction for head tilt	Unknown	21% > 30°
Grabow, 1997	STAAR 4203TF	81 (?)	6+ Not Stated	Unknown	Unknown	5% ≥ 40°

Study (first Author)	Name of IOL	Eyes (Px)	Follow up period (months)	Analysis	Rotation ±(SD)	Rotation description
Ruhswurm, 2000	STAAR 4203TF	37 (30)	20±17 Not stated	Slit-lamp protractor	Unknown	21.6% >5° 2.7% ≥ 40°
Sun, 2000	STAAR 4203TF	130 (99)	3 (106 eyes)	Unknown	Unknown	25% ≥ 20 7% > 40°
Leyland, 2001	STAAR 4203TF	22 (16)	4	Slit lamp protractor	8.9° ±11.6°	22% >10° 13.6%>20° 9% >30°
Till, 2002	Mixed STAAR 4203TF & TL	100 (81) TF 63 TL 37	23±17 (weeks)	Image analysis no correction for head tilt	Unknown	14% >15°
Chang, 2003	STAAR 4203TF & 4203TL	TF 6 (4) TL 50 (37)	1	Slit lamp protractor	Unknown	TF group 50% ≥ 30° TL group 28% > 5° 10% >10° 2% > 15°
Jampaulo, 2008	STAAR 4203TF and 4203TL	25 (19)	2 weeks to 26.2 months Rotation	Image analysis no correction for head tilt	1.36 ±1.85°	100% ≤ 5°
Chang, 2008	STAAR 4203TF and 4203TL

AcrySof SN60T | 90 TL80 TF10

100 | 1 | Slit lamp protractor | 5.56 ±8.49

3.35 ±3.41 | 27% > 5 9% > 10 3% > 15 3.3% repositioned 10% >5 1% > 10 |

Table 6.1 *Methods and findings of toric intraocular lens evaluations*

6.1.1 Rotation and Misalignment

The terms rotation and misalignment of a toric IOL are used interchangeably; however, they refer to two different circumstances and often these terms are incorrectly used. Misalignment refers to the distance in degrees an IOL is away from the intended axis as determined by the corneal power. Rotation refers to the movement of a lens between two points in time. Objective methods utilising image analysis measures rotation between two visits. When these two visits occur is an essential consideration as mechanism of rotation can fall into the early and late time periods. However, it is often difficult to establish the time at which the two images were taken (Shimizu *et al.,* 1994).

6.1.2 Measurement of Decentration

High levels of decentration can degrade the optical image attained from an IOL especially if coupled with lens tilt (Eppig *et al.,* 2009). Decentration also has a prismatic effect, in accordance with the Prentice rule, which can be exploited to correct binocular misalignments (Nishimoto *et al.,* 2007). Extensive *in vitro* studies have examined the degrading effect decentration has on the image acquired through a spherical and aspheric IOLs (Eppig *et al.,* 2009; Wang and Koch, 2005). Aberration neutral aspheric IOLs have been designed to be robust against the effects of decentration as the lenses have a continuous power profile across them. Spherical IOLs are subject to positive spherical aberration; therefore decentration exacerbates these effects resulting in a more positive refractive outcome (Atchison, 1991). Aberration controlling aspherical IOLs have negative spherical aberration and so reduce in power towards the periphery. Baumeister and colleagues (2009) found that the level of decentration of an aberration controlling IOL has no effect on visual quality; however, levels of decentration and tilt in this study were low. Mester and colleagues (2009) noted that with malposition of aberration controlling aspheric IOLs a slight horizontal coma was induced on the post-operative wavefront profile. Oshika and associates (2007) and Taketani and associates (2004) found that spherical IOL tilt induced coma aberration, but decentration of the spherical IOL was not correlated with any aberrations.

Refractive multifocals are sensitive to decentration, the percentage of light focused at each focal point is dependent on the distribution of each refractive zone within the pupil margin. The presence of multiple concentric refractive zones reduces the impact of decentration. *In-vitro* studies demonstrated that decentration has a minimal effect on the optical image from a five zone concentric refractive multifocal IOL if the extent of decentration does not exceed 1 mm (Negishi *et al.,* 2005). *In-vivo* examination of the same multifocal IOL demonstrated a correlation between decentration and visual acuity; VA was significantly reduced once decentration reached 0.7 mm (Hayashi *et al.,* 2001). Theoretically fully diffractive concentric multifocals are robust to decentration (Schwiegerling, 2007). *In-vivo* studies have not found a correlation between the decentration and tilt of an IOL and VA with partially diffractive multifocals and monofocal IOLs (Hayashi *et al.,* 2009b).

Assessment of IOL tilt and decentration is varied, and poses some challenges. Decentration describes the difference between the centre of an IOL and another reference point. The centre of the pupil, centre of the limbus and the predicted line of vision are all used intermittently as the reference points for centration. Early centration studies determined the position of IOLs, during post mortem examinations, using the centre of the ciliary ring as a reference (Hansen *et al.,* 1998). Similarly animal studies examining the effect of IOL design and capsular compression also use the centre of the cilary ring as a reference (Ohmi, 1993), the magnification of the cornea is not an influence on the measurement and so both methods provide actual decentration. Subjective assessment of decentration requires dilation, it describes the position of the IOL by examining the position of the edge of the optic within the pupil. This method allows the assessment of apparent decentration but magnification must be accounted for. Furthermore, as the IOL lies at a different optical plane in comparison to the cornea, parallax effects the results. The subjective measurement can be assisted with concentric rings found on most multifocal IOL.

The 1st, 3rd and 4th purkinje images (P1, P3, P4) can also be used to measure decentration. Purkinje images were first described in 1832, since this time they have been used to examine the curvature of the crystalline lens in the accommodative and non-accommodative eye. The first Ophthalmophacometer was constructed by Tscherning, the instrument was used to assess crystalline lens changes with accommodation (Norn and Jensen, 2004). The use of still photography (Sorsby *et al.,* 1961; Van Veen and Goss, 1988) and video (Mutti *et al.,* 1992) has expanded the potential of Ophthalmophacometry for examination of the eyes geometry. Phacometry was first used in 1988 to assess IOL decentration and tilt. Several iterations of phakometers have been created to allow the objective assessment of decentration. Guyton (1992) described a subjective method using purkinje images where decentration is described as the distance between P1 from the cornea and P3 and P4 from the IOL after these have been aligned. Moving the fixation target of the subject whilst keeping the light source direct to the subject allows alignment of P3 and P4. Opthalmophakometers (often referred to as Purkinje meters; Nishi *et al.,* 2010) use both the pupil (Rosales and Marcos, 2006) and limbal (Kirschkamp *et al.,* 2004) centre as a reference for decentration. However, the mobility of the pupil reduces its reliability as a constant reference point (Barry & Backes, 1997). Incorporating measurement of

corneal power and anterior chamber depth compensates for the magnifying effects of the cornea (Rosales and Marcos, 2006; Nishi *et al.,* 2010).

Scheimflug imaging can be used to measure decentration, the reference point used is a line drawn between the pupil centre and corneal centre believed to approximate the visual axis. The raw images from the scheimflug system are required for decentration analysis, but these do no correct for the distortion of the cornea. Therefore a correction factor needs to be applied to the data to achieve actual decentration (de Castro *et al.,* 2007). Anterior segment optical coherence tomography (OCT) also has the potential for assessing lens tilt. However a distortion correction factor also needs to be applied (Dunne *et al.,* 2007)

Intraocular lens centration has been assessed by image analysis in which an oval is fitted to the IOL optic margin and the limbus and centres are compared; this requires a view through a dilated pupil of the entire IOL optic and can use the dilated pupil centre or limbal centre as a reference point. (Perez-Torregrosa *et al.,* 1995; Becker *et al.,* 2004; Becker *et al.,* 2006). However, the repeatability of analysis and image capture has not been assessed and although image quality is considered an important factor, the effect of poor image quality has not been determined. This method is susceptible to the parallax effect caused by the optical plane of the IOL. The image analysis method measures apparent centration, unless a correction factor is used utilising either the corneal power and anterior chamber depth or the known size of the IOL optic (Pérez-Torregrosa *et al.,* 1995).

6.2 Study Aim

To be effective a toric IOL needs to be rotationally and positionally stable. To measure accurately rotational stability of an IOL, head rotation needs to be accounted for. The purpose of this study is to develop a repeatable, objective method of measuring IOL rotation and centration using image analysis. The effect of image quality on the accuracy of measure was examined along with the consistency of features on the anterior eye.

6.2.1 Subjects

One-hundred and seven subjects (63% female) of mean age 69.9 ± 7.7 years (range 51 to 87 years) were recruited, at each of the six European hospital sites involved with the study, for unilateral implantation of the *Akreos AO aspheric IOL* (Bausch & Lomb, Rochester, NY) with additional orientation marks to facilitate measurement of rotation. The six hospital sites were: Universitat Rostock Germany, Umea University Hospital Sweden, University Hospital Sweden, University Medical Centre Ljubljana, Universitat Niederrhein Germany and Uppsala University Hospital Sweden. A co-investigator at each site according to the following inclusion criteria recruited all subjects:

- The absence of ocular pathology affecting the anterior chamber, including Fuch's endothelial dystrophy and corneal disease.
- Age-related cataract amenable to treatment with standard phacoemulsification and IOL implantation.
- A minimum potential for dilation of at least 5.5 mm.
- Willingness to participate in the study.
- Aged 50 to 80 years
- Willing to attend required additional visits post-operatively.

A 2.8 mm clear corneal incision was completed in all cases; phacoemulsification and IOL implantation were preformed through a 5.5 mm circumlinear capsularhexis. Subjects were excluded intra-operatively if the capsularhaexis was no longer intact. The Ophthalmic Viscoelastic Device (OVD*) Amvisc® PLUS* (Bausch & Lomb, Rochester, NY) was inserted to assist IOL insertion and positioning, the OVD was fully removed both in front and behind the IOL before re-inflating the eye with balanced saline solution (BSS).

6.2.2 Intraocular Lens Design

The *Akreos AO aspheric IOL* is an aberration neutral Aspheric IOL made from acrylic, hydrophilic material. The IOL is 11 mm long with a 6 mm optic, it has a 360° posterior square edge barrier. The haptics are a closed loop design and the IOL can be implanted through a 1.8 mm incision.

6.2.3   Methods

All Subjects were assessed at four visits postoperatively:

Visit 1 (V1) – 1 to 2 days

Visit 2 (V2) – 7 to 14 days

Visit 3 (V3) – 30 to 60 days

Visit 4 (V4) – 120 to 180 days

At each visit, phenylephrine 2.5% and tropicamide 1.0% were used to achieve maximum possible dilation. The principal investigator for each site imaged the subjects using the *CSO* (Costruzione Strumenti Oftalmici) *SL-990 digital slitlamp biomicroscope* set to 10X magnification following training from the author; this slitlamp has a secondary diffuse light source which allows illumination of the external eye. Retroillumination of the IOL, using co-axial light from the main slit beam, was achieved by decoupling the illumination arm of the slit lamp from the observation arm. External illumination was achieved using the secondary light source.

At each site the same object of known size was imaged to establish the correct pixel to distance conversion. A bespoke computer program written in *Labview* determined the axis of rotation and the centrational position of the IOL.

A clinician (PB) subjectively graded the images in random order prior to analysis. The following were rated:

> Iris feature quality, including illumination consideration
>> 0 = poor/ungradeable
>>
>> 1 = moderate
>>
>> 2 = good
>>
>> 3 = excellent
>
> Scleral blood vessel clarity, including under-illumination
>> 0 = poor/ungradeable
>>
>> 1 = moderate/partially obscured markings
>>
>> 2 = good
>>
>> 3 = excellent

Marking clarity of the toric IOL, including under illumination and with dilation

> 0 = at least 1 not visible
>
> 1 = indistinct
>
> 2 = clear
>
> 3 = sharp

Two images of each eye were captured immediately after surgery in a subgroup of 40 patients then analysed to assess intra-session repeatability of the technique. Images from 2 patients were analysed 10 times to assess the repeatability of the analysis.

In a second subgroup of 72 subjects, where image quality was sufficient to identify 2 sets of reference points from both the iris and conjunctiva, the consistency of reference markers was determined.

All patients provided informed consent before IOL implantation, and the ethical committee at each site approved the study. The study was conducted in accordance with the tenets of the Declaration of Helsinki.

6.2.4 The Intraocular Lens Rotation and Centration Program

The axis of rotation and the centrational position of the IOL was determined using a bespoke computer program written in *Labview* (National Instruments, Austin, Texas). To determine rotation, the program was designed to record in triplicate angles between two given points on a single digital image. For centration, ovals were overlaid on the IOL, pupil and limbus using the *Labview* program. The program calculates in pixels the length and width of each oval, it also calculated the distance between the centres of each oval are in X and Y co-ordinates.

6.2.5 Determining Rotation

IOL rotation is determined in a three stages:

- the innermost edges of both toric markings, present on the IOL, are marked with a four pixel white dot defining the two points for the given angle.
- two sets of reference points, consistent on all images, are identified on the iris and conjunctiva and are marked with a four pixel white or black dot. The markings are selected from either the iris architecture or from blood vessels on the conjunctiva and the two features in the pair are on opposite sides of the pupil margin.

- the angle of a line drawn between the matching reference points are determined using the bespoke computer program (Figure 1). The images are analysed in a random order to ensure no bias of results.

The results provide three angles per image; these three angles can be used to determine axis rotation whilst normalizing for head rotation using Equation 6.1.

$$Rotation = \left(aAX - \left(\frac{aAE_1 + aAE_2}{2} \right) \right) - \left(bAX - \left(\frac{bAE_1 + bAE_2}{2} \right) \right)$$ **Equation 6.1**

$Rotation$ = IOL rotation between visit a and b
aAX = Angle between toric markings on visit a
bAX = Angle between toric markings on visit b
aAE_1 = Angle between the first set of anterior eye reference markers at visit a
bAE_1 = Angle between the first set of anterior eye reference markers at visit b
aAE_2 = Angle between the second set of anterior eye reference markers at visit a
bAE_2 = Angle between the second set of anterior eye reference markers at visit b
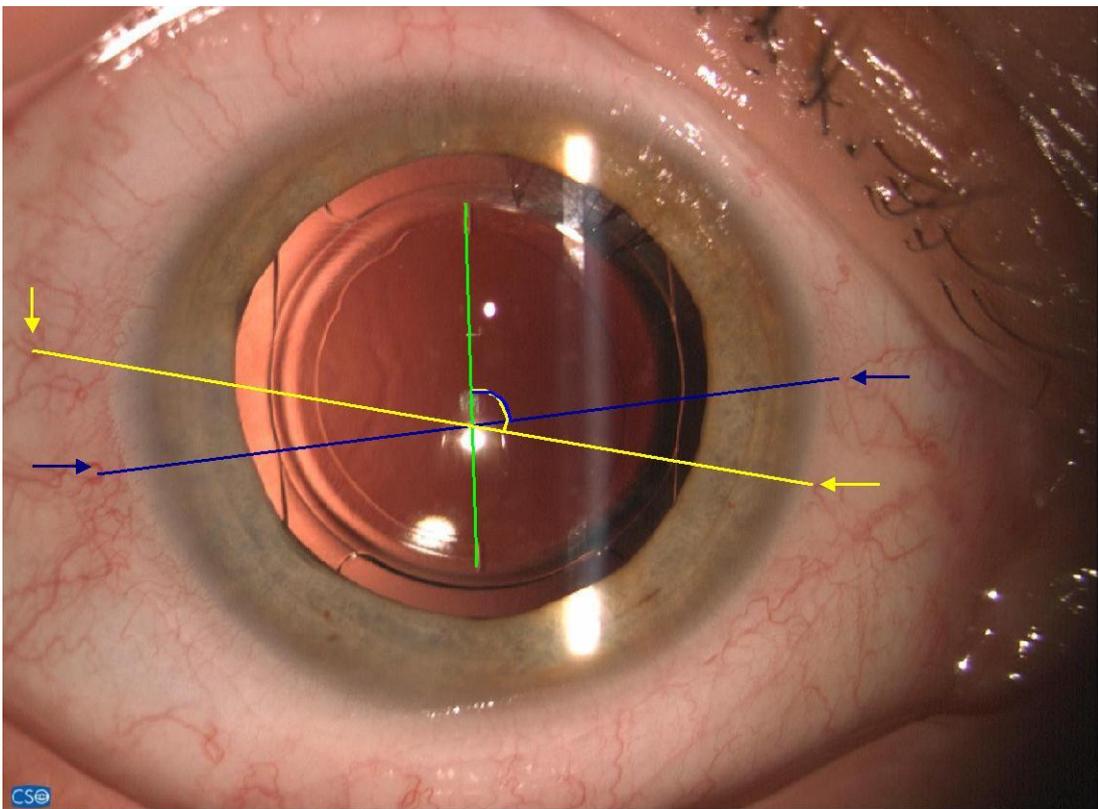
Figure 6.1 *Determining angles between toric markings and between two sets of reference points consistent on all images*

6.2.6 Determining Centration

To calculate centration ovals were over-laid on the IOL optic edge, pupil margin and the limbal margin using the bespoke *Labview* program. Outputs from the program show the height and width of the IOL, the cornea and pupil and the distance of the center of the IOL with respect to the centres of both the limbus and pupil (Figure 6.3).

226

The output measurements describe apparent IOL centration in pixels, to convert this to mm an object with known dimensions was imaged and the length was used to calculate the size of a single pixel. This calibration showed that each pixel = 0.0056 mm. However, this does not take into account the refractive power of the cornea. Using the known optic size to account for the magnifying effect of the cornea allowed the calculation of actual pixel size at the IOL plane (Equation 6.2).

$$pixel size (mm) = \frac{6}{Optic}$$ **Equation 6.2**

Optic = Maximum size in mm of the IOL optic

Centration measurements are in the form of x and y co-ordinates; the total distance can be calculated as the hypotenuse of a triangle (Equation 6.3)

$$h^2 = x^2 + y^2$$ **Equation 6.3**

h = total distance between centers
x = horizontal distance between centers
y = vertical distance between centers
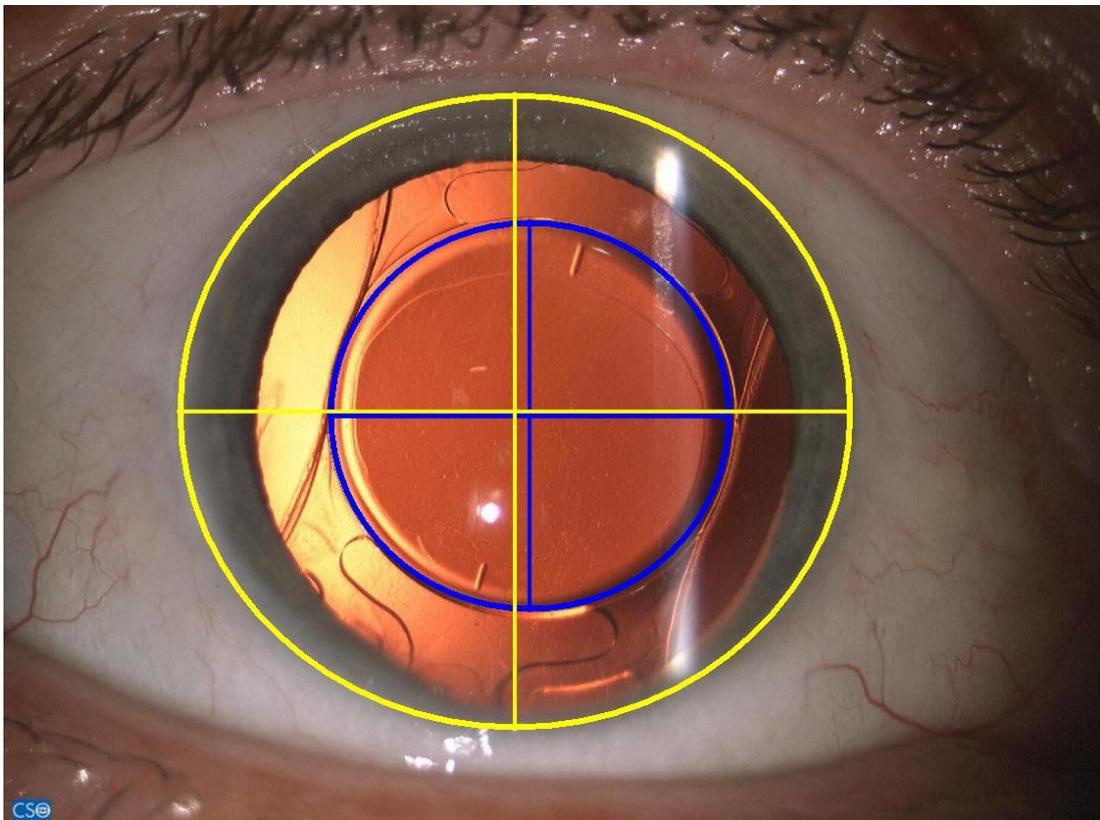
Figure 6.2 *Ovals overlaying the intraocular lens optic and limbus*

6.3 Statistical Analysis

Subjectively rated image-quality elements and the absolute rotation of the IOL and head tilt were not normally distributed. To determine the correlation between image quality and absolute IOL rotation, Spearmans rank correlation was used. Friedman Chi-Square test was used to determine if differences existed within the subjectively rated image-quality elements. If these differences were present then post-hoc testing using the Wilcoxon signed-rank test was applied the data with a Bonferroni adjustment to compensate for multiple comparisons. Absolute head rotation assessed by 1 set or the mean of 2 sets of blood vessel or iris features on either side of the pupil, was compared with the Friedman Chi-Square test. Total rotation values and centration values were normally distributed and student t-tests were used to determine differences. To determine if a difference in image quality was present between sites the Kruskal Wallis test was applied to the data.

Analysis of the average and standard deviation was calculated to assess the intra-session and repeated analysis variability in IOL rotation and centration. The statisitical analysis was preformed using SPSS version 15.0 (SPSS Inc., Chicago, IL., USA.)

6.4 Results

To evaluate the images for rotation, the toric markings needed to be at least partially visible. From the one hundred and seven subjects enrolled in the study only ninety-nine could be evaluated, as pupil dilation was not sufficient in 8 subjects. The subgroup analysis of intra-session repeatability included 40 eyes.

6.4.1 Image Clarity

The mean subjectively rated image quality of the iris architecture was 2.25 ± 0.87 at V1, 2.38 ± 0.73 at V2, 2.56 ± 0.55 at V3 and 2.51 ± 0.68 at V4. Iris clarity was different between groups (χ^2_3=14.362, p=0.002). Post-hoc testing revealed better clarity at visit three than at visits one and two (z=-3.556, P≤0.001; z=−2.836, P=0.005). There was no significant difference in clarity between visits one and two and between visit 4 and the other visits (P>0.0083).

The mean subjectively rated image quality of the blood vessels was 1.99 ± .99 for V1, 1.88 ± 0.89 for V2, 1.83 ± 0.90 for V3 and 1.73 ± 0.94 for V4. Blood vessel clarity was similar between visits (χ^2_3=5.235, P=0.155).

The mean subjectively rated image quality of the toric IOL markings was 2.24 ± 1.02 for V1, 2.29 ± 1.04 for V2, 2.13 ± 1.11 for V3 and 1.94 ± 1.19 for V4. Toric marking clarity was different between groups (χ^2_3=8.795, p=0.031). Post-hoc testing revealed a similar clarity between V1-3 (P>0.0083) but less clarity at V4 in comparison to V1 and V2 (Z=−2.657, P=0.007; Z=3.206, P=0.001).

The sites significantly differed in their ability to capture clear images of the iris architecture (V1: H_5=14.743, P=0.012; V2: H_5=25.084, P<0.001; V3: H_5=18.730, P=0.002; V4: H_5=15.960, p=0.007), conjunctival features (V1: H_5=11.742, P=0.038; V2: H_5=12.614, P=0.027; V3: H_5=11.452, p=0.038; V4: H_5=19.544, p=0.001), and toric IOL markings at each visit (V1: H_5=22.500, P<0.001; V2: H_5=17.653, P=0.003; V3: H_5=34.323, p<0.001; V4: H_5=40.969, p<0.001).

Clarity of the conjunctival vessels was significantly worse than the clarity of the iris architecture at all visits (V1: Z=-3.416, P=0.001; V2: Z=−5.357, P<0.001; V3: Z=−6.547, P<0.001; V4: Z=−6.932, P<0.001). Clarity of the conjunctival vessels was worse than the clarity of toric IOL markings for V2 and V3 (Z=-3.390, P=0.001 and Z=−2.338, P=0.019) but similar for V1 and V4 (Z=−1.439, P=0.152 and Z=−1.476, P=0.140).

Clarity of the toric IOL markings was similar to the clarity of the iris for V1 and V2 (Z=−0.286, P=0.771 and z=−0.540, P=0.595) but worse for V3 and V4 (Z=−3.542, P<0.001 and Z=−4.185, p<0.001).

6.4.2 Head Rotation

Absolute head rotation between visits was assessed using the rotation of blood vessels or iris features on either side of the pupil between visits (table 6.2). The amount of head rotation between visits and at each visit was similar when 1 set of reference points and when the mean 2 sets of images were used (V1-V2: Z=−1.240, P=0.215; V2-V3 Z=−0.385, p=0.700; V3-V4 z=-1.061, p=0.289).

	Between V1 & V2		Between V2 & V3		Between V3 & V4	
No of reference points	1 set	2 sets	1 set	2 sets	1 set	2 sets
Mean (°)	2.16	2.05	1.94	1.81	2.31	2.03
Median (°)	1.80	1.65	1.62	1.60	1.79	1.59
Skew (°)	.91	1.11	1.07	.96	1.19	1.17
Amount of rotation greater than 5°	6%	4%	3%	3%	6%	4%

Table 6.2 *Amount of head rotation between visits*

6.4.3   Consistency of Reference Features

In 73 subjects the image quality was sufficient to identify 4 sets of reference points; 2 from the iris and 2 from conjunctival blood vessels. The difference in angle between the 2 iris reference points was calculated for each image. This angle should be equal for each visit and so calculating the difference determined the consistency of the reference points. The consistency angle was also calculated for both sets of conjunctival blood vessels (table 6.3).

	Consistency of iris features			Consistency of conjunctival features		
	Btw V1&V2	Btw V2&V3	Btw V3&V4	Btw V1&V2	Btw V2&V3	Btw V3&V4
Mean (°)	1.0245	1.1542	1.3679	1.2242	1.1632	1.2615
Median (°)	0.86916	1.11161	1.31556	1.07613	1.15412	1.14247
Skew (°)	1.663	1.286	2.639	1.335	1.695	1.260

Table 6.3 *Consistency of reference points*

Consistency of results was similar at each visit when using both the iris and conjunctival features (V1-V2: Z=−1.259, P=0.208; V2-V3: Z=-0.172, p=0.864; V3-V4: Z=-0.311, p=0.756).

6.4.4   Image Quality and Apparent Rotation

Due to the relationship between blood vessel and iris feature clarity and the reliance on only one of these features to assess head rotation, the maximum score for these two

ratings was taken. Inability to detect either the anterior eye features or the IOL toric marks resulted in an image that could not be graded. Hence the toric marking grade and blood vessel or iris feature grade was multiplied and then divided by the maximum possible value of 9 to give the percentage quality. The average image quality between V1 and V2 and between V3 and V4 exhibited a low but significant correlation with absolute apparent toric IOL rotation between these visits (r_s=-0.422, $p<0.001$; Figure 6.4)
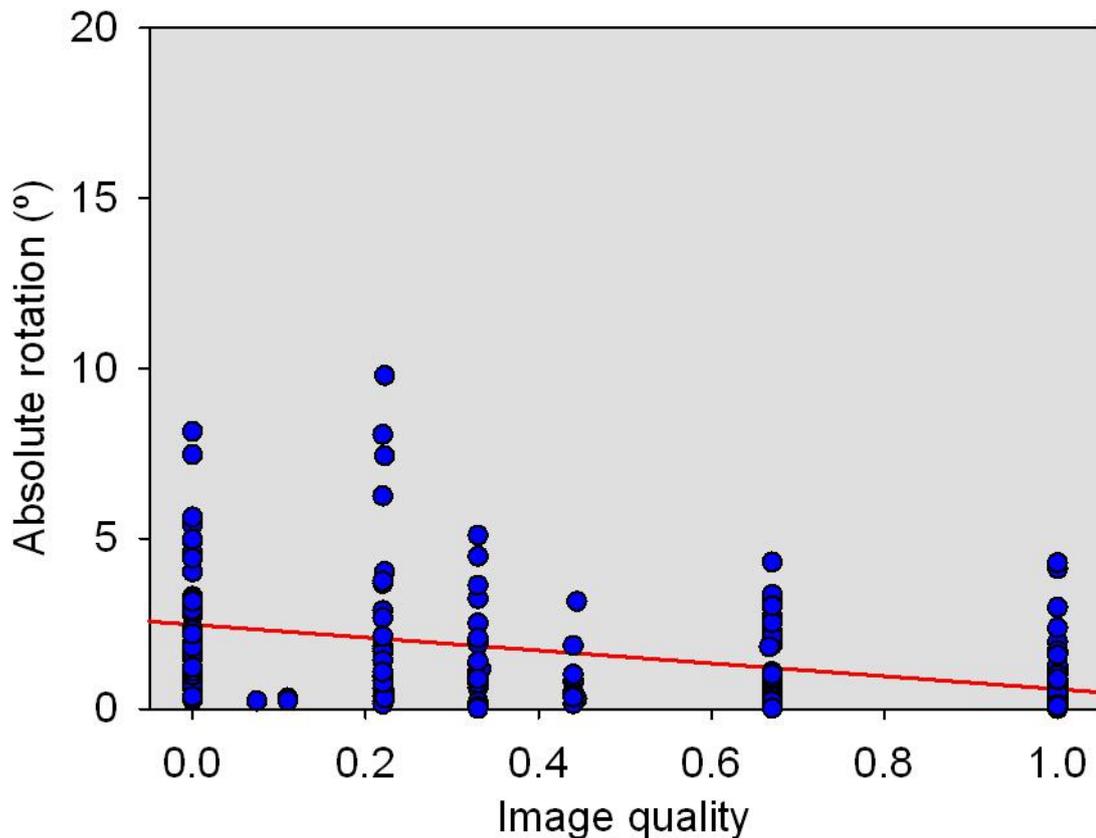
Figure 6.4 *Comparison of image quality and rotation*

6.4.5 Intraocular Lens Centration

	V1		V2		V3		V4	
	Centre of Pupil	**Centre of cornea**	**Centre of pupil**	**Centre of cornea**	**Centre of pupil**	**Centre of cornea**	**Centre of pupil**	**Centre of cornea**
Apparent distance mean±SD (mm)	0.35 ± 0.209	0.47 ± 0.20	0.44 ± 0.22	0.46 ± 0.19	0.44 ± 0.23	0.44 ± 0.22	0.40 ± 0.21	0.43 ± 0.18
Compensated distance mean±SD (mm)	0.23 ± 0.14	0.31 ± 0.13	0.29 ± 0.14	0.30 ± 0.13	0.29 ± 0.15	0.29 ± 0.14	0.26 ± 0.18	0.29 ± 0.12

Table 6.4 *Average amounts of total decentration for each visit*

Compensated and apparent decentration was greater when comparing the centre of the IOL with the centre of the Limbus than when comparing the centre of the IOL with the centre of the pupil for V1 (z=4.301, p<0.001 and z=4.301, p<0.001). This difference was not present in V2 (Z=0.339, p=0.734, Z=0.339, p=0.734), V3 (z=0.814, p=0.416 and z=0.814, p=0.416) and V4 (z=1.736, p=0.082).

Apparent decentration was greater than compensated decentration by a factor of 1.518±0.039 times (range 1.414 to 1.616). Changes in the compensated IOL position between visits were similar when compared to the limbal centre or to the pupil centre, V1 to V2 (0.204±0.131 mm versus 2.53±0.131 mm z=2.124, p=0.033), V1 to V3 (0.229±0.125 mm versus 0.260±0.152 mm z=1.140, p=0.254), and V1 to V3 (0.207±0.108 versus 0.255±0.130 mm z=2.304, p=0.021).

However, the absolute difference in anatomic centre between the pupil and the limbus varied greatly, being significantly larger in the vertical meridian (mean 1.89 ± 1.82 mm) than in the horizontal meridian (mean 0.18 ± 0.19 mm; P < 0.001).

The intra-session SD was ±0.79 degrees for rotation, ±0.10 mm for horizontal compensated centration, and ±0.10 mm for vertical compensated centration. The SD of repeated analysis of the same image IOL was ±0.70 degrees, ±0.02 mm, and ±0.03 mm, respectively.

6.5 Discussion

This study examined the repeatability of objective analysis of IOL rotation and centration, and the effect of image quality. The clarity of the iris features was better than the clarity of the blood vessels for all visits; this was expected, as the iris is closer to the optical plane of the IOL in comparison to the conjunctiva; it is also less dependent on the external diffuse illumination source being closer to the illumination through the pupil. Iris clarity improved after the first two visits, this likely to be due to a reduction in corneal oedema during this period; resulting in increased corneal transparency. Overall blood vessel clarity was rated the worst feature due to the lack of depth-of focus of the imaging system. Some digital systems have an aperture control that can be reduced to enlarge the depth of focus, thus allowing simultaneous imaging of the iris, conjunctiva, and IOL toric markings. However, either the illumination has to

be increased to compensate for the reduced aperture, which can cause patient discomfort, or the sensor gain has to be increased, which can cause a grainy image.

The decrease in visibility of the toric IOL markings at the V4 was related to fibrosis of the anterior capsule; where the toric marking fell outside the capsulorhexis border a reduction of capsular transparency resulted in worse marking visibility. The clinical sites significantly differed in their ability to capture clear images of the IOL and anterior eye features, and no site had consistently high performance; these findings emphasize the need for imaging training and support. Despite the low rotation of the *Akreos AO* IOL platform, apparent image rotation increased with poorer rated image quality. Reduced image quality made it more difficult to accurately establish the position of the IOL and reference points: This confirms the importance of high image quality for objective analysis of IOL rotation and supports the image quality metric devised.

The objective methodology had a repeatability of less than 1 degree in assessment of the IOL rotation. Head rotation between measures was, on average, approximately 2 degrees, and over 5 degrees in many of the images. This finding was consistent with a study of IOL rotation using fundus photography (Viestenz *et al.* 2005), which found a mean rotation of 2.3 ± 1.7 degrees in 400 eyes. The prevalence of eye rotation highlights the importance of accounting for it when measuring IOL rotation. The results show that no difference would be found with the rotational stability results if either the iris architecture or conjunctival features were used to normalize for rotation This is an important consideration as, either can be used to normalize for head rotation provided that image quality is high enough.

Several methods exist that can determine centration. This study highlights the importance of compensating for the magnification of the cornea and highlights the differences in results attained using either the pupil or limbal centre as a reference point especially for the day 1 image. Repeatability was approximately 0.03 mm, an order of magnitude better than subjective estimation. The pupil is not anatomically central to the limbus, particularly in the vertical meridian and the centre may vary with dilation. This could cause further variability in subjective estimation of IOL centration unless the reference anatomical feature is clearly defined. Ideally the centration should be calculated with respect to the visual axis and this method of determining centration

could be combined with the white-to-white visual axis measurement used with the *Lenstar LS900:* this would allow a measure of centration in accordance with the visual axis.

In conclusion, objective analysis of digital retroillumination images at different postoperative periods allowed sensitive assessment of the stability of IOL rotation and centration. Eye rotation between images can lead to significant errors if not taken into account. The quality of the images also significantly affects the accuracy of objective assessment. The aspheric IOL with orientation marks was stable in the eye 3 to 6 months after implantation.

6.6   Limitations of the Study

As highlighted in this study image quality is essential with respect to valid analysis of rotation and centration. Examiner skill is essential, correct set up of the slit-lamp is required and the gaze of the subject is also important. Although this methodology compensates for rotation of the eye it does not compensate for incorrect gaze of a subject. The optical plane of the IOL is behind that of the cornea; this creates a parallax effect, which can have a small effect measurement of rotation. The parallax effect has a larger effect on centration. This is reflected in the relative high intra-session SD for analysis of centration compared to the repeated measurement of analysis of the same image. The method used to measure centration in this study is objective and is valid and repeatable however it is not as robust to non-incident gaze as is Scheimpflug imaging or measurement using phakometry. Therefore it requires incident gaze with the slit lamp observation system. Analysis of centration is also dependent on a best-fit oval. An Irregular pupil and corneal shape may not match that of the fitted oval this may lead to errors. Furthermore, an ill-defined limbus results in errors with decentration calculation.

6.7   Conclusions

The methodology described in this chapter is a valid and repeatable method for evaluating the rotation of a toric IOL, whilst compensating for eye rotation. In Chapter 7 this methodology is used to assess the rotational stability of a closed loop haptic IOL with both an aspherical and toric surface.

6.8 Supporting Publications

Wolffsohn, J.S. & Buckhurst, P.J. (2010). Objective analysis of toric intraocular lens rotation and centration. *J Cataract Refract Surg.* **36,** 778-82.

Chapter 7 Stability of a Closed Loop Haptic Intraocular Lens

7.1   Introduction

Assessment of corneal power and accurate placement of a toric IOL is essential to achieve the best refractive results. There are numerous techniques available for measuring corneal power:

7.1.1   Manual and Automated Keratometry

This measures central anterior corneal radius using reflections from the tear film close to the visual axis (Thebpatiphat *et al.,* 2007).

7.1.2   Videokeratoscopy

Assesses anterior corneal curvatures over the central and peripheral area. An image of the Placido disc is reflected from the tear film and computer analysis of the reflections calculates the complex corneal shape. Videokeratoscopy can better identify irregular astigmatism because of the larger number of data points assessed over the corneal area (Thebpatiphat *et al.,* 2007). Maintenance of the tear film is essential for achieving accurate results: the effect of the tear film has been shown to create errors larger than 0.6 D (Erdélyi *et al.,* 2006).

Techniques to measure the front corneal surface assume standard corneal thickness and a constant anterior to posterior corneal curvature ratio. Following laser refractive surgery, the corneal thickness and the front and back corneal curvature ratio is changed. In these subjects, keratometric and topographic measures are no longer valid (Holliday *et al.,* 2009).

7.1.3   Raster Topography

A slit beam can be passed across or rotated around the cornea (projection system) and imaged multiple times at an angle to the camera axis (in a manner similar to Scheimpflug imaging). This quantifies the curvature of both the front and back surfaces of the cornea, together with the corneal thickness (known as raster topography or posterior apical radius imaging; Liu *et al.,* 1999). Therefore, it can quantify the changes made by corneal refractive surgery (Holliday *et al.,* 2009). The accuracy and reproducibility is similar to Placido-based systems (approximately 4.0 mm in the central cornea and 7.0 mm in the periphery under optimal conditions) and

the technique does not require an intact epithelial surface (Mejía-Barbosa and Malacara-Hernández, 2001). The technique takes longer than imaging the reflections from the tear film and is more susceptible to blinking, loss of fixation, and tear film instability (Reuland *et al.,* 2007; Savini *et al.,* 2009).

With toric IOL implantation, measurement of the axis becomes more important. With hand-held keratometry, incorrect orientation of the instrument or patient causes inaccuracy in measurement (Lam *et al.,* 2004). Therefore, it is essential with any measurement of corneal power that a vertical orientation is achieved for head and instrument. The most common method in the literature for establishing the correct keratometric power and axis for toric implantation is automated keratometry with the *IOLMaster* (Carl Zeiss, California, Germany) and confirmation of this result with a computerised topographer, although which is chosen when they are disparate is not obvious (Bauer *et al.,* 2008; Mendicute *et al.,* 2008; Dardzhikova *et al.,* 2009; Mendicute *et al.,* 2009; Alió *et al.,* 2010; Carey *et al.,* 2010).

In accordance with the corneal measurements, reference markers on opposite sides of the pupil need to be established to demarcate the correct axis for IOL orientation. Eye rotation occurs changing from the prolate and supine position (Chernyak, 2004) and so these markers need to be established pre-operatively. The slitlamp beam axis graticule can be dialled to the correct axis or a bespoke eyepiece graticule can be used to determine marker placement. These markers can be applied to the cornea or conjunctiva using ink or with scratches (Ma and Tseng, 2008). Ink should be applied at the last possible minute as it can diffuse by 10° or disappear before implantation is complete (Osher, 2010). As an alternative, a Yag laser can be used to mark the cornea. It has been suggested that this improves the accuracy and definition of the markers (Wehner, 2009). Specific toric axis marking instruments exist. One step methods, such as the Devgan Axis Marker (Accutome, Pennsylvania, USA) and the Gerten Pendulum Marker (Geuder, Heidelberg, Germany) are used pre-operatively to determine the required axis. They are dependent on a vertical head position when applied to the cornea. Two-step methods require marking the cornea at the zero and 180 degrees position pre-operatively and then aligning a degree gauge with these markings intra-operatively to establish the correct position (Graether, 2009). The iris architecture is intricate and full of natural landmarks that can be used as reference markers for fitting a toric IOL (Osher, 2010). The plane of the iris is closer to the optical plane of the IOL in

comparison to the cornea or conjunctiva, which reduces the problem of parallax when positioning the lens. During dilation, movement of the iris occurs and so the selected iris feature needs to be peripheral and unaffected by dilation.

The Micron-Osher Overlay System (Micron Imaging Systems LLC, Tennessee, USA) has been developed to assist with toric alignment. A grid is placed over high resolution images of the iris, enabling the position of any iris structure in relation to the horizontal to be determined in degrees (Osher, 2010). Automated iris recognition systems have been used in laser *in-situ* keratomileusis (LASIK) and – in terms of reducing astigmatism – provide results comparable to manual limbal marking (Shen *et al.,* 2010).

A recent paper by Cha and colleagues (2010) examined the accuracy of axis markings using three methods:

- A two-step method where the 3, 6, and 9 o'clock positions were first marked pre-operatively using the *AE-2793S* (ASICO LLC, Westmont, Illinois, USA) toric reference marker and then marked intra-operatively using a Mendez degree gauge (accuracy 3.69±1.49°; range 1.17° to 6.60°).
- A two-step method marking the 3 and 6 o'clock positions using a horozontal slit beam pre-operatively and then the Mendez degree gauge interoperatively (accuracy 3.14±1.64°; range 0.43° to 6.46°).
- A mapping method where conjunctival vessels adjacent to the limbus were used as reference points for target alignment (accuracy 0.32° to 4.41°).

Several digital systems have been developed to aid in the alignment of a toric IOL intraoperatively. The Z-align (Carl Zeiss Meditec, Berlin, USA) allows the surgeon to superimpose a line through reference markers on the surgical microscope. This technology is able to track the limbus and provides a visual aid to aligning a toric IOL. *The ORange inter-operative wavefront aberrometer* (WaveTec Vision, California, USA) has also been introduced. It attaches to the surgical microscope and allows real time update on the refractive results at any point during the operation. With toric IOL implantation, this can – in theory – be used to verify correct orientation of the IOL inter-operatively (Holladay, 2009).

Patel and colleagues (1999) have published the only study examining IOL rotation in the early stages immediately post-operative using image analysis. Pre-operatively a reference mark was placed at six o'clock on the limbus. Subjects were implanted with either a plate haptic or open C-loop haptic spherical IOL. To assess early rotation, the orientation of the IOL in patients, at the end of surgery was compared with the orientation at two weeks. A snapshot from the surgical video at the end of surgery was taken; the orientation of this image was adjusted until the reference marking was positioned at six o'clock. This methodology is prone to eye torsion error as it is difficult to guarantee the same head orientation at between the two timeframes. It is also dependent on a precise reference marking at the limbus.

No studies have examined the accuracy of placement of an IOL using image analysis. Similarly, accuracy of placement of the corneal reference marking has not been determined.

The effect of IOL decentration and tilt has previously been examined on spherical (Hayashi *et al.,* 2001b), aspherical (Baumeister *et al.,* 2009), multifocal (Hayashi *et al.,* 2001a), bag in the lens (Verbruggen *et al.,* 2007), and IOLs implanted with a capsular tension ring (Takimoto *et al.,* 2008). The use of purkinje imaging systems and Scheimpflug imaging systems are common for the assessment of decentration and tilt (Rosales *et al.,* 2010). The reference points for decentration vary between studies; image analysis methods utilise either the pupil or limbus as a reference point (Verbruggen *et al.,* 2007); purkinje systems use the purkinje image 1 as a reference point; and Scheimpflug systems use centre of the pupil (Sasaki *et al.,* 1989; de Castro *et al.,* 2007). Most modern IOLs studies demonstrate a mean total decentration of between 0.19 ± 0.12 (Baumeister *et al.,* 2009) to 0.31 ± 0.17 mm (Verbruggen *et al.,* 2007; Ohtani *et al.,* 2009). Where stated, previous studies have shown the decentration of the IOL to occur nasally. The vertical position of the IOL has varied between studies and both inferior (Verbruggen *et al.,* 2007) and superior (Mester *et al.,* 2009) positions have been recorded. The centration of an IOL is an important consideration with aberration controlling aspherical IOLs. If a lens is decentred by more than 0.5 mm then the benefit of the aspheric surface is lost (Holladay *et al.,* 2002; Altmann *et al.,* 2005).

7.2 Purpose of Study

This study was conducted in two stages; first, the rotational and centrational stability of the *Akreos AO Aspheric IOL* (Bausch & Lomb, Rochester, NY.) was determined from the day 1 position to its 6-month position following implantation. Second, was to examine the alignment and rotational stability of the *Akreos AO toric IOL* (Bausch & Lomb, Rochester, NY.) from time of surgery to its 6-month orientation.

7.2.1 Subjects

7.2.1.1 Subjects Implanted with the Akreos AO Aspheric Intraocular Lens

The study of the rotational stability of the *Akreos AO aspheric IOL* was conducted at the following six European hospital sites: Universitat Rostock Germany, Umea University Hospital Sweden, University Hospital Sweden, University Medical Centre Ljubljana, Universitat Niederrhein Germany, and Uppsala University Hospital Sweden.

A total of one hundred and seven subjects (63% female) of mean age 69.5 ± 9.9 years (range 41 to 86 years) were recruited by the hospital sites. A co-investigator at each hospital recruited all subjects, according to the following inclusion criteria:

- The absence of ocular pathology affecting the anterior chamber, including Fuchs endothelial dystrophy and corneal disease.

- Age-related cataract amenable to treatment with standard phacoemulsification and IOL implantation.

- A minimum potential for dilation of at least 5.5 mm.

- Willingness to participate in the study.

- Aged over 18 years

- Willing to attend required additional visits post-operatively.

A 5.5 mm continuous curvilinear capsulorhexis was created through which phacoemulsification was performed. Once the capsular bag was filled with the ophthalmic viscosurgical device (OVD); *Amvisc® PLUS* (Bausch & Lomb, Rochester, NY.), the IOL was inserted using an Akreos single-use insertion device through a 2.8

mm incision. The OVD was then aspirated from in front of and behind the IOL before re-inflating the eye with balanced saline solution (BSS).

7.2.1.2 Subjects Implanted with the Akreos AO Toric Intraocular Lens

The study of the rotational stability of the *Akreos AO Toric IOL* (Bausch & Lomb, Rochester, NY.) was conducted at the following eight European hospital sites: Klinikum der Johann Wolfgang Goethe-Universität Germany, Umea University Hospital Sweden, Uppsala University Hospital Sweden, University Medical Centre Ljubljana, Bucharest Oculus Eye Centre Romania, Medical University of Pécs Hungary and Budapest Semmelweis University Hungary.

A total of one-hundred subjects (64% female) of mean age 69.5 ± 9.9 years (range 41 to 86 years) were recruited by the sites. A co-investigator at each hospital recruited all subjects, according to the following inclusion criteria:

- age-related cataract amenable to treatment with standard phacoemulsification and IOL implantation.

- aged over 18

- subjects must be willing and able to return for scheduled follow up examinations for the duration of the study

- spherical IOL power between 15 to 30 D

- pre-operative BCVA equal or worse than 20/40

- potential post operative BCVA better than 20/30

- absence of any ocular pathology including all corneal pathology potentially affecting topography

- absence of previous ocular surgery

- absence of irregular corneal astigmatism

- absence of the use of any medications known to complicate cataract surgery (e.g. tamsulosin)

- predicted post-operative astigmatism from 0.90 to 2.50 D.

Preoperatively, corneal power was determined using a manual keratometer and *IOLMaster*, following training from the principal investigator of the study (PB). Care was taken to ensure a vertical head position for each measurement of curvature. Keratometry results from the manual keratometer were considered valid provided that the cylindrical axis was measured within ±20° of the axis as determined by the *IOLMaster* and that the cylindrical power was within ±0.50 D. If invalid, both measurements were repeated. The subject was excluded if the repeated measures were also invalid.

The Akreos Toric calculator was used to determine the correct IOL cylindrical power and target IOL orientation axis. The mean spherical equivalent IOL power was calculated separately using the SRK/T, Holladay or Hoffer Q depending on the calculation preference of each hospital site.

Following training by the principal investigator of the study (PB), the surgeon, immediately prior to surgery, marked the operative eye with the subject seated at the slit lamp in order to identify the axis of placement as determined by the Akreos Toric calculator:

- corneal anesthesia was instilled
- the subject was seated at the CSO Digital Slit Lamp (a vertical head position was strictly enforced)
- the subject fixated on a distance object visible to the non-operative eye
- a 2mm wide slit-beam was rotated to the angle of orientation using the degree scale at the top of the slit lamp illumination arm and the slit beam at the correct axis of placement was placed across the cornea with the slit beam passing through the central cornea
- both sides of the peripheral cornea were marked superficially using a needle or Sinskey hook, not penetrating the anterior limiting laminar (Bowman's).

A 5.5 mm continuous curvilinear capsulorhexis was created through which phacoemulsification was performed. Once the capsular bag was filled with the ophthalmic viscosurgical device (OVD) *Amvisc® PLUS* (Bausch & Lomb, Rochester, NY.), the IOL was inserted using an Akreos single-use insertion device through a 2.8 mm incision. A surgical ink marker was used to highlight the corneal reference markers

before rotating the IOL into place following OVD aspiration from in front and behind the IOL and before re-inflating the eye with balanced saline solution (BSS). The surgery was recorded using a live feed from the surgical microscope.

All patients provided informed consent before IOL implantation, and the ethical committee at each site approved the study.

7.2.2   Intraocular Lens Design

Both studies used an IOL based upon the Akreos AO platform. The *Akreos AO aspheric IOL* is an aberration neutral aspheric IOL made from an acrylic, hydrophilic material. The IOL is 11mm long with a 6 mm optic; it has a 360° posterior square edge barrier. The haptics are a closed loop design and the IOL can be implanted through a 1.8 mm incision. The IOL incorporated two additional orientation marks to facilitate measurement of rotation.

The *Akreos AO toric IOL* is also an aberration neutral aspheric IOL of the same design, however it has a toric posterior surface. This lens is available with three torus powers: 1.25, 2.00 and 2.75 D; equivalent to 0.87, 1.40 and 1.92 D at the cornea.

Figure 7.1 *The Akreos AO toric intraocular lens with toric markings*

7.2.3 Methods

7.2.3.1 Assessment of the Akreos AO Aspheric Intraocular Lens

All Subjects were assessed at four visits postoperatively:

- Visit 1 (V1) – 1 to 2 days
- Visit 2 (V2) – 7 to 14 days
- Visit 3 (V3) – 30 to 60 days
- Visit 4 (V4) – 120 to 180 days.

At each visit, phenylephrine 2.5% and Tropicamide 1.0% were used to achieve maximum possible dilation. A single co-investigator from each site imaged the subjects using a *CSO* (Costruzione Strumenti Oftalmici) *SL-990 digital slitlamp biomicroscope* set to 10X magnification. For analysis of rotation using the methods detailed in Chapter 6 good image quality is essential. In the study conducted by Weinand and colleagues (2007) it was only possible to measure rotation in 43% of the subjects. Therefore the principal investigator for the study (PB) trained each co-investigator for image acquisition. The CSO slitlamp has a secondary diffuse light source, which allows illumination of the external eye. Retroillumination of the IOL, using co-axial light from the main slit beam, was achieved by decoupling the illumination arm of the slit lamp from the observation arm and placing the main beam incident with the pupil.

7.2.3.1.1 Determining Rotation

The methodology for rotation analysis is detailed in Chapter 6 (Wolffsohn and Buckhurst, 2010), this analysis was conducted by the principal investigator (PB): The axis of IOL rotation was determined by drawing a line between the IOL orientation marks, comparing the angle between two consistent conjunctival vessels or iris features – on opposite sides of the pupil margin – compensated for eye rotation. The IOL, iris, and conjunctival reference markers needed to be visible on the images captured at every follow-up visit, this prevented rotation analysis in 10 of the 107 eyes.

7.2.3.1.2 Determining Centration

Ovals were overlaid on the IOL optic edge and limbus; the centres of the ovals were compared in order to determine IOL centration as detailed in Chapter 6 (Wolffsohn and

Buckhurst 2010). Analysis of centration was also conducted by the principal investigator for the study (PB). Actual centration was calculated using equation 6.2 (Chapter 6), with the known optic size of 6mm. Measurement of centration with this method cannot be achieved unless pupil dilation is sufficient to allow visualisation of the entire IOL optic. Pupil dilation was sufficient for centration analysis in 76 of the 107 eyes.

7.2.3.2 Assessment of the Akreos AO Toric Intraocular Lens

All Subjects were assessed at four visits postoperatively:

Visit immediately post-operatively (OP) – within 15 minutes

- Visit 1 (V1) – 1 to 2 days
- Visit 2 (V2) – 7 to 14 days
- Visit 3 (V3) – 30 to 60 days
- Visit 4 (V4) – 120 to 180 days.

7.2.3.2.1 Determining Misalignment

The axis of misalignment was determined by drawing a line between the corneal reference markers and the post-operative IOL orientation marks at each visit, comparing the angle between two consistent conjunctival vessels or iris features − on opposite sides of the pupil margin − compensated for eye rotation. The corneal reference markers needed to be clear at the immediate post-operative visit and the IOL markings needed to be visible on the images at each follow up visit; misalignment could only be assessed in 68 of the 100 eyes

A snapshot taken from the surgical video at the end of surgery allowed an assessment of the initial misalignment of the IOL; the angle of the corneal reference markers were compared with the angle of the IOL markings. Initial misalignment could only be assessed in 62 of the 100 eyes.

7.2.3.2.2 Determining Rotation and Centration

The same methodology used to assess the rotation and decentration of the Akreos aspheric IOL was used to assess the between visit rotation and centration for the toric

IOL, rotation assessment was possible in 86 of the 100 eyes and centration assessment was possible in 67 of the 100 eyes.

7.3   Statistical Analysis

The difference in toric mark orientation at each visit was used to assess rotation; Equation 6.1 was used to compensate for eye torsion. The difference between the toric mark orientation and the corneal marking orientation was used to assess misalignment; equation 6.1 was also used to compensate for eye torsion. Initial misalignment was determined as the difference in orientation of the toric markings and corneal markings using the image from the surgical video.

The difference between the corneal and IOL position and the target axis − as determined by the Akreos toric calculator − was also calculated. The orientation of the eye during keratometry was defined as the average eye orientation, calculated from the two sets of reference points for the five visits.

A Friedman's Repeated measure analysis of variance was used to assess orientation stability between visits. Post-Hoc examination of significance was performed using repeated Wilcoxon signed-rank tests; a Bonferroni correction was applied to the significance level. The IOL centration with respect to the limbus at each visit was subtracted from the centration at V1 to give a decentration measure. A one-way repeated measures ANOVA was used to assess the locational stability between visits.

7.4   Results

7.4.1   Rotational Stability of the Akreos AO Aspheric Intraocular Lens

The average and range of rotation at each visit compared to V1 is displayed in Table 7.1 (Figure 7.2). There was no lens rotation greater than 5° between V2 and V1. By V2, 2 eyes (3%) had rotated between 5° and 10°, and this remained stable up to V4. One IOL (1%), in an eye that was clearly inflamed, rotated more than 10 degrees by V3 but subsequently remained stable. There appeared to be no strong bias in the direction of the rotation, with 60% rotating clockwise. The rotation between visits V1 and V2, V2 and V3, and V3 and V4 were similar (χ^2_2=0.993, p=0.650).

	At V2 (7-14 days)	At V3 (30-60 days)	At V4 (120-180 days)
Absolute Rotation from V1 position	1.03 ± 1.08°	1.53 ± 2.16°	1.93 ± 2.33°
Lenses misaligned less than 5°	100%	96%	96%
Lenses misaligned less than 10°	100%	99%	99%

Table 7.1 *Absolute rotation values of the Akreos AO aspheric intraocular lens with toric markings in comparison with V1. n=97*
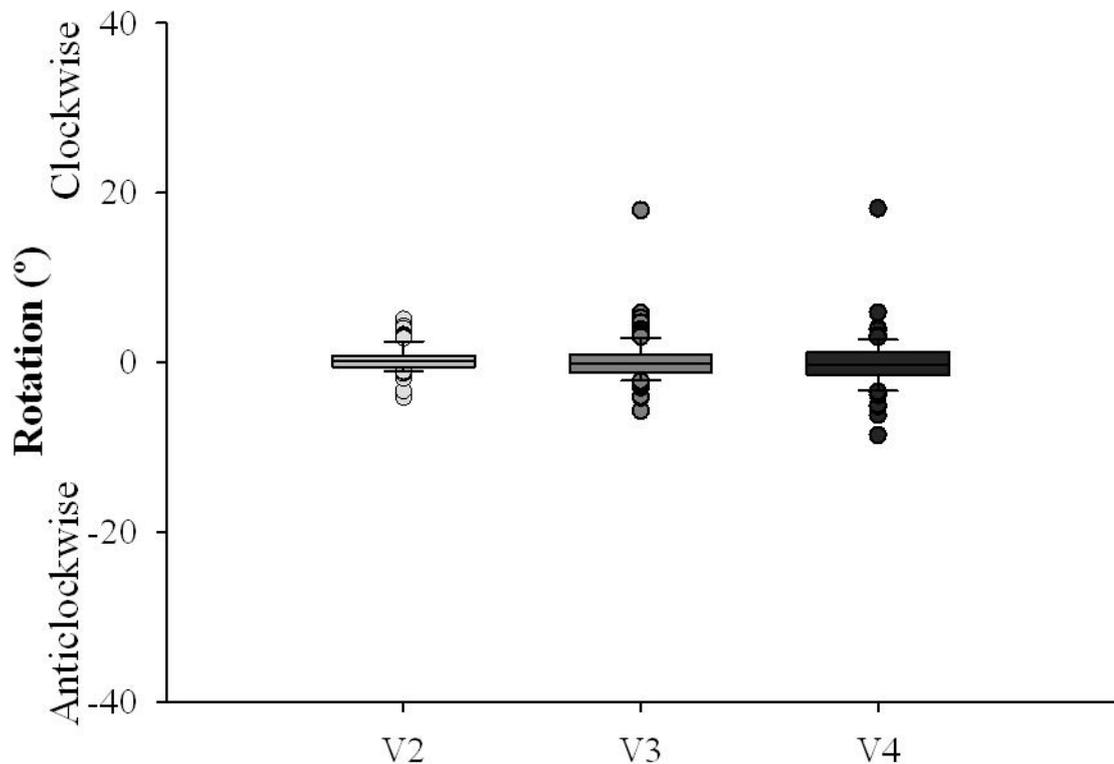
Figure 7.2 *Box and whisker plot of rotation at each of the visits compared to day 1-2 post-implantation. n=97*

7.4.2 Centrational Stability of the Akreos AO Aspheric Intraocular Lens

The position of the IOL following implantation was in general superior (0.18 ± 0.17mm) nasal (0.19 ± 0.15mm). The mean total absolute decentration value was 0.31 ± 0.13 mm at V1, 0.30 ± 0.13 mm at V2, 0.30 ± 0.14 mm at V3, and 0.28 ± 0.12 mm at V4. There were no significant changes in IOL centration over time ($F_{3,228} = 1.61$, P = 0.090), with subsequent decentration appearing random in direction (Figure 7.3, Figure 7.4 and Figure 7.5). All lenses remained within 0.5 mm of the V1 position at all visits (mean change 0.21 ± 0.11 mm).
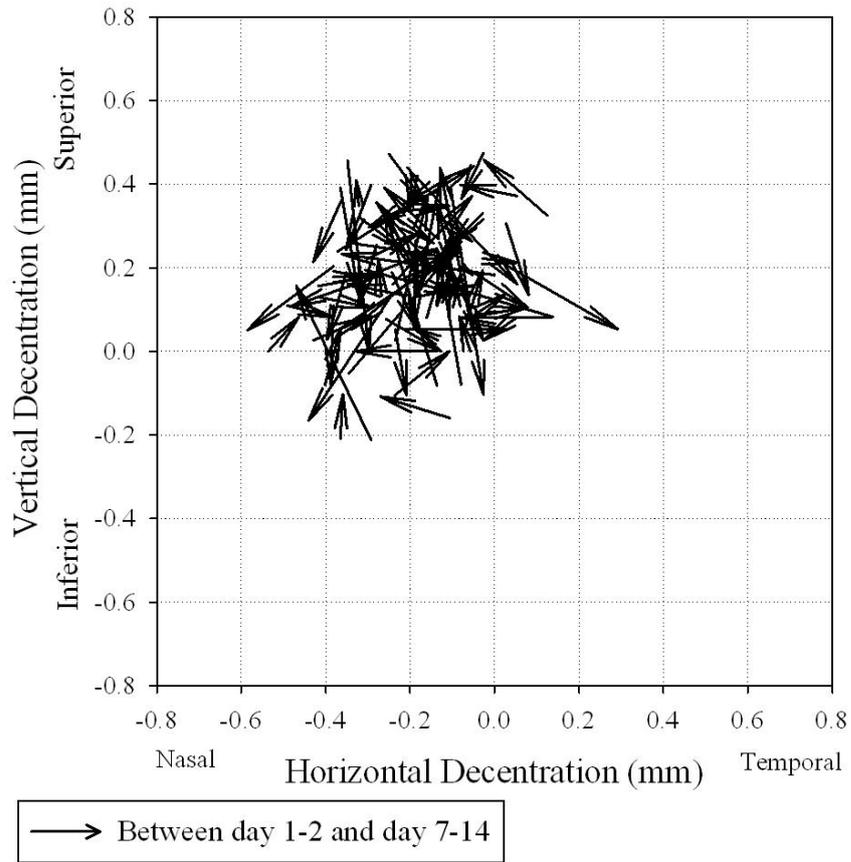
Figure 7.3 *Vector graph of change in intraocular lens centration between day 1-2 and day 7-14 post implantation. n=76*
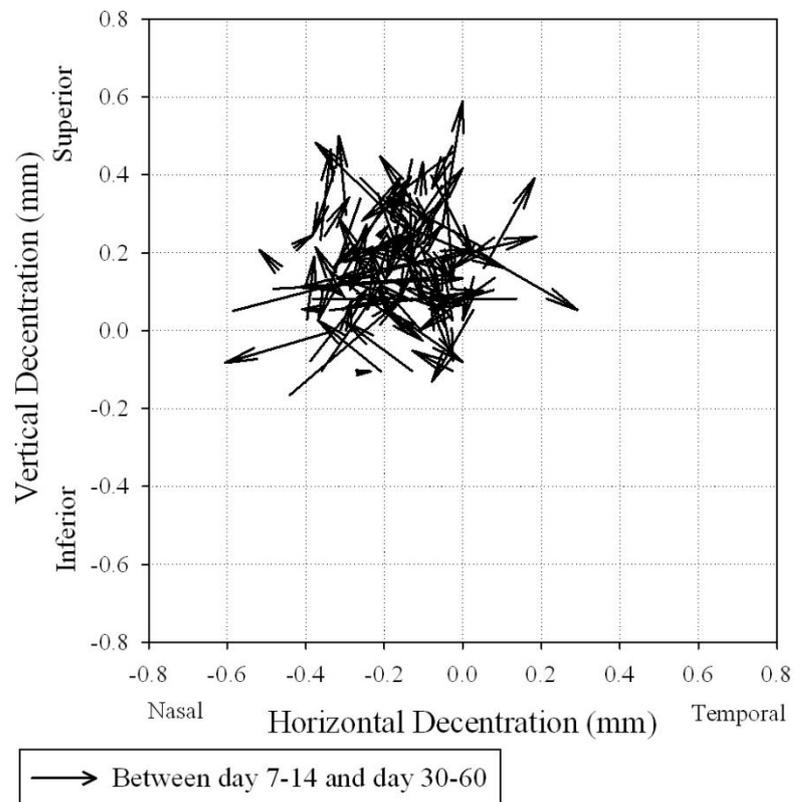
Figure 7.4 *Vector graph of change in intraocular lens centration between day 7-14 and day 30-60 post implantation. n=76*
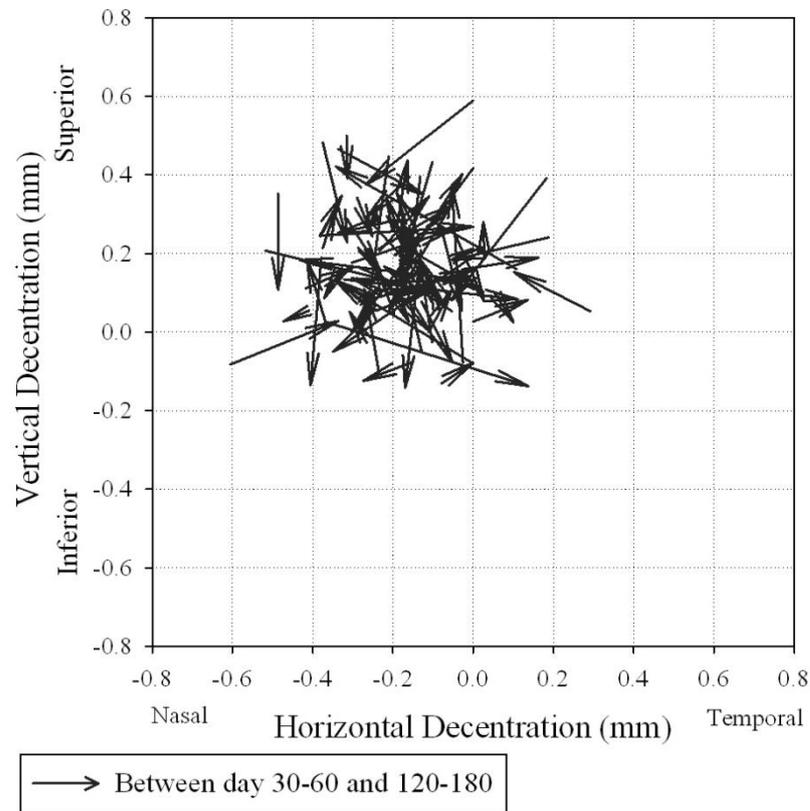
Figure 7.5 *Vector graph of change in intraocular lens centration between day 30-60 and day 120-180 post implantation. n=76*

7.4.3 Misalignment and Rotational Stability of the Akreos AO Toric Intraocular Lens

Of the one hundred eyes, three IOL required surgical repositioning as a result of rotation after the operation. An additional IOL was explanted due to excessive rotation intraoperatively. The results from these four lenses are not included in the misalignment and rotation stability results.

The range and average misalignment of the IOLs, relative to the corneal reference markers, is displayed in Table 7.2 and Figure 7.6.

	At OP	At V1	At V2	At V3	At V4
Absolute misalignment in comparison to reference markers (range)	3.2±4.3° (0.0-23.2)	4.5±4.9° (0.0–23.5)	4.3±4.9° (0.0-23.9)	4.3±4.9° (0.0-24.3)	4.3±4.9° (0.2-24.4)
Lenses misaligned less than 5°	90%	80%	81%	76%	78%
Lenses misaligned less than 10°	95%	88%	90%	90%	90%

Table 7.2 *Absolute misalignment of the Akreos AO toric intraocular lens at each post-operative visit. n=68*
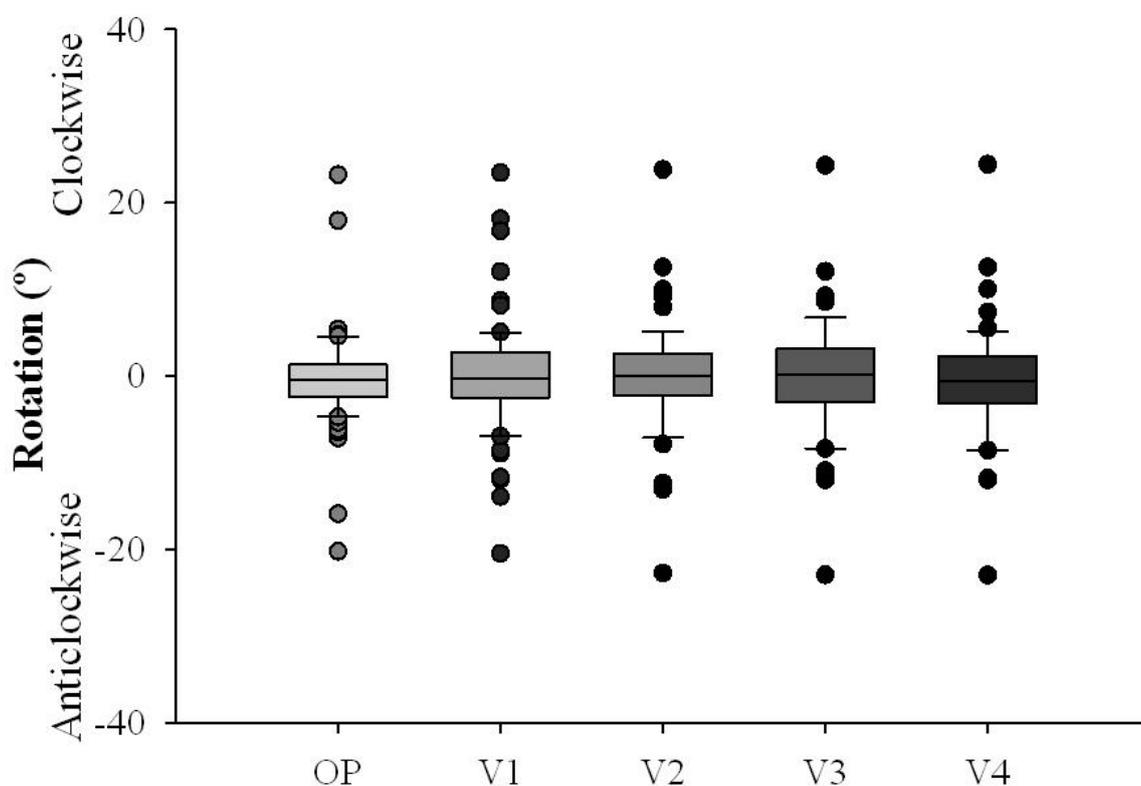
Figure 7.6 *Misalignment of the Akreos AO Toric intraocular lens at each visit. n=68*

At the end of surgery the accuracy of placement of the IOL in relation to the corneal markings was 2.14±2.18°. Two IOLs (3%) were positioned more than 5° away from the target axis and one (2%) was orientated 14° away from the target axis.

The rotation of the IOL at each visit in comparison to its orientation at visit OP is displayed in Table 7.3 and Figure 7.7.

	At V1	At V2	At V3	At V4
Absolute rotation in comparison to OP	2.4±2.5° (0.0-14.1)	2.4±2.5° (0.0-14.1)	2.5±2.4° (0.0-14.7)	2.5±2.4° (0.2-14.6)
Lenses rotating less than 5°	92%	92%	92%	92%
Lenses rotating less than 10°	97%	98%	98%	98%

Table 7.3 *Absolute rotation of the Akreos AO toric intraocular lens at each post-operative visit in comparison with visit OP. n=86*
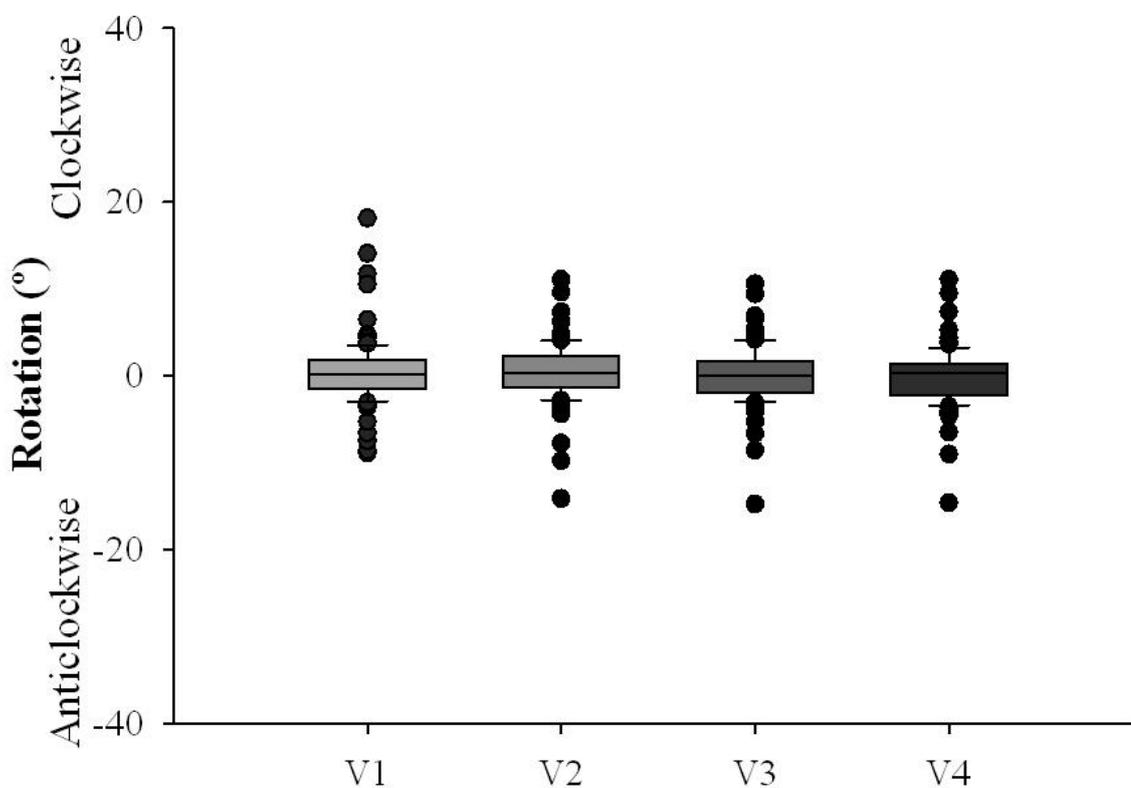
Figure 7.7 *Rotation of the Akreos AO Toric intraocular lens at each visit in comparison with visit OP. n=86*

The rotation of the IOL in comparison to its orientation at visit V1 is displayed in Table 7.3 and Figure 7.8.

	At V2	At V3	At V4
Absolute rotation in comparison to V1	1.3±1.3° (0.0-6.7)	1.4±1.4° (0.0-7.5)	1.3±1.4° (0.0-7.1)
Lenses rotated less than 5°	98%	97%	98%
Lenses rotated less than 10°	100%	100%	100%

Table 7.4 *Absolute rotation of the Akreos AO toric intraocular lens at each post-operative visit following visit V1. n=86*
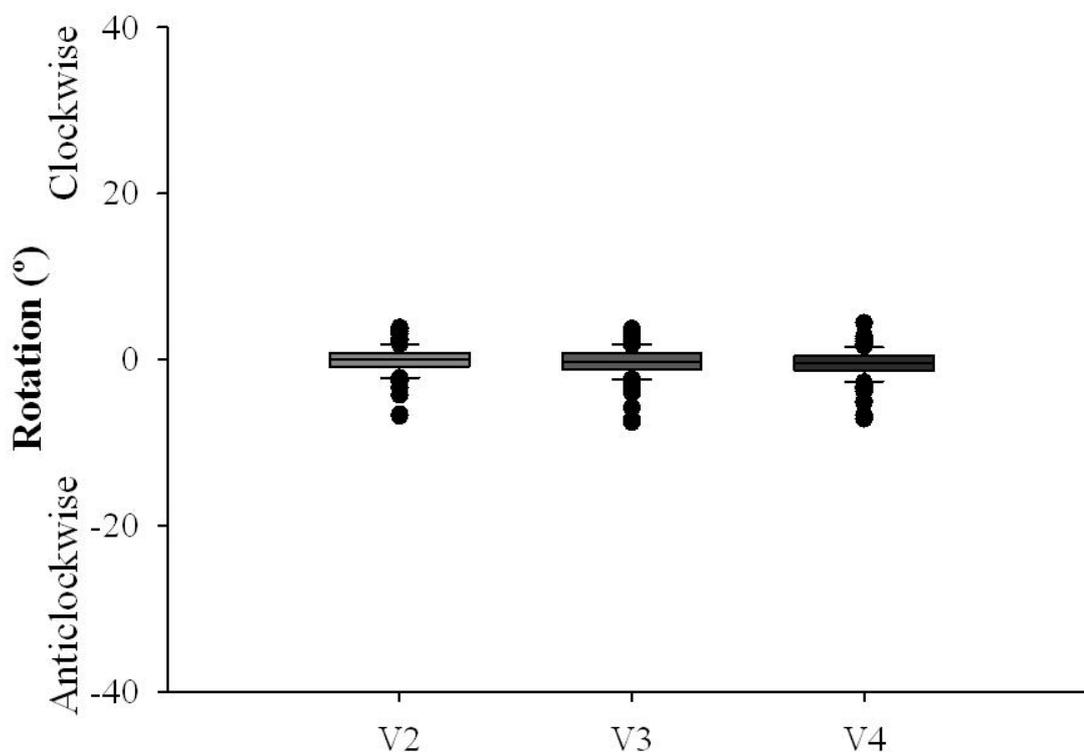
Figure 7.8 *Rotation of the Akreos AO Toric intraocular lens at each visit in comparison with visit V1. n=86*

The rotation of the IOL in comparison to its orientation at visit V2 is displayed in Table 7.4 and Figure 7.9.

	At V3	At V4
Absolute rotation in comparison to V2	1.1±0.9° (0.0-3.9)	1.1±1.0° (0.0-4.4)
Lenses rotated less than 5°	100%	100%
Lenses rotated less than 10°	100%	100%

Table 7.5 *Absolute rotation of the Akreos AO toric intraocular lens at each post-operative visit following visit V2. N=86*
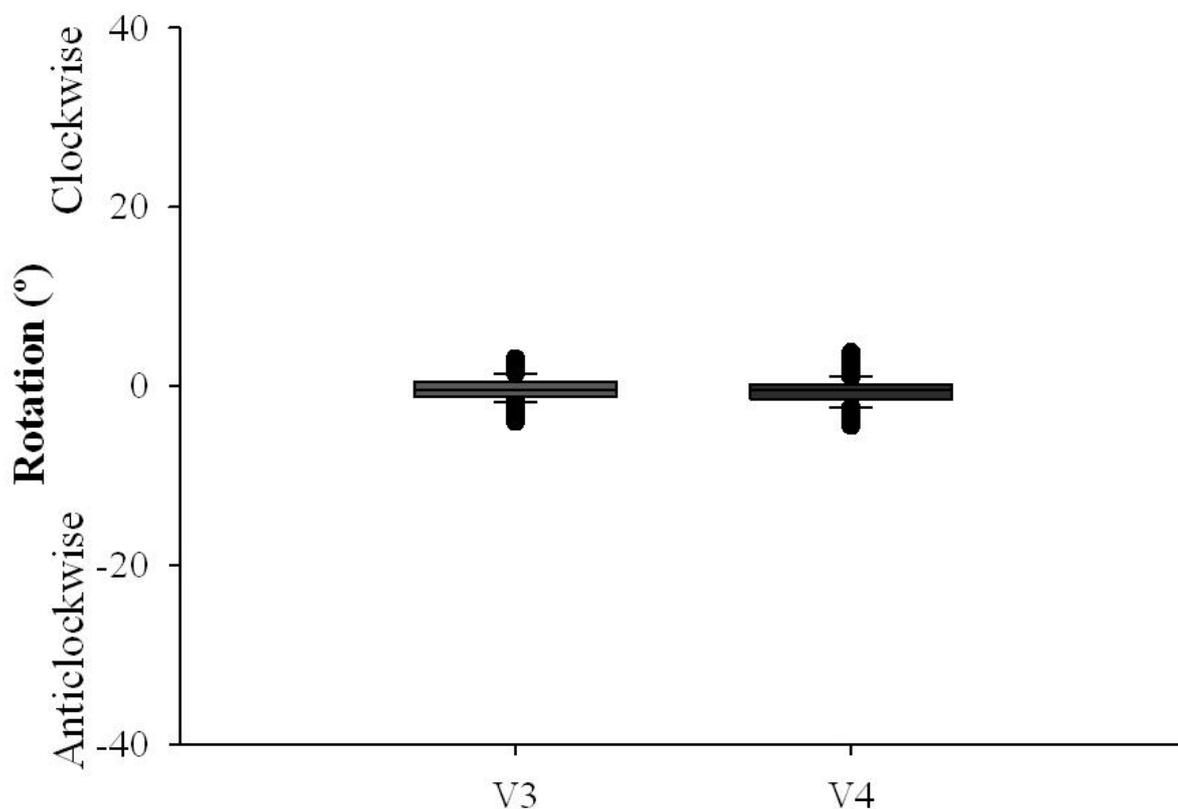
Figure 7.9 *Rotation of the Akreos AO Toric intraocular lens at each visit in comparison with visit V2. N=86*

The mean absolute rotation between V3 and V4 was 0.89±0.75° (range 0 to 3.1); all IOLs remained within 5° of their orientation at V3.

The misalignment of the corneal reference markings (MK), and IOL orientation in comparison to the desired orientation of the IOL as determined using the Akreos toric calculator is displayed in Table 7.5 and Figure 7.10.

	MK	OP	V1	V2	V3	V4
Absolute misalignment in comparison to keratometry (range)	4.26±3.92° (0.0-19.9)	6.6±5.9° (0.0-27.6)	7.2±7.0° (0.0-32.4)	7.4±7.2° (0.0-34.3)	7.3±7.1 (0.1-34.9)	7.2±7.1° (0.0-34.8)
Lenses misaligned less than 5°	73%	59%	63%	55%	50%	53%
Lenses misaligned less than 10°	93%	76%	73%	74%	72%	73%

Table 7.6 *Absolute misalignment of the corneal reference markings and intraocular lens at each visit. n=86 (MK; n=68)*
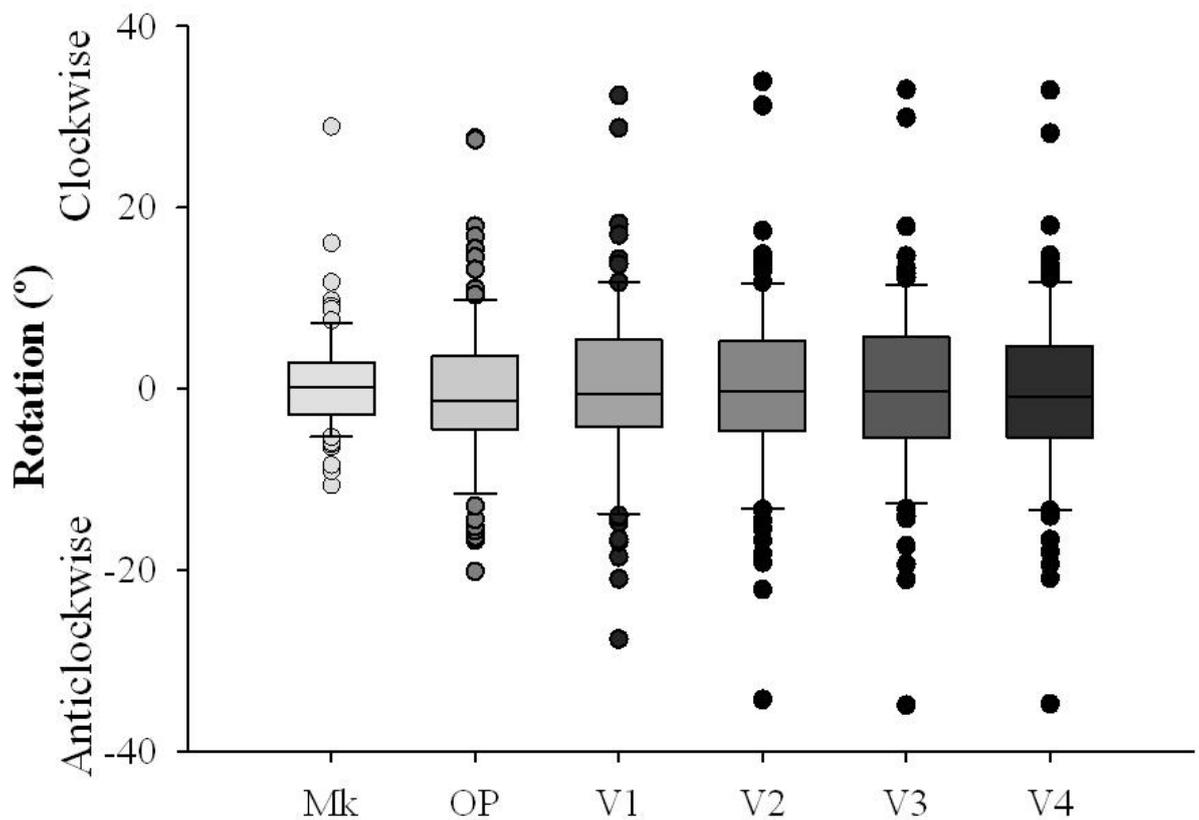
Figure 7.10 *Misalignment of the corneal reference markings and intraocular lens at each visit. n=86 (MK; n=68)*

There was a significant difference in rotation between consecutive visits (χ^2_3=31.396, Z<0.001). More rotation occurred in the OP-V1 period than between any other consecutive visit (Z<0.001). Each subsequent consecutive visit exhibited similar levels of rotation (Z>0.008)

7.4.4 Centrational Stability of the Akreos AO Toric Intraocular Lens

The position of the IOL following implantation was generally superior (0.22 ± 0.14 mm) nasal (0.15 ± 0.15 mm). The mean total absolute decentration value was 0.31 ± 0.14 mm at OP, 0.32 ± 0.14 mm at V1, 0.28 ± 0.13 mm at V2, 0.31 ± 0.14 at V3, and 0.31 ± 0.14 mm at V4. There were no significant changes in IOL centration over time ($F_{4,264}$=1.905, p=0.110) and any movement of the IOL appeared random in direction (Figure 7.11; Figure 7.12; Figure 7.13; Figure 7.14). Two lenses were decentred by more than 0.5 mm, no lenses were decentred more than 7.5 mm
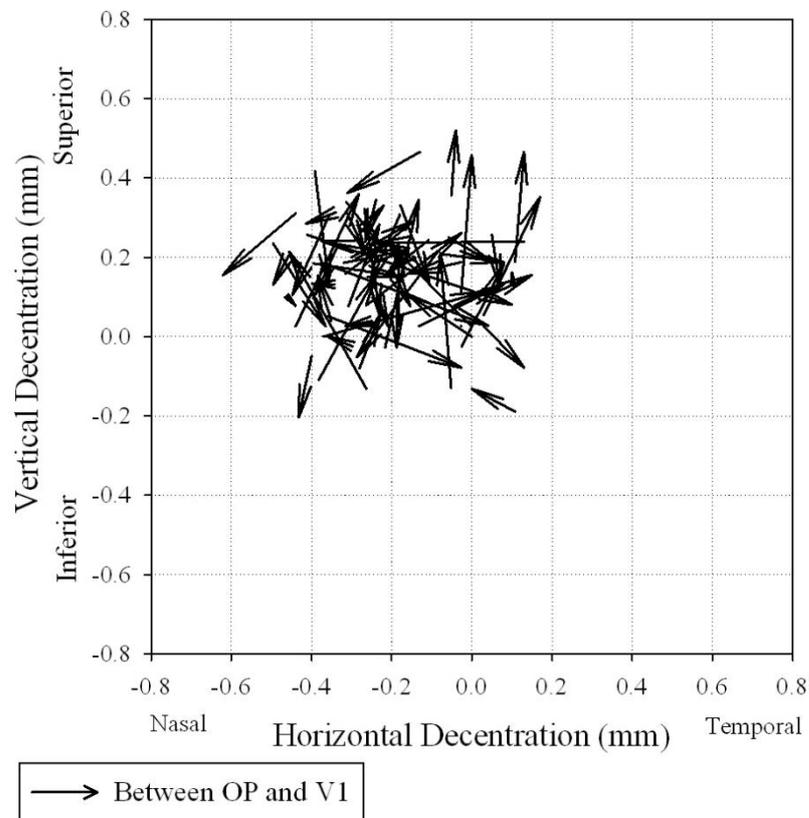
Figure 7.11 *Vector graph of change in intraocular lens centration between 15 minutes post operatively and day 1-2 post implantation. n=67*
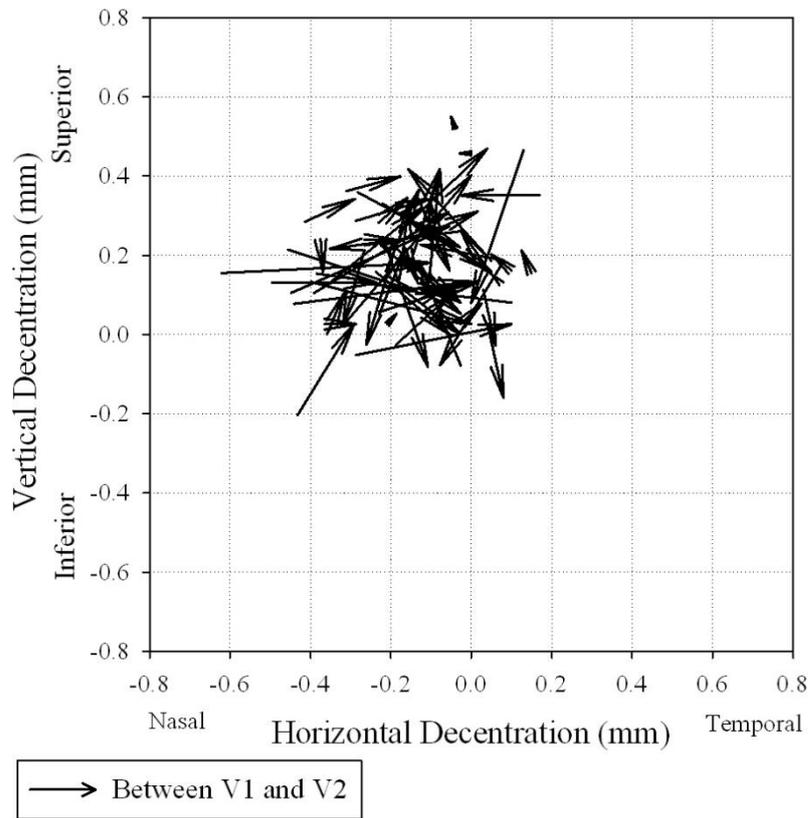
Figure 7.12 Vector graph of change in intraocular lens centration between day 1-2 and day 7-14 post implantation. n=67
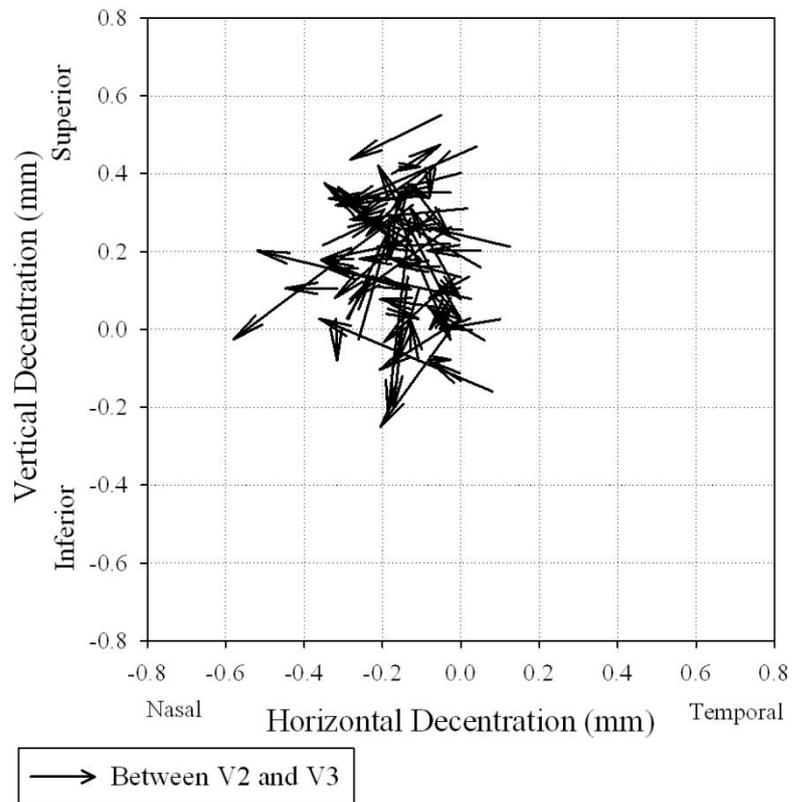
Figure 7.13 *Vector graph of change in intraocular lens centration between day 7-14 and day 30-60 post implantation. n=67*
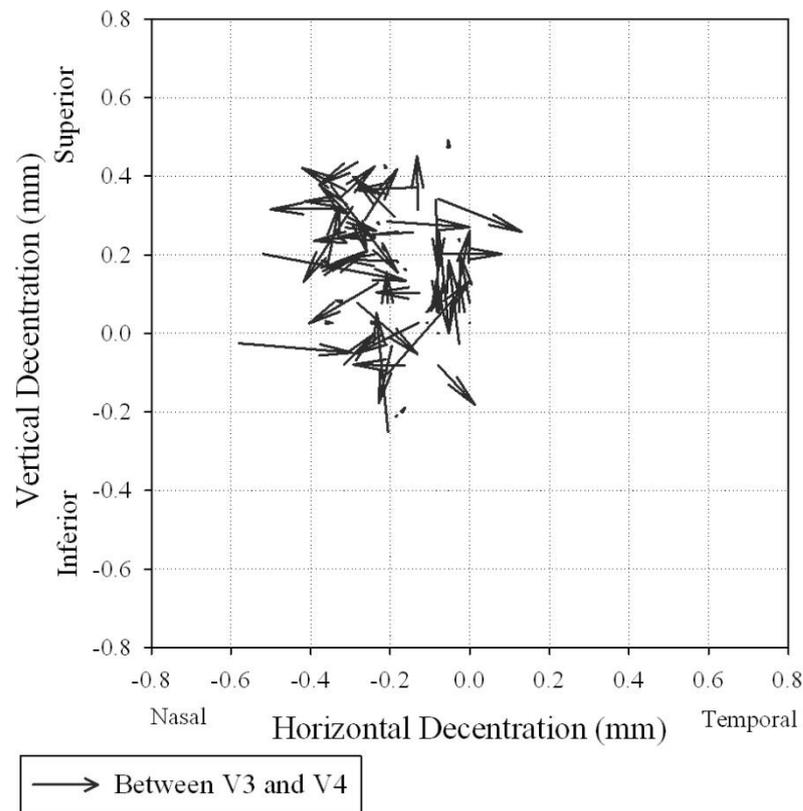
Figure 7.14 *Vector graph of change in intraocular lens centration between 15 minutes post operatively and day 1-2 post implantation. n=67*

7.5 Discussion

It appears that four main contributors to IOL rotation post implantation are:

- poor initial friction between the IOL haptics and the capsular bag; this relates to the design of the IOL, capsular bag size, and removal of OVD
- instability of the anterior chamber related to post-operative intraocular pressure changes and ocular trauma
- a lack of long term IOL fixation within the capsular bag
- compression of the IOL haptics from capsular bag shrinkage.

Movement of IOL haptics within the capsular bag tends to occur during the early postoperative period before fusion between the capsular bag and IOL haptics (Patel *et al.,* 1999). Maximising friction between haptic and capsular bag can reduce this early rotation. Several mechanisms can be employed to increase the friction. A larger lens

diameter ensures more contact with the capsular bag and therefore more friction. However, if too large, distortion of the capsular bag and zonules occurs (Lim *et al.,* 1998). Unfortunately, it is difficult to establish the size of the capsular bag pre-operatively and a reliable link between accessible ocular measurements and capsular bag size are yet to be confirmed (Khng and Osher, 2008). Haptic material is also a consideration. PMMA has the most adhesive force between bag and haptic. Next best is foldable acrylic, and the weakest is silicone (Oshika *et al.,* 1998).

Care needs to be taken to fully remove the OVD. These coat the IOL, decreasing friction and allowing easy manipulation (Myers and Olson, 1999). OVDs vary in viscosity; the type of OVD used may influence the amount of rotation (Chang, 2003). Intraocular pressure can fluctuate in the early period after cataract surgery, causing increased fluid flow within the anterior chamber. In uneventful cataract surgery, IOP can drop to below 5 mmHg in 6.3% of patients (Shingleton *et al.,* 2007). Hypotony causes destabilisation of the anterior chamber reducing its integrity and resulting in a higher risk of rotation (Pereira *et al.,* 2010).

Post-operative ocular trauma can cause IOL rotation. If the force on the eye is sufficient to cause significant wound leakage then large degrees of IOL rotation can occur. Lens positioning holes could help reduce the effect of ocular trauma acting as an anchor to resist traumatic forces (Pereira *et al.,* 2010). Positioning holes, present on many plate haptics, can increase stability. Capsular fibrosis and proliferative lens cortical material migrate through the positioning holes creating an effective anchor. The larger the positioning holes, the more material can migrates, therefore strengthening the fixation within the capsule. This fibrosis typically takes 2 weeks after implantation to establish (Mamalis *et al.,* 1996). If a toric lens is misaligned it is easier to reposition the IOL before this fibrosis occurs (Chang, 2009).

Capsular shrinkage compresses the IOL haptics and, depending on the design, can cause IOL rotation. Plate haptic lenses have no preference in their direction of rotation and show good stability with capsular compression (Jampaulo *et al.,* 2008). However, open loop haptic IOLs can rotate with capsular compression. If sufficient friction between the haptics and capsule occurs, then the lens optic (implanted with the haptics orientated clockwise) rotates clockwise under compression. If there is insufficient

friction, the haptics slip causing anticlockwise rotation (Pärssinen *et al.,* 1998). This pattern of rotation has been demonstrated *in vivo* (Werblin, 1995; Patel *et al.,* 1999).

Between the 1-2 day post-operative and 3-4 month post-operative visits, the rotational stability of the Akreos AO platform was excellent: 96% of the *Akreos AO aspheric IOLs* and 98% of the *Akreos AO toric IOLs* remained within 5°. The amount of rotational stability during this time period is good (or better than) previously studied toric IOLs (Chapter 6; Table 6.1). The 4 large positioning holes should be anchored by fibrosis migration and the use of 4 haptic arms provide resilience to potential rotation caused by compression of the capsular bag. However, in the early post-operative period (before day 1-2) there is a higher chance of rotation. The acrylic material should maximise early friction, however the 11 mm length of the IOL is similar to plate haptic IOLs and shorter than IOls with loop haptics, therefore there is less chance of contact between the IOL and capsular bag in the early post-operative period before capsular compression occurs. The relatively high surgical re-intervention rate due to IOL rotation found with this lens highlights the lack of early rotational stability.

This is the first study to examine the accuracy of lens placement using image analysis and highlights the need for a new method of establishing lens position. Due to the variability in the quality of the surgical videos only 62 of the 100 eyes could be examined for the accuracy of placement intraoperatively. On average, the placement of the IOL was 2.1 ± 2.2° (range 0.0 to 14.3°) away from the orientation of the reference markers. Lens placement, in comparison to the desired IOL axis as determined by the Akreos toric calculator, demonstrated an unacceptably high rate of IOL misalignment. The difference between the target axis and the corneal markings was 4.26 ± 3.92°(0.0 - 19.9) with 93% of the markings within 10° of the target axis. The eye torsion during keratometry is assumed: therefore an error of approximately 2° could be expected (range 0 to 7.1; Chapter 6). Even after compensating for the error, the level of misalignment would be unacceptable.

The difference in orientation between the IOL at 3-4 months and the target orientation (determined by the Akreos toric calculator) was 7.2 ± 7.1° (range 0.0-34.8). 73% of lenses were misaligned by over 10°: This misalignment would result in a loss of toric power by 25 ± 24% (range 0 to 114%; Ma and Tseng, 2008), highlighting the difficulty involved with toric IOL implantation. Head position, when measuring keratometry is

susceptible to error as is the corneal axis marking. Alignment of the IOL to these ink markings as well as the placement of the markings are also susceptible to error. These factors contribute to the overall misalignment before any rotation of the IOL occurs.

The standards set by the American national standards institute (ANSI Z80.30-2010) state that a toric IOL is required to be rotationally stable between two consecutive visits 3 months apart. The standards do not require assessment of positional inaccuracies or require evaluation of the rotational stability in the early post-operative period, which, for this closed haptic IOL, was the main source of error.

Intraocular lens tilt can induce coma aberrations; however, the effect of decentration is difficult to predict as it is dependent on the shape factor of the IOL (Atchison, 1991). Despite the reference for centration differing between studies between the pupil, corneal center, and Purkinje images, the results in this study compare well with modern studies of aspheric IOLs in which no higher-order aberrations were induced by increased decentration of abberation correcting aspheric IOLs (Baumeister *et al.,* 2009). In this study both IOLs had an aberration neutral aspheric surface and should be more robust against the visual affects of decentration (Altmann *et al.,* 2005).

7.6 Limitations of the Study

Several limitations exist in this study that are indicative of the current problems with IOL implantation. Eye torsion, when measuring corneal power, is assumed to be the same as when marking the cornea with reference markings. These corneal markings are susceptible to diffusion which reduces clarity and increases the source of error. New systems are in development, such as the *Z-Align* (Carl Zeiss Jena GmbH, Germany) which image the eye during measurement of corneal power. Using this image an eye-tracking program is used to superimpose axis markings over the eye through the surgeons eye piece. Eye tracking has the potential to reduce the systematic error that results from manually marking the desired axis on the cornea.

Image quality was another limitation of the study. Ninety percent of subjects for the *Akreos AO* study and eighty six percent of subjects for the *Akreos toric* study could be assessed for rotational stability. The number dropped to seventy six percent for the assessment of centration, due to insufficient dilation. The IOL has a diameter of 6 mm, therefore the minimum pupil size to assess centration is 6 mm. The IOL toric markings

are 5 mm apart therefore the minimum pupil size to assess rotation is 5 mm. If decentration is present a larger pupil size may be required. This may cause bias in the results: lenses that are decentered will be more difficult to assess for rotational stability and centration.

Only sixty eight percent were suitable for the assessment of IOL misalignment; this was due to the diffusion of the corneal ink markings. Only sixty two percent could be assessed for the accuracy of placement; the main limitations were a lack of image quality from the surgical microscope and diffusion of the ink markings.

7.7 Conclusion

In its current form the *Akreos* platform does not provide enough stability in the early postoperative period. When coupled with the errors systematic with toric axis determination the misalignment of the toric IOL results in insufficient clinical correction of astigmatism. New methods for marking the cornea or iris and conjunctival recognition systems are needed if alignment accuracy is to be improved.

7.8 Supporting Publications

Buckhurst, P.J., Wolffsohn, J.S., Naroo, S.A. & Davies, L.N. (2010). Rotational and centration stability of an aspheric intraocular lens with a simulated toric design. *J Cataract Refract Surg.* **36,** 1523-1528.

Chapter 8 Summary and conclusions

8.1 Introduction

Cataract surgery has evolved into a precise refractive surgical technique. With the advent of multifocal, accommodative and toric IOLs it is now possible to achieve high levels of spectacle independency. Despite significant advancements in IOL designs, post-operative visual outcome is still highly dependent upon accurate IOL power prediction via precise biometry. The primary aim of the thesis was to develop standardised methods for the assessment of IOLs and to evaluate a range of multifocal, accommodative and toric IOLs using these new methodologies.

8.2 Assessment of Multifocal Intraocular Lenses using Defocus Curves

Two depth-of-focus metrics were explored in Chapter 2: amplitude of accommodation and depth-of-focus. Both metrics provide a single value to quantify the useful range of clear vision, however, as discussed in Chapter 2, these metrics have several limitations. The depth-of-focus metric fails to provide significant detail to allow differentiation between MIOL designs, whilst amplitude of accommodation provides insufficient detail to discriminate between monofocal and MIOL designs.

The direct comparison method can be used to determine differences between IOLs for each level of defocus. This method provides a large amount of information, however the results can be complex to interpret making between study comparisons difficult. In view of these limitations, Chapter 2 proposes the area of defocus as an improved metric for evaluating distance, intermediate and near vision. The area of defocus provides a comprehensive yet simplified means of obtaining an overview of the defocus curve results, thus facilitating cross study comparisons whilst still providing sufficient detail to differentiate MIOL designs.

In comparison to measures of VA, intermediate and near area metrics demonstrate high correlation with the subjective perceptions of vision at these distances. Measurement of VA at a fixed distance has inherent disadvantages especially relevant when assessing multiple MIOLs: the set distance favours the MIOL with a corresponding reading addition. For example an MIOL with an effective spectacle addition of +2.50 D should

perform greater at 40 cm than the same principal design of MIOL with a +3.00 D addition. The area metric reduces this bias as it assesses the MIOL over a range of optical defocuses.

Furthermore the results of Chapter 2 suggest that the refractive +3.50 D provides improved levels of vision within the intermediate range whilst the diffractive +4.00 D provides higher levels of near vision. It was also noted that the relatively high addition of the fully diffractive MIOL results in a reduced level of intermediate VA. A *mix and match* approach with both types of IOLs was shown to provide a compromise between intermediate and near vision. Moreover, the levels of intermediate and near vision with this form of correct were similar to those when both types of IOLs were implanted binocularly.

As expected, subjects implanted with the +3.00 D sectorial refractive MIOL achieved the best intermediate vision in comparison with the +3.50 D and +4.00 D addition MIOLs. Vision within the near range was also impressive considering its lower add power; this supports the theory that a sectorial segment can offer a high level of near vision. These conclusions can be derived from both the direct comparison method and the area of focus method of analysis.

8.3   Assessment of Reading Ability and Near Vision Satisfaction

Reading charts have increased in popularity as a method for assessing near vision in IOL studies. Modern reading charts use standardised logarithmic progression of letter size and as such offer more scientific scope in comparison to often used Jaeger charts. A significant limitation when assessing the results from reading charts is the lack of standardisation in the protocols used to evaluate the results. Reading acuity demonstrates a subject's spot reading acuity. The methods of calculating this metric are standardised but the value it provides does not represent reading acuity over a range of print sizes which is required for an accurate measure of 'real life' near visual acuity and does not take into account the speed of the reading.

Maximum reading speed (MRS) and critical print size (CPS) are two commonly used metrics to describe reading ability, there is a variety of approaches as to how these metrics can be calculated, however, the method used is not always reported. The two methods used to calculate MRS in Chapter 3 produced equivalent results; however, this

measure describes the suprathreshold reading ability of a subject irrespective of vision and as such provides limited insight regarding the near vision performance of an IOL. The measure could be useful for determining if the groups are equal in cognitive reading ability, independent of vision. CPS was calculated using a variety of methods. The visual inspection method demonstrated the highest correlation with the subjective perception of near vision. However this method is by nature more variable than standardised objective analysis techniques. CPS as 90% of the asymptote of the curve provides a close match to the visual inspection method whilst maintaining discriminative ability.

The reading performance index is a new metric derived in the thesis, which can be utilised to assess reading ability and accounts for both reading speed and acuity. It is calculated as the area under an asymptotic curve − fitted to the *MNRead* results after converting reading speed to a logarithmic form − between the print size when reading speed equals 0 and the print size of 1 LogMAR. The metric incorporates measures of reading speed across a range of print sizes and demonstrated a good correlation with the subjective perception of near vision. It is not a subjective method and so is not subject to inter-analyser variability.

On assessing reading ability between different designs of IOLs, Chapter 3 demonstrated similar levels of reading ability (at 40 cm) when comparing monofocal IOL and single optic accommodative IOL groups. In contrast, the reading ability of the MIOL groups was higher than the monofocal and accommodative IOL groups. Each of the MIOL groups demonstrated similar reading ability except for the *ReZoom* group, which did no achieve as high a reading ability in comparison with the *Lentis MPlus* group. In Chapter 2, VA was measured at 40 cm using the *EDTRS* chart and was compared to VA measured using a -2.50 D defocus lens over the distance prescription. The same findings were noted using these measures, VA was better in the MIOL groups in comparison with the monofocal group and a difference between the *ReZoom* and *Lentis MPlus* MIOLs was also found.

Aside from measures of reading ability, a subjective measure of near vision was evaluated with the NAVQ. Rasch analysis was used to validate the NAVQ for subjects implanted with single optic accommodative IOLs, MIOLs and monofocal IOLs. The NAVQ was targeted for validation, as a questionnaire specific to the assessment of near

vision was required. Rasch analysis assesses the fit of the questionnaire items whilst accounting for the difficulty of each item, ability of each subject and provides an adjustment for converting the scores to a linear interval scale. Chapter 3 demonstrated the reduced NAVQ as a valid instrument for the assessment of IOLs as the questionnaire demonstrated a moderate construct validity correlation with the *MNRead* results. The lack of a strong correlation with reading ability highlights the importance of a questionnaire for the assessment of near vision since a clinical assessment does not fully describe a subjects perception of their near vision following implantation of a presbyopic correcting IOL.

8.4 Assessment of Dysphotopsia in Pseudophakic Subjects with Multifocal Intraocular Lenses

Despite the high prevalence levels of dysphotopsia post MIOL implantation there has been little progress in the assessment of this phenomenon. Where attempts have been made to quantify this visual disturbance, these have been mainly based upon questionnaires, which are limited by their subjectivity. A halometer can provide a more objective method of evaluating the extent of dysphotopsia, providing information on both the glare intensity and localisation. Although halometers have been reported in the academic literature, with MIOLs no validated halometer has been used prior to this thesis.

Chapter 4 describes the application of the BD Halometer to assess the extent of dysphotopsia in MIOL subjects. The BD Halometer Mark 1 battery powered glare source demonstrated a drop in output over time; this spurred the development of the Mark 2 that used a mains output to achieve a constant output. The Halometer demonstrated good repeatability in both phakic and pseudophakic subjects for the assessment of dysphotopsia. The amount of Straylight (measured with the *C-Quant*) and photopic scotoma (measured with the BD Halometer) increased as the density of *Bangerter* occlusion increased. However the results of both instruments did not correlate, suggesting that measures of Straylight and Photopic scotoma are not interchangeable. This may explain why the *C-Quant* fails to detect differences between a monofocal and fully diffractive and sectorial refractive MIOLs. In a prior study the *C-Quant* failed to quantify the visual phenomenon with partially diffractive MIOLs (Hofmann *et al.*, 2009).

The subjective assessment of dysphotopsia shows variability; on the 0-10 subjective scale both the fully diffractive MIOL and monofocal IOL produced similar results despite 53% of the monofocal IOL subjects associating their vision with the image representing clear vision and none of the fully diffractive MIOL subjects associating with the same image.

The BD Halometer proved to be a valid and repeatable instrument for the assessment of dysphotopsia. This is the first study to quantify and compare dysphotopsia profiles – using a Halometer – for multiple MIOL designs and the first to assess this phenomenon with a refractive sectorial MIOL. The dysphotopsia for this type of MIOL corresponds with the position of the near segment. In Chapter 4 all IOLs were implanted with the segment inferiorly, however, varying this location should theoretically change the glare position. The *Tecnis ZM900* demonstrates a uniform concentric light scotoma surrounding the glare source; this concurs with the subjective illustration results where 73% of subjects associated their dysphotopsia with either small or large halos.

The subjective perception of dysphotopsia was better in subjects implanted with the *Lentis MPlus* in comparison with the *Tecnis ZM900*. This suggests that restricting the photopic scotoma area to a specific area of visual field is beneficial in reducing the subjective appearance of dysphotopsia.

8.5   New Optical Low Coherence Reflectometry Device for Ocular Biometry in Cataract Patients

Ocular biometry using time domain interferometry has revolutionised the accuracy of IOL implantation as a refractive procedure. The introduction of the partial coherence interferometer has reduced the prevalence of residual postoperative refractive error but not eliminated it. The estimation of the post-operative IOL position is the main source of error in IOL power predictions. In Chapter 5 the *LenStar LS900* was assessed for its validity and its results were compared to those of an Ultrasound A-Scan and the *IOLMaster*. The results of the *LenStar LS900* and *IOLMaster* were similar for the assessment of axial length. However, greater variability was found with applanation ultrasound, which on average measured longer than both interferometry devices. This may be attributed to the lower resolution of the system and the fact that the laser light is

reflected from the retinal pigment epithelium and ultrasound waves are reflected from the internal limiting membrane.

The *LenStar LS900* measures corneal curvature using two sets of markers in a concentric pattern. The inner markers measure corneal curvature at a 1.65 mm zone surrounding the visual axis and the outer markers measure at a 2.3 mm zone curvature is calculated from these two sets of data points. In comparison the *IOLMaster* measures corneal curvature using 6 points of light arranged in a hexagonal pattern 2.3 mm surrounding the visual axis. In Chapter 5 both instruments produced equivalent corneal curvature results however further work is required to determine the effect of these differences with subjects presenting with irregular astigmatism or following corneal refractive surgery.

The *LenStar LS900* demonstrates significant advantages over the IOLMaster as it provides the facility for measuring corneal thickness and lens thickness as well as using interferometry for measuring anterior chamber depth rather than the lower resolution image analysis technique employed by the *IOLMaster*. Assessment of crystalline lens thickness and position using OLCR has many implications. In particular it is useful for IOL calculations as it may provide additional information for predicting the postoperative IOL position.

A specific constraint of the OLCR in IOL studies is its dependency on its trace edge detection ability. In Chapter 5 the *LenStar LS900* was unable to detect both the anterior and posterior surfaces of the IOL in all but one of the subjects. When used on subjects implanted with the *Lentis MPlus* the *LenStar LS900* detected both surfaces in 13 of the 20 subjects tested. This suggests that the design of the IOL significantly influences the ability of the *LenStar LS900* to detect the IOL surfaces.

8.6   Toric Orientation Assessment

Toric IOLs are dependent on their axis of orientation. Chapters 6 and 7 highlight the importance of the accurate assessment of IOL orientation in comparison with the target axis.

Using consistent anatomical landmarks on the eye allows the assessment of IOL rotation whilst compensating for eye torsion. This is an important factor as the average

rotation of the eye is approximately 2 degrees and can be as high as 7 degrees. Chapter 6 evaluated the repeatability of a refined toric analysis technique demonstrating a high level of validity and repeatability. The vulnerability of all imaging techniques to the captured image quality was also demonstrated.

The closed loop haptic IOL investigated in Chapter 7 displayed a high level of rotational stability following the first two days of implantation; only 2% of lenses rotated more than 5 degrees after the day 1-2 visit. This rotational stability in the late stages could be attributed to the closed loop haptic design and to the presence of positioning holes on the IOL haptic. This would satisfy the FDA criteria requiring; 90% of lenses to rotate less than 5°, 95% less than 10° and 100% less than 20° between two postoperative visits separated by 3 months. However, in the early period between the operation and day 1-2 the lens exhibits a higher level of rotation, 8% of the 86 lenses rotated more than 5° during this time, with an additional 3 subjects requiring surgical re-intervention (overall 9% unacceptable rotation).

This high prevalence of rotation may be a consequence of factors affecting early rotation. The relatively small lens diameter (11 mm) of the closed loop haptic IOL results in reduced friction between the capsular bag and the IOL thus increasing the likelihood for lens rotation if the capsular bag is large or if hypotony occurs due to wound leakage.

Aside from postoperative rotation, inaccuracy in the placement of the IOL with reference to the target axis produces a major source of error for toric IOLs. Only 73% of the corneal reference markers were placed within 5° of the target axis. Orientating the IOL to the corneal markings is also not exempt from error. In Chapter 7 two IOLs were positioned further than 5° from the target axis and one was positioned greater than 10° degrees away from the target axis. The cumulative error resulted in only 59% of IOLs being within five degrees of the target orientation (as determined by the *Akreos* toric calculator) when the first image was taken within 15 minutes after surgery.

In comparison to the target axis (determined by the toric calculator) the total rotational error culminated in an average misalignment of 7.2 ± 7.1° (25 ± 24%; range 0 to 114%) at the 6 month visit. The study determined that the centre of the IOL was positioned superior nasally in comparison with the centre of the cornea. This position proved to be

consistent for each visit and decentration proved to be stable over time. The *Akreos AO* aspheric and toric IOL are aberration neutral IOLs and so are robust to decentration. In contrast, if this displacement in centration were found with a refractive sectorial IOL it would increase the proportion of the near segment present in the pupil.

8.7 Limitations of Current Investigations and Proposals for Future Research

8.7.1 Evaluation of Defocus Curves using Spline Curves

To establish the distance, intermediate, and near areas of focus, 9th order polynomials were fitted to the data sets of each subject. High order polynomials are susceptible to the effects of Runge's phenomenon thereby requiring the assessment of additional data points outside of the limits of integration. Future work will explore the possibility of fitting spline curves to the data set which are unaffected by Runge's phenomenon.

8.7.2 Pupil Size and Defocus Curves

Most MIOLs are dependent upon pupil size. In Chapter 2, the affect of pupil size on the clear range of vision was explored indirectly by using different lighting conditions. To affectively evaluate the direct influence of pupil size on visual outcome, future studies should evaluate a large number of subjects with variable pupil sizes whilst maintaining constant illumination.

8.7.3 The *Radner Reading Chart*

Chapter 3 described the reading performance index (RPI) as a viable means of evaluating reading ability. By using the MNRead chart this metric provided a single value for reading area across a range of print sizes. As multiple versions of the MNRead are not available, multiple examinations cannot be conducted without being influenced by the effects of memorisation. *Radner reading charts* are ideal for evaluating reading ability over a range of distances, as multiple charts are available. Future studies will investigate the development of a metric similar to the RPI that may be applied to the *Radner reading chart* for use at multiple distances.

8.7.4   The Halometer

In Chapter 4 a new halometer was designed and developed for measuring the extent of dysphotopsia in subjects implanted with MIOLs. The glare source used in the study was limited to a single peak wavelength emission. It is envisaged that levels of dysphotopsia may exhibit wavelength specific characteristics. Therefore a tuneable LED, allowing wavelength targeting, could be utilised as the glare source for the halometer.

A significant limitation of Chapter 4 was the assumption that the *Lentis Mplus* segment was situated, and remained, in an inferior position. To verify the link between segment position and location of dysphotopsia, slit lamp imaging or aberrometry should be preformed along with halometery.

8.7.5   Assessment of Post-Operative Intraocular Lens Position

Accurate prediction of the post-operative IOL position from pre-operative biometry measurements is essential for reducing residual refractive error. A limitation presented by the *LenStar LS900* was its inability to detect the surface of the *Softec 1* IOL. This limitation may be characteristic of specific IOL designs. To confirm this proposition, future studies will assess post-operative IOL position with a variety of IOL designs. Furthermore, dependent on it edge detection properties, the *LenStar LS900* may be utilised for the assessment of accommodative IOL movement.

8.7.6   Assessment of Centration

In Chapter 6, IOL centration was assessed using slit lamp images. Although more accurate than the subjective evaluation of centration, this method is gaze dependent and is influenced by the refractive effects of the cornea.

Future studies will examine the position of IOLs using phakometry. Furthermore, phakometry results could be combined with that of the *LenStar LS900* to provide centration co-ordinates with respect to the visual axis.

8.7.7   Assessment of Rotation and Misalignment

A method for assessing IOL rotation was developed and validated in Chapter 6. The process requires the subjective identification of consistent anatomical conjunctival and

iris features. As the determination of these reference features requires subjective judgement, it is susceptible to human error and is further exacerbated by poor image quality. Future work will explore the possibility of developing a computer program, which can automatically identify these features, thus objectively measuring IOL rotation.

In addition to investigating rotation, studies examining misalignment are also needed. Misalignment appears to be the primary source of error with toric IOL implantation. By implementing eye tracking systems or intra-operative aberrometers misalignment may be reduced, however these systems are in the early prototype stages and require further development and validation.

8.8 Conclusion

This thesis has achieved its aim of standardizing methods of assessment of IOLs and to use these techniques to evaluate current multifocal, accommodative and toric IOLs. Adoption of these techniques by the academic community will allow more comprehensive evaluation of future IOL design enhancements. In addition larger studies of patient demographics, analysis of expectations, comprehensive IOL performance assessment and examination of patient satisfaction post implantation will allow better IOL selection for individual patients to optimise their quality of life.

Chapter 9 References

Absolon, M. (1991). Intracapsular techniques. IN: Percival, S.P.B. *A Colour atlas of lens implantation*. Aylesbury, UK, Wolfe Publishing Ltd. 23-26**.**

Akutsu, H., Legge, H.G.E., Showalter, M., Lindstrom, R.L., Zabel, R.W. & Kirby, V.M. (1992). Contrast sensitivity and reading through multifocal intraocular lenses. *Arch Ophthalmol*. **110**, 1076-80.

Akutsu, H., Legge, G.E., Luebker, A.R., Lindstrom, L., Zabel, R.W. & Kirby, V.M. (1993). Multifocal intraocular lenses and glare. *Optom Vis Sci*. **70**, 487-95.

Al-Ghoul, K. J. and Costello, M. J. (1997). Light microscopic variation of fiber cell size, shape and ordering in the equatorial plane of bovine and human lenses. *Mol Vis*. **3,** 2.

Al-Ghoul, K.J., Nordgren, R.K., Kuszak, A.J., Freel, C.D., Costello, M.J. & Kuszak, J.R. (2001). Structural evidence of human nuclear fiber compaction as a function of ageing and cataractogenesis. *Exp Eye Res*. **72,** 199-214.

Alfonso, J.F., Fernández-Vega, L., Señaris, A. & Montés-Micó, R. (2007). Quality of vision with the Acri. Twin asymmetric diffractive bifocal intraocular lens system. *J Cataract Refract Surg*. **33,** 197-202.

Alfonso, J.F., Fernández-Vega, L., Baamonde, M.B. & Montés-Micó, R. (2007b). Prospective visual evaluation of apodized diffractive intraocular lenses. *J Cataract Refract Surg*. **33**, 1235-43.

Alfonso, J.F., Madrid-Costa, D., Poo-López, A. & Montés-Micó, R. (2008). Visual quality after diffractive intraocular lens implantation in eyes with previous myopic laser in situ keratomileusis. *J Cataract Refract Surg*. **34,** 1848-54.

Alfonso, J.F., Puchades, C., Fernández-Vega, L., Montés-Micó, R., Valcárcel, B. & Ferrer-Blasco, T. (2009). Visual acuity comparison of 2 models of bifocal aspheric intraocular lenses. *J Cataract Refract Surg*. **35**, 672-6.

Alfonso, J.F., Fernández-Vega, L., Amhaz, H., Montés-Micó, R., Valcárcel, B. & Ferrer-Blasco, T. (2009b). Visual function after implantation of an aspheric bifocal intraocular lens. *J Cataract Refract Surg*. **35**, 885-92.

Alfonso, J.F., Fernández-Vega, L., Puchades, C. & Montés-Micó. R. (2010). Intermediate visual function with different multifocal intraocular lens models *J Cataract Refract Surg*. **36**, 733-9.

Alió, J.L., Tavolato, M., de la Hoz, F., Claramonte, P., Rodríguez-Prats, J. & Galal, A. (2004). Near vision restoration with refractive lens exchange and pseudoaccommodating and multifocal refractive and diffractive intraocular lenses: comparative clinical study. *J Cataract Refract Surg*. **30,** 2494-503.

Alió, J.L., Elkady, B., Ortiz, D. & Bernabeu, G. (2008a). Clinical outcomes and intraocular optical quality of a diffractive multifocal intraocular lens with asymmetrical light distribution. *J Cataract Refract Surg*. **34**, 942-8.

Alió, J.L., Elkady, B., Ortiz, D. & Bernabeu, G. (2008b). Microincision multifocal intraocular lens with and without a capsular tension ring: optical quality and clinical outcomes. *J Cataract Refract Surg*. **34**, 1468-75.

Alió, J.L., Agdeppa, M.C.C., Pongo, V.C. & Kady, B.C. (2010). Microincision cataract surgery with toric intraocular lens implantation for correcting moderate and high astigmatism: pilot study. *J Cataract Refract Surg,* **36**, 44–52.

Allen, E.D., Burton, R.L., Webber, S.K., Haaskjold, E., Sandvig, K., Jyrkkiö, .H, Leite, E., Nyström, A. & Wollensak, J. (1996) Comparison of a diffractive bifocal and a monofocal intraocular lens. *J Cataract Refract Surg.* **22,** 446-51.

Allen, R., Ho-Yen, G.O., Beckingsale, A.B., Fitzke, F.W., Sciscio, A.G. & Saleh, G.M. (2009) Post-capsulotomy dysphotopsia in monofocal versus multifocal lenses. *Clin Exp Optometry.* **92,** 104-9.

Altmann, G.E., Nichamin, L.D., Lane, S.S. & Pepose, J.S. (2005). Optical performance of 3 intraocular lens designs in the presence of decentration. *J Cataract Refract Surg.* **31**, 574-85.

Amesbury, E.C. & Miller, K.M. (2009). Correction of astigmatism at the time of cataract surgery. *Curr Opin Ophthalmol* **20**, 19–24.

Anderson, H.A., Hentz, G., Glasser, A., Stuebing, K.K. & Manny, R.E. (2008). Minus-lens-stimulated accommodative amplitude decreases sigmoidally with age: a study of objectively measured accommodative amplitudes from age 3. *Invest Ophthalmol Vis Sci.* **49,** 2919-26.

Andley, U.P. (2007). Crystallins in the eye: Function and pathology. *Prog Retin Eye Res.* **26,** 78-98.

Aralikatti, A.K.V., Tu, K.L., Kamath, G.G., Phillips, R.P. & Prasad, S. (2004). Outcomes of sulcus implantation of Array multifocal intraocular lenses in second-eye cataract surgery complicated by vitreous loss. *J Cataract Refract Surg.* **30,** 155-60.

Artigas, J. M., Menezo, J.L., Peris, C., Felipe, A. & Díaz-Llopis, M. (2007). Image quality with multifocal intraocular lenses and the effect of pupil size: comparison of refractive and hybrid refractive-diffractive designs. *J Cataract Refract Surg.* **33,** 2111-7.

Arens, B., Freudenthaler, N. & Quentin, C.D. (1999). Binocular function after bilateral implantation of monofocal and refractive multifocal intraocular lenses. *J Cataract Refract Surg.* **25**, 399-404.

Aslam, T.M., Dhillon, B., Tallentire, V.R., Patton, N. & Aspinal, P. (2004) Development of a forced choice photographic questionnaire for photic phenomena and its testing - repeatability, reliability and validity. *Ophthalmologica.* **218**, 402-10.

Aslam, S.A., Kashani, S., Jones, E. & Claoué, C. (2009) Pilot study and functional results following implantation of the M-flex 630F multifocal intraocular lens. *J Cataract Refract Surg.* **35,** 792

Atchison, D.A. (1991). Design of aspheric intraocular lenses. *Ophthalmic Physiol Opt.* **11,** 137-46.

Atchison, D.A., Charman, W.N. & Woods, R.L. (1997). Subjective depth-of-focus of the eye. *Optom Vis Sci.* **74,** 511-20.

Atchison, D.A. & Charman, W.N. (2010). Thomas Young's contribution to visual optics: the Bakerian Lecture "on the mechanism of the eye". *J Vis.* 10, 16.

Andley, U.P. (2007). Crystallins in the eye: Function and pathology. *Prog Retin Eye Res,* **26,** 78-98.

Auffarth, G.U., Hunold, W., Wesendahl, T.A. & Mehdorn, E. (1993). Depth of focus and functional results in patients with multifocal intraocular lenses: a long-term follow-up. *J Cataract Refract Surg.* **19,** 685-9.

Auffarth, G.U., Hunold, W., Breitenbach, S., Wesendahl, T.A. & Mehdorn, E. (1993). [Long-term results of contrast perception and glare sensitivity in patients with diffraction multifocal lenses]. *Klinische Monatsblätter für Augenheilkunde.* **203,** 336-40.

Babizhayev, M.A., Minasyan, H. & Richer, S.P. (2009). Cataract halos: a driving hazard in aging populations. Implication of the Halometer DG test for assessment of intraocular light scatter. *Applied ergonomics.* **40**, 545-53.

Bacskulin, A., Martin, H., Kundt, G., Terwee, T. & Guthoff, R. (2000). [Analysis of the dynamics of the ciliary muscle during accommodation]. *Der Ophthalmologe.* **97,** 855-9.

Baïkoff, G., Matach, G., Fontaine, A., Ferraz, C. & Spera, C. (2004). Correction of presbyopia with refractive multifocal phakic intraocular lenses. *J Cataract Refract Surg.* **30**, 1454-60.

Bailey, I.L. & Lovie, J.E. (1976). New design principles for visual acuity letter charts *Am J Optom Physiol Opt.* **53,** 740-5.

Bailey, I.L. & Bullimore, M.A. (1991). A new test for the evaluation of disability glare. *Optom Vis Sci.* **68**, 911-7.

Bailey, I.L. (2006). Visual Acuity. IN Benjamin, W. J. *Borish's Clinical Refraction.* 2nd ed. Philadelphia, USA, W.B. Saunders Company. 217-246.

Baldasare, J., Watson, G.R., Whittaker, S.G. & Millershaffer, H. (1986). The Development and Evaluation of a Reading Test For Low Vision Individuals With Macular Loss. *J Vis Impair Blindness.* **80,** 785-789.

Bamashmus, M.A. (2010). Traditional Arabic technique of couching for cataract treatment in Yemen. *European J Ophthalmology.* **20,** 340-4.

Barisić, A., Dekaris, I., Gabrić, N., Bohac, M., Romac, I., Mravicić, I. & Lazić, R. (2008). Comparison of diffractive and refractive multifocal intraocular lenses in presbyopia treatment. *Coll Antropol.* **32**, 27-31.

Baron, A. (1953). Tolerance di l'oeil a matiere plastique: prostheses optiques corneennes. *Bull Soc Ophthalmol Paris.* **9**. 982-988.

Bauer, N.J.C., de Vries, N.E., Webers, C.A.B., Hendrikse, F. & Nuijts R.M.M.A. (2008). Astigmatism management in cataract surgery with the AcrySof toric intraocular lens. *J Cataract Refract Surg.* **34,** 1483-8.

Baumeister, M., Bühren, J. & Kohnen, T. (2009). Tilt and decentration of spherical and aspheric intraocular lenses: effect on higher-order aberrations. *J Cataract Refract Surg.* **35,** 1006-12.

Bautista, C.P., González, D.C., Gómez, A.C. & Bescos, J.A.C. (2009). Evolution of visual performance in 250 eyes implanted with the Tecnis ZM900 multifocal IOL *European J Ophthalmology.* **19**, 762-8.

Becker, K.A., Auffarth, G.U. & Völcker, H.E. (2004). [Evaluation of rotation and decentration of intraocular lenses]. *Ophthalmologe.* **101,** 600–603.

Becker, K.A., Holzer, M.P., Reuland, A.J. & Auffarth, G.U. (2006). [Accuracy of lens power calculation and centration of an aspheric intraocular lens]. *Ophthalmologe.* **103,** 873-6.

Beebe, D.C. (2003). The Lens. IN: Kaufman, P.L. & Alm, A. *Adler's Physiology of the Eye – Clinical Application.* 10th ed. Missouri, USA. Mosby, Inc. 117-158.

Beiko, G.H.H. (2007). Personalized correction of spherical aberration in cataract surgery. *J Cataract Refract Surg.* **33,** 1455-60.

Bellucci, R. & Giardini, P. (1993). Pseudoaccommodation with the 3M diffractive multifocal intraocular lens: a refraction study of 52 subjects. *J Cataract Refract Surg.* **19,** 32-5.

Ben-Simon, G.J. & Desatnik, H. (2005). Correction of pre-existing astigmatism during cataract surgery: comparison between the effects of opposite clear corneal incisions and a single clear corneal incision. *Graefes Arch Clin Exp Ophthalmol.* **243,** 321–326.

Bender, L., Spalton, D.J., Uyanonvara, B., Boyce, J., Heatley, C., Jose, R. & Khan, J. (2004). POCOman: new system for quantifying posterior capsule opacification. *J Cataract Refract Surg.* **30,** 2058–2063

Bi, H., Ma, X., Cai, W., Wang, X., Chen, W., Liu, D. & Xie, X. (2004). [Clinical application of multifocal intraocular lens]. *Zhonghua Yan Ke Za Zhi.* **40,** 385-8.

Bi, H., Cui, H., Ma, X., Cai, W., Wang, G., Ji, P. & Xie, X. (2008). Early clinical evaluation of AcrySof ReSTOR multifocal intraocular lens for treatment of cataract. *Ophthalmologica.* **222,** 11-6.

Bissen-Miyajima, H., Minami, K., Yoshino, M., Nishimura, M. & Oki, S. (2010). Autorefraction after implantation of diffractive multifocal intraocular lenses. *J Cataract Refract Surg.* **36,** 553-6.

Bland, J.M. & Altman, D.G. (1986). Statistical methods for assessing agreement between two methods of clinical measurement. *Lancet.* **1,** 307-10.

Blaylock, J.F., Si, Z. & Vickers, C. (2006). Visual and refractive status at different focal distances after implantation of the ReSTOR multifocal intraocular lens. *J Cataract Refract Surg.* **32,** 1464-73.

Blaylock, J.F., Si, Z., Aitchison, S. & Prescott, C. (2008). Visual function and change in quality of life after bilateral refractive lens exchange with the ReSTOR multifocal intraocular lens. *J Refract Surg.* **24,** 265-73.

Blaylock, J.F., Si, Z., Prescott, C. & Aitchison, S. (2009). Intermediate optimization of vision with bilateral nonaspheric multifocal intraocular lens implantation. *J Cataract Refract Surg.* **35,** 303-11.

Bleckmann, H., Schmidt, O., Sunde, T. & Kaluzny, J. (1996). Visual results of progressive multifocal posterior chamber intraocular lens implantation. *J Cataract Refract Surg.* **22,** 1102-7.

Blinkhorst, C.D. (1975). Twenty Years Experience with Pseudophakia: Some Thoughts on the Fixation of Intraocular Lenses. *Contact Intraocular Lens Med J.* **1,** 115-120.

Bluestein, E.C., Wilson, M.E., Wang, X.H., Rust, P.F. & Apple, D.J. (1996). Dimensions of the pediatric crystalline lens: implications for intraocular lenses in children. *J Pediatric Ophthalmol Strab*. **33,** 18-20.

de Boer, M.R,M., Moll, A.C., de Vet, H.C.W., Terwee, C.B., Völker-Dieben, H.J.M. & van Rens, G.H.M.B. (2004). Psychometric properties of vision-related quality of life questionnaires: a systematic review. *Ophthalmic Physiol Opt*. **24,** 257-73.

Bonnet, P., Robinet, A., Colin J. (1991). [Comparative study of 2 types of bifocal implants by measurement of visual acuity and contrast sensitivity]. *J français d'ophtalmologie*. **14,** 295-9.

Borderie, V.M., Touzeau, O. & Laroche, L. (1998). Videokeratography, keratometry and refraction after penetrating keratoplasty. *J Refract Surg*. **15,** 32–37.

Borkenstein, A.F.M., Reuland, A., Limberger, I., Rabsilber, T.M. & Auffarth, G.U. (2009). Transscleral fixation of a toric intraocular lens to correct aphakic keratoplasty with high astigmatism. *J Cataract Refract Surg*. **35,** 934–938.

Braswell, J. & Rine, R.M. (2006). Evidence that vestibular hypofunction affects reading acuity in children. *Int J Pediatr Otorhinolaryngol*. **70,** 1957-65.

Brian, G. & Taylor, H. (2001) Cataract blindness--challenges for the 21st century. *Bull World Health Organ,* **79,** 249-56.

Bron, A.J., Tripathi, R.C. & Tripathi, B.J. (1997). The lens and zonules. IN: Wolff's Anatomy of the Eye and Orbit. 8th ed. London, Chapman & Hall. 411-443.

Brown, N. (1974). The change in lens curvature with age. *Exp Eye Res*. **19,** 175-83.

Brown, D., Dougherty, P., Gills, J.P., Hunkeler, J., Sanders, D.R. & Sanders, M.L. (2009). Functional reading acuity and performance: Comparison of 2 accommodating intraocular lenses. *J Cataract Refract Surg*. **35,** 1711-4.

Brydon, K.W., Tokarewicz, A.C. & Nichols, B.D. (2000). AMO array multifocal lens versus monofocal correction in cataract surgery. *J Cataract Refract Surg*. **26,** 96-100.

Buchwald, H. & Lang, G.K. (2004). [Cataract surgery with implantation of toric silicone lenses for severe astigmatism after keratoplasty]. *Klin Monbl Augenheilkd*. **221,** 489–494.

Buratto, L. & Meglio, G.D. (2006). Accommodative intraocular lenses: short-term visual results of two different lens types. *European J Ophthalmology*. **16,** 33-9.

Butcher, J.M. & O'Brien, C. (1991). The reproducibility of biometry and keratometry measurements. *Eye*. **5,** 708–11.

Buznego, C. & Trattler, W.B. (2009). Presbyopia-correcting intraocular lenses. *Curr Opin Ophthalmol*. **20,** 13-18.

Caporossi, A., Martone, G., Casprini, F. & Rapisarda, L. (2007). Prospective randomized study of clinical performance of 3 aspheric and 2 spherical intraocular lenses in 250 eyes. *J Refract Surg*. **23**, 639-48.

Carey, P.J., Leccisotti, A., McGilligan, VE., Goodall, E.A. & Moore, C.B.T. (2010). Assessment of toric intraocular lens alignment by a refractive power/corneal analyzer system and slitlamp observation. *J Cataract Refract Surg*. **36,** 222-9.

de Castro, A., Rosales, P. & Marcos, S. (2007). Tilt and decentration of intraocular lenses in vivo from Purkinje and Scheimpflug imaging. Validation study. *J Cataract Refract Surg.* **33,** 418-29.

Central Bureau of the Commission Internationale de l'Eclairage. Vienna. (1989). Mesopic Photometry: History, Spacial Problems and Practival Solutions, *CIE publication.* **81.**

Cerviño, A., Hosking, S.L., Montés-Micó, R. & Alió, J.L. (2008a). Retinal straylight in patients with monofocal and multifocal intraocular lenses. *J Cataract Refract Surg.* **34,** 441-6.

Cerviño, A., Montes-Mico, R. & Hosking L.S. (2008a). Performance of the compensation comparison method for retinal straylight measurement: effect of patient's age on repeatability. *Br J Ophthalmol.* **92**, 788-91.

Cha, D., Kang, S.Y., Kim, S., Song, J. & Kim, H. (2010). New Axis-Marking Method for a Toric Intraocular Lens: Mapping Method. *J Refract Surg.* doi:10.3928/1081597X-20101005-01 [Epub ahead of print].

Chang, D.F. (2003). Early rotational stability of the longer Staar toric intraocular lens: fifty of opposite power. consecutive cases. *J Cataract Refract Surg.* **29,** 935–940.

Chang, D.F. (2008a). Comparative rotational stability of single-piece open-loop acrylic and plate-haptic silicone toric intraocular lenses. *J Cataract Refract Surg.* **34,** 1842–1847.

Chang, D.F. (2008b). Prospective functional and clinical comparison of bilateral ReZoom and ReSTOR intraocular lenses in patients 70 years or younger. *J Cataract Refract Surg.* **34,** 934-41.

Chang, D.F. (2009). Repositioning technique and rate for toric intraocular lenses. *J Cataract Refract Surg.* **35,** 1315–1316.

Chen, W., Meng, Q., Ye, H., Liu, Y. (2010) Reading ability and stereoacuity with combined implantation of refractive and diffractive multifocal intraocular lenses *Acta ophthalmologica.* doi: 10.1111/j.1755-3768.2009.01702.x 2009 [Epub ahead of print].

Chen, W., Meng, Q., Ye, H., Liu, Y. (2009) [Comparative assessment of visual quality after combined implantation of multifocal intraocular lens.]. *Zhonghua Yan Ke Za Zhi.* **45,** 1084-8.

Chernyak, D.A. (2004). Cyclotorsional eye motion occurring between wavefront measurement and refractive surgery. *J Cataract Refract Surg.* **30**, 633-8.

Chiam, P.J.T., Chan, J.H., Haider, S.I., Karia, N., Kasaby, H., Aggarwal R.K., (2007). Functional vision with bilateral ReZoom and ReSTOR intraocular lenses 6 months after cataract surgery. *J Cataract Refract Surg.* **33,** 2057-61.

Choi, J. & Schwiegerling, J. (2008). Optical performance measurement and night driving simulation of ReSTOR, ReZoom, and Tecnis multifocal intraocular lenses in a model eye. *J Refract Surg.* **24,** 218-22.

Chylack, L.T., Wolfe, J.K., Singer, D.M., Leske, M.C., Bullimore, M.A., Bailey, I.L., Friend, J., McCarthy, D. & Wu, S.Y. (1993a). The Lens Opacities Classification System III. The Longitudinal Study of Cataract Study Group. *Arch Ophthalmol.* **111,** 831-6.

Chylack, L.T., Jakubicz, G., Rosner, B., Khu, P., Libman, J., Wolfe, J.K., Padhye, N. & Friend, J. (1993b). Contrast sensitivity and visual acuity in patients with early cataracts. *J Cataract Refract Surg.* **19,** 399-404.

Cillino, S., Casuccio, A., Pace, F.D., Morreale, R., Pillitteri, F., Cillino, G. & Lodato, G. (2008) One-year outcomes with new-generation multifocal intraocular lenses. *Ophthalmology.* **115,** 1508-16.

Cionni, R.J., Chang, D.F., Donnenfeld, E.D., Lane, S.S., McCulley, J.P. & Solomon, K.D. (2009a). Clinical outcomes and functional visual performance: comparison of the ReSTOR apodised diffractive intraocular lens to a monofocal control. *Br J Ophthalmol.* **93,** 1215-9.

Cionni, R.J., Osher, R.H., Snyder, M.E. & Nordlund, M.L. (2009b). Visual outcome comparison of unilateral versus bilateral implantation of apodized diffractive multifocal intraocular lenses after cataract extraction: prospective 6-month study. *J Cataract Refract Surg.* **35,** 1033-9.

Cionni, R.J., Chang, D.F., Donnenfeld, E.D., Lane, S.S., McCulley, J.P. & Solomon, K.D. (2009c). Clinical outcomes and functional visual performance: comparison of the ReSTOR apodised diffractive intraocular lens to a monofocal control. *Br J Ophthalmol*. **93,** 1215-9.

Cheung, S., Kallie, C.S., Legge, G.E. & Cheong, A.M.E. (2008). Nonlinear mixed-effects modeling of MNREAD data. *Invest Ophthalmol Vis Sci.* **49,** 828-35.

Cheong, A.M.Y., Legge, G.E., Cheung, S. & Massof, R. (2008). Development of a scale to measure reading ability. *Invest Ophthalmol Vis Sci.* ARVO E-Abstract 4108.

Chiam, P.J.T., Chan, J.H., Aggarwal, R.K. & Kasaby, S. (2006). ReSTOR intraocular lens implantation in cataract surgery: quality of vision. *J Cataract Refract Surg*. **32,** 1459-63.

Christie, B., Nordan, L., Chipman, R., & Gupta, A. (1991). Optical performance of an aspheric multifocal intraocular lens. J Cataract Refract Surg. **17,** 583-91.

Chung, S.T.L., Mansfield, J.S. & Legge, G.E. (1998). Psychophysics of reading. XVIII. The effect of print size on reading speed in normal peripheral vision. *Vision Res*. **38**, 2949-2962.

Cleary, G., Spalton, D.J. & Marshall, J. (2010a). Pilot study of new focus-shift accommodating intraocular lens. *J Cataract Refract Surg*. **36,** 762-70.

Cleary, G., Spalton, D.J. & Gala, K.B. (2010b). A randomized intraindividual comparison of the accommodative performance of the bag-in-the-lens intraocular lens in presbyopic eyes. *Am J Ophthalmol.* **150,** 619-627.

Coeckelbergh, T.R.M., Brouwer, W.H., Cornelissen, F.W., Van Wolffelaar, P. & Kooijman, A.C. (2002). The effect of visual field defects on driving performance: a driving simulator study. *Arch Ophthalmol*. **120,** 1509-16.

Coleman, D.J. (1970). Unified model for accommodative mechanism. *Am J Ophthalmol.* **69,** 1063-1979.

Colvard, M. (2003). Defining mesopic and scotopic. *J Cataract Refract Surg*. **29,** 6-7.

Correia, R.J.B., Moreira, H., Netto, S.U.L. & Pantaleão, G.R. (2009). Visual performance after toric IOL implantation in patients with corneal astigmatism. *Arquivos brasileiros de oftalmologia*. **72,** 636-40.

Croft, M.A., McDonald, J.P., Nadkarni, N.V., Lin, T. & Kaufman, P.L. (2009). Age-related changes in centripetal ciliary body movement relative to centripetal lens movement in monkeys. *Exp Eye Res.* **89,** 824-32

Cruysberg, L.P.J., Doors, M., Verbakel, F., Berendschot, T.T.J.M., De Brabander, J. & Nuijts, R.M.M.A. (2010). Evaluation of the Lenstar LS 900 all-in-one non contact biometry meter. *Br J Ophthalmol.* **94,** 106-110.

Cumming, J.S. (2004). History and function of the Crystalens. *Cataract Refract Surg Today.* **4**, 38-40.

Cumming, J.S., Colvard, D.M., Dell, S.J., Doane, J., Fine, I.H., Hoffman, R.S., Packer, M. & Slade, S.G. (2006). Clinical evaluation of the Crystalens AT-45 accommodating intraocular lens: results of the U.S. Food and Drug Administration clinical trial. *J Cataract Refract Surg.* **32**, 812-25.

Dardzhikova, A., Shah, C.R. & Gimbel, H.V. (2009). Early experience with the AcrySof toric IOL for the correction of astigmatism in cataract surgery. *Can J Ophthalmol.* **44**, 269–273.

Datiles, M.B., Magno, B.V. & Freidlin, V. (1995). Study of nuclear cataract progression using the National Eye Institute Scheimpflug system. *Br J Ophthalmol.* **79,** 527-34.

Day, M., Seidel, D., Gray, L.S. & Strang, N.C. (2009). The effect of modulating ocular depth of focus upon accommodation microfluctuations in myopic and emmetropic subjects. *Vision Res.* **49**, 211-8.

Dick, H.B., Krummenauer, F., Schwenn, O., Krist, R. & Pfeiffer, N. (1999). Objective and subjective evaluation of photic phenomena after monofocal and multifocal intraocular lens implantation. *Ophthalmology.* **106,** 1878-86.

Dick, H.B., Gross, S., Tehrani, M., Eisenmann, D. & Pfeiffer, N. (2002). Refractive lens exchange with an array multifocal intraocular lens. *J Refract Surg.* **18**, 509-18.

Dick, H.B. (2005). Accommodative intraocular lenses: current status. *Curr Opin Ophthalmol.* **16,** 8-26.

Dick, H.B., Krummenauer, F. & Tröber, L. (2006). [Compensation of corneal astigmatism with toric intraocular lens: results of a multicentre study]. *Klin Monbl Augenheilkd.* **223**, 593–608.

Dong, E.Y. & Joo, C.K. (2001). Predictability for proper capsular tension ring size and intraocular lens size. *Korean J Ophthalmol.* **15,** 22–26.

Dua, H.S., Said, D.G. & Otri, A.M. (2009). Are we doing too many cataract operations? Cataract surgery: a global perspective. *Br J Ophthalmol.* **93,** 1-2.

Duane, A. (1922). Studies in Monocular and Binocular Accommodation, with Their Clinical Application. *Trans Am Ophthalmol Soc.* **20,** 132-57.

Dunne, M.C.M., Davies, L.N. & Wolffsohn, J.S. (2007). Accuracy of cornea and lens biometry using anterior segment optical coherence tomography. *J Biomed Optics.* **12,** 064023.

Ehrmann, K., Ho, A. & Parel, J. (2008). Biomechanical analysis of the accommodative apparatus in primates. *Clin Exp Optom.* **91,** 302-12.

Eisenmann, D., Jacobi, F.K., Dick, B., Jacobi, K.W. & Pabst, W. (1996). [Glare sensitivity of phakic and pseudophakic eyes]. *Klinische Monatsblätter für Augenheilkunde.* **208,** 87-92.

Eleftheriadis, H. (2003). IOLMaster biometry: refractive results of 100 consecutive cases. *Br J Ophthalmol.* **87,** 960-963.

Elgohary, M.A. & Beckingsale, A.B. (2006). Effect of illumination on visual function after monofocal and multifocal intraocular lens implantation. *Eye.* **20**, 144-9.

Elliot, R.H. (1924). A Halometer. *BMJ.* **1**, 624.

Elliott, D.B., Hurst, M.A. & Weatherill, J. (1990). Comparing clinical tests of visual function in cataract with the patient's perceived visual disability. *Eye.* **4**, 712-7.

Eppig, T., Scholz, K., Löffler, A., Messner, A. & Langenbucher, A. (2009). Effect of decentration and tilt on the image quality of aspheric intraocular lens designs in a model eye. *J Cataract Refract Surg.* **35,** 1091-100.

Erdélyi, B., Csákány, B. & Németh, J. (2006). Reproducibility of keratometric measurements decreases with time after blinking. *European J Ophthalmology.* **16,** 371-5.

Evans, M. (2009) Anatomy of the Uvea. IN: Yanoff, M. & Duker, J.S. *Ophthalmology.* 3rd edition. London, Elsevier publishing. 775-776.

Farnsworth, P.N. & Shyne, S.E. (1979). Anterior zonular shifts with age. *Exp Eye Res.* **28,** 291-7.

Fea, A.M., Annetta, F., Cirillo, S., Campanella, D., De Giuseppe, M., Regge, D. & Grignolo F.M. (2005). Magnetic resonance imaging and Orbscan assessment of the anterior chamber. *J Cataract Refract Surg.* **31,** 1713-8.

Fenzl, R.E., Gills, J.P. & Cherchio, M. (1998) Refractive and visual outcome of hyperopic cataract cases operated on before and after implementation of the Holladay II formula. *Ophthalmology.* **105**, 1759–64.

Fercher, A.F., Mengedoht, K. & Werner, W. (1988). Eye-length measurement by interferometry with partial coherent light. *Opt Lett.* **13**, 186–8.

Ferrer-Blasco, T., Montés-Micó, R., Peixoto-de-Matos, S.C., González-Méijome, J.M. & Cerviño, A. (2009). Prevalence of corneal astigmatism before cataract surgery. *J Cataract Refract Surg.* **35,** 70-5.

Fincham, E.F. (1937). The mechanism of accommodation. *Br J Ophthalmol.* **8,** 7-80.

Fine, I.H. & Hoffman, R.S. (2000). The AMO array foldable silicone multifocal intraocular lens. *International ophthalmol clinics.* **40,** 245-52.

Fisher, R.F. (1983). Is the vitreous necessary for accommodation in man. *Br J Ophthalmol.* **67,** 206.

Forte, R. & Ursoleo, P. (2009). The ReZoom multifocal intraocular lens: 2-year follow-up. *European J Ophthalmology.* **19,** 380-3.

Franssen, L., Coppens, J.E. & van den Berg T.J.T.P. (2006). Compensation comparison method for assessment of retinal Straylight. *Invest Ophthalmol Vis Sci.* **47,** 768-76.

Friedman, S.M., Munoz, B., Rubin, G.S., West, S.K., Bandeen-Roche, K. & Fried, L.P. (1999). Characteristics of discrepancies between self-reported visual function and

measured reading speed. Salisbury Eye Evaluation Project Team. *Invest Ophthalmol Vis Sci.* **40**, 858-64.

Frohn, A., Dick, H.B. & Thiel, H.J. (1999). Implantation of a toric poly(methyl methacrylate) intraocular lens to correct high astigmatism. *J Cataract Refract Surg*. **25,** 1675–1678.

Fu, E.R., Yong, V.S. (1990). Multifocal intraocular lens: a new development in aphakic visual rehabilitation. *Ann Acad Med Singap.* **19,** 817-9.

Fujimoto, K., Honda, K., Wada, Y.R., Tanaka, M. & Irie, T. (2010). Four-year experience with a silicone refractive multifocal intraocular lens. *J Cataract Refract Surg*. **36,** 1330-5.

Gale, R.P., Saha, N. & Johnston R.L. (2004). National biometry audit. *Eye.* **18**, 63-6.

Gerten, G., Michels, A. & Olmes, A. (2001). [Toric intraocular lenses. Clinical results and rotational stability]. *Der Ophthalmologe*. **98**, 715-20.

Gierek-Ciaciura, S., Cwalina, L., Bednarski, L. & Mrukwa-Kominek, E. (2010). A comparative clinical study of the visual results between three types of multifocal lenses. *Graefes Arch Clin Exp Ophthalmol*. **248,** 133-40.

Gills, J.P. & Gayton, J.L. (1998). Reducing pre-existing astigmatism. In: Gills, J.P., Fenzl, R. & Martin, R.G. *Cataract Surgery; the State of the Art.* New Jersey, USA, Thorofare. 53–66.

Gills, J.P. & Van der Karr, M.A. (2002). Correcting high astigmatism with piggyback toric intraocular lens implantation. *J Cataract Refract Surg*. **28,** 547–549.

Gills, J.P. (2003). Sutured piggyback toric intraocular lenses to correct high astigmatism. *J Cataract Refract Surg*. **29,** 402–404.

Gilmartin, B. (1986). A review of the role of sympathetic innervation of the ciliary muscle in ocular accommodation. *Ophthalmic Physiol Opt.* **6,** 23-37.

Gimbel, H.V., Sanders, D.R. & Raanan, M.G. (1991). Visual and refractive results of multifocal intraocular lenses. *Ophthalmology.* **98,** 881-7; discussion 888.

Glasser, A., Croft, M.A., Brumback, L. & Kaufman, P.L. (2001). Ultrasound biomicroscopy of the aging rhesus monkey ciliary region. *Optom Vis Sci*. **78,** 417-24.

Glasser, A. (2006). Accommodation: mechanism and measurement. *Ophthalmology. Clinics of North America*. **19,** 1-12.

Glasser, A. (2008). Restoration of accommodation: surgical options for correction of presbyopia. *Clin Exp Optom.* **91,** 279-95.

Goes, F. (1991). Personal results with the 3M diffractive multifocal intraocular lens. *J Cataract Refract Surg*. **17,** 577-82.

Gobbi, P.G., Fasce, F., Bozza, S., Calori, G. & Brancato, F. (2007). Far and near visual acuity with multifocal intraocular lenses in an optomechanical eye model with imaging capability. *J Cataract Refract Surg*. **33,** 1082-94.

Goes, F.J. (2008a). Visual results following implantation of a refractive multifocal IOL in one eye and a diffractive multifocal IOL in the contralateral eye. *J Refract Surg*. **24,** 300-5.

Goes, F.J. (2008b). Refractive lens exchange with the diffractive multifocal Tecnis ZM900 intraocular lens. J Refract Surg. **24,** 243-50.

Gothwal, V.K., Wright, T.A., Lamoureux, E.L. & Pesudovs, K. (2009a). Using Rasch analysis to revisit the validity of the Cataract TyPE Spec instrument for measuring cataract surgery outcomes. *J Cataract Refract Surg.* **35,** 1509-17.

Gothwal, V.K., Wright, T.A., Lamoureux, E.L. & Pesudovs, K. (2009b). Cataract symptom score questionnaire: Rasch revalidation. *Ophthalmic epidemiology.* **16,** 296-303.

Gothwal, V.K., Wright, T.A., Lamoureux, E.L., Lundström, M. Pesudovs, K. (2009c). Catquest questionnaire: re-validation in an Australian cataract population. *Clin Experiment Ophthalmol.* **37,** 785-94.

Gothwal, V.K., Wright, T.A., Lamoureux, E.L. & Pesudovs, K. (2010) Measuring outcomes of cataract surgery using the Visual Function Index-14. *J Cataract Refract Surg.* **36,** 1181-8.

Grabow, H.B. (1997). Toric intraocular lens report. *Ann Ophthalmol-Glauc.* **29,** 161-163.

Graether, J.M. (2009). Simplified system of marking the cornea for a toric intraocular lens. *J Cataract Refract Surg.* **35,** 1498-500.

Green, D.G., Powers, M.K. & Banks M.S. (1980). Depth of focus, eye size and visual acuity. *Vision Res.* **20,** 827-35.

Grewal, D.S., Brar, G.S. & Grewal, S.P.S. (2009). Correlation of nuclear cataract lens density using Scheimpflug images with Lens Opacities Classification System III and visual function. *Ophthalmology.* **116,** 1436-43.

Gross, R.H. & Miller, K.M. (1996). Corneal astigmatism after phacoemulsification and lens implantation through unsutured scleral and corneal tunnel incisions. *Am J Ophthalmol.* **121,** 57–64.

Grosskopf, U., Wagner, R., Jacobi, F.K., Krzizok, T. (1998). [Twilight vision and glare sensitivity in monofocal and multifocal pseudophakia]. *Der Ophthalmologe.* **95,** 432-7.

Gullstrand, A. (1909): Die Dioptrik des Auges. IN: Helmholz, H. *Handbuch der Physiologischen.* Optik. L Voss. 41–375.

Gunenc, U. & Celik, L. (2008). Long-term experience with mixing and matching refractive array and diffractive CeeOn multifocal intraocular lenses. *J Refract Surg.* **24,** 233-42.

Gupta, N., Naroo, S.A. & Wolffsohn, J.S. (2007). Is randomisation necessary for measuring defocus curves in pre-presbyopes? *Cont Lens Anterior Eye.* **30,** 119-24.

Gupta, N., Wolffsohn, J.S., Naroo, S.A., Davies, L.N., Gibson, G.A. & Shah, S. (2007b). Development of a near activity visual questionnaire to assess accommodating intraocular lenses. *Cont Lens Anterior Eye.* **30,** 134-43.

Gupta, N., Wolffsohn, J.S. & Naroo, S.A. (2008). Optimizing measurement of subjective amplitude of accommodation with defocus curves. *J Cataract Refract Surg.* **34,** 1329-38.

Gupta, N., Naroo, S.A. & Wolffsohn, J.S. (2009). Visual comparison of multifocal contact lens to monovision. *Optom Vis Sci.* **86,** E98-105.

Gutiérrez, R., Jiménez, J.R., Villa, C., Valverde, J.A. & Anera, R.G. (2003). Simple device for quantifying the influence of halos after lasik surgery. *J Biomedical Optics.* **8,** 663-7.

Guyton, D.L. (1977). Prescribing cylinders: the problem of distortion. *Surv Ophthalmol.* **22,** 177-88.

Guyton, D.L., Uozato, H. & Wisnicki, H.J. (1990). Rapid determination of intraocular lens tilt and decentration through the undilated pupil. *Ophthalmology.* **97,** 1259-64.

Haigis W. (2004). The Haigis formula. IN: Shammas, H.J. *Intraocular Lens Power Calculations.* N.J, USA, Slack. 41–57.

Hancox, J., Spalton, D., Heatley, C., Jayaram, H. & Marshall, J. (2006). Objective measurement of intraocular lens movement and dioptric change with a focus shift accommodating intraocular lens. *J Cataract Refract Surg.* **32,** 1098-103.

Hancox, J., Spalton, D., Heatley, C., Jayaram, H., Yip, J., Boyce, J. & Marshall, J. Fellow-eye comparison of posterior capsule opacification rates after implantation of 1CU accommodating and AcrySof MA30 monofocal intraocular lenses. *J Cataract Refract Surg.* **33,** 413-7.

Hansen, T.E., Corydon, L., Krag, S. & Thim, K. (1990) New multifocal intraocular lens design *J Cataract Refract Surg.* **16,** 38-41.

Hansen, S.O., Tetz, M.R., Solomon, K.D., Borup, M.D., Brems, R.N., O'Morchoe, D.J., Bouhaddou, O. & Apple, D.J. (1988). Decentration of flexible loop posterior chamber intraocular lenses in a series of 222 postmortem eyes. *Ophthalmology.* **95,** 344-9.

Häring, G., Dick, H.B., Krummenauer, F., Weissmantel, U. & Kröncke, W. (2001). Subjective photic phenomena with refractive multifocal and monofocal intraocular lenses. results of a multicenter questionnaire. *J Cataract Refract Surg.* **27,** 245-9.

Harman, F.E., Maling, S., Kampougeris, G., Langan, L., Khan, I., Lee, N., Bloom, P.A. (2008). Comparing the 1CU accommodative, multifocal, and monofocal intraocular lenses: a randomized trial. *Ophthalmology.* **115,** 993-1001.

Hartley, J.T., Stojack, C.C., Mushaney, T.J., Annon, T.A. & Lee, D.W. (1994). Reading speed and prose memory in older and younger adults. *Psychol Aging.* **9,** 216-23.

Hansen, T.A., Corydon, L., Krag, S. & Thim, K. (1990). New multifocal intraocular lens design. *J Cataract Refract Surg.* **16,** 38-41.

Hayashi, K., Hayashi, H., Nakao, F. & Hayashi, F. (1995). The correlation between incision size and corneal shape changes in sutureless cataract surgery. *Ophthalmology.* **102,** 550-6.

Hayashi, K., Hayashi, H., Nakao, F., Hayashi, F. (2001a). Correlation between pupillary size and intraocular lens decentration and visual acuity of a zonal-progressive multifocal lens and a monofocal lens. *Ophthalmology.* **108,** 2011-7.

Hayashi, K., Hayashi, H., Nakao, F. & Hayashi, F. (2001b) Anterior capsule contraction and intraocular lens decentration and tilt after hydrogel lens implantation. *Br J Ophthalmol.* **85,** 1294-7.

Hayashi, K., Yoshida, M. & Hayashi, H. (2009). All-distance visual acuity and contrast visual acuity in eyes with a refractive multifocal intraocular lens with minimal added power. *Ophthalmology*. **116,** 401-8.

Hayashi, K., Masumoto, M. & Hayashi, H. (2009a). All-distance visual acuity in eyes with a nontinted or a yellow-tinted diffractive multifocal intraocular lens. *Jpn J Ophthalmol.* **53,** 100-6.

Hayashi, K, Manabe, S. & Hayashi, H. (2009c). Visual acuity from far to near and contrast sensitivity in eyes with a diffractive multifocal intraocular lens with a low addition power. *J Cataract Refract Surg*. **35,** 2070-6.

Hazel, C.A. & Elliott, D.B., (2002). The dependency of logMAR visual acuity measurements on chart design and scoring rule. *Optom Vis Sci*. **79,** 788-92.

He Y., Rea, M.S., Bierman, A. & Bullough, J. (1997). Evaluating light source efficacy under mesopic conditions using reaction times. *J Illuminating Engineer Soc.* **26,** 125-138.

He, Y., Zhang, C., Wang, K. & Zhu, S. (2009). [Quality of vision in patients with aspherical diffractive multifocal intraocular lens implantation]. *Zhonghua Yi Xue Za Zhi*. **89,** 2175-8.

Helmholtz, H.H. (1855). Accommodation des Auges. *Archiv fur Ophthalmologie.* **1,** 1-74.

Hermans, E.A., Pouwels, P.J.W., Dubbelman, M., Kuijer, J.P.A., van der Heijde, R.J.L. & Heethaar, R.M. (2009). Constant volume of the human lens and decrease in surface area of the capsular bag during accommodation: an MRI and Scheimpflug study. *Invest Ophthalmol Vis Sci.* **50,** 281–289.

Hessemer, V., Frohloff, H., Eisenmann, D. & Jacobi, K.W. (1994). [Mesoptic vision in multi- and monofocal pseudophakia and in phakic control eyes]. *Der Ophthalmologe*. **91,** 465-8.

Hill, W., Angeles, R. & Otani, T. (2008). Evaluation of a new IOL master algorithm to measure axial length. *J Cataract Refract Surg.* **34,** 920-924.

Hitzenberger, C.K. (1991). Optical measurement of the axial eye length by laser Doppler interferometry. *Invest Ophthalmol Vis Sci*. **32,** 616–24.

Hitzenberger, C.K., Drexler, W. & Dolezal, C. (2001). Measurement of the axial length of cataract eyes by laser Doppler interferometry. *Invest Ophthalmol Vis Sci*. **34,** 1886–93.

Hoffman, R.S., Fine, I.H. & Packer, M. (2004). Refractive lens exchange as a refractive surgery modality. *Curr Opin Ophthalmol.* **15,** 22-8.

Hofmann, T., Zuberbuhler, B., Cervino, A., Montés-Micó, R. & Haefliger, E. (2009). Retinal straylight and complaint scores 18 months after implantation of the AcrySof monofocal and ReSTOR diffractive intraocular lenses. *J Refract Surg.* **25,** 485-92.

Hoffer, K.J. (1980). Biometry of 7,500 cataractous eyes. *Am J Ophthalmol.* **90,** 360-8.

Hoffer, K.J. (2000). Clinical results using the Holladay 2 intraocular lens power formula. *J Cataract Refract Surg.* **26,** 1233-7.

Hoffer, K.J. (1993). The Hoffer Q formula: a comparison of theoretic and regression formulas. *J Cataract Refract Surg.* **19,** 700–712.

Hoffer, K.J. (2000). Clinical results using the Holladay 2 intraocular lens power formula. *J Cataract Refract Surg.* **26,** 1233-7.

Hoffer, K.J. (2009). The Evolution of the Intraocular Lens. IN: *Cataract surgery.* Roger F. Steinert. 3rd ed. Philadelphia, USA, Saunders Inc. 419-438.

Hoffer, K.J., Shammas, H.J. & Savini, G. (2010). Comparison of 2 laser instruments for measuring axial length. *J Cataract Refract Surg.* 36, 644-8.

Hoffman, R.S., Fine, I. & Packer, M. (2005). New phacoemulsification technology. *Curr Opin Ophthalmol.* **16,** 38-43.

Holladay, J.T., Prager, T.C., Chandler, T.Y., Musgrove, K.H., Lewis, J.W. & Ruiz, R.S. (1988). A three-part system for refining intraocular lens power calculations. *J Cataract Refract Surg.* **14,** 17–24.

Holladay, J.T., Van Dijk, H., Lang, A., Portney, V., Willis, T.R., Sun, R. & Oksman, H.C. (1990). Optical performance of multifocal intraocular lenses. *J Cataract Refract Surg.* **16,** 413-22.

Holladay, J.T. (1997). Proper method for calculating average visual acuity. *J Refract Surg.* **13,** 388-91

Holladay, J.T., Piers, P.A. Koranyi, G., van der Mooren, M. & Norrby, N.E.S. (2002). A new intraocular lens design to reduce spherical aberration of pseudophakic eyes *J Refract Surg.* **18,** 683-91.

Holladay, J.T. Hill, W.E. & Steinmueller, A. (2009). Corneal power measurements using scheimpflug imaging in eyes with prior corneal refractive surgery. *J Refract Surg.* **25,** 862-8.

Holland, E., Lane, S., Horn, J.D., Ernest, P., Arleo, R. & Miller, K.M. (2010). The AcrySof Toric Intraocular Lens in Subjects with Cataracts and Corneal Astigmatism A Randomized, Subject-Masked, Parallel-Group, 1-Year Study. *Ophthalmology.* **117,** 2104-11.

Holzer, M.P., Mamusa, M. & Auffarth, G.U. (2009). Accuracy of a new partial coherence interferometry analyser for biometric measurements. *Br J Ophthalmol.* **93,** 807-10.

Huber, S., Nguyen, N.X. & Seitz, B. (2003). Cardinal points and image-object magnification with an accommodative lens implant (1 CU). *Ophthal Physiol Opt.* **23,** 61-70.

Hunkeler, J.D., Coffman, T.M., Paugh, J., Lang, A., Smith, P., Tarantino, N. (2002). Characterization of visual phenomena with the Array multifocal intraocular lens. *J Cataract Refract Surg.* **28,** 1195-204.

Hunold, W., Auffarth, G., Wesendahl, T., Mehdorn, E. & Kuck, G. (1993). [Pseudo-accommodation of diffractive multifocal lenses and monofocal lenses]. *Klinische Monatsblätter für Augenheilkunde.* **202,** 19-23.

Hütz, W.W., Eckhardt, H.B., Röhrig, B. & Grolmus, R. (2006). Reading ability with 3 multifocal intraocular lens models. *J Cataract Refract Surg.* **32,** 2015-21.

Hütz, W.W., Eckhardt, H.B., Röhrig, B. & Grolmus, R. (2008). Intermediate vision and reading speed with array, Tecnis, and ReSTOR intraocular lenses. *J Refract Surg.* **24,** 251-6.

Hütz, W.W., Bahner, K., Röhrig, B. & Hengerer, F. (2010a). The combination of diffractive and refractive multifocal intraocular lenses to provide full visual function after cataract surgery. *European J Ophthalmol.* **20,** 370-5.

Hütz, W.W., Jäckel, R. & Hoffman, P.C. (2010b). Comparison of visual performance of silicone and acrylic multifocal IOLs utilizing the same diffractive design. *Acta ophthalmologica.* doi: 10.1111/j.1755-3768.2010.01984.x [Epub ahead of print].

Hyon, J.Y., Yeo, H.E. (2010). Rotational stability of a single-piece hydrophobic acrylic intraocular lens during removal of ophthalmic viscosurgical devices. *Am J Ophthalmol.* **149,** 253–257.

Ito, M. & Shimizu, K. (2009). Reading ability with pseudophakic monovision and with refractive multifocal intraocular lenses: comparative study. *J Cataract Refract Surg.* **35,** 1501-4.

Jacobi, K.W. & Eisenmann, D. (1993). [Asymmetric multizone lenses--a new concept in multifocal intraocular lenses]. *Klinische Monatsblätter für Augenheilkunde.* **202,** 309-14.

Jacobi, P.C. & Konen, W. (1995). Effect of age and astigmatism on the AMO Array multifocal intraocular lens. *J Cataract Refract Surg.* **21,** 556-61.

Jacobi, F.K., Kammann, J., Jacobi, K.W., Grosskopf, U. & Walden, K. (1999) Bilateral implantation of asymmetrical diffractive multifocal intraocular lenses. *Arch Ophthalmol.* **117,** 17-23.

Jacobi, P.C., Dietlein, T.S., Lüke, C. & Jacobi, F.K. (2002). Multifocal intraocular lens implantation in prepresbyopic patients with unilateral cataract. *Ophthalmology.* **109,** 680-6.

Jacobi, P.C., Dietlein, T.S., Lueke, C. & Jacobi, F.K. (2003) Multifocal intraocular lens implantation in patients with traumatic cataract. *Ophthalmology.* **110,** 531-8.

Jaffe, N.S. (1998). The History of Cataract Surgery. IN: Kwitko, M.L. & Kelman, C.D. *The History of Modern Cataract Surgery.* The Hague, Netherlands, Kugler Publications Inc. 3-15.

Jampaulo, M., Olson, M.D. & Miller, K.M. (2008). Long-term Staar toric intraocular lens rotational stability. *Am J Ophthalmol.* **146,** 550–553.

Javitt, J.C., Wang, F., Trentacost, D.J., Rowe, M. & Tarantino, N. (1997). Outcomes of cataract extraction with multifocal intraocular lens implantation: functional status and quality of life. *Ophthalmology.* **104,** 589-99.

Javitt, J., Brauweiler, H.P., Jacobi, K.W., Klemen, U., Kohnen, S., Quentin, C.D., Teping, C., Pham, T., Knorz, M.C. & Pöetzsch, D. (2000). Cataract extraction with multifocal intraocular lens implantation: clinical, functional, and quality-of-life outcomes. Multicenter clinical trial in Germany and Austria. *J Cataract Refract Surg.* **26,** 1356-66.

Jiang, B.C. & Morse, S.E. (1999). Oculomotor functions and late-onset myopia. *Ophthalmic Physiol Optics.* **19,** 165-72.

Jiang, J., Le, Q., Yang, J. & Lu, Y. (2006). Changes in corneal astigmatism and higher order aberrations after clear corneal tunnel phacoemulsification guided by corneal topography. *J Refract Surg.* **22,** S1083–S1088.

Jin, H., Limberger, I., Borkenstein, A.F.M., Ehmer, A., Guo, H. & Auffarth, G.U. (2010). Pseudophakic eye with obliquely crossed piggyback toric intraocular lenses. *J Cataract Refract Surg*. **36,** 497–502.

Kamlesh, S., Dadeya, S. & Kaushik, S. (2001). Contrast sensitivity and depth of focus with aspheric multifocal versus conventional monofocal intraocular lens. *Can J Ophthalmol*. **36,** 197-201.

Kanski, J.J. & Packard, R.B.S. (1985). Intracapsular Extraction. IN: *Cataract and lens implant surgery : a systematic manual.* Edinburgh, UK, Churchill Livingstone. 4-13.

Kasthurirangan, S., Markwell, E.L., Atchison, D.A. & Pope, J.M. (2008). *In vivo* study of changes in refractive index distribution in the human crystalline lens with age and accommodation. *Invest Ophthalmol Vis Sci*. **49,** 2531-40.

Kaufmann, C., Peter, J., Ooi, K., Phipps, S., Cooper, P. & Goggin, M. (2005). Limbal relaxing incisions versus on-axis incisions to reduce corneal astigmatism at the time of cataract surgery. *J Cataract Refract Surg*. **31,** 2261–2265.

Kawamorita, T. & Uozato, H. (2005). Modulation transfer function and pupil size in multifocal and monofocal intraocular lenses in vitro. *J Cataract Refract Surg*. **31,** 2379-85.

Kawamorita, T., Uozato, H., Aizawa, D., Kamiya, K. & Shimizu, K. (2009). Optical performance in rezoom and array multifocal intraocular lenses in vitro. *J Refract Surg*. **25,** 467-9.

Kaymak, H. & Mester, U. (2007). [First results with a new aberration correcting bifocal intraocular lens]. *Der Ophthalmologe*. **104,** 1046-51

Keates, R.H., Pearce, J.L. & Schneider, R.T. (1987). Clinical results of the multifocal lens. *J Cataract Refract Surg*. **13,** 557-60.

Keates, R.H. (1989). The first American experience with the multifocal lens. *Develop Ophthalmol*. **18,** 121-4.

Kelman, C.D. (1967). Phaco-emulsification and aspiration. A new technique of cataract removal. A preliminary report. *Am J Ophthalmol*. **64,** 23-35

Kersey, J.P., O'Donnell, A. & Illingworth, C.D. (2007). Cataract surgery with toric intraocular lenses can optimize uncorrected postoperative visual acuity in patients with marked corneal astigmatism. *Cornea*. **26,** 133–135.

Khng, C. & Osher, R.H. Evaluation of the relationship between corneal diameter and lens diameter. *J Cataract Refract Surg*. **34,** 475–479.

Khokhar, S., Lohiya, P., Murugiesan, V. & Panda, A. (2006). Corneal astigmatism correction with opposite clear corneal incisions or single clear corneal incision: comparative analysis. *J Cataract Refract Surg*. **32,** 1432–1437.

Kiel, A.W., Butler, T. & Alwitry, A. (2003). Visual acuity and legal visual requirement to drive a passenger vehicle. *Eye*. **17,** 579-82.

Kim, J.H., Lee, D., Cha, Y.D., Oh, S.H., Mah, K.C. & Lee, M.S. (2008). The analysis of predicted capsular bag diameter using modified model of capsule measuring ring in Asians. *Clin Experiment Ophthalmol*. **36,** 238–244.

Kirschkamp, T., Dunne, M. & Barry, J. (2004). Phakometric measurement of ocular surface radii of curvature, axial separations and alignment in relaxed and accommodated human eyes. *Ophthal Physiol Optics*. **24,** 65-73.

Knorz, M.C., Claessens, D., Schaefer, R.C., Seiberth, V. & Liesenhoff, H. (1993). Evaluation of contrast acuity and defocus curve in bifocal and monofocal intraocular lenses. *J Cataract Refract Surg*. **19,** 513-23.

Koch, D.D. & Wang, L. (2007). Custom optimization of intraocular lens asphericity. *Transactions of the American Ophthalmological Society*. **105,** 36-41.

Kohnen, T., Allen, D., Boureau, C., Dublineau, P., Hartmann, C., Mehdorn, E., Rozot, P., Tassinari, G. (2006). European multicenter study of the AcrySof ReSTOR apodized diffractive intraocular lens. *Ophthalmology*. **113,** 584-9.

Kohnen, T., Klaproth, O.K., Bühren, J. (2009). Effect of intraocular lens asphericity on quality of vision after cataract removal: an intraindividual comparison. *Ophthalmology*. **116,** 1697-706.

Kohnen, T., Nuijts, R., Levy, P., Haefliger, E., Alfonso, J.F. (2009). Visual function after bilateral implantation of apodized diffractive aspheric multifocal intraocular lenses with a +3.0 D addition. *J Cataract Refract Surg*. **35,** 2062-9.

Koretz, J.E., Strenk, S.A., Strenk, L.M. & Semmlow, J.L. (2004). Scheimpflug and high-resolution magnetic resonance imaging of the anterior segment: a comparative study. *J Opt Soc Am*. **21,** 346-54.

Krag, S. & Andreassen, T.T. (2003). Biomechanical characteristics of the human anterior lens capsuale in relation to age. *Invest Ophthalmol Vis Sci*. **38,** 357-363.

Kupersmith, M.J., Speira, R., Langer, R., Richmond, M., Peterson, M., Speira, H., Mitnick, H., Paget, S. (2001). Visual function and quality of life among patients with giant cell (temporal) arteritis. *J Neuroophthalmol*. **21,** 266-73.

Lackner, B., Pieh, S., Schmidinger, G., Hanselmayer, G., Simader, C., Reitner, A. & Skorpik, C. (2003). Glare and halo phenomena after laser in situ keratomileusis. *J Cataract Refract Surg*. **29,** 444-50.

Lacmanović-Loncar, V., Pavicić-Astalos, J., Petric-Vicković, I., Mandić, Z., (2008). Multifocal intraocular "mix and match" lenses. *Acta clinica Croatica*. **47,** 217-20.

Lam, A.K.C., Chan, R. & Chiu, R. (2004). Effect of instrument rotation on handheld keratometry. *J Cataract Refract Surg*. **30,** 2590-4.

Lan, J., Huang, Y. & Xie, L. (2009). [Clinical observation of visual performance in patients with a apodized diffractive multifocal intraocular lens]. *Zhonghua Yan Ke Za Zhi*. **45,** 122-6.

Lang, A.J., Lakshminarayanan, V. & Portney, V. (1993). Phenomenological model for interpreting the clinical significance of the in vitro optical transfer function. *J Optical Soc Am*. **10,** 1600-10.

Langenbucher, A., Huber, S., Nguyen, N.X., Seitz, B., Gusek-Schneider, G.C., Küchle, M. (2003). Measurement of accommodation after implantation of an accommodating posterior chamber intraocular lens. *J Cataract Refract Surg*. **29,** 677-85.

Laurendeau, C., Lafuma, A. & Berdeaux, G. (2009). Modelling lifetime cost consequences of toric compared with standard IOLs in cataract surgery of astigmatic patients in four European countries. *J Med Econ*. **12,** 230-7.

Lee, J.E., Fos, P.J., Sung, J.H., Amy, B.W., Zuniga, M.A., Lee, W.J. & Kim, J.C. (2005). Relationship of cataract symptoms of preoperative patients and vision-related quality of life. *Quality of life research.* **14,** 1845-53.

Lee, H.K., Choe, C.M., Ma, K.T. & Kim, E.K. (2006). Measurement of contrast sensitivity and glare under mesopic and photopic conditions following wavefront-guided and conventional LASIK surgery. *J Refract Surg*. **22,** 647-55.

Lee, J.H., You, Y.S., Choe, C.M. & Lee, E.S. (2008). Efficacy of brimonidine tartrate 0.2% ophthalmic solution in reducing halos after laser in situ keratomileusis. *J Cataract Refract Surg*. **34,** 963-7.

Legeais, J.M., Werner, L., Werner, L., Abenhaim, A. & Renard G. (1999). Pseudoaccommodation: BioComFold versus a foldable silicone intraocular lens. *J Cataract Refract Surg*. **25,** 262-7.

Legge, G.E., Mullen, K.T., Woo, G.C., CAMPBELL, F.W. (1987a). Tolerance to visual defocus. *J Optical Soc Am*. **4,** 851-63.

Legge, G.E., Rubin, G.S. & Luebker, A. (1987b). Psycophysics of reading 5. The role of contrast in normal vision. *Vision Res*. **27,** 1165-1177.

Legge, G.E., Ross, J.A., Luebker, A. & LaMay, J.M. (1989). Psychophysics of reading 8. The Minnesota Low-Vision Reading Test. *Optom Vis Sci*. **66,** 843-53.

Legge, G.E. (2007). Visual Mechanisms in Reading. IN: *Psychophysics of reading in normal and low vision*. New Jersey, USA, Lawrence Erlbaum Associates Inc. 43-67.

Lesueur, L., Gajan, B., Nardin, M., Chapotot, E. & Arne, J.L. (2000). [Comparison of visual results and quality of vision between two multifocal intraocular lenses. Multifocal silicone and bifocal PMMA]. *J français d'ophtalmologie*. **23,** 355-9.

Lévy, P., Elies, D., Dithmer, O., Gil-Campos, I., Benmedjahed, K., Berdeaux, G. & Arnould, B. (2010). Development of a new subjective questionnaire: the Freedom from Glasses Value Scale (FGVS). *J Refract Surg*. **26,** 438-46.

Leyland, M.D., Zinicola, E., Bloom, P. & Lee, N. (2001). Prospective evaluation of a plate haptic toric intraocular lens. *Eye*. **15,** 202–205.

Leyland, M.D., Langan, L., Goolfee, F., Lee, N., Bloom, P.A. (2002). Prospective randomised double-masked trial of bilateral multifocal, bifocal or monofocal intraocular lenses. *Eye*. **16,** 481-90.

Leyland, M. & Zinicola, E. (2003). Multifocal versus monofocal intraocular lenses in cataract surgery: a systematic review. *Ophthalmology*. **110,** 1789-98.

Liekfeld, A., Walkow, T., Anders, N., Pham, D.T. & Wollensak, J. (1998). [Prospective comparison of 2 multi-focal lens models]. *Der Ophthalmologe*. *95,* 253-6.

Liekfeld, A., Torun, N. & Friederici, L. (2010). [A new toric diffractive multifocal lens for refractive surgery.]. *Der Ophthalmologe*. **107,** 258-61.

Likert, R. (1932). A technique for the measurement of attitudes. *Arch Psychol*. **22,** 1-55.

Lim, S.J., Kang, S.J., Kim, H.B. & Apple, D.J. (1998a). Ideal size of an intraocular lens for capsular bag fixation. *J Cataract Refract Surg*. **24,** 397–402.

Lim, S.J., Kang, S.J., Kim, H.B., Kurata, Y., Sakabe, I. & Apple, D.J. (1998b). Analysis of zonular-free zone and lens size in relation to axial length of eye with age. *J Cataract Refract Surg*. **24,** 390–396.

Liu, Z., Huang, A.J. & Pflugfelder, S.C. (1999). Evaluation of corneal thickness and topography in normal eyes using the Orbscan corneal topography system. *Br J Ophthalmol*. **83,** 774-8.

Lloyd, I.C., Goss-Sampson, M., Jeffrey, B.G., Kriss, A., Russell-Eggitt, I. & Taylor, D. (1992) Neonatal cataract: aetiology, pathogenesis and management. *Eye*. **6,** 184-96

Lubiński, W., Gronkowska, J., Barnyk, K., Szych, Z. & Karczewicz, D. (2007). Visual function and complications after cataract surgery with bilateral multifocal intraocular lens implantation. *Klinika oczna*. **109,** 261-6.

Lubiński, W., Gronkowska-Serafin, J., Podboraczyńska-Jodko, K. & Karczewicz, D. (2009). Cataract surgery with bilateral multifocal ReZoom intraocular lens implantation--comparison of 3 and 12 month follow-up. *Klinika oczna*. **111,** 327-31.

Ludwig, K., Wegscheider, E., Hoops, J.P. & Kampik, A. (1999). In vivo imaging of the human zonular apparatus with high-resolution ultrasound biomicroscopy. *Graefes Arch Clin Exp Ophthalmol*. **237,** 361-71

Ma, J.J.K. & Tseng, S.S. (2008). Simple method for accurate alignment in toric phakic and aphakic intraocular lens implantation. *J Cataract Refract Surg*. **34,** 1631–1636.

Maaijwee, K., Mulder, P., Radner, W., van Meurs, J.C. (2008). Reliability testing of the Dutch version of the Radner Reading Charts. *Optom Vis Sci*. **85,** 353-8.

Mallinson, T., Stelmack, J., Velozo, C. (2004). A comparison of the separation ratio and coefficient alpha in the creation of minimum item sets. *Medical care*. **42,** I17-24.

Mamalis, N., Omar, O., Veiga, J., Tanner, D., Pirayesh, A. & Fernquist, D.S. (1996). Comparison of two plate-haptic intraocular lenses in a rabbit model. *J Cataract Refract Surg*. **22,** 1291-5.

Mamalis, N., Omar, O., Veiga, J., Tanner, D., Pirayesh, A., Fernquist, D.S. (1998). Comparison of two plate-haptic intraocular lenses in a rabbit model. *J Cataract Refract Surg*. **22,** 1291–1295.

Mamalis, N., Brubaker, J., Davis, D., Espandar, L. & Werner, L. (2008). Complications of foldable intraocular lenses requiring explantation or secondary intervention--2007 survey update. *J Cataract Refract Surg*. **34,** 1584-91.

Mangione, C.M., Phillips, R.S., Seddon, J.M., Lawrence, M.G., Cook, E.F., Dailey, R. & Goldman, L. (1992). Development of the 'Activities of Daily Vision Scale'. A measure of visual functional status. *Medical care*. **30,** 1111-26.

Mansfield, J.S., Ahn, S.J., Legge, G.E. & Luebker, A. (1993). A New Reading-Acuity Chart for Normal and Low Vision Ophthalmic and Visual Optics/ Noninvasive Assessment of the Visual System. *Technical Digest (Opt Soc Am)*. **3,** 232-235.

Marcos, S., Moreno, E. & Navarro, R. (1999). The depth-of-field of the human eye from objective and subjective measurements. *Vision Res*. **39,** 2039-49.

Maxwell, W.A., Cionni, R.J., Lehmann, R.P. & Modi, S.S. (2009). Functional outcomes after bilateral implantation of apodized diffractive aspheric acrylic intraocular lenses with a +3.0 or +4.0 diopter addition power Randomized multicenter clinical study. *J Cataract Refract Surg.* **35,** 2054-61.

Mayer, S., T Böhm, H Häberle, D-T Pham, C Wirbelauer. (2008). [Combined implantation of monofocal and multifocal intraocular lenses for presbyopia correction in cataract patients]. *Klinische Monatsblätter für Augenheilkunde.* **225,** 812-7.

McAlinden, C., Pesudovs, K. & Moore, J.E. (2010). The development of an instrument to measure quality of vision; the Quality of Vision (QoV) questionnaire. *Invest Ophthalmol Vis Sci.* doi: 10.1167 [Epub ahead of print].

McLeod, S.D., Portney, V., Ting, A. (2003). A dual optic accommodating foldable intraocular lens. *Br J Ophthalmol.* **87,** 1083-5.

McLeod, S.D., Vargas, L.G., Portney, V. & Ting, A. (2007). Synchrony dual-optic accommodating intraocular lens. Part 1: optical and biomechanical principles and design considerations. *J Cataract Refract Surg.* **33,** 37-46.

McMullan, T.F.W., Goldsmith, C. & Illingworth, C.D. (2007). Toric posterior chamber (in-the-bag) intraocular lens implantation to correct postpenetrating keratoplasty astigmatism. *Eye.* **21,** 150–152.

Mejía-Barbosa, Y. & Malacara-Hernández, D. (2001). A review of methods for measuring corneal topography. *Optom Vis Sci.* **78,** 240-53.

Mendicute, J., Irigoyen, C., Aramberri, J., Ondarra, A. & Montés-Micó, R. (2008). Foldable toric intraocular lens for astigmatism correction in cataract patients. *J Cartaract Refract Surg.* **34,** 601-7.

Mendicute, J., Irigoyen, C., Ruiz, M., Illarramendi, I., Ferrer-Blasco, T. & Montés-Micó, R. (2009). Toric intraocular lens versus opposite clear corneal incisions to correct astigmatism in eyes having cataract surgery. *J Cataract Refract Surg.* **35,** 451–458.

Mester, U., Dillinger, P., Anterist, N. & Kaymak, H. (2005). [Functional results with two multifocal intraocular lenses (MIOL). Array SA40 versus Acri.Twin]. *Der Ophthalmologe.* **102,** 1051-6.

Mester, U., Hunold, W., Wesendahl, T. & Kaymak, H. (2007). Functional outcomes after implantation of Tecnis ZM900 and Array SA40 multifocal intraocular lenses. *J Cataract Refract Surg.* **33,** 1033-40.

Mester, U., Sauer, T. & Kaymak, H. (2009). Decentration and tilt of a single-piece aspheric intraocular lens compared with the lens position in young phakic eyes. *J Cataract Refract Surg.* **35,** 485-90.

Michael, R., van Rijn, L.J., van den Berg, T.J.T.P., Barraquer, R.I., Grabner, G., Wilhelm, H., Coeckelbergh, T., Emesz, M., Marvan, P. & Nischler, C. (2009). Association of lens opacities, intraocular straylight, contrast sensitivity and visual acuity in European drivers. *Acta ophthalmologica.* **87,** 666-71.

Miller, D. (1991). Optics and Contrast: Questions Connected with the Bifocal IOL. IN: Maxwell, A. & Nordan, L.T. *Current Concepts of Multifocal Intraocular Lens.* Phoenixville, USA, Thorofare. 53-66.

Millodot, M. (2002). Cataract. IN: *Dictionary of Optometry and Visual Science*. 7th ed. London. Butterworth Heinemann Inc. 52-54

Millodot, M. (2002). Vision. IN: *Dictionary of Optometry and Visual Science*. 7th ed. London. Butterworth Heinemann Inc. 401-402.

Mitchell, P., Cumming, R. G., Attebo, K. and Panchapakesan, J. (1997). Prevalence of cataract in Australia: the Blue Mountains eye study. *Ophthalmology*. **104,** 581-8.

Moghimi, S., Esfahani, M.R. & Maghsoudipour, M. (2007). Visual function after implantation of aniridia intraocular lens for traumatic aniridia in vitrectomized eye. *European J Ophthalmol*. **17,** 660-5.

Mönestam, E. & Wachtmeister, L. (1997). The impact of cataract surgery on low vision patients. A population based study. *Acta Ophthalmol Scand*. **75,** 569-76.

Montés-Micó, R., España, E., Bueno, I., Charman, W.N., Menezo, J.L. (2004). Visual performance with multifocal intraocular lenses: mesopic contrast sensitivity under distance and near conditions. *Ophthalmology*. **111,** 85-96.

Muñoz, G., Albarrán-Diego, C. & Sakla, H.F. (2007). Validity of autorefraction after cataract surgery with multifocal ReZoom intraocular lens implantation. *J Cataract Refract Surg*. *33,* 1573-8.

Murray, A., Lawrence, G.P. & Clayton. R.H. (1991). Repeatability of dynamic eye pupil response measurement using the Pupilscan instrument. *Clin Phys Physiol Meas*. **12,** 377-385.

Mutti, D.O., Zadnik, K. & Adams, A.J. (1992). A video technique for phakometry of the human crystalline lens. *Invest Ophthalmol Vis Sci*. **33,** 1771-82.

Mutti, D.O., Zadnik, K. & Adams, A.J. (1995). The equivalent refractive index of the crystalline lens in childhood. *Vis Research*. **35,** 1565-73.

Myers, T.D. & Olson, R.J. (1999). Comparison of the effects of viscoelastic agents on clinical properties of the Unfolder lens injection system. *J Cataract Refract Surg*. **25,** 953-8.

Namiki, M. & Tagami, Y. (1993). [Perimetric glare test and evaluation of intraocular lenses]. *Nippon Ganka Gakkai Zasshi*. **97,** 210-6.

Narendran, R., Vyas, A. & Bacon, P. (2009). Centration, rotational stability and outcomes of Rayner T-flexTM toric lens implantation: 2 year results. Proceedings of the XXVII congress of the ESCRS, Barcelona.

Navas, A. & Suárez, R. (2009). One-year follow-up of toric intraocular lens implantation in forme fruste keratoconus. *J Cataract Refract Surg*. **35,** 2024–2047.

Negishi, K., Nagamoto, T., Hara, E., Kurosaka, D. & Bissen-Miyajima H. (1996). Clinical evaluation of a five-zone refractive multifocal intraocular lens. *J Cataract Refract Surg*. **22,** 110-5.

Negishi, K., Bissen-Miyajima, H., Kato, K., Kurosaka, D. & Nagamoto, T. (1997). Evaluation of a zonal-progressive multifocal intraocular lens. *Am J Ophthalmol*. **124,** 321-30.

Negishi, K., Ohnuma, K., Ikeda, T. & Noda, T. (2005). Visual simulation of retinal images through a decentered monofocal and a refractive multifocal intraocular lens. *Jpn J Ophthalmol*. **49,** 281-6.

Nemeth, J., Fekete, O. & Pesztenlehrer, N. (2003). Optical and ultrasound measurement of axial length and anterior chamber depth for intraocular lens power calculation. *J Cataract Refract Surg.* **29,** 85–8.

Nguyen, T.M. & Miller, K.M. (2000). Digital overlay technique for documenting toric intraocular lens axis orientation. *J Cataract Refract Surg.* **26,** 1496–1504.

Nichols, J.J., Mitchell, G.L., Saracino, M. & Zadnik, K. (2003). Reliability and validity of refractive error-specific quality-of-life instruments. *Arch Ophthalmol.* **121,** 1289-96.

Nichols, J.J., Twa, M.D., Mitchell, G.L. (2005). Sensitivity of the National Eye Institute Refractive Error Quality of Life instrument to refractive surgery outcomes. *J Cataract Refract Surg.* **31,** 2313-8.

Nijkamp, M.D., Dolders, M.G.T., de Brabander, J., van den Borne, B., Hendrikse, F. & Nuijts, R.M.M.A. (2004). Effectiveness of multifocal intraocular lenses to correct presbyopia after cataract surgery: a randomized controlled trial *Ophthalmology.* **111,** 1832-9.

Ninn-Pedersen, K., Stenevi, U. & Ehinger, B. (1994). Cataract patients in a defined Swedish population 1986-1990. II. Preoperative observations. *Acta Ophthalmologica.* **72,** 10-5.

Nishi, Y., Hirnschall, N., Crnej, A., Gangwani, V., Tabernero, J., Artal, P. & Findl, O. (2010). Reproducibility of intraocular lens decentration and tilt measurement using a clinical Purkinje meter. *J Cataract Refract Surg.* **36,** 1529-35.

Nishimoto, H., Shimizu, K., Ishikawa, H. & Uozato, H. (2007). New approach for treating vertical strabismus: decentered intraocular lenses. *J Cataract Refract Surg.* **33,** 993-8.

Nordan, L.T. (1991). The Nordan Aspheric Multifocal Intraocular Lens – Concepts and Current Status. IN: Maxwell, A. & Nordan, L.T. *Current Concepts of Multifocal Intraocular Lenses.* Phoenixville, USA, Slack Inc. 117-126.

Norn, M. & Jensen, O.A. (2004). Marius Tscherning (1854-1939): his life and work in optical physiology. *Acta Ophthalmol Scand.* **82,** 501-8.

Norrby, S. (2008). Sources of error in intraocular lens power calculation. *J Cataract Refract Surg.* **34,** 368-76.

Novis, C. (2000). Astigmatism and toric intraocular lenses. *Curr Opin Ophthalmol.* **11,** 47-50.

Nygaard, R.W., Echt, K.V. & Schuchard, R.A. (2008). Models of reading performance in older adults with normal age-related vision. *J Rehab Res Devel.* **45,** 901-10.

Ohmi, S. (1993). Decentration associated with asymmetric capsular shrinkage and intraocular lens size. *J Cataract Refract Surg.* **19,** 640-3.

Ohtani, S., Gekka, S., Honbou, M., Kataoka, Y., Minami, K., Miyata, K. & Oshika, T. (2009). One-year prospective intrapatient comparison of aspherical and spherical intraocular lenses in patients with bilateral cataract. *Am J Ophthalmol.* **147,** 984-9.

Olaru, G., Gavriş, M., Horge, I., Marian, N., Popa, D., Levai, L., Ghindea, C. & Bran, L. (2008). [Toric intraocular lens implantation in cataract patients--6 months results]. *Oftalmologia.* **52,** 100-4.

Olsen, T. & Corydon, L. (1990). Contrast sensitivity as a function of focus in patients with the diffractive multifocal intraocular lens. *J Cataract Refract Surg.* **16,** 703-6.

Ogle, K.N. & Madigan, L.F. (1945). Astigmatism at oblique axes and binocular stereoscopic spatial localization. *Arch Ophthalmol.* **33,** 116-127.

Osher, R.H. (2009). Deliberate use of unequal adds with aspheric ReSTOR intraocular lens. *J Cataract Refract Surg.* **35,** 1646.

Osher, R.H. (2010). Iris fingerprinting: new method for improving accuracy in toric lens orientation. *J Cataract Refract Surg.* **36,** 351-2.

Oshika, T., Nagata, T. & Ishii, Y. (1998). Adhesion of lens capsule to intraocular lenses of polymethylmethacrylate, silicone and acrylic foldable materials: an experimental study. *Br J Ophthalmol.* **82,** 549–553.

Oshika, T., Sugita, G., Miyata, K.,Tokunaga, T., Samejima, T., Okamoto, C., Ishii, Y. (2007). Influence of tilt and decentration of scleral-sutured intraocular lens on ocular higher-order wavefront aberration. *Br J Ophthalmol.* **91,** 185-8.

Ossma, I.L., Galvis, A., Vargas, L.G., Trager, M.J., Vagefi, M.R. & McLeod, S.D. (2007). Synchrony dual-optic accommodating intraocular lens. Part 2: pilot clinical evaluation. *J Cataract Refract Surg.* **33,** 47-52.

Ostrin, L.A. & Glasser, A. (2007). Edinger-Westphal and pharmacologically stimulated accommodative refractive changes and lens and ciliary process movements in rhesus monkeys. *Exp Eye Res.* **84,** 302-13.

Ozawa, S., Sugiyama, Y., Mitsuhashi, J. & Inaba, M. (1989). Kinetic analysis of cell killing effect induced by cytosine arabinoside and cisplatin in relation to cell cycle phase specificity in human colon cancer and Chinese hamster cells. *Cancer Res.* **49,** 3823-8.

Packer, M., Fine, I.H. & Hoffman, R.S. (2002). Immersion A-scan compared with partial coherence interferometry—outcomes analysis. *J Cataract Refract Surg.* **28,** 239–42.

Packer, M., Chu, Y.R., Waltz, K.L., Donnenfeld, E.D., Wallace, R.B., Featherstone, K., Smith, P., Bentow, S.S. & Tarantino, N. (2010). Evaluation of the Aspheric Tecnis Multifocal Intraocular Lens: One-Year Results from the First Cohort of the Food and Drug Administration Clinical Trial. *Am J Ophthalmol.* **149,** 577-584.

Packer, M., Fine, I.H. & Hoffman, R.S. (2009). Aspheric intraocular lens selection based on corneal wavefront. *J Refract Surg.* **25,** 12-20.

Palmer, A.M., Faiña, P.G., Albelda, A.E., Serrano, M.C., Saad, D.N. & Céspedes, M.C. (2008). Visual function with bilateral implantation of monofocal and multifocal intraocular lenses: a prospective, randomized, controlled clinical trial. *J Refract Surg.* **24,** 257-64.

Pardue, M.T & Sivak, J.G. (2000). Age-related changes in human ciliary muscle *Optom Vis Sci.* **77,** 204-10.

Parravano, M., Oddone, F., Sampalmieri, M. & Gazzaniga, D. (2007). Reliability of the IOLMaster in axial length evaluation in silicone oil-filled eyes. *Eye.* **21,** 909–11.

Pärssinen, O., Räty, J., Vainikainen, J., Timonen, J. & Lyyra, A.L. (1998). Compression forces of haptics of freely rotating posterior chamber intraocular lenses. *J Cataract Refract Surg.* **24,** 415–425.

Patel, C.K., Ormonde, S., Rosen, P.H. & Bron, A.J. (1999). Postoperative intraocular lens rotation: a randomized comparison of plate and loop haptic implants. *Ophthalmology.* **106,** 2190–2195.

Peckar, C. (1991). Extracapsular techniques. IN: Percival, S.P. *A Colour atlas of lens implantation.* Aylesbury, UK, Wolfe Publishing Ltd. 27-32.

Pepose, J.S., Qazi, M.A., Davies, J., Doane, J.F., Loden, J.C., Sivalingham, V. & Mahmoud, A.M. (2007). Visual performance of patients with bilateral vs combination Crystalens, ReZoom, and ReSTOR intraocular lens implants. *Am J Ophthalmol.* **144,** 347-357.

Pérez, A.L., Muñoz, L.A., Gimeno, J.A.S., Jorge, M.A.M. & Rahhal M.S. (2003). [Comparative clinical study of visual results between two different types of bifocal intraocular lenses]. *Arch Soc Esp Oftalmol.* **78,** 665-73.

Pérez, G.A., Archer, S.M. & Artal, P. (2010). Optical characterization of Bangerter foils. *Invest Ophthalmol Vis Sci.* **51,** 609-13.

Pérez-Torregrosa, V.T., Menezo, J.L., Harto, M.A. & Maldonado, M.J. & Cisneros, A. (1995). Digital system measurement of decentration of Worst-Fechner iris claw myopia intraocular lens. *J Refract Surg.* **11,** 26-30.

Percival, S.P. (1989). Prospective study of the new diffractive bifocal intraocular lens *Eye.* **3,** 571-5.

Percival, S.P. (1990). Indications for the multizone bifocal implant. *J Cataract Refract Surg.* **16,** 193-7.

Percival, S.P. & Setty, S.S. (1991). Comparative analysis of three prospective trials of multifocal implants. *Eye.* **5,** 712-6.

Percival, S.P. (1992). An update on multifocal lens implants. *Doc ophthalmologica.* **81,** 285-92

Percival, S.P. & Setty, S.S. (1993). Prospectively randomized trial comparing the pseudoaccommodation of the AMO ARRAY multifocal lens and a monofocal lens. *J Cataract Refract Surg.* 19, 26-31.

Pereira, F., Milverton, E., Coroneo, M. (2010). Miyake-Apple study of the rotational stability of the Acrysof toric intraocular lens after experimental eye trauma. *Eye.* **24,** 376–378.

Pesudovs, K. & Coster, D.J. (1998). An instrument for assessment of subjective visual disability in cataract patients. *Br J Ophthalmol.* **82,** 617-24.

Pesudovs, K., Garamendi, E., Keeves, J.P. & Elliott, D.B. (2003). The Activities of Daily Vision Scale for cataract surgery outcomes: re-evaluating validity with Rasch analysis. *Invest Ophthalmol Vis Sci*. **44,** 2892-9.

Petermeier, K. & Szurman, P. (2007). [Subjective and objective outcome following implantation of the apodized diffractive AcrySof ReSTOR]. *Der Ophthalmologe*, **104,** 399-404.

Petermeier, K., Gekeler, F., Spitzer, M.S. & Szurman, P. (2009). Implantation of the multifocal ReSTOR apodised diffractive intraocular lens in adult anisometropic patients with mild to moderate amblyopia. *Br J Ophthalmol*. **93,** 1296-301.

Pick, Z.S., Leaming, D.V. & Elder, M.J. (2008). The fourth New Zealand cataract and refractive surgery survey: 2007. *Clin Experiment Ophthalmol.* **36,** 604–619.

Pieh, S., Weghaupt, H. & Skorpik, C. (1998). Contrast sensitivity and glare disability with diffractive and refractive multifocal intraocular lenses. *J Cataract Refract Surg.* **24,** 659-62.

Pieh, S., Lackner, B., Hanselmayer, G., Zöhrer, R., Sticker, M., Weghaupt, H., Fercher, A. & Skorpik, C. (2001a). Halo size under distance and near conditions in refractive multifocal intraocular lenses. *Br J Ophthalmol.* **85,** 816-21.

Pieh, S., Hanselmayer, G., Lackner, B., Marvan, P., Grechenig, A., Weghaupt, H., Vass, C. & Skorpik, C. (2001b). Tritan colour contrast sensitivity function in refractive multifocal intraocular lenses. *Br J Ophthalmol.* **85,** 811-5.

Pieh, S., Kellner, C., Hanselmayer, G., Lackner, B., Schmidinger, G., Walkow, T., Sticker, M., Weghaupt, H., Fercher, A.F. & Skorpik, C. (2002). Comparison of visual acuities at different distances and defocus curves. *J Cataract Refract Surg.* **28,** 1964-7.

Pieh, S., Marvan, P., Lackner, B., Hanselmayer, G., Schmidinger, G., Leitgeb, R., Sticker, M., Hitzenberger, C.K., Fercher, A.F. & Skorpik, C. (2002). Quantitative performance of bifocal and multifocal intraocular lenses in a model eye: point spread function in multifocal intraocular lenses. *Arch Ophthalmol.* **120,** 23-8.

Pierscionek, B.K. & Chan, D.Y. (1989). Refractive index gradient of human lenses. *Optom Vis Sci.* **66,** 822-9.

Pierscionek, B.K. and Weale, R.A. (1995). The optics of the eye-lens and lenticular senescence. A review. *Doc Ophthalmol,* **89,** 321-35.

Post, C.T. (1992). Comparison of depth of focus and low-contrast acuities for monofocal versus multifocal intraocular lens patients at 1 year. *Ophthalmology.* **99,** 1658-63; discussion 1663-4.

Prieto, L., Alonso, J. & Lamarca, R. (2003). Classical Test Theory versus Rasch analysis for quality of life questionnaire reduction. *Health Qual Life Outcomes.* **1,** 27.

Raasch, T.W., Bailey, I.L. & Bullimore, M.A. (1998). Repeatability of visual acuity measurement. *Optom Vis Sci.* **75,** 342-8.

Rabbetts, R.B. (2007). General Introduction. IN: *Bennett & Rabbetts Clinical Visual Optics.* 4th ed. London. Butterworth-Heinemann Inc. 1-19.

Rabsilber, T.M., Jepsen, C., Auffarth, G.U. & Holzer, M.P. (2010). Intraocular lens power calculation: clinical comparison of 2 optical biometry devices. *J Cataract Refract Surg.* **36,** 230-4.

Radner, W., Willinger, U., Obermayer, W., Mudrich, C., Velikay-Parel, M., Eisenwort, B. (1998). [A new reading chart for simultaneous determination of reading vision and reading speed]. *Klinische Monatsblätter für Augenheilkunde.* **213,** 174-81.

Raj, P.S., Ilango, B. & Watson, A. (1998). Measurement of axial length in the calculation of intraocular lens power. *Eye.* **12,** 227–9.

Rasch, G. (1961). On general laws and the meaning of measurment in psychology *Proceedings of the Fourth Berkeley Symposium on Mathematical Statistics and*

Probability, IV. Berkeley, California: University of California press. Available free from Project Euclid. 321-334.

Rau, M. & Bach, C. (2003). [Initial results obtained with the multifocal lens MF4]. *Klinische Monatsblätter für Augenheilkunde*. **220,** 24-8.

Ravalico, G., Parentin, F., Sirotti, P. & Baccara, F. (1998). Analysis of light energy distribution by multifocal intraocular lenses through an experimental optical model. *J Cataract Refract Surg.* **24,** 647-52.

Renieri, G., Kurz, S., Schneider, A. & Eisenmann, D. (2007). ReSTOR diffractive versus Array 2 zonal-progressive multifocal intraocular lens: a contralateral comparison. *European J Ophthalmol.* **17,** 720-8.

Retzlaff JA, Sanders DR, Kraff MC. (1990). Development of the SRK/T intraocular lens implant power calculation formula. *J Cataract Refract Surg.* **16,** 333–340; correction, 528

Reuland, M.S., Reuland, A.J., Nishi, Y. & Auffarth, G.U. (2007). Corneal radii and anterior chamber depth measurements using the IOLmaster versus the Pentacam. *J Refract Surg.* **23,** 368-73.

Rice, M.L., Birch, E.E. & Holmes, J.M. (2005). An abbreviated reading speed test. *Optom Vis Sci.* **82,** 128-33.

Richter-Mueksch, S., Weghaupt, H., Skorpik, C., Velikay-Parel, M. & Radner, W. (2002). Reading performance with a refractive multifocal and a diffractive bifocal intraocular lens. *J Cataract Refract Surg.* **28,** 1957-63.

Ridley, H. (1952). Intra-ocular acrylic lenses after cataract extraction. *Lancet.* **1,** 118-21.

Rohen, J.W. (1979). Scanning electron microscopic studies of the zonular apparatus in human and monkey eyes. *Invest Ophthalmol Vis Sci.* **18**, 133–144.

Rohrer, K., Frueh, B.E., Wälti, R., Clemetson, I.A., Tappeiner, C. & Goldblum, D. (2009). Comparison and evaluation of ocular biometry using a new noncontact optical low-coherence reflectometer. *Ophthalmology*. **116,** 2087-92.

Rosales, P. & Marcos, S. (2006). Phakometry and lens tilt and decentration using a custom-developed Purkinje imaging apparatus: validation and measurements. *J Opt Soc Am.* **23,** 509-20.

Rosales, P., de Castro, A., Jiménez-Alfaro, I. & Marcos, S. (2010). Intraocular lens alignment from Purkinje and Scheimpflug imaging. *Clin Exp Optom.* **93,** 400-8

Rose, L.T. & Moshegov, C.N. (2003). Comparision of the Zeiss IOLMaster and applanation A-scan Ultrasound: biometry for intraocular lens calculation. *Clin Exp Ophthalmol*. **31,** 121-124.

Rossetti, l., Carraro, F., Rovati, M. & Orzalesi, N. (1994). Performance of diffractive multifocal intraocular lenses in extracapsular cataract surgery. *J Cataract Refract Surg*. **20,** 124-8.

Ruhswurm, I., Scholz, U., Zehetmayer, M., Hanselmayer, G., Vass, C., Skorpik, C. (2000). Astigmatism correction with a foldable toric intraocular lens in cataract patients. *J Cataract Refract Surg.* **26**, 1022–1027.

Ruíz-Mesa, R., Carrasco-Sánchez, D., Díaz-Alvarez, S.B., Ruíz-Mateos, M.A., Ferrer-Blasco, T. & Montés-Micó, R. (2009). Refractive lens exchange with foldable toric intraocular lens. *Am J Ophthalmol*. **147,** 990-6.

Runge, C., (1901). Über empirische Funktionen und die Interpolation zwischen äquidistanten Ordinaten. *Zeitschrift für Mathematik und Physik* **46,** 224–243. available at www.archive.org

Rüther, K., Eisenmann, D., Zrenner, E., Jacobi, K.W. (1994). [Effect of diffractive multi-focal lenses on contrast vision, glare sensitivity and color vision]. *Klinische Monatsblätter für Augenheilkunde*. **204,** 14-9.

Salati, C., Salvetat, M.L., Zeppieri, M. & Brusini, P. (2007). Pupil size influence on the intraocular performance of the multifocal AMO-Array intraocular lens in elderly patients. *European J Ophthalmol*. **17,** 571-8.

Sanders, D.R. & Sanders, M.L. (2010). FDA Clinical Trial of the Tetraflex Potentially Accommodating IOL: Comparison to Concurrent Age-Matched Monofocal Controls. *J Refract Surg*. **26,** 723-30.

Santodomingo-Rubido, J., Mallen, E.A.H., Gilmartin, B., Wolffsohn, J.S. (2002). A new non-contact optical device for ocular biometry. *Br J Ophthalmol*. **86,** 458-62.

Sasaki, K., Sakamoto, K., Shibata, T., Nakaizumi, H., Emori, Y. (1989). Measurement of postoperative intraocular lens tilting and decentration using Scheimpflug images. *J Cataract Refract Surg*. **15,** 454-7.

Sasaki, A. (2000). Initial experience with a refractive multifocal intraocular lens in a Japanese population. *J Cataract Refract Surg*. **26,** 1001-7.

Savini, G., Barboni, P., Carbonelli, M., Hoffer, K.J. (2009). Agreement between Pentacam and videokeratography in corneal power assessment. *J Refract Surg*. **25,** 534-8.

Schachar, R.A. (2006). The mechanism of accommodation and presbyopia. *Int Ophthalmol Clin*. **46,** 39-61.

Schachar, R.A., Tello, C., Cudmore, D.P., Liebmann, J.M., Black, T.D. & Ritch, R. (1996). In vivo increase of the human lens equatorial diameter during accommodation. *Am J Physiol*. **271,** 670-6.

Scheffel, M., Kuehne, C. & Kohnen, T. (2010). Comparison of monocular and binocular infrared pupillometers under mesopic lighting conditions. *J Cataract Refract Surg*. **36,** 625-30.

Schmidinger, G., Geitzenauer, W., Hahsle, B., Klemen, U., Skorpik, C., Pieh, S. (2006). Depth of focus in eyes with diffractive bifocal and refractive multifocal intraocular lenses. *J Cataract Refract Surgery*. **32,** 1650-6.

Schmidt, F.U., Häring, G., Rochels, R. (1994). [Functional results after implantation of Array type refractive multifocal intraocular lenses]. *Der Ophthalmologe*. **91,** 469-72.

Schmitz, S., Dick, H.B., Krummenauer, F., Schwenn, O. & Krist, R. (2000). Contrast sensitivity and glare disability by halogen light after monofocal and multifocal lens implantation. *Br J Ophthalmol*. **84,** 1109-12.

Schor, C.M. (2009). Charles F. Prentice award lecture 2008: surgical correction of presbyopia with intraocular lenses designed to accommodate. *Optom Vis Sci*. **86,** 1028-41.

Schwiegerling, J. (2007). Analysis of the optical performance of presbyopia treatments with the defocus transfer function. *J Refract Surg.* **23,** 965-71.

Scott, I.U., Smiddy, W.E., Schiffman, J. Feuer, W.J., Pappas, C.J. (1999). Quality of life of low-vision patients and the impact of low-vision services. *Am J Ophthalmol*. **128,** 54-62.

Sedgewick, J.H., Orillac, R. & Link, C. (2002). Array multifocal intraocular lens in a charity hospital training program: a resident's experience. *J Cataract Refract Surg*. **28,** 1205-10.

Seland, J.H. (1974). Ultrastructural changes in the normal human lens capsule from birth to old age. *Acta ophthalmologica*. **52,** 688-706.

Sen, H.N., Sarikkola, A., Uusitalo, R.J., Laatikainen, L. (2004). Quality of vision after AMO Array multifocal intraocular lens implantation. *J Cataract Refract Surg*. **30,** 2483-93.

Shah GD, Praveen MR, Vasavada AR, Rampal NV, Vasavada VA, Asnani PK, Pandita, D. (2009). Software-based assessment of postoperative rotation of toric intraocular lens. *J Cataract Refract Surg*. **35,** 413–418.

Shen, E.P., Chen, W. & Hu, F. (2010). Manual limbal markings versus iris-registration software for correction of myopic astigmatism by laser in situ keratomileusis. *J Cataract Refract Surg*. **36,** 431-436.

Sheppard, A.L. & Davies, L.N. (2010) In vivo analysis of ciliary muscle morphologic changes with accommodation and axial ametropia. *Invest Ophthalmol Vis Sci.* **51,** 6882-9.

Sheppard, A.L. & Davies, L.N. (2010). The effect of ageing on in vivo human ciliary muscle morphology and contractility. *Invest Ophthalmol Vis Sci*. doi: 10.1167. [Epub ahead of print].

Sherwood, M.B., Garcia-Siekavizza, A., Meltzer, M.I., Hebert, A., Burns, A.F. & McGorray, S. (1998). Glaucoma's impact on quality of life and its relation to clinical indicators. A pilot study. *Ophthalmology*. **105,** 561-6.

Shimizu, K., Misawa, A. & Suzuki, Y. (1994). Toric intraocular lenses: correcting astigmatism while controlling axis shift. *J Cataract Refract Surg*. **20,** 523-6.

Shingleton, B.J., Rosenberg, R.B., Teixeira, R. & O'Donoghue, M.W. (2007). Evaluation of intraocular pressure in the immediate postoperative period after phacoemulsification. *J Cataract Refract Surg*. **33,** 1953–1957.

Shoji, N. & Shimizu, K. (1996). Clinical evaluation of a 5.5 mm three-zone refractive multifocal intraocular lens. *J Cataract Refract Surg*. **22,** 1097-101.

de Silva, D.J., Ramkissoon, Y.D. & Bloom, P.A. (2006). Evaluation of a toric intraocular lens with a Z-haptic. *J Cataract Refract Surg*. **32,** 1492–1498.

Shoji, N. & Shimizu, K. (2002). Binocular function of the patient with the refractive multifocal intraocular lens. *J Cataract Refract Surg*. **28,** 1012-7.

Smith, G. (2003). The optical properties of the crystalline lens and their significance *Clin Exp Optom*. **86,** 3-18.

Snell, R. S. and Lemp, M. A. (1998). The Eyeball. IN: *Clinical Anatomy of the Eye*. 2nd ed. MA, USA, Blackwell Science, Inc. 132-213.

Sorsby, A., Benjamin, B., Sheridan, M., Stone, J. & Leary, G.A. (1961). Refraction and its components during the growth of the eye from the age of three. *Memo Med Res Counc*. **301,** 1-67.

Souza, C.E., Muccioli, E., Soriano, E.S., Chalita, M.R., Oliveira, F., Freitas, L.L., Meire, L.P., Tamaki, C., Belfort, R. (2006). Visual performance of AcrySof ReSTOR apodized diffractive IOL: a prospective comparative trial. *Am J Ophthalmol*. **141,** 827-832.

Sparrow, J.M., Bron, A.J., Brown, N.A., Ayliffe, W. & Hill, A.R. (1986). The Oxford Clinical Cataract Classification and Grading System. *Int Ophthalmol*. **9,** 207-25.

Steinberg, E.P., Tielsch, J.M, Schein, O.D., Javitt, J.C., Sharkey, P., Cassard, S.D., Legro, M.W., Diener-West, M., Bass, E.B., Damiano, A.M. (1994). The VF-14. An index of functional impairment in patients with cataract. *Arch Ophthalmol*. 112, 630-8.

Steinert, R.F., Post, C.T., Brint, S.F., Fritch, C.D., Hall, D.L., Wilder, L.W., Fine, I.H., Lichtenstein, S.B., Masket, S., Casebeer, C. (1992). A prospective, randomized, double-masked comparison of a zonal-progressive multifocal intraocular lens and a monofocal intraocular lens. *Ophthalmology*. **99,** 853-60; discussion 860-1.

Steinert, R.F., Aker, B.L., Trentacost, D.J., Smith, P.J., Tarantino, N. (1996). A prospective comparative study of the AMO ARRAY zonal-progressive multifocal silicone intraocular lens and a monofocal intraocular lens. *Ophthalmology*. 106, 1243-55.

Stelmack, J. Stelmack, T.R., Fraim, M. & Warrington, J. (1987). Clinical use of the Pepper Visual Skills for Reading Test in low vision rehabilitation. *Am J Optom Physiol Optic*. **64,** 829-31.

Stelmack, J., Szlyk, J.P., Stelmack, T., Babcock-Parziale, J., Demers-Turco, P., Williams, R.T. & Massof, R.W. (2004). Use of Rasch person-item map in exploratory data analysis: A clinical perspective. *J Rehabil Res Dev*. **41,** 233-41.

Streiner, D. L. & Norman, G. R. (1995). Selecting the items. IN: *Health measurement scales: A guide to their development and Use*. 2nd Ed. Oxford, Oxford University Press Inc. 54-68.

Strenk, S.A., Semmlow, J.L., Strenk, L.M., Munoz, P., Gronlund-Jacob, J. & Demarco, J.K. (1999). Age related changes in human ciliary muscle and Lens: a magnetic resonance imaging study. *Invest Ophthalmol Vis Sci*. **40,** 1162-1149.

Strenk, S.A., Strenk, L.M. & Koretz, J.F. (2005). The mechanism of presbyopia Prog. *Retin Eye Res*. **24,** 379-93.

Strenk, S.A., Strenk, L.M. & Guo, S. (2006). Magnetic resonance imaging of aging, accommodating, phakic, and pseudophakic ciliary muscle diameters. *J Cataract Refract Surg*. **32,** 1792-8.

Stockman, A. & Sharpe, L.T. (2006). Into the twilight zone: the complexities of mesopic vision and luminous efficiency. *Ophthalmic Physiol Opt*. **26,** 225-39.

Storey, J.K. & Rabie, E.P. (1983). Ultrasound—a research tool in the study of accommodation. *Ophthalmic Physiol Opt*. **3,** 315–20.

Subramanian, A. & Pardhan, S. (2006). The repeatability of MNREAD acuity charts and variability at different test distances. *Optom Vis Sci*. **83,** 572-6.

Subramanian, A. & Pardhan, S. (2009). Repeatability of reading ability indices in subjects with impaired vision. *Invest Ophthalmol Vis Sci.* **50,** 3643-7.

Sun, X.Y., Vicary, D., Montgomery, P. & Griffiths, M. (2000). Toric intraocular lenses for correcting astigmatism in 130 eyes. *Ophthalmology.* **107,** 1776–1781.

Sushmita, S., Kaushik, S. & Kamlesh, S. (2002). A clinical evaluation of an aspheric multifocal intraocular lens and its implications for the developing world. *Ophthalmic Surg Laser.* **33,** 298-303.

Taketani, F., Matuura, T., Yukawa, E., Hara, Y. (2004). Influence of intraocular lens tilt and decentration on wavefront aberrations. *J Cataract Refract Surg.* **30,** 2158-62.

Takimoto, M., Hayashi, K. & Hayashi, H. (2008). Effect of a capsular tension ring on prevention of intraocular lens decentration and tilt and on anterior capsule contraction after cataract surgery. *Jpn J Ophthalmol.* **52,** 363-7.

Tamm, E., Lütjen-Drecoll, E., Jungkunz, W. & Rohen, J.W. (1991). Posterior attachment of ciliary muscle in young, accommodating old, presbyopic monkeys *Investigat Ophthalmol & Vis Sci.* **32,** 1678-92.

Tamm, E.R. & Lütjen-Drecoll, E. (1996). Ciliary body. *Microsc Res Tech,* **33,** 390-439.

Thebpatiphat, N., Hammersmith, K.M., Rapuano, C.J., Ayres, B.D. & Cohen, E.J. (2007). Cataract surgery in keratoconus. *Eye Contact Lens.* 33, 244-6.

Tehrani, M., Stoffelns, B. & Dick, H.B. (2003). Implantation of a custom intraocular lens with a 30-diopter torus for the correction of high astigmatism after penetrating keratoplasty. *J Cataract Refract Surg.* **29,** 2444–2447.

Tehrani, M., Krummenauer, F., Blom, E. & Dick, H.B. (2003). Evaluation of the practicality of optical biometry and applanation ultrasound in 253 eyes. *J Cataract Refract Surg.* **29,** 741–6.

Tennant, A., McKenna, S.P. & Hagell, P. (2004). Application of Rasch analysis in the development and application of quality of life instruments. *Value Health.* **7,** S22-6.

Teping, C., Oran, E. & Backes-Teping, C. (1994). [Visual acuity at twilight and contrast vision in patients with bifocal IOL]. *Ophthalmologe.* **91,** 460-4.

Terwee, T., Weeber, H., van der Mooren, M. & Piers, P. (2008). Visualization of the retinal image in an eye model with spherical and aspheric, diffractive, and refractive multifocal intraocular lenses. *J Refract Surg.* **24,** 223-32.

Thylefors, B., Chylack, L.T., Konyama, K., Sasaki, K., Sperduto, R., Taylor, H.R. & West, S. (2002). A simplified cataract grading system. *Ophthalmic epidemiology.* **9,** 83-95.

Till, J.S. (2001). Piggyback silicone intraocular lenses of opposite power. *J Cataract Refract Surg.* **27,** 165–168.

Till, J.S., Yoder, P.R., Wilcox, T.K. & Spielman, J.L. (2002). Toric intraocular lens implantation: 100 consecutive cases. *J Cartaract Refract Surg.* **28,** 295-301.

Toto, L., Falconio, G., Vecchiarino, L., Scorcia, V., Nicola, M.D., Ballone, E. & Mastropasqua, L. (2007). Visual performance and biocompatibility of 2 multifocal diffractive IOLs: six-month comparative study. *J Cataract Refract Surg.* **33,** 1419-25.

Tseng, S.S. & Ma, J.J.K. (2008). Calculating the optimal rotation of a misaligned toric intraocular lens. *J Cataract Refract Surg*. **34,** 1767–1772.

Tsinopoulos, I.T., Tsaousis, K.T., Tsakpinis, D., Ziakas, N.G. & Dimitrakos, S.A. (2010). Acrylic toric intraocular lens implantation: a single center experience concerning clinical outcomes and postoperative rotation. *Clin Ophthalmol.* **4,** 137-42.

Tucker, J. & Charman, W.N. (1975). The depth-of-focus of the human eye for Snellen letters. *Am J Optom Physiol Opt.* **52,** 3-21.

Tucker, J. & Charman, W.N. (1986). Depth of focus and accommodation for sinusoidal gratings as a function of luminance. *Am J Optom Physiol Opt.* **63,** 58-70.

Turuwhenua, J. (2005). A theoretical study of intraocular lens tilt and decentration on perceptual image quality. *Ophthal Physiol Opt.* **25,** 556-67

Uhlhorn, S.R., Borja, D., Manns, F. & Parel, J. (2008). Refractive index measurement of the isolated crystalline lens using optical coherence tomography. *Vision Res.* **48,** 2732-8.

Uusitalo, R.J., Brans, T., Pessi, T. & Tarkkanen, A. (1999). Evaluating cataract surgery gains by assessing patients' quality of life using the VF-7. *J Cataract Refract Surg.* **25,** 989-94.

Uvijls, A., Baets, R., Leroy, B.P. & Kestelyn, P. (2001). Mesopic visual acuity requirements for driving licenses in the European Union-Research Report. *Bulletin de la Société belge d'ophtalmologie*. **282,** 71-7.

Valle, P., Oti, J., Canales, V. & Cagigal, M. (2005). Visual axial PSF of diffractive trifocal lenses. *Optics express*. **13,** 2782-92.

Vanderschueren, I., Zeyen, T. & D'heer, B. (1991). Multifocal IOL implantation: 16 cases. *Br J Ophthalmol*. **75,** 88-91.

Vaquero, M., Encinas, J.L. & Jimenez, F. (1996). Visual function with monofocal versus multifocal IOLs. *J Cataract Refract Surg.* **22,** 1222-5.

Vaquero-Ruano, M., Encinas, J.L., Millan, I., Hijos, M. & Cajigal, C. (1998). AMO array multifocal versus monofocal intraocular lenses: long-term follow-up. *J Cataract Refract Surg.* **24,** 118-23.

Vass, C., Menapace, R., Schmetterer, K., Findl, O., Rainer, G. & Steineck, I. (1999) Prediction of pseudophakic capsular bag diameter based on biometric variables. *J Cataract Refract Surg,* **25,** 1376–1381.

Vass, C. & Menapace, R. (2007). Computerized statistical analysis of corneal topography for the evaluation of changes in corneal shape after surgery. *Am J Ophthalmol.* **118,** 177–184.

Van Veen, H.G. & Goss, D.A. (1988). Simplified system of Purkinje image photography for phakometry. *Am J Optom Physiol Optics.* **65,** 905-8.

Velozo, C.A., Lai, J.S., Mallinson, T., Hauselman, E. (2000). Maintaining instrument quality while reducing items: application of Rasch analysis to a self-report of visual function. *J Outcome Meas*. **4,** 667-80.

Verbruggen, K.H.M., Rozema, J.J., Gobin, L., Coeckelbergh, T., Groot, V.D. & Tassignon, M. (2007). Intraocular lens centration and visual outcomes after bag-in-the-lens implantation. *J Cataract Refract Surg.* **33,** 1267-72.

Viestenz, A., Seitz, B. & Langenbucher, A. (2005). Evaluating the eye's rotational stability during standard photography: effect on determining the axial orientation of toric intraocular lenses. *J Refract Surg.* **31,** 557–561.

Vilupuru, A.S., Roorda, A. & Glasser, A. (2004). Spatially variant changes in lens power during ocular accommodation in a rhesus monkey eye. *J Vis.* **4,** 299-309.

Vingolo, E.M., Grenga, P., Iacobelli, L. & Grenga, R. (2007). Visual acuity and contrast sensitivity: AcrySof ReSTOR apodized diffractive versus AcrySof SA60AT monofocal intraocular lenses. *J Cataract Refract Surg.* **33,** 1244-7.

Virgili, G., Pierrottet, C., Parmeggiani, F., Pennino, M., Giacomelli, G., Steindler, P., Menchini, U. & Orzalesi, N. (2004a). MNREAD charts Reading performance in patients with retinitis pigmentosa: a study using the MNREAD charts. *Invest Ophthalmol Vis Sci.* **45,** 3418-24.

Virgili, G., Cordaro, C., Bigoni, A., Crovato, S., Cecchini, P. & Menchini, U. (2004b) Reading acuity in children: evaluation and reliability using MNREAD charts. *Invest Ophthalmol Vis Sci.* **45,** 3349-54.

Vogel, A., Dick, H.B. & Krummenauer, F. (2001). Reproducibility of optical biometry using partial coherence interferometry : intraobserver and interobserver reliability. *J Cataract Refract Surg.* **27,** 1961-8.

Vos, J.J. (1984). Disability glare state of the art report. *CIE-Journal.* **3,** 39-53.

de Vries, N.E., Franssen, L., Webers, C.A.B., Tahzib, N.G., Cheng, Y.Y.Y., Hendrikse, F., Tjia, K.F., van den Berg, T.J.T.P. & Nuijts, R.M.M.A. (2008a). Intraocular straylight after implantation of the multifocal AcrySof ReSTOR SA60D3 diffractive intraocular lens. *J Cataract Refract Surg.* **34,** 957-62.

de Vries, N.E., Webers, C.A.B., Montés-Micó, R., Tahzib, N.G., Cheng, Y.Y.Y., de Brabander, J., Hendrikse, F. & Nuijts, R.M.M.A. (2008b). Long-term follow-up of a multifocal apodized diffractive intraocular lens after cataract surgery. *J Cataract Refract Surg.* **34,** 1476-82.

de Vries, N.E., Webers, C.A.B., Montés-Micó, R., Ferrer-Blasco, T., Nuijts, R.M.M.A. (2010). Visual outcomes after cataract surgery with implantation of a +3.00 D or +4.00 D aspheric diffractive multifocal intraocular lens: Comparative study. *J Cataract Refract Surg.* **36,** 1316-22.

Walkey, H.C., Harlow, J.A. & Barbur, J.L. (2006). Changes in reaction time and search time with background luminance in the mesopic range *Ophthalmic Physiol Opt.* **26,** 288-99.

Walkow, T., Liekfeld, A., Anders, N., Pham, D.T., Hartmann, C. & Wollensak, J. (1997) A prospective evaluation of a diffractive versus a refractive designed multifocal intraocular lens. *Ophthalmology.* **104,** 1380-6.

Walkow, L. & Klemen, U.M. (2001). Patient satisfaction after implantation of diffractive designed multifocal intraocular lenses in dependence on objective parameters. *Graefes Arch Clin Exp Ophthalmol.* **239,** 683-7.

Wang, B. & Ciuffreda, K.J. (2004). Depth-of-focus of the human eye in the near retinal periphery. *Vision Res.* **44,** 1115-25.

Wang, J.C., Tan, A.W.T., Monatosh, R. & Chew, P.T.K. (2005). Experience with ARRAY multifocal lenses in a Singapore population. *Singapore Med J.* **46,** 616-20.

Wang, L. & Koch, D.D. (2005). Effect of decentration of wavefront-corrected intraocular lenses on the higher-order aberrations of the eye. *Arch Ophthalmol.* **123,** 1226-30.

Wang, L., Pitcher, J.D., Weikert, M.P. & Koch, D.D. (2010). Custom selection of aspheric intraocular lenses after wavefront-guided myopic photorefractive keratectomy. *J Cataract Refract Surg.* **36,** 73-81.

Weghaupt, H., Pieh, S. & Skorpik, C. (1996). Visual properties of the foldable Array multifocal intraocular lens. *J Cataract Refract Surg.* **22,** 1313-7.

Weghaupt, H., Pieh, S. & Skorpik, C. (1998). Comparison of pseudoaccommodation and visual quality between a diffractive and refractive multifocal intraocular lens. *J Cataract Refract Surg.* **24,** 663-5.

Wehner, H. (2007). [Microincision intraocular lens with plate haptic design. Evaluation of rotational stability and centering of a microincision intraocular lens with plate haptic design in 12-19 months of follow-up]. *Der Ophthalmologe.* **104,** 393-4.

Weinand, F., Jung, A., Stein, A., Pfützner, A., Becker, R. & Pavlovic, S. (2007). Rotational stability of a single-piece hydrophobic acrylic intraocular lens: new method for high-precision rotation control. *J Cataract Refract Surg.* **33,** 800–803.

Werblin, T.P. (1995). Do three-piece PMMA IOLs rotate after implantation in the capsular bag? *J Refract Surg.* **11,** 468–471.

Werner, L., Izak, A.M., Isaacs, R.T., Pandey, S.K. & Apple, D.J. (2009). Evolution of Intraocular Lens Implantation. IN: *Ophthalmology.* Yanoff, M. & Duker, J.S. London. Elsevier Inc. 394-409.

West, S.K., Rosenthal, F., Newland, H.S. & Taylor, H.R. (1988). Use of photographic techniques to grade nuclear cataracts. *Invest Ophthalmol Vis Sci.* **29,** 73-7.

Whittaker, S.G. & Lovie-Kitchin, J. (1993). Visual requirements for reading. *Optom Vis Sci.* **70,** 54-65.

Wiemer, C., Pham, D.T. & Wollensak, J. (1994). [Can the diffractive multifocal posterior chamber lens be implanted in routine lens implantation?]. *Der Ophthalmologe.* **91,** 450-3.

Winther-Nielsen, A., Corydon, L., Olsen, T. (1993). Contrast sensitivity and glare in patients with a diffractive multifocal intraocular lens. *J Cataract Refract Surg.* **19,** 254-7.

Winther-Nielsen, A. & Gyldenkerne, G. L (1995). Corydon Contrast sensitivity, glare, and visual function: diffractive multifocal versus bilateral monofocal intraocular lenses. *J Cataract Refract Surg.* **21,** 202-7.

Wolffsohn, J.S. & Cochrane, A.L. (2000). Design of the low vision quality-of-life questionnaire (LVQOL) and measuring the outcome of low-vision rehabilitation. *Am J Ophthalmol.* **130,** 793-802.

Wolffsohn, J.S., Hunt, O.A., Naroo, S., Gilmartin, B., Shah, S., Cunliffe, I.A., Benson, M.T. & Mantry, S. (2006). Objective accommodative amplitude and dynamics with the 1CU accommodative intraocular lens. *Invest Ophthalmol Vis Sci*. **47,** 1230-5.

Wolffsohn, J.S. & Davies, L.N. (2007). Advances in anterior segment imaging. *Curr Opin Ophthalmol.* **18,** 32–38.

Wolffsohn, J.S. & Buckhurst, P.J. (2010). Objective analysis of toric intraocular lens rotation and centration. *J Cataract Refract Surg.* **36,** 778-82.

Wolffsohn, J.S., Davies, L.N., Gupta, N., Naroo, S.A., Gibson, G.A., Mihashi, T., Shah, S. (2010). Mechanism of Action of the Tetraflex Accommodative Intraocular Lens. *J Refract Surg.* **26,** 858-862.

Wolffsohn, J.S., Davies, L.N., Naroo, S.A., Buckhurst, P.J., Gibson, G.A., Gupta, N., Craig, J.P., Shah, S. (2010b). Evaluation of an open-field autorefractor's ability to measure refraction and hence potential to assess objective accommodation in pseudophakes. *Br J Ophthalmol.* doi: 10.1136/bjo.2010.185009 [Epub ahead of print].

Woodward, M.A., Randleman, J.B. & Stulting, D.R. (2009). Dissatisfaction after multifocal intraocular lens implantation. *J Cataract Refract Surg.* **35,** 992-7.

Wright, B.D. & Linacre, J.M. (1994). Reasonable mean-square fit values. Raasch Measurement Transactions. **8,** 370.

Yang, Y., Thompson, K. & Burns, S.A. (2002). Pupil location under mesopic, photopic, and pharmacologically dilated conditions. *Invest Ophthalmol Vis Sci.* **43,** 2508-12.

Ypma, T.J. (1995). Historical Development of the Newton-Raphson Method. *Soc Indust App Math.* **37,** 531-551.

Zeng, M., Liu, Y., Liu, X., Yuan, Z., Luo, L., Xia, Y. & Zeng, Y. (2007). Aberration and contrast sensitivity comparison of aspherical and monofocal and multifocal intraocular lens eyes. *Clin Experiment Ophthalmol.* **35,** 355-60.

Zhang, W., Sun, K., Xie, J., Luo, S., Lu, Q., Hong, J. & Huang, Y. (2007). [The observation of visual quality after the implantation of apodized diffractive multifocal intraocular lens]. *Yan ke xue bao.* **23,** 79-83.

Zhao, Y., Li, J., Zhu, J., Wang, D., Wang, Q. (2009). Evaluation of long-term visual performance following AcrySof ReSTOR lens implantation. *Chin Med J.* **122,** 2705-10.

Zuberbuhler, B., Signer, T., Gale, R., Haefliger, E. (2008). Rotational stability of the AcrySof SA60TT toric intraocular lenses: a cohort study. *BMC Ophthalmol.* **8,** 8.

Appendix

A1   Power calculation

A1.1   Sample Size for Chapter Two

Previous studies evaluating defocus curves in subjects implanted with Multifocal IOLs have used variable group sizes (range 4 to 141 subjects); often these group sizes are unequal (Chapter 2).

Sample size calculations prior to the study could not be reliably conducted due to:

- The disparity in defocus curve methodology

- The variability of analysis

- The lack of literature evaluating sectorial multifocals

Correlation between defocus curve results and measures of VA require a minimum sample size of 68 subjects to achieve a power of 80% for a correlation coefficient of 0.3 at a significance level of 0.05 (Cohen, 1988).

Correlation between defocus curve results and the subjective questionnaire requires a minimum sample size of 75 (68 adjusted by the asymptotic relative efficiency (ARE) correction (0.910))

Post hoc power analysis (multiple one- way fixed effects ANOVAs) using the results from Chapter 2 revealed a power of 81%, 100%, and 100% for the distance, intermediate, and near 'areas of focus' ($\alpha = 0.05$).

A1.2   Sample Size for Chapter Three

Rasch analysis requires a large sample size, however, there is no definition for how large this sample size should be.

For construct validity, a low level of correlation can be expected (Gupta *et al.,* 2007), a minimum sample size of 68 subjects is therefore required for a low correlation coefficient of 0.3 at a significance level of 0.05 (with a power of 80%).

The effect of ten variables was examined using multiple linear regressions in Chapter 3. Using a conservative estimate at least one hundred subjects should be included in the study (ten times the number of variables).

Previous studies examining reading ability in subjects implanted with MIOLs have involved a range of group sizes varying between 7 to 124 subjects. Due to the variability in MNread analysis and the lack of information regarding sectorial MIOLs, a priory analysis cannot be reliably conducted.

Post hoc analysis of the MNRead (one-way fixed effects ANOVA) revealed a power of 100% ($\alpha = 0.05$).

Post hoc analysis of the NAVQ (one-way fixed effects ANOVA) revealed a power of 100% ($\alpha = 0.05$).

A1.3   Sample Size for Chapter Four

The DG Halometer is a new instrument for the measurement of dysphotopsia. As such no sample size power analysis can be conducted *a-priori*.

Correlation between the halometer results and C-Quant requires a minimum sample size of at least 10 (80% statistical power for a correlation coefficient of 0.3 and significance level of 0.05).

 Correlation between defocus curve results and the subjective questionnaire requires a minimum sample size of 11 (10 adjusted by the ARE correction (0.910))

Post-hoc analysis of the BD Halometer results (one-way fixed effects ANOVA) revealed a power of 92% ($\alpha = 0.05$).

A1.4   Sample Size for Chapter Five

Several studies have evaluated the IOLmaster all with varying numbers of subjects:

- Santodomingo-Rubido and colleages (2002) involved 104 eyes of 52 subjects.

- Connors and associates (2002) involved 111 eyes of 91 subjects.

- Lam and colleagues (2001) involved 26 subjects

- Packer and colleages (2002) involved 50 eyes.

A range of parameters are measured by both instruments, a high level of correlation was expected between axial length measurements, a minimum of 16 subjects was required to achieve a power of 80% for a correlation coefficient of 0.7 with a significance level of 0.01.

A Low level of correlation were predicted for the other parameters, a sample size of least 108 was required for a correlation coefficent of 0.3 at the p=0.01 level.

A1.5   Sample Size for Chapters Six and Seven

This was the first study to examine the validity of the rotation image analysis compensating for eye rotation. The extent of apparent rotation was compared with image quality this required a minimum of 75 subjects. To achieve a power of 80% for a correlation coefficent of 0.3 with a significance level of 0.05 after applying an ARE correction.

The sample sizes of previous toric IOL studies have ranged between 17 and 244 subjects (Table 6.1). The American national standards institute stipulate a minimum of 100 recruited subjects for the assessment of IOL rotation (ANSI Z80.30-2010).

A2 Summary of Mesopic Illumination Levels in Studies Assessing Multifocal Intraocular Lenses

Paper	Mesopic Conditions	Adaption time(Min)	Outcome measure	Multifocal design
Alfonso 2010	3 cdm^2	5	CS	Acrylisa & ReSTOR
Felipe 2010a	3cdm^2	Not stated	VA	Tecnis, ReZoom & ReSTOR
Alfonso 2010b	5 cdm^2	5	CS	ReSTOR
Fernandez-Vega 2010	5 cdm^2	5	CS	Acrylisa
Vries 2010a	0.4 Lux & 4 Lux	Not stated	Pupil Size	ReSTOR +3/+4 D
Vries 2010b	0.4 Lux & 4 Lux	Not stated	Pupil Size	ReSTOR +4 D
Alfonso 2010c	3 cdm^2	5	CS	ReSTOR & Acrylisa
Mesci 2010	5 cdm^2	5	CS	1CU ReSTOR Preziol
Maxwell 2009	2cdm^2	Not Stated	VA	ReSTOR +3/+4 D
Hayashi 2009	2 cdm^2	Not stated	CS	Hoya SFX MV1
Chen 2009	6 cdm^2	Not Stated	VA	ReZoom, Tecnis
Petermeier 2009	6 cdm^2	Not Stated	CS	ReSTOR
Fernández-Vega 2009	5 cdm^2	5 minutes	CS	Acrylisa
Cionni 2009	3 cdm^2	Not Stated	CS	ReSTOR
Lan 2009	6 cdm^2	Not Stated	CS	ReSTOR
Blaylock 2009	3 cdm^2	Not Stated	CS	RESTOR
Alfonso 2009	5 cdm^2	5 Minutes	CS	ReSTOR
Forte 2009	6 cdm^2	Not Stated	VA	ReZoom
Hida 2009	6 cdm^2	Not Stated	CS	ReSTOR

Paper	Mesopic Conditions	Adaption time(Min)	Outcome measure	Multifocal design
Ferrer-Blasco 2008	5 & 2 cdm^2	5 minutes	CS	ReSTOR
Alfonso 2008	3 cdm^2	Not Stated	CS	ReSTOR & Acri.LISA 366D
Cillino 2008	6 cdm^2	Not Stated	VA	Array, ReZoom & Tecnis
Chang 2008	Not stated	Not Stated	CS	ReZoom & ReSTOR
Palmer 2008	10 Lux	Not Stated	CS	Tecnis, ReZoom, TwinSet

Table A1 *Table of mesopic illumination levels and adaption times in studies examining multifocal intraocular lenses*

A3   Summary of Studies Assessing Multifocal Intraocular Lenses by use of Questionnaires

Author	IOLs	Type of questionnaire	Questions			Validated	
			Satisfaction	Photopic phenomenon	Spectacle dependence	Pseudophakic	Other
Percival 1989	3M Diffractive +3.5 D n=55	Bespoke	X	X	X		
Percival 1990	Diffractive +3.5 D n=55	Bespoke	X	X			
Gimbel 1991	Diffractive +3.5 D n=149 Monofocal n=101	Bespoke	X	X	X		
Steinert 1992	Refractive +3.5 D n=32 Monofocal n=20	Bespoke	X	X	X		
Lindstrom 1992	Diffractive +3.5 D n=869	Bespoke	X				
Lindstrom 1993	Diffractive +3.5 D n=671	Bespoke	X		X		
Percival 1993	Refractive +3.5 D n=25 Monofocal n=25	Bespoke	X		X		
Winther-Nielsen 1993	Diffractive +3.5 D n=25 Monofocal n=23	Bespoke	X	X	X		
Eisenmann 1993	Diffractive +3.5 D n=15 Refractive +3.5 D n=15	Bespoke		X			
Auffarth 1993	Diffractive +3.5 D n=35 Monofocal n=45	Bespoke	X		X		
Rossetti 1994	Diffractive +3.5 D n=38 Monofocal n=42	Bespoke	X	X			
Winther-Nielsen 1995	Diffractive +3.5 D n=9 Monofocal n=9	Bespoke	X	X			

311

Author	IOLs	Type of questionnaire	Questions			Validated	
			Satisfaction	Photopic phenomenon	Spectacle dependence	Pseudophakic	Other
Jacobi 1995	Array n=25	Verbal interview	X				
Allen 1996	Diffractive +4 D n=79 Monofocal n=70	Bespoke	X	X	X		
Bleckmann 1996	Refractive +4.75 D n=59	Bespoke	X	X			
Javitt 1997	Refractive +3.5 D n=100 Monofocal 103	Cataract TyPE specification & Bespoke	X	X	X	X	X
Negishi 1997	Refractive +3.5 D n=25	Bespoke	X	X	X		
Walkow 1997	Diffractive +4 D n=40 Refractive +3.5 D n=40	Bespoke	X	X			
Jacobi 1999	Asymmetrical Diffractive +4 D n=29	Bespoke			X		
Steinert 1999	Refractive +3.5 D n=400	Bespoke	X	X	X		
Avitabile 1999	Diffractive +4 D n=35	Bespoke	X				
Dick 1999	Refractive +3.5 D n=28 Monofocal	Bespoke		X			
Brydon 2000	Refractive +3.5 D n=15 Monofocal n=13	Modified VF-14 & bespoke	X	X	X		X

Author	IOLs	Type of questionnaire	Questions			Validated	
			Satisfaction	Photopic phenomenon	Spectacle dependence	Pseudophakic	Other
Sasaki 2000	Refractive +3.5 D n=31	Bespoke	X	X	X		
Javitt 2000a	Refractive +3.5 D n=64 Monofocal n=60	Modified cataract TyPE specification	X	?	?	X	X
Javitt 2000b (ophthalmology)	Refractive +3.5 D n=127 Monofocal n=118	Modified cataract TyPE specification	X	?	?	X	X
Häring 2001	Refractive +3.5 D n=138 Monofocal n=93	Bespoke Arnold 1994		X			
Kamlesh 2001	Refractive +5 D n=20 Monofocal n=20	Bespoke	X	X	X		
Walkow 2001	Diffractive +4 D n=50	Bespoke	X	X	X		
Dick 2002	Refractive +3.5 D n=25	Bespoke Dick 1999		X			
Kaushik 2002	Refractive +5 D n=20 Monofocal n=20	Bespoke	X	X	X		
Jacobi 2002	Refractive +3.5 D n=54 Monofocal n=41	Verbal interview	X	X	X		
Shoji 2002	Refractive +4 D n=66	Verbal interview			X		
Sedgewick 2002	Refractive +3.5 D n=17 Monofocal n=15	Bespoke	X	X	X		
Leyland 2002	Refractive +3.5 D n=29 Sorz truevista IOL n=15 Monofocal n=16	Modified cataract TyPE specification	X	X	X	X	X

313

Author	IOLs	Type of questionnaire	Questions			Validated	
			Satisfaction	Photopic phenomenon	Spectacle dependence	Pseudophakic	Other
Aralikatti 2004	Refractive +3.5 D n=15	VF14	X	X	X		X
Nijkamp 2004	Refractive +3.5 D n=68 Monofocal n=69	VF14 & VQOL	X	X	X		X
Claoué 2004	Refractive +3.5 D n=28 Single Optic accommodative n=5	Bespoke			X		
Alió 2004	Single optic Accommodating n=12 Refractive +3.5 D n=16	Bespoke	X	X	X		
Sen 2004	Refractive +3.5 D n=35 Monofocal n=40	VF-7, CS-5 & bespoke	X	X	?	X	X
Lee 2005	Refractive +3.5 D n=163	VF-14	X	X	X		X
Wang 2005	Refractive +3.5 D n=27	Bespoke	X	X	X		
Elgohary 2006	Refractive +3.5 D n=17 Monofocal n=10	Bespoke	X	X	X		
Kohnen 2006	Apodized diffractive +4 D n=127	Bespoke	X	X	X		
Blaylock 2006	Apodized diffractive +4 D n=20	NEI-RQL-42	X	X	X		X
Cumming 2006	Single Optic accommodative n=263	Bespoke	X		X		
Chiam 2006	Apodized diffractive +4 D n=40	Bespoke	X	X	X		
Salati 2007	Refractive +3.5 D n=62	Bespoke	X	X	X		

Author	IOLs	Type of questionnaire	Questions			Validated	
			Satisfaction	Photopic phenomenon	Spectacle dependence	Pseudophakic	Other
Lubiński 2007	Refractive +3.5 D n=20	Modified cataract TyPE specification	X	X	X		X
Gupta 2007	Single Optic accommodative n=22	NAVQ	X		X	X	
Petermeier 2007	Apodized Diffractive +4 D n=32	Bespoke	X	X	X		
Mester 2007	Diffractive +4 D n=25 Refractive +3.5 D n=25	Bespoke	X	X	X		
Alfonso 2007	Apodized diffractive +4 D n=325 Blue filter Apodized diffractive +4 D n=335	Bespoke	X	X	X		
Chen 2007	Refractive +3.5 D n=20 Monofocal n=20	Bespoke	X		X		
Pepose 2007	Single Optic accommodating n=14 Apodized Diffractive +4 D n=12 Refractive +3.5 D n=14 Diffractive accommodative combination n=6 Refractive accommodative combination n=3	NEI-RQL-42	X	X	X		X
Chiam 2007	Refractive +3.5 D n=50 Apodized diffractive +4D n=50	Bespoke	X	X	X		
Akaishi 2007	Diffractive +4 D n=12	Bespoke	X	X	X		
Kaymak 2007	Refractive/Diffractive +3.75 D n=20	Bespoke		X			
Bi 2008	Apodized diffractive +4 D n=20 Monofocal n=18	Bespoke	X	X	X		

Author	IOLs	Type of questionnaire	Questions			Validated	
			Satisfaction	Photopic phenomenon	Spectacle dependence	Pseudophakic	Other
Gunenc 2008	Diffractive +4 D n=10 Refractive +3.5 D n=10 Refractive/Diffractive combination n=10	Bespoke	X	X	X		
Palmer 2008	Diffractive +4 D n=26 Refractive +3.5 D n=32 Monofocal n=24	Bespoke	X	X	X		
Blaylock 2008	Apodized diffractive +4 D n=30	NEI-RQL-42	X	X	X		X
Goes 2008a	Diffractive +4 D n=30	Bespoke	X	X	X		
Goes 2008b	Diffractive/Refractive combination n=20	Bespoke	X	X	X		
Elgohary 2008	Refractive +3.5 D n=9 Monofocal n=25	Bespoke	X	X			
Chang 2008	Refractive +3.5 D n=15 Apodized Diffractive +4D n=15	Bespoke	X	X	X		
Harman 2008	Refractive +3.5 D n=30 Single Optic Accommodating n=30 Monofocal n=30	Self-perceived quality of vision questionnaire	X	X		X	X
Alió 2008a	Refractive/diffractive +3.75 D n=52	Verbal interview		X			
Alio 2008b	Refractive/diffractive +3.75 D n=47	Verbal interview		X			
Cillino 2008	Refractive +3.5 D(a) n=16 Refractive +3.5 D(b) n=15 Diffractive +4 D n=16 Monofocal n=15	Modified VF-7 & Bespoke	X	X	X	X	

Author	IOLs	Type of questionnaire	Questions			Validated	
			Satisfaction	Photopic phenomenon	Spectacle dependence	Pseudophakic	Other
de Vries 2008	Apodized diffractive +4 D n=22	Bespoke	X	X	X		
Mayer 2008	Monofocal/Apodized diffractive +4 D combination n=12	Bespoke	X	X	X		
Barisić 2008	Refractive +3.5 D n=50 Diffractive +4 D n=50	Bespoke	X	X	X		
Lacmanović-Loncar 2008	Refractive +3.5D/Appodized diffractive +4 D combination n=10	Bespoke	X	X	X		
Lubiński 2009	Refractive +3.5 D n=20	Bespoke	X	X	X		
Forte 2009	Refractive +3.5 D n=35	VF-7 & Bespoke	X	X	X	X	
Bautista 2009	Diffractive +4 D n=137	Bespoke	X	X			
Blaylock 2009	Apodized diffractive +4 D n=32	NEI-RQL-42	X	X	X		X
Ferko 2009	Single Optic accommodative n=35	Bespoke	X				
Allen 2009	Refractive +3.5 D n=20 Monofocal n=29	Tester 2000 Javitt 1997 Winther-Neilson 1995 Sedgewich 2002		X		X	X
Hayashi 2009a	Refractive +3 D n=22	Bespoke	X		X		

Author	IOLs	Type of questionnaire	Questions			Validated	
			Satisfaction	Photopic phenomenon	Spectacle dependence	Pseudophakic	Other
Hayashi 2009b	Blue filtered Apodized diffractive n=30 Apodized diffractive n=34 Monofocal n=17	Bespoke		X			
Cionni 2009a	Apodized diffractive +4 D n=73 Monofocal n=53	Bespoke	X	X	X		
Cionni 2009b	Apodized diffractive +4 D n=15 Apodized diffractive/ monofocal combination n=20 Apodized diffractive/ phakic combination n=32	Bespoke	X	X	X		
Hofmann 2009	Apodized diffractive +4 D n=20	Bespoke		X			
Petermeier 2009	Apodized diffractive +4 D n=3	Bespoke	X	X	X		
Chen 2009	Refractive +3.5 D/diffractive +4 D combination n=15 Monofocal n=16	NEI-RQL-42	X	X	X		X
Kohnen 2009	Apodized diffractive +3 D n=93	Modified NEI-VFQ-25 & modified TyPE questionnaire	X	X	X		X
Maxwell 2009	Apodized diffractive +3 D n=138 Apodized diffractive +4 D n=134	Cataract TyPE questionnaire & Bespoke	X	X	X		X

Author	IOLs	Type of questionnaire	Questions			Validated	
			Satisfaction	Photopic phenomenon	Spectacle dependence	Pseudophakic	Other
Alfonso 2009b	Apodized diffractive +3 D n=20	Modified NEI-VFQ-25 and modified TyPE questionnaire	X		X		X
Sanders 2010	Single Optic accommodative n=239 Monofocal n=96	Bespoke	X	X	X		
Gierek-Ciaciura 2010	Apodized diffractive +4 D n=10 Refractive +3.5 D n=10 Diffractive +4 D n=10	VF-14 & Bespoke	X	X	X		X

Table A2 *Summary of studies involving subjective questionnaires given to subjects implanted with a multifocal and accommodating*

intraocular lenses

A4 Rasch analysis of the Near Activity Visual Questionnaire for Chapter 3

The category function for the first 23 items, before item and category reduction, is displayed in Table A3 and the category function probability curve for the items is displayed in figure A1. Categories 1 and 5 of the original 23-item questionnaire demonstrated a close fit to the Rasch model. The category function table describes the slight deviation from the Rasch model for category 3 and 4. Category 3 failed the outfit MNSQ statistic and the expected and observed averages for category 4 differed by 4.99. The category probability curve demonstrated that category 2 had a peak probability of less than 50% (Figure A1).

Category Label	Observed Count %	Observed average	Sample expected	Infit MNSQ	Outfit MNSQ	Structure calibration	Category Measure
1	62	-28	-27.7	0.85	0.92	NONE	-20.83
2	18	-12.73	-13.8	0.97	1.00	-11.67	-9.84
3	11	-5.02	-5.08	1.04	2.13	-5.87	-1.25
4	7	-2.35	2.74	1.08	0.99	1.99	9.47
5	2	10.62	11.97	1.45	1.31	15.55	23.69

Table A3 *Summary of category function for the first 23-items of the Near Activity Visual Questionnaire before reduction of the items*
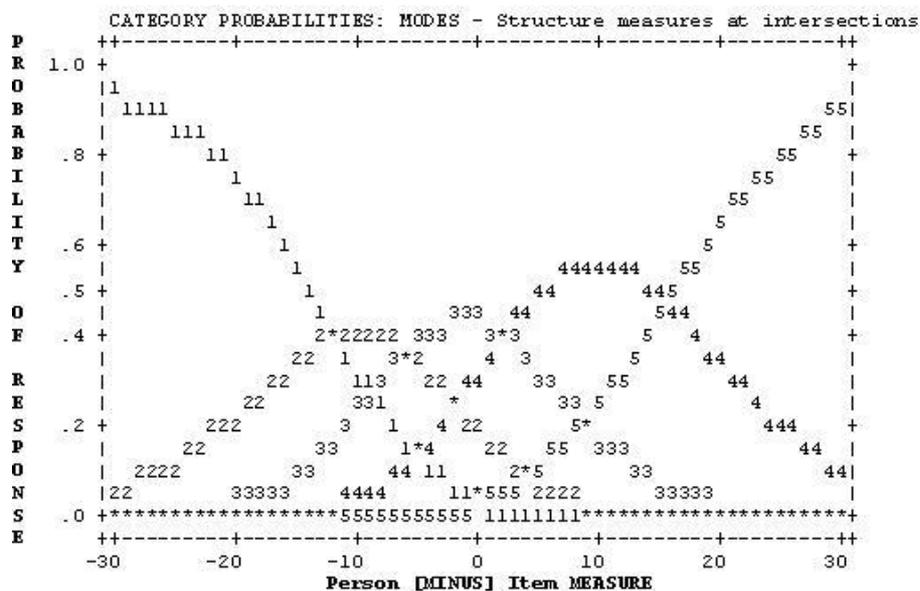
Figure A1 *Category probability curves for items 1 to 23*

The initial Rasch separation index, before category and item reduction, was 3.08 and the reliability index was 0.90. The item fit statistics (Table A4), item map (Figure A2), frequency of endorsement (Table A5) and skew and kertosis (Table A6) all show several items displaying a poor fit to the Rasch model indicating that a reduction of items may improve the validity of the questionnaire.

	Infit MNSQ	Infit ZSTD	Outfit MNSQ	Outfit ZSTD
1	0.79	-1.60	0.71	-2.1
2	0.85	-1.10	0.93	-0.40
3	0.60	-2.9	0.49	-2.80
4	1.23	0.8	0.57	-0.50
5	0.64	-2.40	0.45	-2.70
6	0.85	-0.90	0.84	-0.80
7	0.83	-1.00	0.75	-1.10
8	1.25	1.40	0.77	-0.80
9	0.92	-0.30	0.54	-1.30
10	0.75	-1.60	0.61	-1.80
11	0.86	-1.00	0.89	-0.60
12	1.05	0.30	0.61	-1.40
13	0.87	-0.60	0.74	-0.50
14	1.31	1.00	0.56	-0.50
15	1.02	0.20	0.56	-1.10
16	1.02	0.20	1.74	1.70
17	1.02	0.20	0.69	-0.20
18	1.15	0.70	2.97	2.90
19	2.54	2.90	7.82	3.60
20	1.02	0.20	0.34	-0.50
21	1.51	3.20	1.48	2.80
22	1.70	3.90	2.01	4.20
23	0.98	-0.1	0.94	-0.3

Table A4 *Item fit statistics for the original 23-items*

```
      <more>|<rare>
 70            +   Q20
               |T
               |
               |   Q19
               |
               |
 60      XX   +   Q4        Q14        Q17
               |S
               |
               |
               |   Q18
               |   Q13      Q15
 50        T+   Q9        Q16
         X    |
         XX   |M Q12
         X    |   Q8
         XXX  |   Q5        Q10
      XXXXXXX |   Q3        Q7
 40      X   +   Q6
      XXXXXX S|   Q22
         XX   |S
         XX   |   Q11      Q23
         XXX  |   Q1        Q2        Q21
        XXXX  |
 30    XXXXXX +
        XXXX  |
        XXX M|T
    XXXXXXXXXX |
    XXXXXXXXXX |
        XXX   |
 20  XXXXXXXX +
      XXXXXXX |
      XXXXXXX S|
               |
        XXXX  |
               |
 10            +
      XXXXXX  |
               |
         T|
               |
               |
  0    XXXXXXX +
      <less>|<frequ>
```

Figure A2 Person map of items for the original 23-item questionnaire

Answer	Frequency of endorsement (%) for each question																						
	1	2	3	4	5	6	7	8	9	10	11	12	13	14	15	16	17	18	19	20	21	22	23
0	0	0	0	0	0	3	1	3	1	1	12	5	2	1	1	1	0	1	0	0	0	0	1
1	31	26	53	81	61	46	51	60	70	58	22	63	71	85	73	70	86	70	86	88	43	30	33
2	29	28	15	8	10	22	21	13	9	14	23	9	10	3	9	13	2	16	4	3	24	38	31
3	10	18	12	3	13	13	12	7	11	8	14	8	8	1	7	7	3	5	2	1	13	20	15
4	16	18	11	0	7	7	5	8	1	8	18	3	2	0	3	0	2	0	0	0	9	2	8
5	6	3	1	0	2	2	3	1	0	3	3	3	0	2	0	2	0	0	0	0	3	2	3

Table A5 *Frequency of endorsement for the 23-item data set*

	Skew	Kertosis
1	0.525707	-0.9688
2	0.35586	-0.96835
3	1.064746	-0.19681
4	3.056056	9.075747
5	1.408143	0.829845
6	0.992006	0.205435
7	1.365044	1.186686
8	1.549287	1.516001
9	1.709108	1.878376
10	1.398632	0.879018
11	0.430701	-0.90461
12	1.845609	3.044604
13	1.99163	3.447886
14	5.354196	31.72129
15	2.165279	4.161707
16	2.636673	7.968144
17	4.368067	18.89858
18	1.709533	2.464325
19	4.439393	20.37459
20	6.072936	39.81311
21	0.529939	-0.90812
22	0.836383	0.9426
23	0.603348	-0.55958

Table A6 *Skew and kurtosis of entire 23-item questionnaire*

Questions 24, 25 and 26 were exempt from the item reduction as they formed three independent question categories. The scale response was examined using the category function table (Table A7) and the category probability curve (Figure A3).

Category Label	Observed Count %	Observed average	Sample effect	Infit MNSQ	Outfit MNSQ	Structure calibration	Category Measure
0	17	-29.14	-32.30	1.72	1.36	NONE	-45.06
1	31	-21.84	-19.60	0.99	1.01	-32.61	-21.98
2	27	-5.46	-4.89	0.74	0.75	-10.28	-2.02
3	11	6.13	5.06	0.7	0.63	8.32	10.12
4	7	15.64	14.10	0.78	0.75	14.87	19.87
5	7	23.91	23.25	0.71	0.68	18.70	34.07

Table A7 *Category function for items 24, 25, and 26*
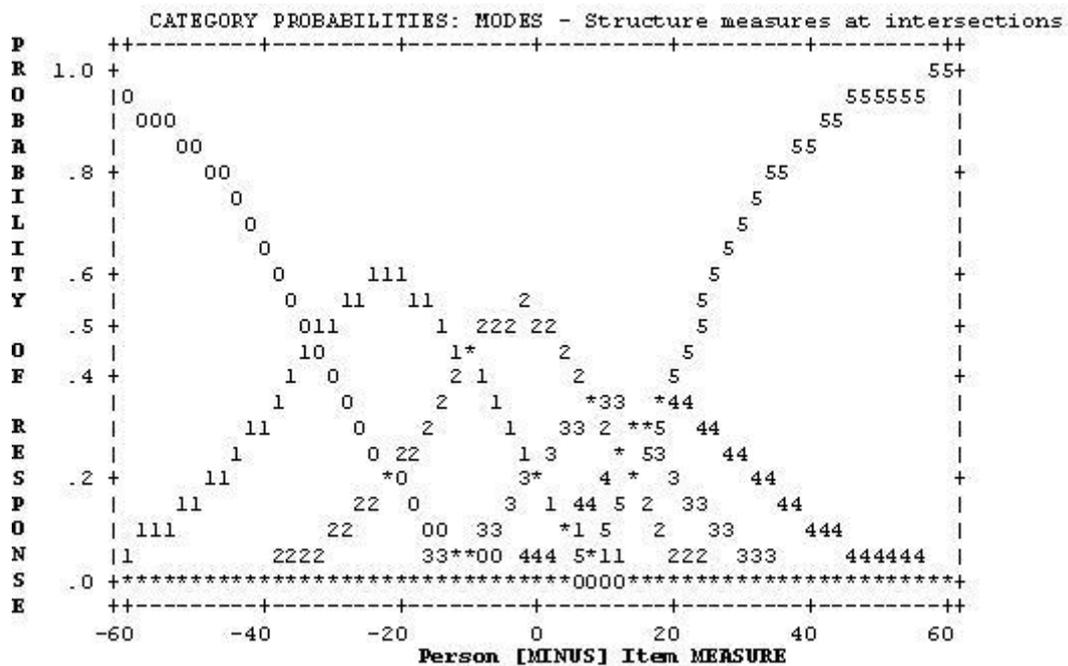
Figure A3 *Category probability curves for items 24, 25 and 26*

A4.1 Results of the Near Activity Visual Questionnaire Item and Category Reduction

As categories 2, 3 and 4 did not match the Rasch model a combination of categories was required. A 4-category scale combining categories 2 and 3 provided the best fit to the Rasch model (Table A8; Figure A4).

Category Label	Observed Count %	Observed average	Sample effect	Infit MNSQ	Outfit MNSQ	Structure calibration	Category Measure
1	367	-55.90	-54.90	0.83	0.84	NONE	-49.90
2	350	-21.11	-22.90	1.03	0.93	-38.82	-16.78
3	104	5.26	7.88	1.18	1.16	5.39	19.44
4	25	29.32	30.26	1.19	1.34	33.43	44.85

Table A8 *summary of category structure for the remaining 9-items of the Near Activity Visual Questionnaire after item and category reduction*
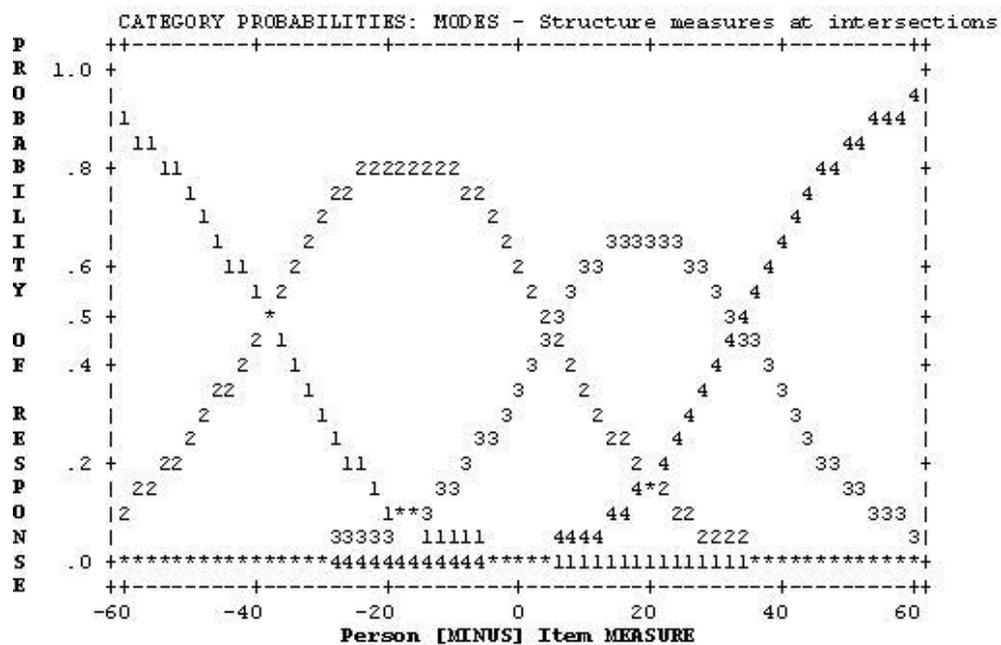
Figure A4 *Category probability curves for the remaining 9-items*

For questions 24, 25 and 26 combining categories 3 and 4 provided the best fit to the Rasch model, reducing the number of responses to each category to 5 (Table A9; Figure A5). Table A10 displays the three items with the reduced 5-scale category

Category Label	Observed Count %	Observed average	Sample effect	Infit MNSQ	Outfit MNSQ	Structure calibration	Category Measure
0	17	-26.86	-29.40	1.52	1.39	NONE	-41.65
1	31	-19.49	-17.60	0.95	1.03	-29.84	19.76
2	27	-3.29	-2.76	0.81	0.77	-8.49	-0.24
3	18	12.56	11.52	0.77	0.78	7.92	19.73
4	7	30.83	29.66	0.73	0.80	30.41	42.14

Table A9 *Summary of category structure for items 24, 25 and 26 after item and category reduction*
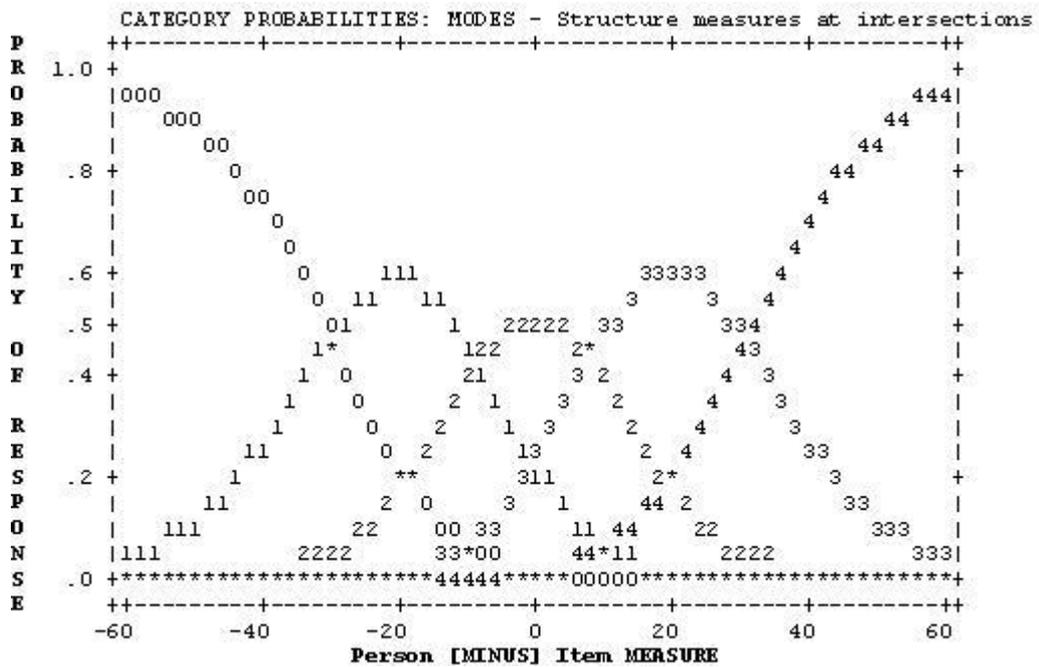
Figure A5 *Category probability curves for items 24, 25 and 26 after the category reduction*

	Instantly	Quickly	Moderate speed	Slowly	Never changes
24. How quickly does your focus change from distance vision to near vision	0	1	2	3	4
	Never	Rarely	Occasionally	Most of the time	Always
25. How often do you have to rely on reading or magnifying aids to do near tasks?	0	1	2	3	4
	Completely satisfied	Very satisfied	Moderately satisfied	A little satisfied	Completely unsatisfied
26. Overall how satisfied are you with the near visual ability that you have?	0	1	2	3	4

Table A10 *Response choices for items 24,25 and 26*

The item reduction procedure resulted in the removal of 14-items from the initial 23-items. The item fit statistics for the reduced 9-item can be seen in Table A11 and the item MAP can be seen in Figure A6. Item 8 did not meet the Rasch model, however, removal of this item reduced the separation index and negatively impacted on the item map and therefore this item was not excluded. The Rasch separation index was 2.78 and the reliability index was 0.89 after reduction.

Question number	Infit MNSQ	Infit ZSTD	Outfit MNSQ	Outfit ZSTD
1	0.94	-0.30	0.94	-0.3
2	0.95	-0.30	0.86	-0.90
3	0.76	-1.7	0.62	-2.00
6	0.84	-1.1	0.91	-0.40
7	1.03	0.30	1.22	1.00
8	1.50	2.6	1.13	0.50
9	0.68	-1.50	0.81	0.00
10	1.08	0.60	1.00	0.10
23	1.26	1.70	1.27	1.70

Table A11 *Item fit statistics for the reduced 9-item questionnaire*

```
                    Persons MAP OF Items
                      <more>|<rare>
                         #  |
                            |
      70                    +T  Q9
                            |
                            |
                            |
                         T  |
                         #  |
      60                    +S
                        . # |   Q8
                         .  |
                            |   Q10
                         .  |   Q3          Q7
                       .### |M  Q6
      50                    +
                      #### S|
                            |
                            |
                         .  |   Q23
                            |S
      40                 #  +   Q2
                            |   Q1
                       ###  |
                            |
                      . ##  |
                         M  |T
      30             .###   +
                            |
                     .####  |
                            |
                       ###  |
                            |
      20           ######   +
                            |
                            |
                    .##### S|
                            |
                            |
      10                    +
                    .#####  |
                            |
                            |
                            |
                            |
       0         ######## +
                      <less>|<frequ>
     EACH '#' IS 2.
```
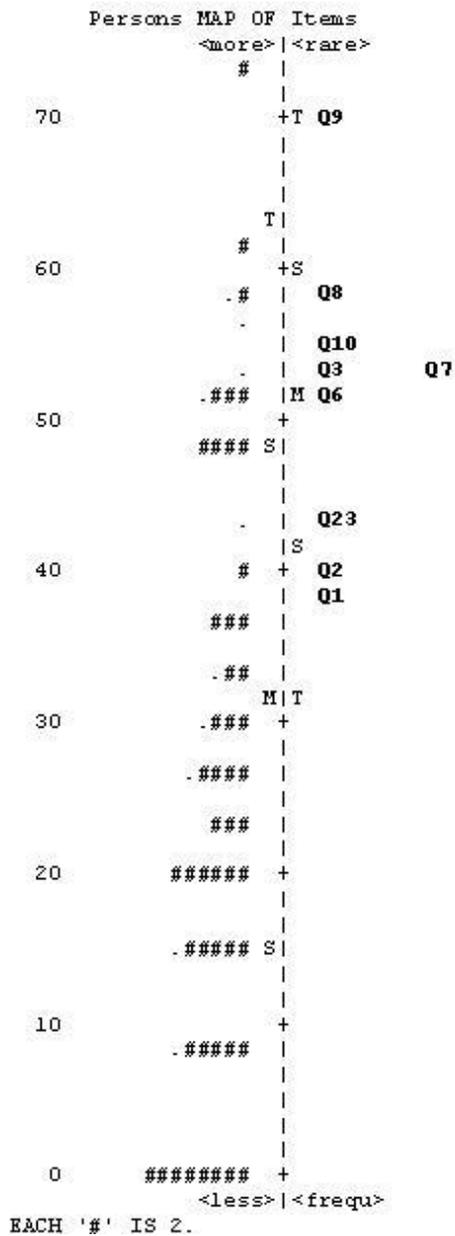
Figure A6 *Person map of items for the reduced 9-item questionnaire*

The final reduced 9-question questionnaire follows a 4-category scale from 1-5 and an additional response if the question is not applicable (Table A12). Figure A7 details the scale required to adjust the total 9 item response score into a Rasch score from 0 to 100

Question	Not applicable or stopped for non visual reasons	No difficulty	A little difficulty	Moderate difficulty	Extreme difficulty
1. Reading small print, e.g. newspaper articles, books, magazine articles, menus at a restaurant, telephone directories, etc.?	0	1	2	3	4
2. Reading labels/ instructions/ prices on, e.g. medicine bottles, food packaging, etc.?	0	1	2	3	4
3. Reading your post/ mail, e.g. electric bills, greeting cards, bank statements, letters from friends and family, etc.?	0	1	2	3	4
6. Seeing the display & keypad on a computer or calculator?	0	1	2	3	4
7. Seeing the display and keypad on a mobile or fixed telephone?	0	1	2	3	4
8. Seeing the display/ face of your wrist watch	0	1	2	3	4
9. Handling money and identifying different coins and notes by appearance?	0	1	2	3	4
10. Seeing objects close toy you to engage in your hobbies, e.g. playing games such as cards, bingo and dominoes, gardening, seeing photographs and pictures etc.?	0	1	2	3	4
23. Maintaining focus for prolonged near work?	0	1	2	3	4

Table A12 *The reduced 9-item Near Activity Visual Questionnaire*

```
+-------------------------------------------------------------------------------+
| RAW   ADJUSTED           | RAW    ADJUSTED          | RAW    ADJUSTED          |
| SCORE MEASURE     S.E.   | SCORE  MEASURE    S.E.   | SCORE  MEASURE    S.E.   |
|--------------------------+--------------------------+-------------------------|
|    9     .00E    12.01   |   19   43.27      4.32   |   29   68.19      3.98   |
|   10    8.86      7.19   |   20   46.16      4.23   |   30   70.75      4.08   |
|   11   15.18      5.73   |   21   48.92      4.12   |   31   73.47      4.22   |
|   12   19.82      5.17   |   22   51.54      4.02   |   32   76.44      4.46   |
|   13   23.78      4.86   |   23   54.03      3.92   |   33   79.86      4.88   |
|   14   27.35      4.66   |   24   56.41      3.85   |   34   84.18      5.66   |
|   15   30.70      4.56   |   25   58.74      3.82   |   35   90.67      7.40   |
|   16   33.95      4.51   |   26   61.04      3.82   |   36  100.00E    12.23   |
|   17   37.14      4.47   |   27   63.36      3.85   |                          |
|   18   40.26      4.41   |   28   65.74      3.91   |                          |
+-------------------------------------------------------------------------------+
```

Figure A7 *Conversion to Rasch Logit scores*

Cronbach's alpha Coefficient was 0.945 and the item total correlation was high. Reduction of further items would reduce the Cronbach Alpha Coefficient (Table A13).

	Q1	Q2	Q3	Q6	Q7	Q8	Q9	Q10	Q23
Corrected Item-Total Correlation	0.838	0.738	0.888	0.799	0.790	0.723	0.761	0.848	0.742
Cronbach's Alpha if Item Deleted	0.936	0.941	0.932	0.937	0.938	0.941	0.942	0.935	0.941

Table A13 *Item total correlation and Cronbach's alpha for each additional deleted item*

The ROC curve is displayed in Figure A8. 15 subjects were regarded as having near vision problems and the calculated area under the curve was 0.941.
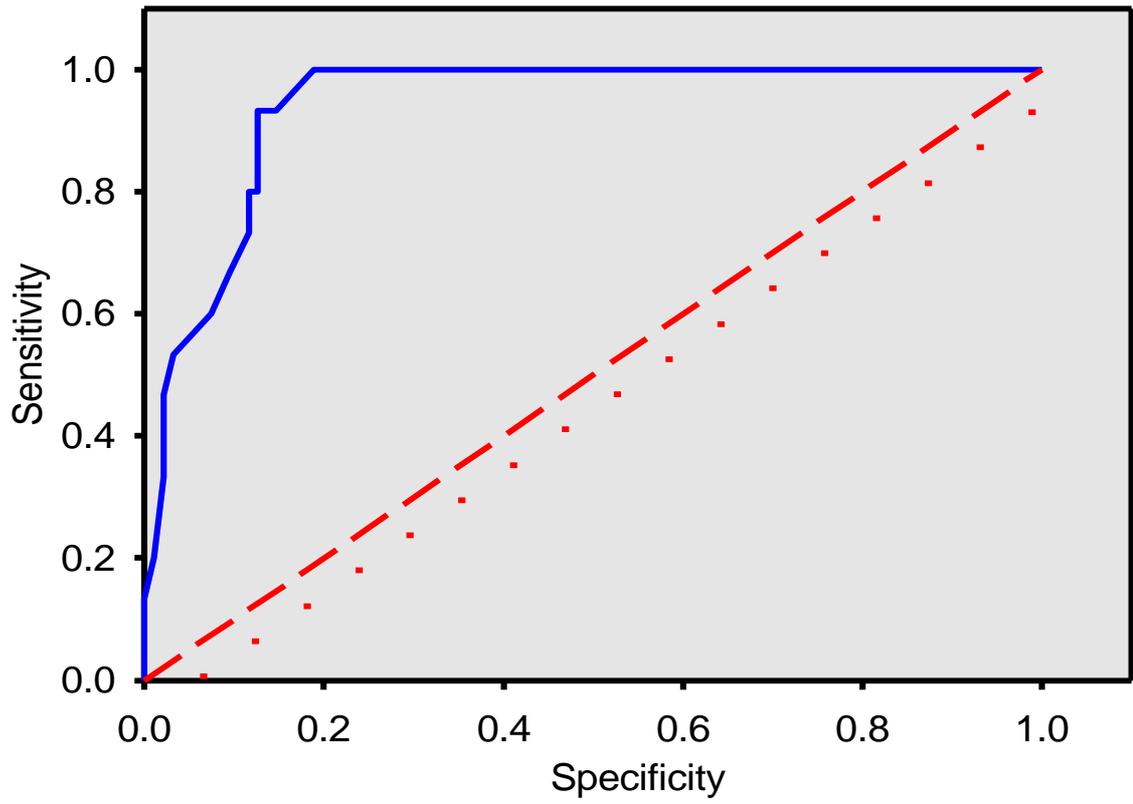
Figure A8 *The ROC curve for the remaining 9-item NAVQ*

A5 Power Vector Conversion for Assessment of Corneal Power

The corneal power, measured by the *LenStar LS900* and *IOLMaster* (n' = 1.332; Chapter 5), was converted into its mean spherical equivalent power (Equation A1) and vector power representation (Equation A2 & Equation A3; Thibos *et al.,* 1997).

$$MSE = S + \frac{C}{2} \qquad\qquad \textbf{Equation A1}$$

$$J0 = -\left(\frac{C}{2}\right)\cos(2 \times A) \qquad\qquad \textbf{Equation A2}$$

$$J45 = -\left(\frac{C}{2}\right)\sin(2 \times A) \qquad\qquad \textbf{Equation A3}$$

MSE is the mean spherical equivalent
S is the magnitude of sphere (flattest corneal meridian)
C is the magnitude of cylinder (difference in power between the two meridians)
A is the axis of astigmatism
J0 is the Jackson Cross cylinder magnitude of power at the zero degree meridian
J45 is the Jackson cross cylinder magnitude of power at the forty-five degree meridian
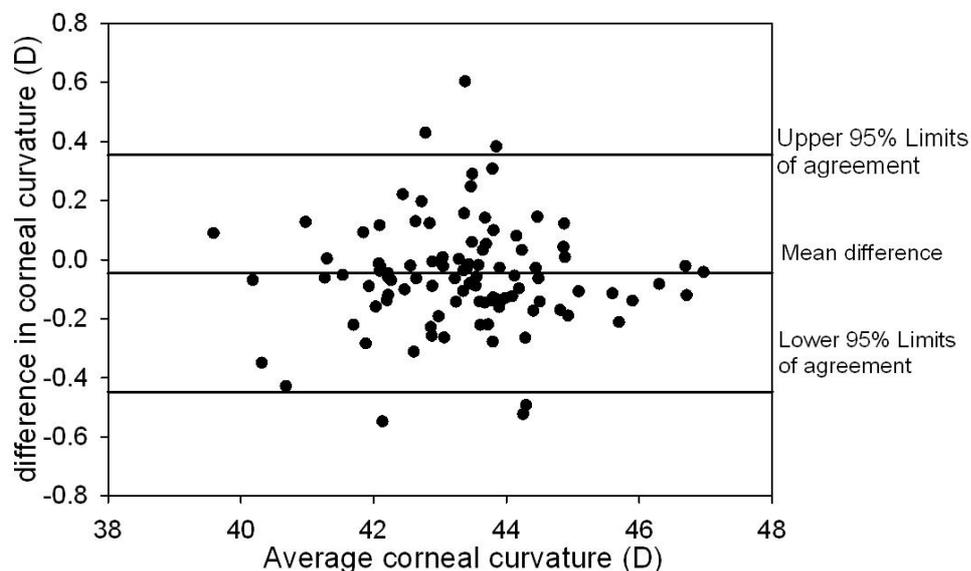
Figure A9 *Mean spherical equivalent corneal curvature: difference between LenStar and IOLMaster for the means spherical equivalent power of the cornea. n=112 eyes*

The mean difference (95% confidence interval), for the mean spherical corneal power, between the *LenStar LS900* and *IOLMaster* was 0.04 D (±0.42 D). The *LenStar LS900* read as much as 0.90 D above and 0.54 D below the *IOLMaster* for corneal curvature

(Figure A9). Both sets of results were similar (p = 0.06) and demonstrated a high correlation (r = 0.989).
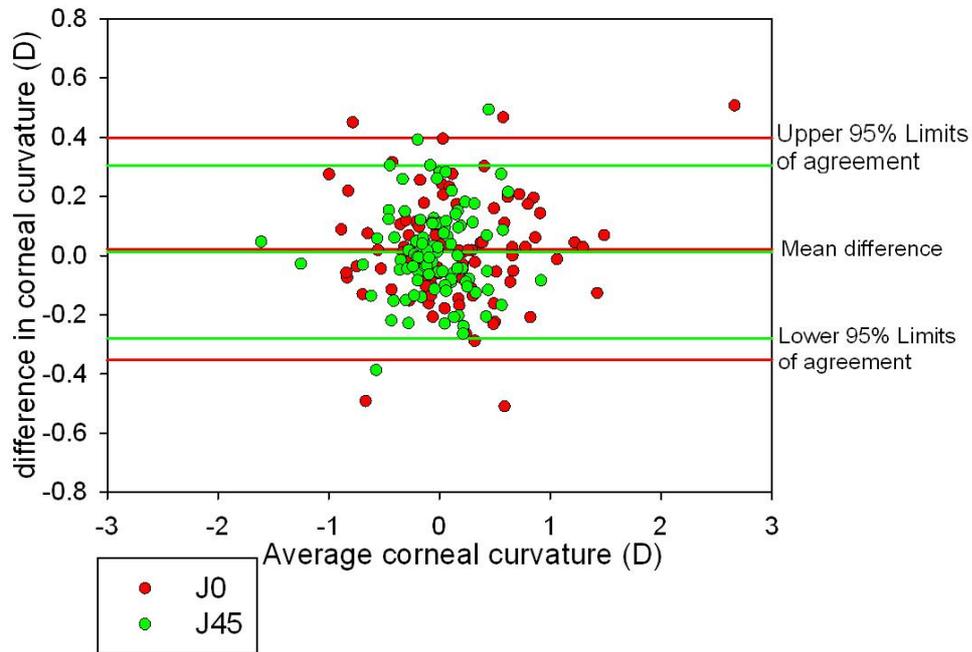
Figure A10 *Vector power analysis of corneal curvature: difference between LenStar and IOLMaster for the Jackson cross cylinder zero degree meridian and the forty-five degree meridian. n=112 eyes*

With regards to the Jackson cross cylinder power the mean difference (95% confidence interval) between the *LenStar LS900* and *IOLMaster* was 0.02 D (±0.37 D) at the zero degree meridian and 0.01 D (±0.29 D) at the forty-five degree meridian. The results of both instruments at the zero degree and forty-five degree meridians were similar (p>0.05) and there was a high correlation of the results at both the zero degree (r = 0.947) and forty-five degree meridians (r = 0.913).

A6   Additional References used in the Appendix

Akaishi, L., Tzelikis, P.F., Gondim, J. & Vaz, R. (2007). Primary piggyback implantation using the Tecnis ZM900 multifocal intraocular lens: case series. *J Cataract Refract Surg.* **33,** 2067-71.

Alfonso, J.F., Fernández-Vega, L., Ortí, S., Ferrer-Blasco, T. & Montés-Micó, R. (2009). Refractive and visual results after implantation of the AcrySof ReSTOR IOL in high and low hyperopic eyes. European J Ophthalmol. **19,** 748-53.

Alfonso, J.F., Puchades, C., Fernández-Vega, L., Merayo, C. & Montés-Micó, R. (2010a). Contrast Sensitivity Comparison Between AcrySof ReSTOR and Acri.LISA Aspheric Intraocular Lenses. *J Refract Surg.* **26,** 471-7.

Alfonso, J.F., Fernández-Vega, L., Ortí, S., Ferrer-Blasco, T. & Montés-Micò, R. (2010b). Differences in visual performance of AcrySof ReSTOR IOL in high and low myopic eyes. *European J Ophthalmol*. **20,** 333-9..

Andley, U.P. (2007). Crystallins in the eye: Function and pathology. *Prog Retin Eye Res.* **26,** 78-98.

Avitabile, T., Marano, F., Canino, E.G., Biondi, S. & Reibaldi, A. (1999). Long-term visual results of bifocal intraocular lens implantation. *J Cataract Refract Surg*. **25,** 1263-9.

Chen, M., Atebara, N.H. & Chen, T.T. (2007). A comparison of a monofocal Acrysoft IOL using the "blended monovision" formula with the multifocal array IOL for glasses independence after cataract surgery. *Annals Ophthalmol*. 39, 237-40.

Chiam, P.J.T., Chan, J.H., Aggarwal, R.K., Kasaby, S. (2006). ReSTOR intraocular lens implantation in cataract surgery: quality of vision. *J Cataract Refract Surg*. **32,** 1459-63.

Cillino, S., Casuccio, A., Pace, F.D., Morreale, R., Pillitteri, F., Cillino, G. & Lodato, G. (2008). One-year outcomes with new-generation multifocal intraocular lenses. Ophthalmology. **115,** 1508-16.

Claoué, C. (2004). Functional vision after cataract removal with multifocal and accommodating intraocular lens implantation: prospective comparative evaluation of Array multifocal and 1CU accommodating lenses. *J Cataract Refract Surg*. **30,** 2088-91.

Connors, R., Boseman, P. & Olson, R.J. (2002). Accuracy and reproducibility of biometry using partial coherence interferometry. *J Cataract Refract Surg.* **28,** 235-8.

Eisenmann, D. & Jacobi, K.W. (1993). [The Array multifocal lens--functional principle and clinical results]. Klinische Monatsblätter für Augenheilkunde. **203,** 189-94.

Elgohary, M.A. & Beckingsale, A.B. (2008). Effect of posterior capsular opacification on visual function in patients with monofocal and multifocal intraocular lenses. *Eye*. **22,** 613-9.

Felipe, A., Pastor, F., Artigas, J.M., Diez-Ajenjo, A., Gené, A. & Menezo, J.L. (2010). Correlation between optics quality of multifocal intraocular lenses and visual acuity: tolerance to modulation transfer function decay. Journal of cataract and refractive surgery. **36,** 557-62.

Ferko, J. & Ferkova, A. (2009). IOL Tetraflex, KH 3500--presbyopia treatment *Oftalmologia*. **53,** 72-3.

Fernández-Vega, L., Alfonso, J.F., Baamonde, B., Madrid-Costa, D., Montés-Micó, R. & Lozano, J. (2009). Visual and refractive outcomes in hyperopic pseudophakic patients implanted with the Acri.LISA 366D multifocal intraocular lens. Am J Ophthalmol. **148,** 214-220.

Fernandez-Vega, L., Madrid-Costa, D., Alfonso, JF., Poo-Lopez, A. & Montes-Micò, R. (2010). Bilateral implantation of the Acri.LISA bifocal intraocular lens in myopic eyes European journal of ophthalmology. **20,** 83-9.

Ferrer-Blasco, T., Montés-Micó, R., Cerviño, A., Alfonso, J.F., Fernández-Vega, L. (2008). Contrast sensitivity after refractive lens exchange with diffractive multifocal intraocular lens implantation in hyperopic eyes. *J Cataract Refract Surg.* **34,** 2043-8.

Hida, W.T., Motta, A.F.P., Kara-José Junior, N., Alves, E., Tadeu, M., Cordeiro, L.N. & Nakano, C.T. (2009). Comparison between OPD-Scan results and visual outcomes of monofocal and multifocal intraocular lenses. *Arquivos brasileiros de oftalmologia*. **72,** 526-32.

Javitt, J.C. & Steinert, R.F. (2000b). Cataract extraction with multifocal intraocular lens implantation: a multinational clinical trial evaluating clinical, functional, and quality-of-life outcomes. *Ophthalmology*. **107,** 2040-8.

Kaushik, S. & Kamlesh. (2002). A clinical evaluation of an aspheric multifocal intraocular lens and its implications for the developing world. *Ophthalmic surgery and lasers.* **33,** 298-303.

Lam, A.K., Chan, R. & Pang, P.C. (2001). The repeatability and accuracy of axial length and anterior chamber depth measurements from the IOLMaster. *Ophthalmic Physiol Opt.* **21,** 477-83.

Lee, E.S., Lee, S.Y., Jeong, S.Y., Moon, Y.S., Chin, H.S., Cho, S.J., Oh, J.H. (2005). Effect of postoperative refractive error on visual acuity and patient satisfaction after implantation of the Array multifocal intraocular lens. *J Cataract Refract Surg.* **31,** 1960-5.

Lindstrom, R.L. (1992). Results of clinical investigation of the 3M diffractive multifocal intraocular lens. *Semin Ophthalmol.* **7,** 261-8.

Lindstrom, R.L. (1992). Food and Drug Administration study update. One-year results from 671 patients with the 3M multifocal intraocular lens. *Ophthalmology*. **100,** 91-7.

Mesci, C., Erbil, H., Ozdoker, L., Karakurt, Y., Bilge, A.D. (2010). Visual acuity and contrast sensitivity function after accommodative and multifocal intraocular lens implantation. *European J Ophthalmol.* **20,** 90-100.

Shoji, N. & Shimizu, K. (2002). Binocular function of the patient with the refractive multifocal intraocular lens. *J Cataract Refract Surg.* **28,** 1012-7.

Thibos, L.N., Wheeler, W. & Horner, D. (1997). Power vectors: an application of Fourier analysis to the description and statistical analysis of refractive error. *Optom Vis Sci.* **74,** 367-75.

de Vries, N,E., Webers, C.A.B., Verbakel, F., de Brabander, J., Berendschot, T.T., Cheng, Y.Y.Y., Doors, M. & Nuijts, R.M.M.A. (2010b). Visual outcome and patient

satisfaction after multifocal intraocular lens implantation: aspheric versus spherical design. *J Cataract Refract Surg.* **36,** 1897-904.

A7 Supporting Publications

Buckhurst, P.J., Wolffsohn, J.S., Shah, S., Naroo, S.A., Davies, L.N. & Berrow, E.J. (2009). A new optical low coherence reflectometry device for ocular biometry in cataract patients. *Br J Ophthalmol*. **93,** 949-53.

Wolffsohn, J.S. & Buckhurst, P.J. (2010). Objective analysis of toric intraocular lens rotation and centration. *J Cataract Refract Surg*. **36,** 778-82

Buckhurst, P.J., Wolffsohn, J.S., Naroo, S.A. & Davies, L.N. (2010). Rotational and centration stability of an aspheric intraocular lens with a simulated toric design. *J Cataract Refract Surg*. **36,** 1523-1528.

Buckhurst, P.J., Wolffsohn, J.S., Davies, L.N. & Naroo, S.A. (2010). Surgical correction of astigmatism during cataract surgery. *Clin Exp Optom.* **93,** 409-18.

Buckhurst, P.J., Naroo, S.A. & Shah, S. (2010). Advanced Intraocular Lens Designs. *European Ophthalmic Review*. **4,** 82-86.

Wolffsohn, J.S., Davies, L.N., Naroo, S.A., Buckhurst, P.J., Gibson, G.A., Gupta, N., Craig, J.P. & Shah, S. (2010). Evaluation of an open-field autorefractor's ability to measure refraction and hence potential to assess objective accommodation in pseudophakes. *Br J Ophthalmol.* doi:10.1136/bjo.2010.185009 [Epub ahead of print].